

Spring 2010

Digital Image Correlation application to structural health monitoring

Philip A. Brogan

University of New Hampshire, Durham

Follow this and additional works at: <https://scholars.unh.edu/thesis>

Recommended Citation

Brogan, Philip A., "Digital Image Correlation application to structural health monitoring" (2010). *Master's Theses and Capstones*. 538.
<https://scholars.unh.edu/thesis/538>

This Thesis is brought to you for free and open access by the Student Scholarship at University of New Hampshire Scholars' Repository. It has been accepted for inclusion in Master's Theses and Capstones by an authorized administrator of University of New Hampshire Scholars' Repository. For more information, please contact nicole.hentz@unh.edu.

NOTE TO USERS

This reproduction is the best copy available.

UMI[®]

**DIGITAL IMAGE CORRELATION APPLICATION
TO STRUCTURAL HEALTH MONITORING**

BY

PHILIP A. BROGAN

B.S., University of New Hampshire, 2009

A.S., New Hampshire Technical Institute, 2006

THESIS

Submitted to the University of New Hampshire
in Partial Fulfillment of
the Requirements for the Degree of

Master of Science
in
Civil Engineering

May, 2010

UMI Number: 1485415

All rights reserved

INFORMATION TO ALL USERS

The quality of this reproduction is dependent upon the quality of the copy submitted.

In the unlikely event that the author did not send a complete manuscript and there are missing pages, these will be noted. Also, if material had to be removed, a note will indicate the deletion.



UMI 1485415

Copyright 2010 by ProQuest LLC.

All rights reserved. This edition of the work is protected against unauthorized copying under Title 17, United States Code.

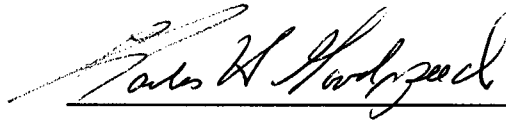


ProQuest LLC
789 East Eisenhower Parkway
P.O. Box 1346
Ann Arbor, MI 48106-1346


This thesis has been examined and approved.



Thesis Director, Dr. Erin Santini Bell
Assistant Professor of Civil Engineering



Dr. Charles H. Goodspeed
Associate Professor of Civil Engineering



Dr. Ricardo A. Medina
Assistant Professor of Civil Engineering

May 12, 2010

Date

ACKNOWLEDGEMENTS

Funding for this research was provided by the National Science Foundation (NSF) division of Civil, Mechanical, and Manufacturing Innovation (CMMI) Career grant number 0644683, “Integrating Structural Health Monitoring, Intelligent Transportation Systems, and Model Updating into a Bridge Condition Assessment”, and by the NSF Major Research Instrumentation (MRI) Program grant number 0821517, “Acquisition of a Digital Image Correlation System to Advance Research, Training, and Education in Engineering.”

Many thanks to fellow graduate researchers Paul Lefebvre and Heather Newton for their assistance in collecting data. I also want to recognize undergraduate researcher Jason Peddle, who has also helped me with data collection and will be continuing my research upon my departure.

Without Prof. Erin Bell, I would not have completed this research. Thank you for encouraging me to do my best and pursue my graduate degree. Many thanks to Prof. Charlie Goodspeed and Prof. Ricardo Medina for their help and support in editing this thesis.

TABLE OF CONTENTS

ACKNOWLEDGEMENTS.....	iii
TABLE OF CONTENTS.....	iv
LIST OF TABLES.....	vii
LIST OF FIGURES.....	viii
ABSTRACT.....	x
CHAPTER 1: INTRODUCTION TO INTELLIGENT TRANSPORTATION SYSTEMS AND STRUCTURAL HEALTH MONITORING	1
1.1 - State of Bridges in the United States	1
1.2 - Current Bridge Management	2
1.3 - The Opportunity for SHM and ITS.....	4
1.3.1 - SHM Definition	4
1.3.2 - ITS Definition	11
1.3.3 - Opportunities for Overlap.....	13
1.4 - Digital Image Correlation	14
1.5 - Research Goals.....	15
CHAPTER 2: THE SHIFTING PARADIGM OF BRIDGE MANAGEMENT TOWARD LONG-TERM MONITORING	16
2.1 - Overview	16
2.2 - Model Verification.....	17
2.3 - Measurement Types	19
2.3.1 - Value of Deflection Measurements	19
2.3.2 - Measurement Enhancement	20
CHAPTER 3: DIC DEVELOPMENT AND PROCESSING THEORY	21
3.1 - Traditional DIC.....	21
3.1.1 - Material Science.....	21

3.1.2 - Mechanical Engineering	22
3.1.3 - Civil Engineering	23
3.1.4 - Software Applications	27
3.2 - Challenges	34
3.2.1 - Environmental Conditions.....	34
3.2.2 - Geographic Limitations	36
3.2.3 - Speckle Pattern Development and Application	38
3.2.4 - Camera Limitations	40
3.2.5 - General Guidelines.....	41
3.2.6 - Testing Protocol for using DIC to Capture the Behavior of Civil Structures.....	42
CHAPTER 4: DIC EXPERIMENTS AND RESULTS.....	45
4.1 - Controlled (Laboratory) Experiments	45
4.1.1 - Board Test	45
4.1.2 - Slab Tests.....	48
4.1.3 - Shake Table Tests	57
4.2 - Field Experiments.....	66
4.2.1 - Pond Bridge Road Bridge Test.....	66
4.2.2 - Vernon Avenue Test.....	77
CHAPTER 5: CASE STUDY—VERNON AVENUE BRIDGE	78
5.1 - Introduction	78
5.2 - Concrete Deck Pour Test.....	81
5.2.1 - Setup	81
5.2.2 - Speckle Pattern Issues.....	81
5.2.3 - Results	82
5.3 - Load Test	84
5.3.1 - Background	84
5.3.2 - Center Span Data	86
5.3.3 - South Span Data	89
5.3.4 - Results	91
5.3.5 - SAP2000 Model Deflection Comparison	100
5.3.6 - Speckle Pattern Comparison	102

5.3.7 - Weather Conditions	103
5.3.8 - Examples of Poor Data	105
5.3.9 - Remarks.....	109
CHAPTER 6: CONCLUSIONS AND RECOMMENDATIONS FOR FUTURE WORK.....	111
6.1 - Conclusions	111
6.2 - Future Work	112
WORKS CITED.....	115
APPENDICES	118
APPENDIX A: TEST RESULTS	119
APPENDIX B: SAMPLE BRIDGE INSPECTION REPORT	180

LIST OF TABLES

Table 4-1: Pond Bridge Road Bridge testing summary.....68
Table 4-2: Pond Bridge Road Bridge test error values71
Table 5-1: Load test schedule.....85

LIST OF FIGURES

Figure 1-1: Percent deficiency of bridges with age (FHWA, 2004)	2
Figure 1-2: Strain gauge (Strain Gauges, 2010).....	5
Figure 1-3: Triple-axis accelerometer (Reiker, 2010)	6
Figure 1-4: Tilt sensor (Applied Geomechanics, 2010).....	7
Figure 1-5: LVDT schematic (Macro Sensors, 2009).....	8
Figure 1-6: LVDT (Digi-key, 2010).....	8
Figure 1-7: Masonry Arch Bridge LVDT setup	9
Figure 1-8: Loop detectors (FHWA, 2006).....	12
Figure 1-9: Traffic camera monitor (A&M University, 2004)	13
Figure 2-1: Bridge modeling flowchart.....	18
Figure 3-1: A Kevlar cloth is penetrated by a bullet (CSlb, 2009).....	22
Figure 3-2: Strain in a gear tooth (CSlb, 2009).....	23
Figure 3-3: DIC equipment (CSI, 2007).....	25
Figure 3-4: A typical DIC setup (CSI, 2007).....	26
Figure 3-5: Screenshot from Vic-Snap (CSI, 2007).....	28
Figure 3-6: Vic-3D screenshot with calibration image (CSI, 2007)	29
Figure 3-7: Vic-3D Calibration parameters.....	30
Figure 3-8: More Vic-3D Calibration parameters.....	31
Figure 3-9: Processed test image in Vic-3D.....	32
Figure 3-10: Auto plane-fit feature in Vic-3D (CSI, 2007).....	33
Figure 3-11: Vic-3D screenshot of strain computation	34
Figure 3-12: Examples of acceptable speckle patterns (CSI, 2007).....	38
Figure 3-13: Paper speckle pattern on bridge girder in Tiverton, Rhode Island	40
Figure 4-1: Board test setup.....	46
Figure 4-2: Deflection of board in Board Test 1	47
Figure 4-3: Deflection of board in Board Test 2	47
Figure 4-4: Examples of precast bridge deck panel connections (Robert, 2009).....	49
Figure 4-5: UNH loading frame.....	50
Figure 4-6: Slab test loading setup.....	51
Figure 4-7: Slab test DIC setup with cameras, loaded slab, and computer	52
Figure 4-8: Slab after failure.....	53
Figure 4-9: Precast Slab test ambient data	54
Figure 4-10: Precast slab Test 1.....	55
Figure 4-11: Precast slab Test 2.....	56
Figure 4-12: Precast slab Test 3.....	57

Figure 4-13: Shake table DIC setup	58
Figure 4-14: Shake table speckle target	59
Figure 4-15: Shake table Test 1, DIC velocity and acceleration versus time	60
Figure 4-16: Shake table Test 2, DIC displacement and velocity versus time	61
Figure 4-17: Shake table Test 1, acceleration versus time comparison	62
Figure 4-18: Shake table Test 1, acceleration versus time comparison detail	63
Figure 4-19: Shake table Test 2, acceleration versus time comparison	64
Figure 4-20: Shake table Test 2, acceleration versus time comparison detail	65
Figure 4-21: Test truck passing over the Pond Bridge Road Bridge	67
Figure 4-22: Pond Bridge Road Bridge DIC test setup	69
Figure 4-23: Example of the speckle pattern used at the Pond Bridge test	70
Figure 4-24: Vertical deflection of Pond Bridge Road Bridge at Midspan-Test 1	72
Figure 4-25: Vertical deflection of Pond Bridge Road Bridge at Midspan-Test 4	74
Figure 4-26: Vertical deflection of Pond Bridge Road Bridge at Midspan-Test 11	75
Figure 4-27: BDI data for two load truck locations at Pond Bridge Road Bridge	76
Figure 5-1: Deck spall at Vernon Avenue Bridge (MHD, 2007)	79
Figure 5-2: Girder 1 being installation with speckle pattern in place	80
Figure 5-3: Vernon Avenue Bridge speckle pattern with obstructions	82
Figure 5-4: Vernon Ave Bridge deflection during concrete deck pour	83
Figure 5-5: Concrete deck pour and heavy equipment operation	84
Figure 5-6: Vernon Ave plan showing truck lanes and DIC setup locations	86
Figure 5-7: Middle span DIC setup	87
Figure 5-8: Updated speckle pattern at middle span	88
Figure 5-9: Calibration target in front of the speckle pattern at the middle span	89
Figure 5-10: DIC setup at south span	90
Figure 5-11: Speckle pattern and calibration target at south span	91
Figure 5-12: Vertical deflection of Vernon Ave Bridge at both spans-Test 3-X1-1	93
Figure 5-13: Vertical deflection of Vernon Ave Bridge at both spans-Test 8-X2-3	95
Figure 5-14: Vertical deflection of Vernon Ave Bridge near midspan-Test 14-X1-3	96
Figure 5-15: Vertical deflection of Vernon Ave Bridge near midspan-Test 103-X2-4_1	97
Figure 5-16: Load truck hitting speed bump during impact test	98
Figure 5-17: Vertical deflection of Vernon Ave Bridge near midspan-Test 25-X1-1	99
Figure 5-18: SAP2000 model of the Vernon Avenue Bridge	100
Figure 5-19: SAP2000 model deflection data versus DIC data from Vernon Ave Load Test	102
Figure 5-20: DIC camera with visor	104
Figure 5-21: Vertical deflection of Vernon Ave Bridge near midspan-Test 7-X2-2	105
Figure 5-22: Computer error at Vernon Avenue Bridge-Test 4-X1-2	107
Figure 5-23: Trending of Vernon Avenue data near midspan-Test 10-X3-2	108

ABSTRACT

DIGITAL IMAGE CORRELATION APPLICATION TO STRUCTURAL HEALTH MONITORING

by

Philip A Brogan

University of New Hampshire, May, 2010

Bridge inspectors have historically relied on previous inspection reports and photographs to assess bridge health. The inclusion of instrumentation including sensors such as strain gauges, tilt sensors, LVDTs, or accelerometers can greatly enhance bridge management. This instrumentation and data interpretation is classified under a new field of study called Structural Health Monitoring (SHM). A relatively new application called Digital Image Correlation (DIC) can be deployed for SHM of civil structures. DIC uses multiple digital cameras to capture sequenced images of a target object and provide displacement information. This research has sought to incorporate DIC systems into bridge inspection and eventually a long-term SHM program. Several experiments were conducted as part of this research in both the laboratory and the field to determine the physical limits of the DIC system. The research provided insight into these limits and illuminated several key areas which require further testing.

CHAPTER 1

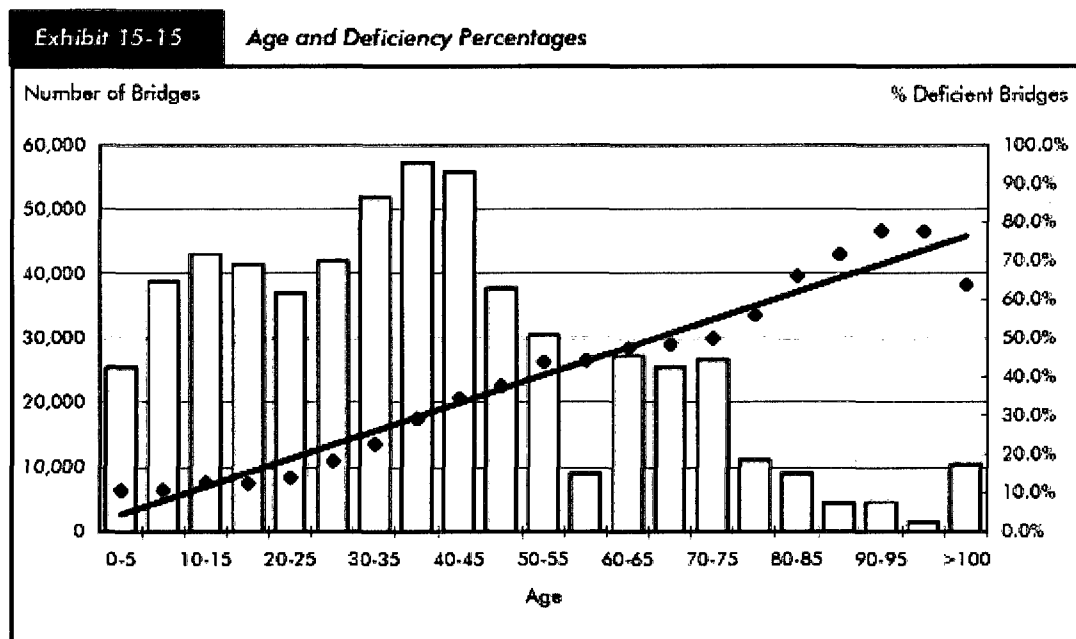
INTRODUCTION TO INTELLIGENT TRANSPORTATION SYSTEMS AND STRUCTURAL HEALTH MONITORING

1.1 - State of Bridges in the United States

An increasing number of critically deteriorating and high profile bridge failures in the past several decades has highlighted the deteriorating condition of the bridge infrastructure in America and the need for new monitoring techniques and advanced management. According to the American Society of Civil Engineers (ASCE) infrastructure report card, America's bridges have consistently received a rating of "C" for the past ten years (ASCE, 2010). Meanwhile, construction costs have inflated by at least 50 percent and neither Federal nor State transportation budgets have been able to keep pace with the increasing expenses of bridge replacement and maintenance. (AASHTO, 2008).

The 1950s and 1960s featured a highway building boom under the Eisenhower administration as the country tried to overcome the lack of high-speed ground transportation encountered during the Second World War (FHWA, 2010). As a result, nearly one half of America's bridges today are between the ages of 35 and 55 years. Collected data shows that bridge deterioration accelerates rapidly after 40 years of age. The average design life for most of these bridges is 50 years, placing many bridges in precarious condition (AASHTO, 2008). Figure 1-1 from the Federal Highway

Administration shows the increasing deficiency of bridges as they age. The number of bridges is shown with bars and quantified on the left axis and the percentage of deficient bridges is depicted with the diamonds and quantified on the right axis.



Source: National Bridge Inventory.

Figure 1-1: Percent deficiency of bridges with age (FHWA, 2004)

1.2 - Current Bridge Management

The collapse of the I-35W Bridge in Minneapolis, Minnesota during rush hour on August 1, 2007, resulted in the deaths of 13 people and reawakened the call for increased bridge monitoring (AASHTO, 2008). Traditionally, the structural integrity of bridges has been monitored by visual inspections according to the National Bridge Inspection Standards (NBIS) or PONTIS software. An “initial inspection” is conducted immediately following construction completion to establish a baseline for future inspections. After this, “routine inspections” take place at least every two years, with

“special inspections” to investigate any anomalies in the structure (Phares, Rolander, Graybeal, & Washer, 2000). Sample bridge inspection reports are included in Appendix B.

Although these inspections are standardized for each state, the inspection process is still fairly subjective, with each inspector using his own judgment and personal expertise on the condition of each bridge component (Phares, Rolander, Graybeal, & Washer, 2000). One study conducted by Phares, Rolander, Graybeal, and Washer (2001) demonstrated that there is almost always a statistically significant difference in bridge inspection ratings between multiple inspectors for a given bridge. This ambiguity, along with the collective deterioration of bridge infrastructure, has led to the realization that a more long-term, objective approach needs to be applied to bridge management. This realization has initiated advancements in a field of study in bridge engineering referred to as Structural Health Monitoring (SHM).

Traditionally, bridge design and operation has been considered a separate discipline from bridge maintenance. Design and operation include the design of the bridge, a regular inspection procedure after construction is completed, and signage, among other things. Bridge maintenance involves repairing the roadway surface, salting, painting girders, etc. However, the desire for long-term bridge monitoring has created opportunities for these two disciplines to overlap. For example, an SHM program may employ thermometers to monitor the temperature of the bridge deck and update a structural model with that data; these temperature readings can also notify bridge

maintenance personnel when the bridge surface drops below freezing and salt application is required.

1.3 - The Opportunity for SHM and ITS

SHM is closely tied to another set of technologies referred to as Intelligent Transportation Systems (ITS). ITS instrumentation includes things such as traffic lights and camera traffic monitors. Both SHM and ITS are monitoring systems deployed in bridge transportation systems.

1.3.1 - SHM Definition

SHM is a comprehensive effort to transform bridge management into a long-term, objective process. According to Catbas et al (2008), SHM can be defined as “tracking the responses of a structure along with inputs, if possible, over a sufficiently long duration to determine anomalies, to detect deterioration and to identify damage for decision making.” Many forms of instrumentation have been used in SHM to create a comprehensive picture of bridge health. A few of the most popular sensors used in SHM that are part of this research are presented in detail.

Strain Gauges. Strain is the unitless measure of displacement relative to overall length, essentially giving an indication of the elongation or contraction of a material. Assuming linear-elastic behavior, strain is proportional to stress, and thus is a very good indicator of the condition of a structural element.

A typical strain gauge consists of an extremely thin layer of foil interwoven with conducting wires. An example of a strain gauge used in this research is shown in (Figure

1-2). It is an Omega KFG-5-350-C1-11L3M3R three-wire, uni-axial strain gauge with 350-ohm resistance. A small amount of electric current is fed through the gauge, and as the sensor stretches or contracts, the resistance to the current increases or decreases, changing the output voltage. Thus the strain gauge output is a simple variation of millivolts of current, which is then translated into a strain reading.

Gauge installation on steel or concrete involves preparing the surface of the structural element to a very smooth finish and attaching the sensor with a strong adhesive (Strain Gauges, 2010). The gauge must then be connected to a data acquisition (DAQ) system for data collection. There is also a “gauge factor” which is unique to each gauge.



Figure 1-2: Strain gauge (Strain Gauges, 2010)

Accelerometers and Tilt Sensors. Similarly, accelerometers and tilt sensors can be mounted to any element of a structural member using mechanical fasteners,

adhesives, or even magnets. Accelerometers can measure the acceleration along all three orthogonal axes, giving data about dynamic response of the structure (see Figure 1-3).

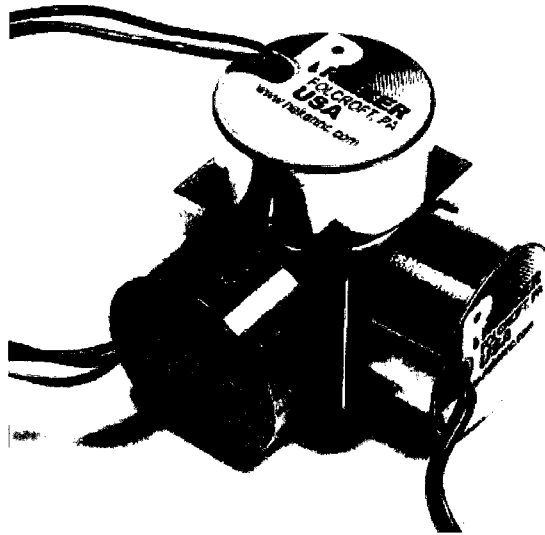


Figure 1-3: Triple-axis accelerometer (Reiker, 2010)

Tilt sensors give an indication of how much an element is rotating about the vertical axis, essentially giving the slope of the deflected shape. These sensors are similar to strain gauges in that they are reference-independent; they can be wired to a hub to provide real-time measurement of several gauges at a time (see Figure 1-4).

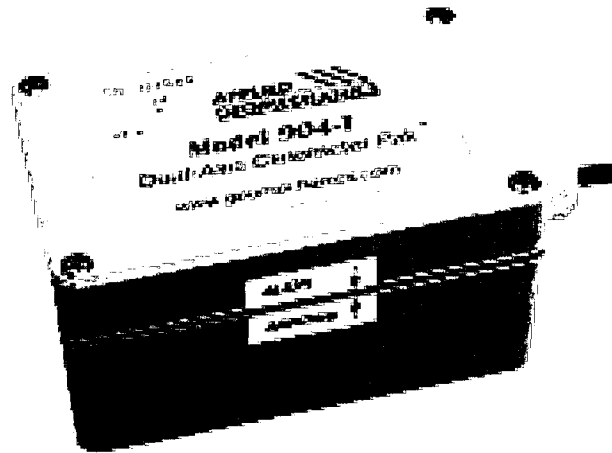


Figure 1-4: Tilt sensor (Applied Geomechanics, 2010)

LVDT and SWP. Several types of displacement measurement have been traditionally used in SHM. Displacement is a reference-dependent measurement, making it more difficult to measure in the field. One of those is the linear variable differential transformer, or LVDT. An LVDT is a transformer that consists of a central magnetic wire surrounded by a solenoid (Figure 1-5).

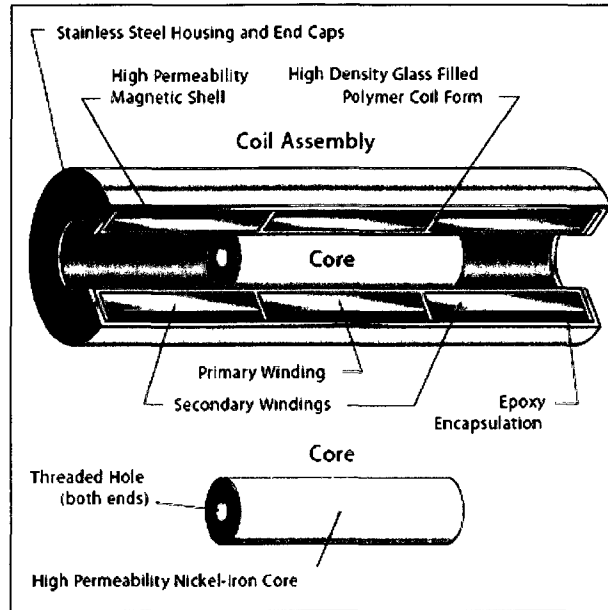


Figure 1-5: LVDT schematic (Macro Sensors, 2009)

The term “linear” explains the measurement limitations of the device—because of the wire configuration, the LVDT can only measure displacement in one dimension (Figure 1-6). The wire and solenoid make no contact, creating a highly-efficient frictionless measurement. Also, since there are no mechanical parts in contact, LVDTs are durable and weather-resistant (Macro Sensors, 2009).

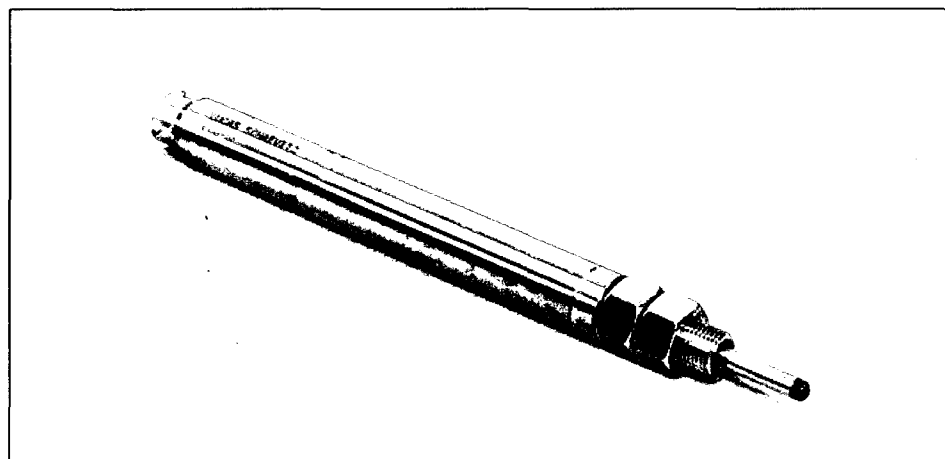


Figure 1-6: LVDT (Digi-key, 2010)

Field application of LVDT's is difficult for bridge testing since they must be positioned firmly beneath the bridge structure and attached to an object with a stationary baseline. For example, Bridge Diagnostics Inc. conducted a test on a masonry arch bridge in Rhode Island in the fall of 2009. To gather deflection data, LVDTs were mounted on tripods which were sitting on scaffolding in a river bed (Figure 1-7).



Figure 1-7: Masonry Arch Bridge LVDT setup

GPS and Radar. Other types of displacement measurement feature more modernized methods. Two of the newest techniques are Global Positioning System (GPS) and radar distance measurement. A recent study on the Manhattan Bridge in Brooklyn, New York compared these two systems (Mayer, Yanev, Olson, & Smyth, 2010). For years the travel of heavy subway cars across opposite sides of the bridge

created large torsional forces across the bridge section. A thirty-year bridge-stiffening project began in the early 1980s; the study measured the vertical bridge deflection after the stiffening was completed. The GPS system used a central antenna located near a bridge abutment, with four local GPS receivers located along the span of the bridge. The main antenna provided absolute displacement measurements of the bridge deck relative to the central antenna (Mayer, Yanev, Olson, & Smyth, 2010).

The same researchers then used an interferometric radar system to measure the bridge deflections. The radar system can be set up underneath the bridge, detect each of the girders, and measure the deflection of each (a metal reflector may be required if the bridge structure is concrete). The data from both the GPS and radar tests proved comparable; both provided a quick, accurate way to measure bridge deflection without substantial traffic interruption (Mayer, Yanev, Olson, & Smyth, 2010).

Laser. Probably the most promising technology of all in SHM is laser measuring devices. One such device was developed by four engineers in the southeastern United States (Fuchs, Washer, Chase, & Moore, 2004). The system is fully automated, and can measure with ± 0.03 inch accuracy to a distance of one hundred feet. The lasers send a constant signal, and noise is filtered out using frequency modulation. Because of its noise-reducing capabilities, the laser can get an accurate reading off any non-polished surface, including steel and concrete.

The laser is typically set up under a bridge, and measurements are taken from the underside of the bottom flange of the bridge girders. Readings are collected every

few feet along each girder. Several measurements are taken in a small square at each location to obtain an average vertical displacement. There are two drawbacks to the system. The first is speed; because it only takes about seven measurements per second, only static load testing is possible (Fuchs, Washer, Chase, & Moore, 2004). The second drawback is accuracy; since the laser system can only measure to ± 0.03 inches, bridge deflection must be significantly greater than that value to collect meaningful results.

Surveying. One final SHM measurement type that is frequently used is surveying. Total stations have greatly increased the simplicity and accuracy of survey operations. As such, they are often used to collect deflection data of a bridge structure. However, even with advanced equipment, there are still many variables, mostly due to human error. For example, total-station measurements often depend on a person who is holding a measuring rod, which must be plum for an accurate reading. It is also very difficult to create reproducible results when shooting points on a leveling rod since accuracy is generally only ± 0.01 inches (Sipple, 2008).

1.3.2 - ITS Definition

Another set of innovative technologies developed in recent years is Intelligent Transportation Systems (ITS). ITS is a network of instruments that seeks to streamline the relationship between driver, vehicle, and user. Essentially, ITS is a traffic management system that enhances vehicular flow (Japanese Ministry of Land, 2008). There are several types of sensors used for ITS that monitor how a bridge is being used.

Ground Sensors. Loop detectors (Figure 1-8) automatically conduct traffic counts on a roadway, saving the time and energy of personnel conducting such counts manually. This information is used for road widening and access design decisions.



Figure 1-8: Loop detectors (FHWA, 2006)

Weigh-in-Motion. A weigh-in-motion station, or WIM, is a scale embedded in the road surface to measure dynamic vehicle loads. WIMs identify and locate heavy or overloaded trucks, which is pertinent information in areas with structurally deficient bridges. WIMs also can record when and where traffic is passing, vehicle speed, and classification of vehicles (NJDOT, 2010). This capability makes WIMs very useful when conducting bridge load testing and assessing transportation needs.

Camera Traffic Monitoring. Video monitors are quite common on many bridges; they are used to monitor ice dams under bridges in northern regions, and to observe

traffic flow in congested areas (see Figure 1-9). These cameras are also used to record traffic violations such as running red lights.



Figure 1-9: Traffic camera monitor (A&M University, 2004)

1.3.3 - Opportunities for Overlap

SHM and ITS have been interwoven into many so-called “smart” bridges. These bridges make use of an array of both SHM and ITS instrumentation to create a complete picture of bridge health (Sleiman, 2009). This overlap provides many opportunities for instrument infrastructure sharing. Several components of ITS and SHM can be shared, such as power, connectivity, and equipment.

Power. In general, it can be assumed that ITS components will be in place before SHM hardware. Obviously, power will be required to operate video monitors and embedded roadway gauges. Many states, including New Hampshire, have mandated

that all new bridges include conduit in the bridge deck to provide for future power wiring. With electricity already onsite, it requires little additional effort to power SHM devices, whether temporarily or permanently.

Connectivity. Whatever the data transmission method, SHM and ITS devices are generally highly compatible, and assuming sufficient capacity, can be run on the same network. Data acquisition (DAQ) devices (either a computer or specialized device) can handle several various data input channels in a single unit, providing the opportunity to operate numerous devices from one location.

Equipment. DAQ devices can handle inputs from both SHM and ITS devices, since most instrumentation uses low-voltage electricity for data transmission. A DAQ setup can be programmed to identify and process information from each instrument and compile data on one computer.

1.4 - Digital Image Correlation

Digital Image Correlation (DIC) is one of the more recent innovations in Structural Health Monitoring. To explain the DIC process simply, it is a series of calibrated digital images that are post-processed to determine pixel movement across the frame. The pixel displacement can be converted to a physical distance through a calibration process using specialized calibration “targets.” This distance measurement can be converted to velocity, acceleration, strain, and rotation very quickly.

DIC has great promise to replace or enhance many SHM instruments. Because it is a non-contacting measurement technology, it is especially useful to record data during destructive testing or where traditional SHM instrumentation is difficult to install. DIC will be explained further in Chapter 3.

1.5 - Research Goals

Six specific research goals have been defined:

- 1) *Examine the need for DIC inclusion in bridge testing***
- 2) *Use the DIC system for laboratory experiments in controlled environments to validate DIC with traditional SHM measurements***
- 3) *Deploy DIC at field bridge tests***
- 4) *Post-process collected data for deflection***
- 5) *Compare deflection with predicted response of a structural model***
- 6) *Assess the usefulness of DIC in bridge testing***

CHAPTER 2

THE SHIFTING PARADIGM OF BRIDGE MANAGEMENT TOWARD LONG-TERM MONITORING

2.1 - Overview

Traditionally, Structural Health Monitoring protocol has primarily consisted of the annual or biannual visual inspection of bridges. These inspections are conducted by trained professionals who follow a checklist of key concerns. The inspector decides the condition of each part of the bridge, and then the bridge as a whole. However, this decision is subjective and depends on the personal experience or opinion of each inspector (Washer, 1998). One inspector may assess a bridge as acceptable, while another declares it in need of repair. Bridge managers rely upon these inspection reports for planning bridge repair and replacement, and allocation of very limited funding and manpower.

In recent years, engineers and government leaders have begun to question the reliability of visual inspection and to investigate objective metrics of bridge performance (Washer, 1998). States looking to optimize the public benefit of tight budgets have

sponsored research in bridge health monitoring. Recent bridge catastrophes have intensified the effort to reform bridge management.

A group of engineers created a non-profit organization called the International Society for Structural Health Monitoring of Intelligent Infrastructure (ISHMII) to “enhance the connectivity and information exchange between participating institutions and to increase the awareness for structural health monitoring disciplines and tools among end users” (ISHMII, 2010). Such organizations have helped engineers and bridge managers to realize the value of bridge instrumentation data to validate structural models.

2.2 - Model Verification

The structural model is verified using collected data under given loading conditions for a healthy bridge soon after construction is completed. Specialized programs using parameter estimation algorithms and model updating have been created to transform collected bridge response into a calibration medium for the structural model. One such program being developed at UNH is the Model Updating Structural Analysis Program (MUSTANG). MUSTANG compares predicted bridge response with collected bridge response. The difference between the two set of data is used to calibrate unknown or uncertain parameters of the bridge (Bell, Sanayei, Javdekar, & Slavsky, 2007). These parameters can include elemental properties that are not visible or the damage level is not easily measured.

The collected data validates the models, creating a baseline model. If the bridge is instrumented from initial construction, then data can be collected to confirm the model or show how the baseline model reflects the actual bridge behavior. All future testing and monitoring can be referenced back to this baseline point.

As illustrated in Figure 2-1, this process combines post-processed images collected from DIC and response parameters from a structural model into a program like MUSTANG. The program compares the data sets and reintroduces them into a calibrated model with new section properties. From this new model a bridge load rating (maximum allowable live load) can be assigned.

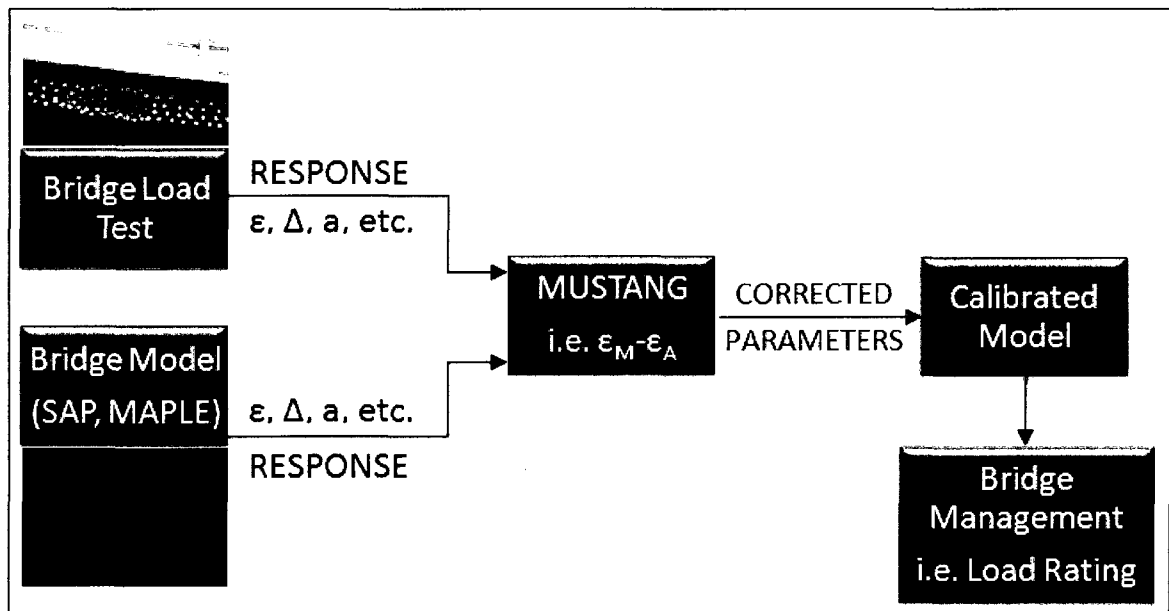


Figure 2-1: Bridge modeling flowchart

2.3 - Measurement Types

2.3.1 - Value of Deflection Measurements

Smart bridges are instrumented with multiple sensors such as strain gauges, video monitors, and loop detectors. Most of these technologies require cables for power and data transfer to be run under the bridge deck, which can be a painstaking and time-consuming process. These sensors require significant installation time and a DAQ to collect data. Because DIC does not need wiring or sensors installed, it has large potential in SHM. The only instrumentation that it requires on the bridge itself is a small speckle pattern that can be applied using spray paint or chalk. The remaining equipment—computer, tripod, and cameras—can be placed on a nearby embankment or shore providing a clear view of the target element. The data produced by DIC is in the form of deflections, which can be a physical representation of the health of a structure when compared to the predicted response at a point in time.

Since raw DIC data is in the form of images, photographic records of the bridge are recorded. Since most bridges are already equipped with traffic cameras, security cameras, or ice monitors, it would be quite sensible to combine all of these technologies into one single instrument. DIC data can be collected from video cameras just as well as from still cameras, since video is merely a collection of images in series. Once the camera is calibrated images can be captured to create a time history of deflection.

2.3.2 - Measurement Enhancement

The addition of DIC will enhance the ability to capture bridge performance. Strain is a local measurement that, although widely accepted, is limited in its ability to capture overall bridge behavior. Displacement and acceleration are global measurements which are much more useful in determining overall behavior. In addition, displacement measurements provide a static signature of a bridge and show the effects of seasonal changes on the structure.

CHAPTER 3

DIC DEVELOPMENT AND PROCESSING THEORY

3.1 - Traditional DIC

As mentioned previously, DIC is not a new technology, but application to SHM is a recent development. DIC has been used extensively in several fields of study including material science, mechanical engineering, and some aspects of civil engineering.

3.1.1 - Material Science

Those in the material science field use DIC extensively to determine material properties such as Young's modulus, Poisson's ratio, etc. In one such case, a DIC system took 10,000 images per second of a Kevlar cloth being hit by a bullet traveling at full speed (see Figure 3-1). Such an analysis can show scientists the limits of a material's strength and many of its properties. More traditional applications include examining molecular movement of materials under load such as steel, concrete, bone, and rubber (Dantec Dynamics, 2010).

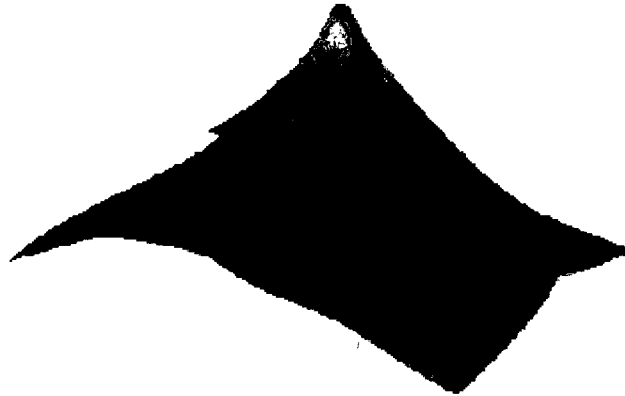


Figure 3-1: A Kevlar cloth is penetrated by a bullet (CSIB, 2009)

3.1.2 - Mechanical Engineering

Mechanical engineers have been using DIC for many years to analyze the stresses and strains in machine parts. These analyses are usually conducted in two dimensions, where a flat plane is stretched and stresses and strains are measured along that plane. However, three-dimensional analyses are sometimes conducted on components such as gears, as seen in Figure 3-2. Typical applications involve testing machine parts to collect strain distribution data and to pinpoint crack growth during destructive testing (Dantec Dynamics, 2010).

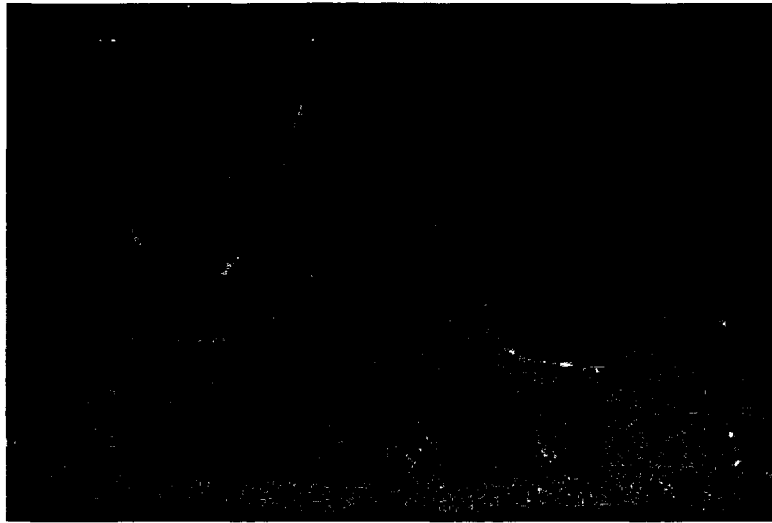


Figure 3-2: Strain in a gear tooth (CSib, 2009)

3.1.3 - Civil Engineering

DIC has also been used in civil engineering applications, although these cases are largely experimental. Extensive research has been conducted on geotextile applications using DIC (Aydilek, Oguz, & Edil, 2002). Other uses of DIC in civil engineering include bridge testing. Jong Jae Lee of the Korea Advanced Institute of Science and Technology and Masanobu Shinozuka of the University of California Irvine are two leading researchers in this growing field (Lee & Shinozuka, 2006). At the University of New Hampshire, Dr. Erin Bell is also conducting extensive research in DIC testing (Gamache & Santini-Bell, 2009).

With funding from the NSF-MRI Program Number 644683, the departments of Civil and Mechanical Engineering at the University of New Hampshire purchased a DIC package in 2008 in a joint venture to further the research activities in the areas of material science and mechanical and civil engineering. The package was purchased from

Correlated Solutions Inc. (CSI) of Columbus, South Carolina. CSI was founded in 1998 by the original developers of DIC at the University of South Carolina, and is the world leader in DIC technology today, serving customers across the globe in the academic, military, and private sectors (CSIa, 2009). CSI originally developed the DIC system for laboratory experimentation; however, the cameras can also be deployed for field tests.

The package that the university purchased contained the following components, which are depicted in Figure 3-3:

- A. Tripod
- B. Tripod 3-axis adjustable head
- C. Tripod quick-release adapter
- D. Slide block
- E. 23" Aluminum profiles
- F. Adjustable extrusion mounting hinge
- G. Cameras (4 low-speed and 2 high-speed)
- H. Lenses (2-17mm and 4-35mm)

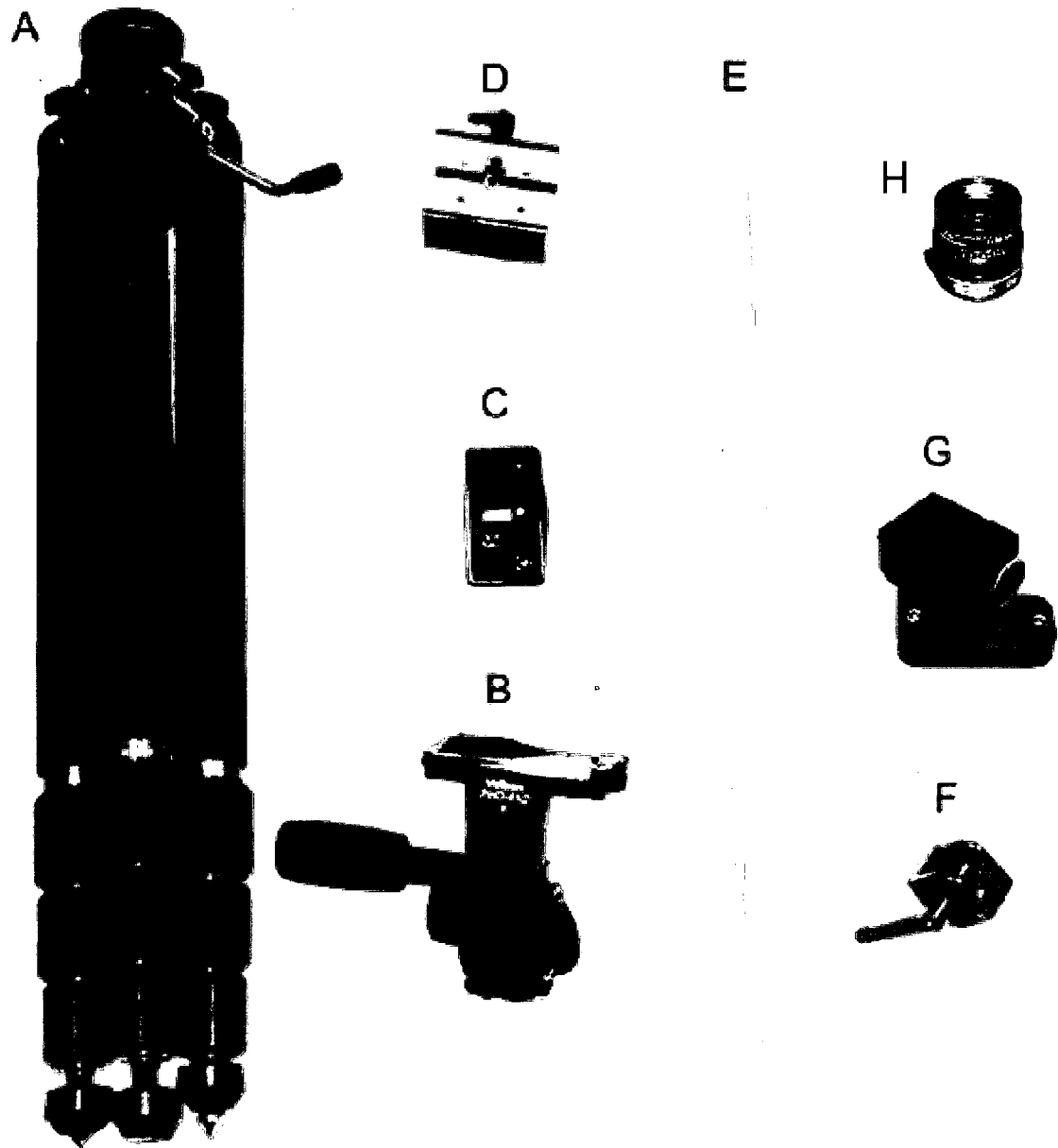


Figure 3-3: DIC equipment (CSI, 2007)

Setup. A typical DIC setup for a test with the aforementioned components consists of the following. A three-axis bracket sits atop a sturdy tripod, giving full range of motion for the camera system. On top of the bracket rests a slide block—so named because it supports an extruded aluminum rod that slides through the block and locks

into place. It is on this 23-inch aluminum rod that the cameras are mounted, one on either end. This provides sufficient separation distance between the cameras to gather displacement information along all three axes. A typical DIC setup is depicted in Figure 3-4.

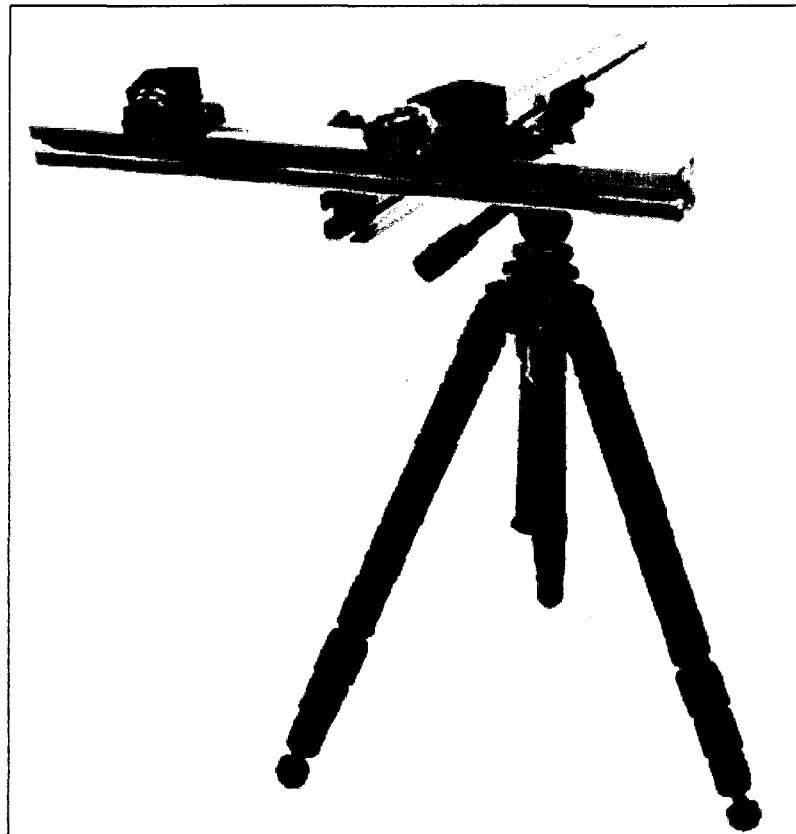


Figure 3-4: A typical DIC setup (CSI, 2007)

A fire-wire cable connects the cameras to each other and to a computer that controls image collection; the cameras must be remotely controlled to reduce camera shake. The cameras should be placed such that the angle between the cameras and target object they are facing is between 15 and 45 degrees; more or less is permissible, but some data may be lost if these limits are not maintained.

Calibration. The camera setup must be calibrated for accurate post-processing of the images. Correlated Solutions provides specialized calibration targets covered with dots that have a known geometry (see Figure 3-6). After the cameras have been adjusted and focused on the selected field of view, about 20-30 images of the calibration target are taken while rotating the target along all three axes, rotating it in plane, moving it toward and away from the cameras, and moving it to each corner of the image frame.

Post-processing software created by Correlated Solutions called Vic-3D analyzes each of the images. The software detects the dots in each of the calibration images and automatically determines the camera orientation and relation to each other. The program then issues a report indicating the calibration parameters and the standard deviation of the analysis. If the standard deviation is below 0.035, the calibration can be saved and the cameras are ready to take test images (CSI, 2007). If the standard deviation exceeds this limit, any calibration images with high standard deviations should be deleted and the calibration process repeated. If the value is still too high, check the camera focus and retake calibration images, preferably with a larger calibration target.

3.1.4 - Software Applications

Correlated Solutions provides software to control image collection (Vic-Snap) and to post-process images (Vic-3D). In the case of this research, the software used was Vic-Snap 2009 and Vic-3D 2009.

Vic-Snap. Vic-Snap has a very simple user interface yet is a powerful tool for collecting data from multiple images simultaneously. As seen in the screenshot of Vic-3D (Figure 3-5), the software shows a live feed from both cameras that are connected to the computer. Images can be enlarged to aid in focusing, and the shutter can either be triggered manually or set to take images at regular intervals. The image capture is completely controlled by the software at a prescribed sampling rate.

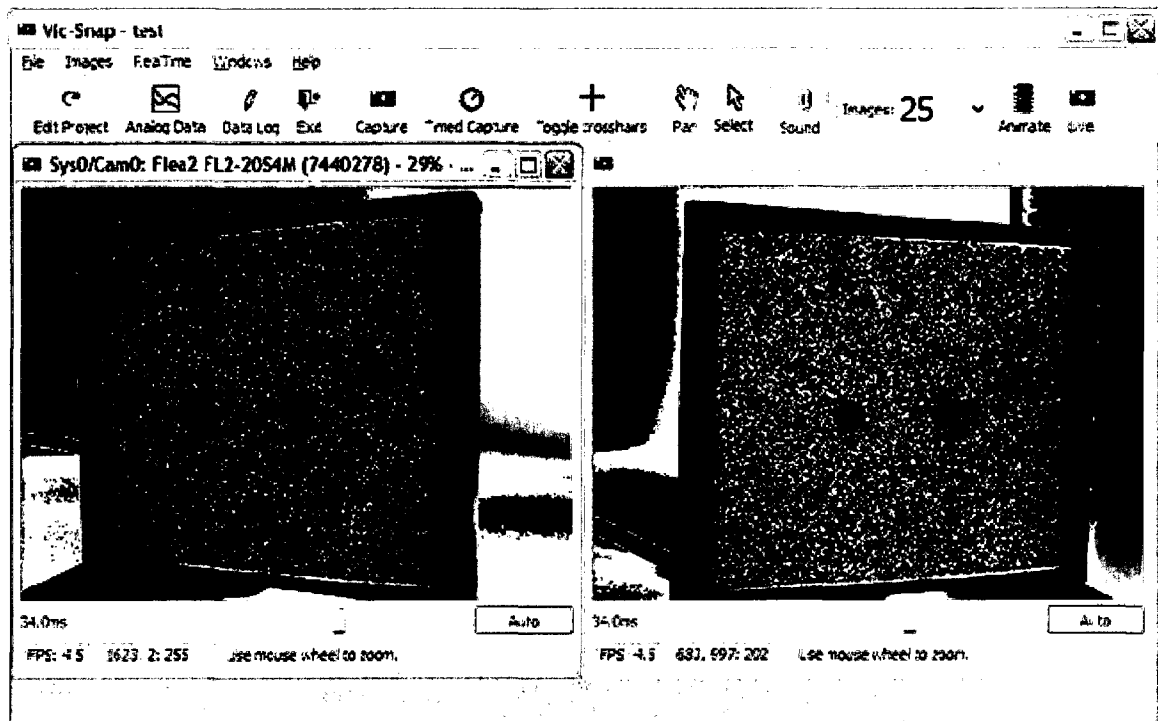


Figure 3-5: Screenshot from Vic-Snap (CSI, 2007)

Vic-3D. The Vic-3D software post-processes the images captured with Vic-Snap. To begin, the software analyzes each of the calibration images to determine the orientation and separation distance of the cameras. The calibration target contains an array of dots with a known spacing. Three of these dots have a hollow center. The

software locates these dots in each calibration image from both cameras, and from this determines the camera position. Images are taken with the target in various orientations to give the software a full perspective of the camera locations. See Figure 3-6 for an example of a processed calibration image; in this case, the software has successfully recognized and highlighted the three hollow dots and identified them with different colors

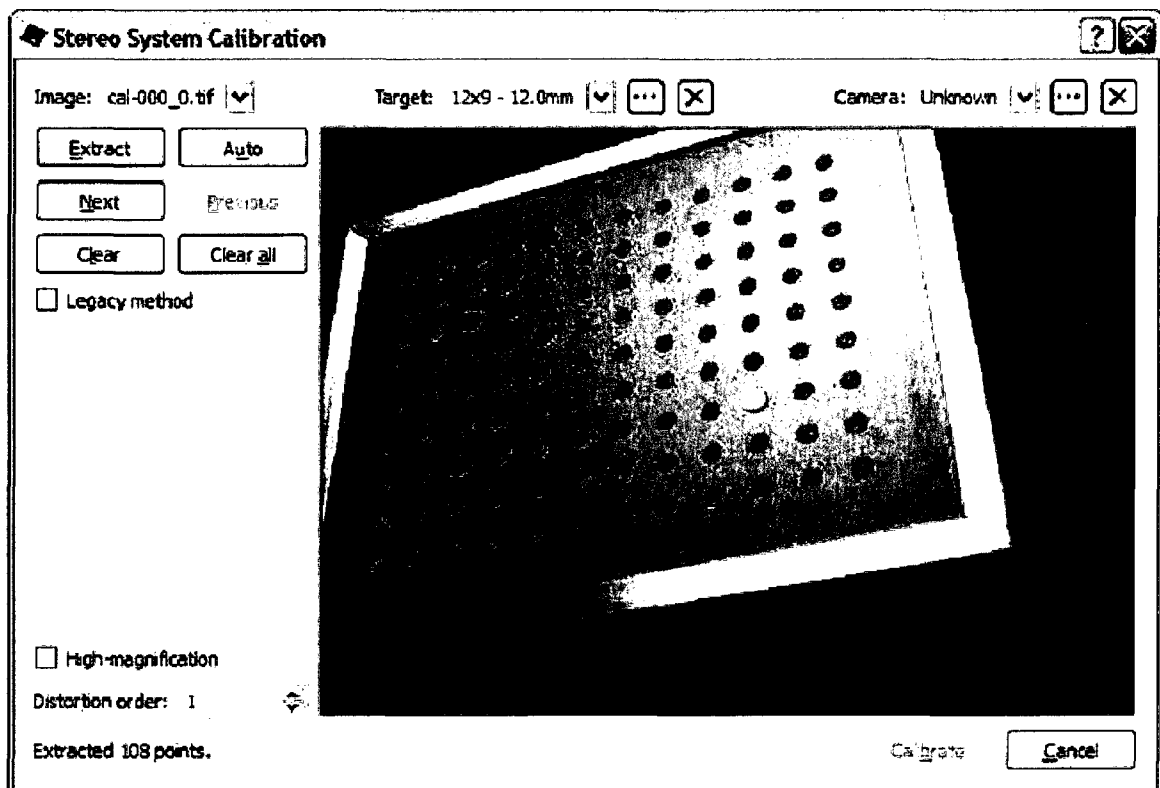


Figure 3-6: Vic-3D screenshot with calibration image (CSI, 2007)

The software calculates a series of camera parameters that identify the location, orientation and properties of each camera (see Figure 3-7 and Figure 3-8). The definition

of some of these properties is as follows, adapted from the Vic-3D Testing Guide (CSI, 2007):

- Center (x,y): the position on the sensor where the lens is centered. It should be roughly in the physical center of the sensor.
- Focal length (x,y): the focal length of the lens, in pixels. Multiplying this number by the known pixel size of the camera will give a number roughly equal to the specified focal length of the lens.
- Skew: indicates the out-of-square of the sensor grid.
- Kappa (1, 2, 3): the radial distortion coefficients of the lens.
- Orientation parameters (rotation and translation): the geometry, described as the relationship of camera 2 to camera 1.

<i>Parameter</i>	Camera 1	Camera 2
center (x)	715.7 ± 22.35	716.5 ± 19.08
center (y)	524.6 ± 16.73	533.7 ± 18.02
Focal length (x)	3544.8 ± 2.74	3555.8 ± 3.67
Focal length (y)	3544.8 ± 2.70	3555.7 ± 3.78
Skew	0.451 ± 6.10e-02	0.056 ± 5.98e-02
kappa 1	-0.195 ± 1.81e-05	-0.195 ± 1.86e-05

Figure 3-7: Vic-3D Calibration parameters

<i>Parameter</i>	Rotation [°]	Translation [mm]
X axis	0.06434 ± 3.2e-05	181.3 ± 0.0084
Y axis	-23.18 ± 3.9e-05	0.5277 ± 0.003
Z axis	0.1833 ± 4.6e-06	42.27 ± 0.094

Figure 3-8: More Vic-3D Calibration parameters

When processing test images of a speckle pattern, Vic-3D tracks each of the pixels in each image by analyzing pixel intensity, using the first image as a reference, and plotting how far and in which direction each pixel has moved through the course of the test. The dependence on pixel intensity for analysis makes it essential to have a high-contrast target for accurate pixel recognition. A good speckle pattern will allow Vic-3D to not only measure displacements, but also the strains in the material. Notice in the speckle pattern shown in Figure 3-9 that there is very little lost data because the pattern is well distributed.

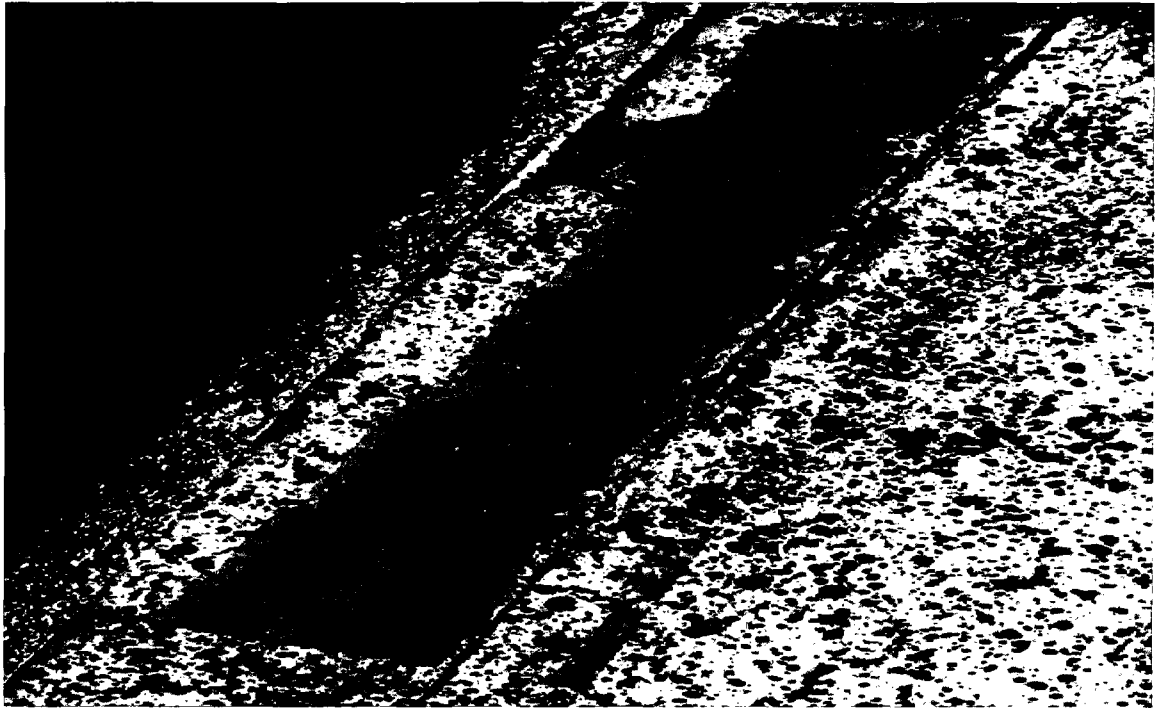


Figure 3-9: Processed test image in Vic-3D

A common concern in DIC analysis is the orientation of the three axes within the images. By default, the x-axis is “left-right”, the y-axis is “up-down”, and the z-axis is out-of-plane (in-out) relative to the camera setup. If the desired measurement direction is not along one of these three axes, the camera axes can be manipulated in Vic-3D to account for the difference. If measurements out-of-plane of the target surface are desired, a feature called “Auto plane-fit” in Vic-3D will automatically detect the plane of the target surface and orient the z-axis perpendicular to that plane (see Figure 3-10).

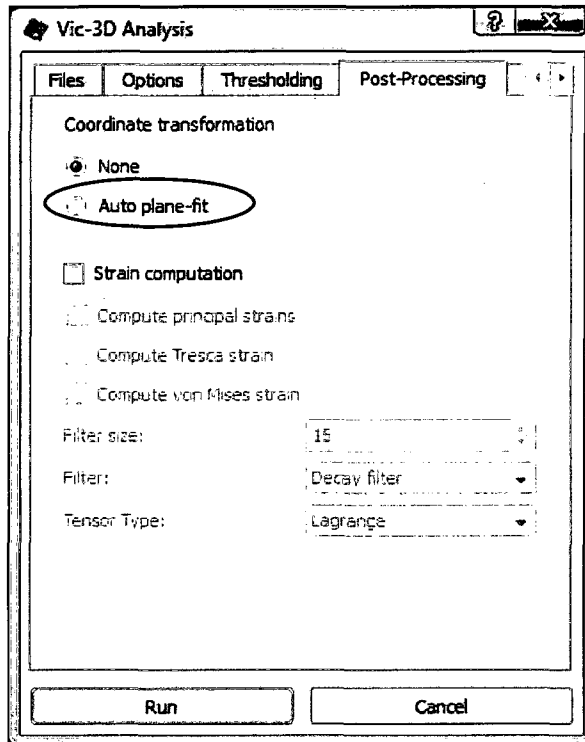


Figure 3-10: Auto plane-fit feature in Vic-3D (CSI, 2007)

Vic-3D is capable of calculating displacements, velocities, strains, rotations, and curvature directly. Figure 3-11 shows an example of the software computing strain. These powerful capabilities make Vic-3D a very useful tool in bridge testing with DIC.

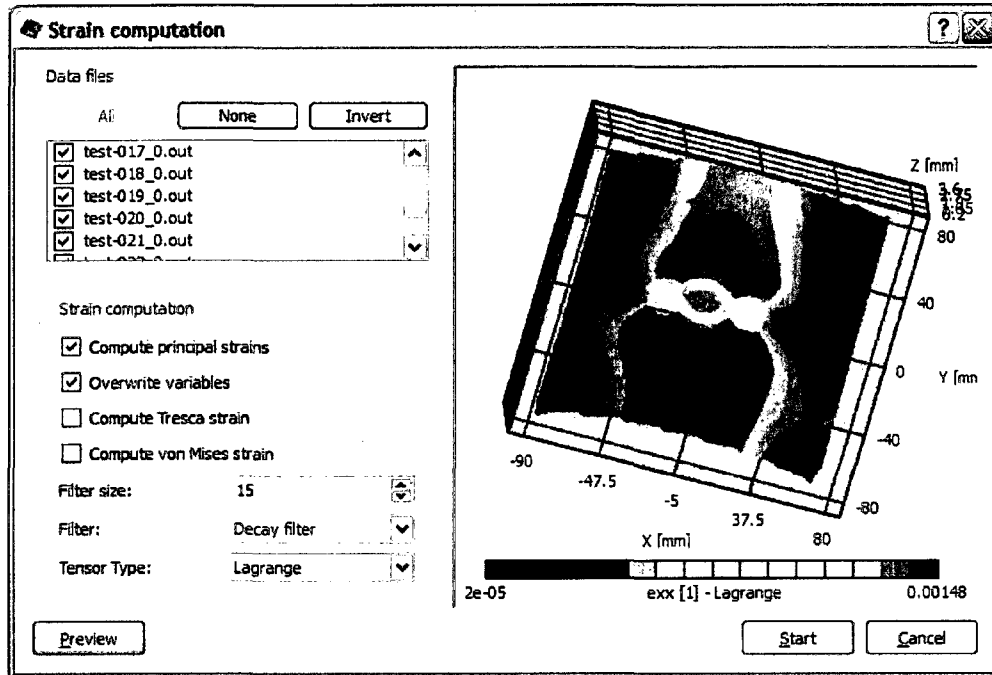


Figure 3-11: Vic-3D screenshot of strain computation

3.2 - Challenges

Several factors create challenges for anyone conducting a digital image correlation test. These challenges specific to the research include environmental conditions, geography of the bridge site, and camera limitations. Each of these can adversely impact the collected response for DIC.

3.2.1 - Environmental Conditions

Up until now, DIC has been almost exclusively used in a controlled laboratory setting. In order to use it for bridge monitoring it must be deployed at the bridge site. The unpredictable environmental conditions during a load test create several potential

hindrances during testing, most relating to weather such as temperature, sun exposure, precipitation, and wind.

Temperature. Temperature gradients will cause changes in the length of the tripod legs, shifting the focus of the cameras and causing an apparent movement of the target object. In fact, the greatest challenge to DIC in general is maintaining the position of the cameras. Since the entire process of DIC revolves around the motion of the target object across the frame, if the cameras move at all, erroneous results will be obtained, and may or may not be obvious. Therefore for greatest accuracy it is essential that the temperature of the tripod be fairly consistent throughout the course of the test.

Sunlight. In addition to interfering with the aperture settings in the camera lenses, sunlight plays a major role in temperature variation. For example, consider if the sun were shining on only one leg of the camera tripod. That one leg would expand to an extent greater than the other two legs, causing the two cameras to rotate relative to one another, in turn causing an apparent rotation or torsion of the target object. If the sun shines on the entire tripod, distortion can still occur due to non-uniform warming of the tripod legs.

Another problem that can arise is glare across the lenses if the cameras are facing toward the sun. Lastly, heat from the sun can create heat shimmer between the cameras and target object as bubbles of warmer air rise from the ground surface and distort light waves (Gamache & Santini-Bell, 2009). Therefore greatest accuracy can be achieved by doing outdoor tests on cloudy days or in shaded areas and using artificial

lighting to provide sufficient illumination of the target. If the DIC system must be set up in direct sunlight, it is recommended that a canopy be provided to shield the equipment.

Precipitation. Generally speaking, DIC systems need to be kept dry. Water will not only infiltrate and damage electronic components of the DIC setup, but also even a few tiny raindrops on the lens surface will seriously interfere with the images, creating apparent distortion or worse yet lost data in each image. However, any precipitation will typically preclude DIC field use.

Wind. Though it does not seem like a significant factor, in actuality wind can cause significant problems with a DIC setup. Heavy cameras are typically set up on a relatively lightweight tripod, leaving the configuration top-heavy and susceptible to tip-over in gusty winds. The test engineer has to be careful even in very light winds; if the tripod is subjected to a steady wind throughout the course of several hours, that lateral force will be transferred to one or two of the tripod legs, tending to push them farther into the ground, and altering the camera orientation.

3.2.2 - Geographic Limitations

The geography of the test site will play a large role in where and how the DIC system will be set up, and can even make the difference between a successful test and a complete failure. Often bridge sites are over water, making access to set up the DIC equipment difficult. Embankments can be steep or loose, posing a hazard for equipment tipping.

Site Conditions. The most obvious limitation in using DIC for bridge analysis is the fact that all bridges are far above the surrounding terrain, and are very often underlain by a body of water. Setting up a DIC system close enough to the bridge to gather data can be a tremendous challenge in these conditions. If it is impossible to set up near the middle of the structure, one possibility is to place the cameras next to the end of the span, and put the target perpendicular to the span using clamps or an adhesive.

Soil Conditions. Soil conditions play a large role in DIC accuracy, mainly because of the small area of the tripod legs that transfer the weight of the cameras to the ground below. If the soil is soft or clayey, the tripod will slowly settle during a test, giving erroneous results. If the ground is very hard, particularly if it is rock, the tripod will be very susceptible to “kicking out” or the legs shifting. If the soil is soft, it is critical to press each of the tripod legs firmly into the soil to prevent long-term settlement; if possible, provide a platform for even load distribution on the soil. If on rock, try to place the legs in a hole or against an obstruction on the rock surface so each leg is well-anchored.

Traffic Vibrations. DIC bridge testing will always be conducted near a roadway. Traffic, especially heavy trucks, can create vibrations that travel through the ground surface and initiate vibration in the camera tripod. Trains traveling near the setup pose an even greater risk for significant vibration (Gamache & Santini-Bell, 2009). If excessive vibrations are expected, rubber shock-absorbing pads should be placed under the tripod feet to absorb the impact.

3.2.3 - Speckle Pattern Development and Application

Speckle patterns are one of the key components of DIC testing that can make a test either a success or failure. The post-processing software requires contrast in the test images; this contrast facilitates easier tracking of pixel movement. Some general guidelines to follow when creating a speckle pattern for a specimen are reviewed below.

General Features. As specified in the Vic-3D Testing Guide published by CSI, speckle patterns should be non-repetitive, isotropic, and high-contrast. If the pattern is repetitive or non-isotropic, the post-processing software may confuse the pixels from one image to the next, producing a faulty deformation. If the pattern is not high-contrast (blacks and whites), the edges of the speckles will fade into the background, creating a gray area that the software does not recognize; this will most likely introduce a significant error. Figure 3-12 shows examples of good speckle patterns. The dots are evenly and randomly distributed, and are not all the same size.

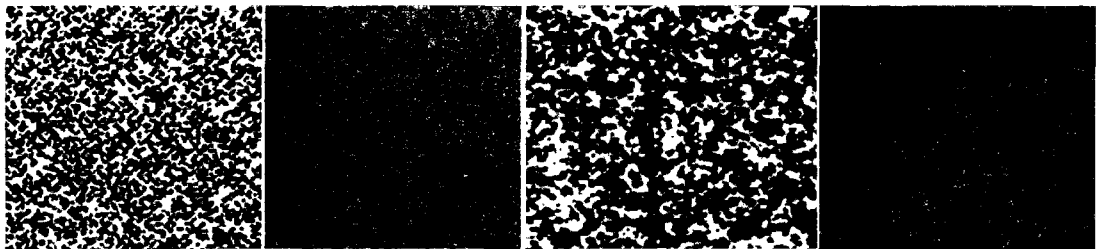


Figure 3-12: Examples of acceptable speckle patterns (CSI, 2007)

Development. The pattern is most commonly applied to the test surface using several thin coats of bright white non-reflective spray paint. Once these layers of paint

dry, a mist of black spray paint is applied; this creates a very-high contrast speckle pattern with consistently-sized dots and a random pattern.

Speckle patterns can be created in many different ways and with many varying materials. When dealing with a steel structure, an array of small magnets can be applied to the surface to create the pattern. If it is weathering steel, white chalk can be rubbed over the material surface to create very fine speckles if the DIC system is set up at close range. In Chapter 5, Figure 5-11 shows an example of white chalk rubbed onto a weathering-steel girder. It is sometimes possible to retrieve data from a plain concrete surface using only the natural variation in the material. However, if permissible, rubbing black chalk over the concrete will enhance the pattern.

Placement. Speckle patterns can either be applied directly to the testing surface, or placed on another disposable object that can be strongly adhered or clamped to the surface. If strain data is desired, it is very important that the speckle pattern be either applied directly to the surface or be adhered completely and of material that will deform exactly like the test surface. Note that a target that is only clamped or loosely adhered to the surface will not move with the surface itself. For example, if a pattern is applied to a piece of paper, which is then taped to the testing surface, any strain data collected will be the strain of the paper itself, not the testing surface.

Figure 3-13 shows the speckle pattern that was used on a bridge load test in Tiverton, Rhode Island. Several pieces of paper with a digitally created speckle pattern were taped onto the bridge girder. No strain data could be collected because the paper

did not flex proportionally with the girder. This target was also not ideal because the paper was loose enough to be affected by wind currents.

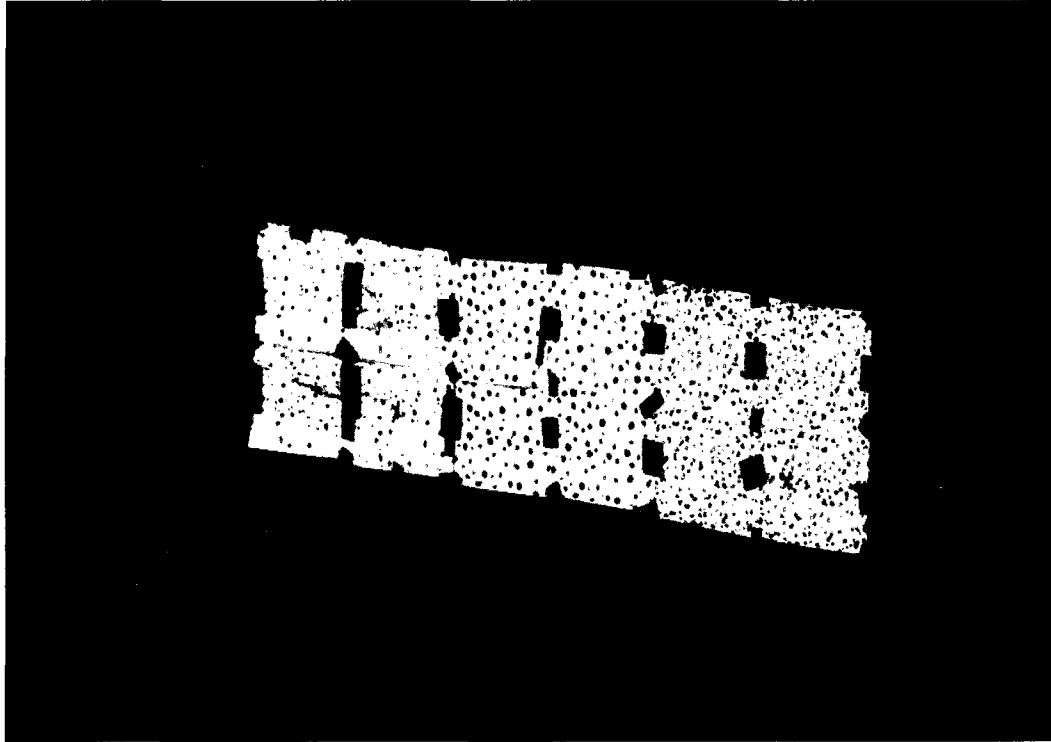


Figure 3-13: Paper speckle pattern on bridge girder in Tiverton, Rhode Island

3.2.4 - Camera Limitations

Data collection with a DIC system is greatly influenced by the quality and resolution of the cameras used. Appropriate focal length lenses need to be selected to place the target in the field of view. However, using telephoto lenses will increase apparent vibrations in the setup, especially when dealing with very small target displacements.

Resolution. One of the greatest limitations in determining how far the cameras can be set up from the target surface is the resolution of the cameras. As the cameras

get farther away, the dots in the pattern get smaller from the point of view of the cameras. When the dots get too small, they are no longer well-defined as distinct pixels, and the post-processing algorithm can no longer produce usable results. The problem of low-resolution can largely be resolved by using lenses with a longer focal length. However, this leads to another issue referred to as camera shake, which can severely impair the quality of measurements.

If tests are being conducted at long distances, camera shake becomes a serious issue. Any movement of the cameras in such instances will be tremendously amplified, especially if lenses with greater than 50mm focal length are used. Camera shake may be caused by people walking near the cameras, heavy equipment or vehicles adjacent to the setup, or wind (Gamache & Santini-Bell, 2009).

The impact of resolution and camera shake depends on the level of deformation that is being measured. If the deflections are very small, any amount of shake will produce a large error, and may be confused with the actual deformation being measured, rendering the results meaningless. If the displacements are large, then significantly more camera movement can be permitted but will still impact the quality of the collected data.

3.2.5 - General Guidelines.

In conclusion, it is clearly ideal to place the cameras in close proximity to the test subject. Place the cameras in a position that will introduce the least amount of interference. There are many variables in play with each set of cameras and each

individual test that can affect the accuracy of the test data and the error introduced. Many of these guidelines are easily adhered to in the laboratory, but field applications are highly variable and site dependent.

3.2.6 - Testing Protocol for using DIC to Capture the Behavior of Civil Structures

The goal of this research is to prove the effectiveness of Digital Image Correlation in Structural Health Monitoring. Several experiments were conducted both in the laboratory and in the field with this purpose in mind. The lessons learned from each test are applied to the next. As discussed in the previous section, there are several challenges associated with deploying DIC at a bridge site. Each test was designed to address a challenge and provide guidance for field application.

Board Test. As in any project, it is critical that the researcher be confident that the instruments in use are functioning properly. If the instruments are cutting-edge technologies, it is very important to vet them against more respected measurement methods. In the case of the DIC system, it was decided that the best way to prove its accuracy would be to compare it with dial gauge readings. A simple test was constructed using a piece of wood and a small weight that would verify correct application of the DIC system (see Section 4.1.1).

Slab Tests. The first civil engineering application of the DIC system was an ongoing research project at UNH in the development of a rapid bridge deck replacement system using precast concrete panels. The project testing included the development of several different panel-to-panel connections in the UNH laboratory. Working with

graduate student Christopher Robert and Prof. Charles Goodspeed, three different connection configurations were destructively tested. Displacement measurements needed to be collected to compare the three different designs. Given that each slab would be tested to failure, there was great concern that the instruments would be destroyed. This was an ideal application for DIC, since it is a no-contact technology. This experiment provided a proof of concept for low-speed DIC (Section 4.1.2).

Shake Table Tests. The next test challenged the capabilities of the high-speed DIC system (Section 4.1.3). Testing was conducted using structural models on the UNH Shake Table in collaboration with fellow graduate student researcher Heather Newton and Prof. Ricardo Medina. Accelerations were gathered using accelerometers and a data acquisition system. However, there was no practical means to measure deflection of the model during the tests because of the rapid movements involved. The high-speed DIC setup was employed to gather the displacement data. The high image rate (between 125 and 1,000 frames per second) allowed the displacements to be converted to accelerations. The acceleration values from the DIC system match very closely with those from the accelerometers.

Pond Bridge Road Bridge Tests. Visual inspections of the bridge across Nonquit Pond on Pond Bridge Road in Tiverton, Rhode Island revealed significant deterioration of the structure. The bridge was not designed for heavy truck loads; however, a nearby potato farm transported heavy loads of potatoes across the structure daily. Bridge Diagnostics Inc. (BDI) of Boulder, Colorado was asked to provide a load rating for the

bridge. BDI instrumented the bridge with multiple strain gauges and drove a loaded dump truck over the structure several times. Instead of using scaffolding and LVDTs under the bridge, the DIC setup was used to acquire deflection data. These deflections compared well with those produced by a structural computer model of the bridge developed by BDI using in-house software (Section 4.2.1).

Vernon Avenue Tests. The final test of the DIC system was in September of 2009 at the Vernon Avenue Bridge in Barre, Massachusetts (Chapter 5). A collaborative research team from UNH and Tufts University had fully instrumented the newly constructed bridge with strain gauges, accelerometers, and tilt sensors. A load test included a preloaded truck making twenty seven passes across the bridge at various stop locations and speeds. Two separate DIC setups recorded deflections at two locations on the bridge. This test stretched the limits of the DIC system in outdoor conditions and at various angles. DIC, SHM, and ITS all converged during this test and the subsequent post-processing.

This series of tests create a comprehensive picture of the capabilities of the DIC system in civil engineering applications. Many lessons were learned while conducting these tests, and can be applied to future applications of DIC in Structural Health Monitoring.

CHAPTER 4

DIC EXPERIMENTS AND RESULTS

A progression of tests was conducted, beginning in the climate-controlled laboratory and eventually out in the field. Initial testing was a simple verification of the accuracy of the DIC system compared to more traditional measurement types. With each successive test, lessons were learned and applied to the following tests. All of these tests were preparation for a load test on a bridge structure, which will be discussed as a case study in Chapter 5.

4.1 - Controlled (Laboratory) Experiments

4.1.1 - Board Test

One of the first tests conducted at the University of New Hampshire using the DIC system was a simple verification of the accuracy of the cameras and the functionality of the post-processing software. A piece of plywood was placed across two blocks, and three dial gauges were mounted such that they would measure vertical deflection across the span. A speckle pattern was applied to the board surface underneath the dial gauges (see Figure 4-1). With help from graduate students David Salzer and Patrick Santoso, a constant load was applied cyclically to the board at a specified location; readings were taken from each gauge, and an image taken with the

DIC for every zero point and every loaded point, for a total of ten load cycles. The process was repeated a second time with the same load placement, and results from the DIC and one of the dial gauges were then plotted in Figure 4-2 and Figure 4-3.

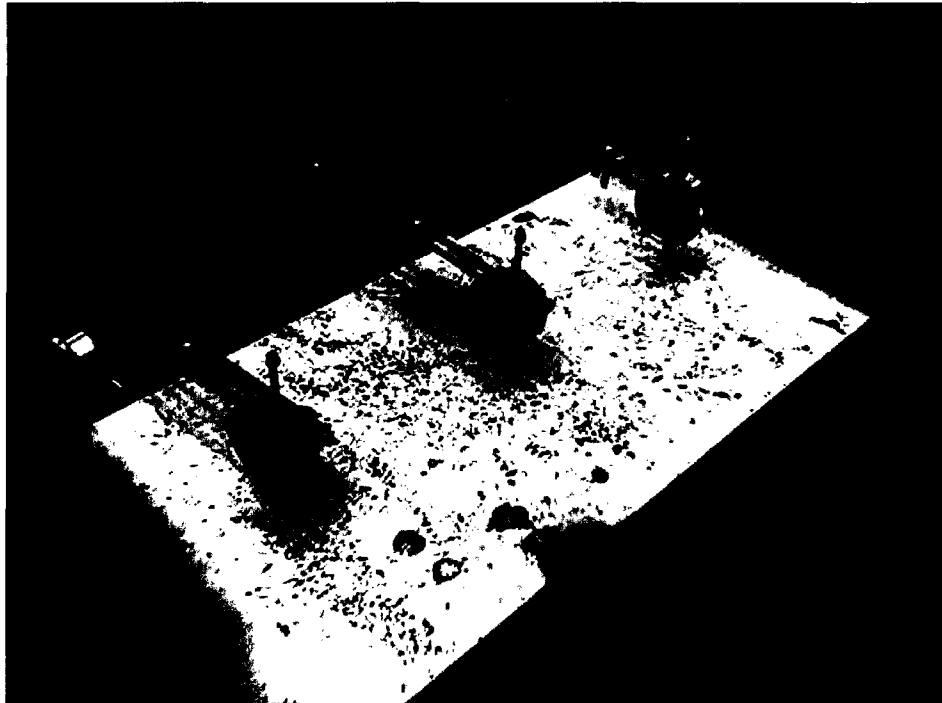


Figure 4-1: Board test setup

Error was calculated by taking the difference between the dial gauge reading and the DIC measurement at each loaded point and dividing this value by the dial gauge reading. The first test contained an average error of 4.20% between the dial gauge readings and the DIC data. The second test improved slightly to 3.11% error. Given that dial gauges depend on visual inspection to collect readings, it is likely that the discrepancy was introduced through human error. For example, notice in Figure 4-2 that the data from the DIC is very constant but the dial gauge readings start to drift upward toward the end.

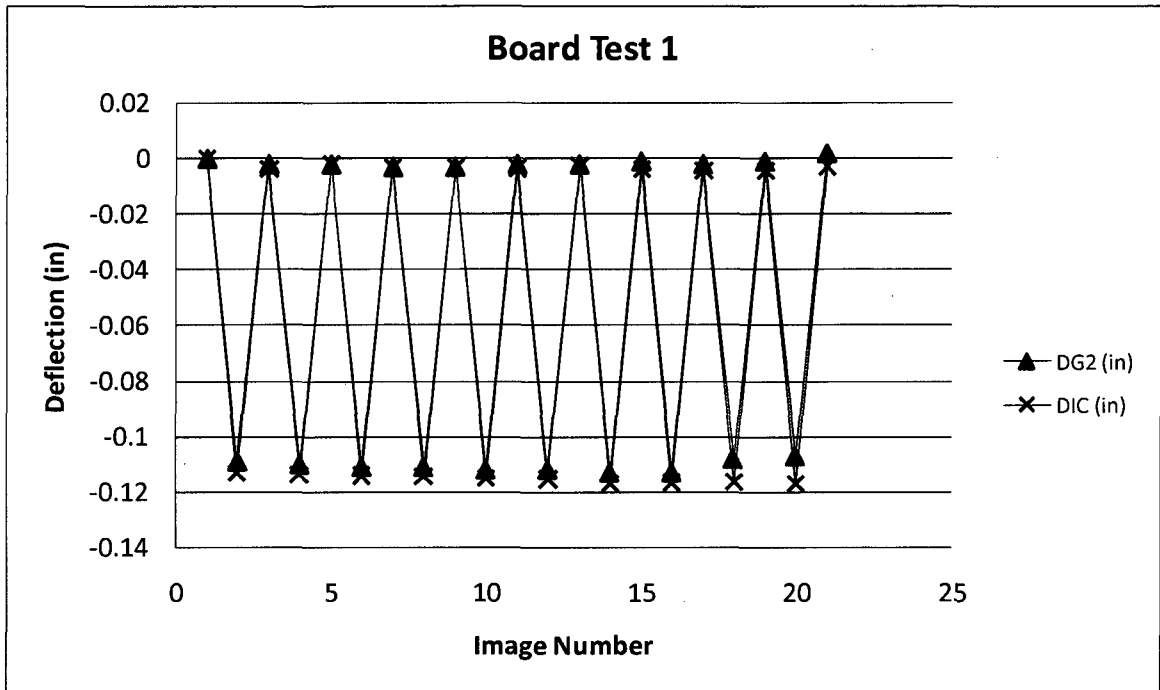


Figure 4-2: Deflection of board in Board Test 1

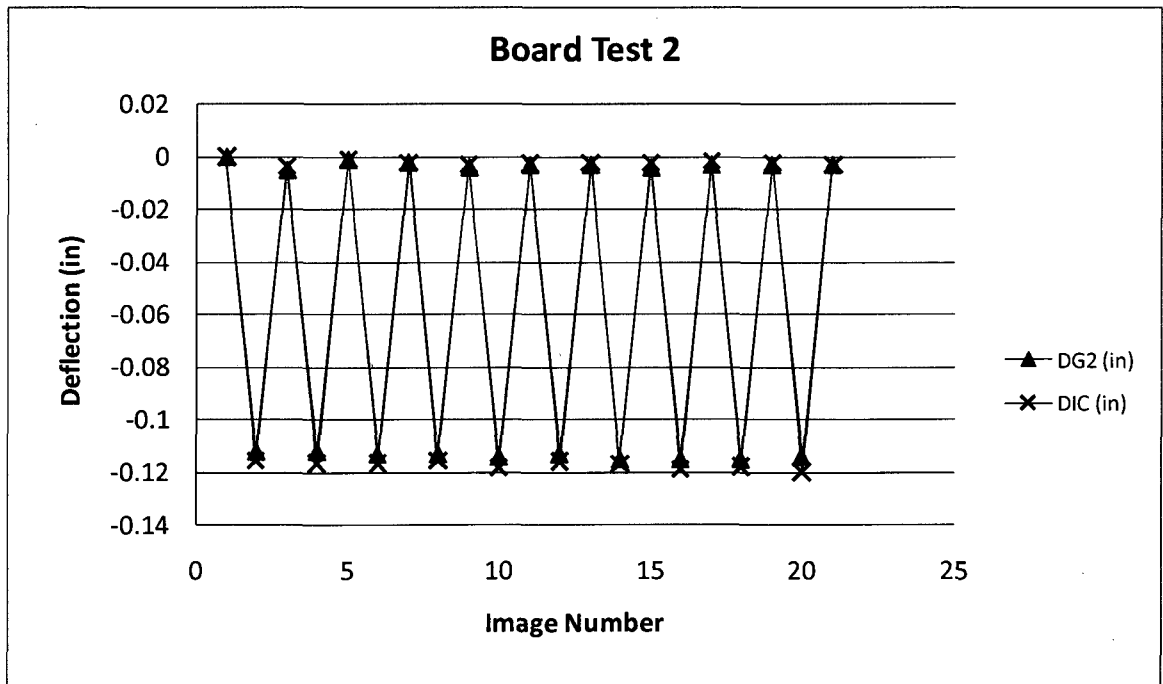


Figure 4-3: Deflection of board in Board Test 2

Remarks. The board test verified that the software provided by Correlated Solutions is fully functional and accurate results are easy to obtain. The test also showed that data measured using the DIC system is comparable to that measured with traditional displacement measuring techniques. Lastly, this test demonstrated that the low-speed camera setup can be successfully used for laboratory testing, and that the DIC tests are repeatable.

4.1.2 - Slab Tests

Background. Bridge deck replacement is typically a lengthy process involving formwork construction, rebar placement, concrete placement, curing, and formwork removal. Under the oversight of the New Hampshire Department of Transportation (NHDOT) and Dr. Charles Goodspeed of the University of New Hampshire, three graduate students have been developing a rapid bridge-deck replacement method. Christopher Robert, David Salzer, and Patrick Santoso have spent several years creating a workable system of precast concrete panels that can be installed in minimal time.

The key area of this research involves finding the best configuration of connecting the panel interface. The panels have a four-foot width and span from girder to girder. The connections in question are those that lie perpendicular to the direction of travel. If these fail, cracks will develop in the road surface and worsen quickly. Three different interlocking patterns were developed and tested for this joint on this specific test day. Some were rounded, others were angular, and still others were simply butt

joints (see Figure 4-4). In addition to this, some of the panels used post-tensioning steel rods, while others were simply grouted or epoxied together (Robert, 2009).

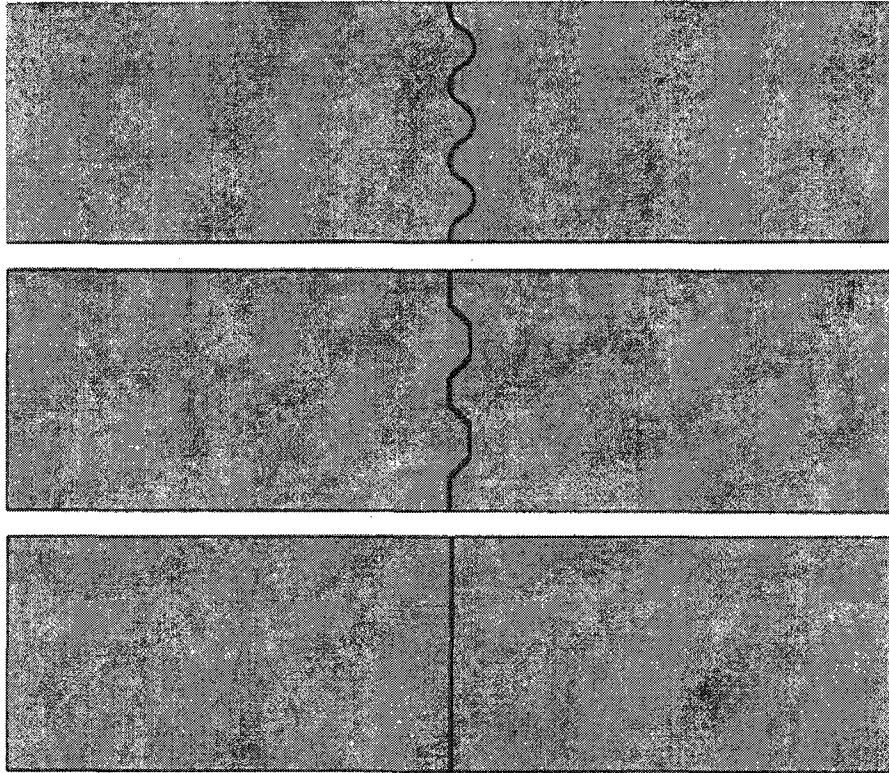


Figure 4-4: Examples of precast bridge deck panel connections (Robert, 2009)

Setup. Tests were conducted using the civil engineering department's steel loading frame, which has a maximum capacity of 300 kips (Figure 4-5). Two 4'-0" x 1'-4" x 8-1/2" thick panels were fastened together by one of the above methods and set flat on two steel roller-type supports.

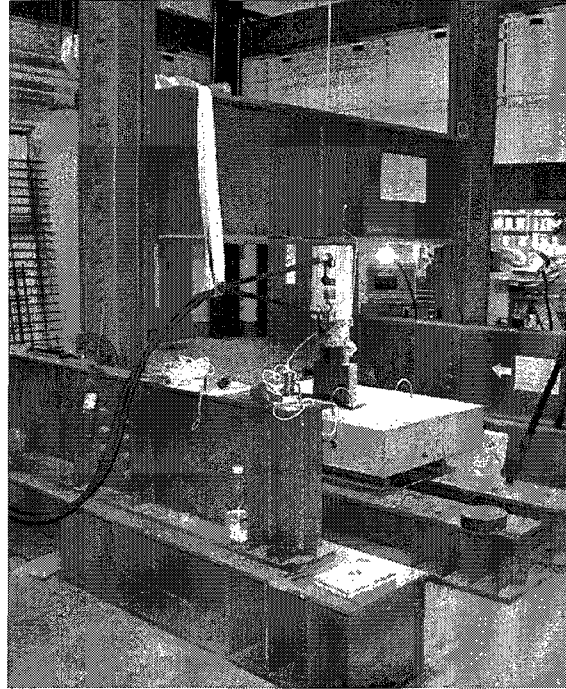


Figure 4-5: UNH loading frame

The load was applied using a hydraulic loading piston and steel plates at two inches to the side of the joint (see Figure 4-6). The tests forced the slab section to break at or near the connection. Ideally, the concrete would fail near the joint but the connection itself would remain intact, indicating that the joint was stronger than the concrete itself.

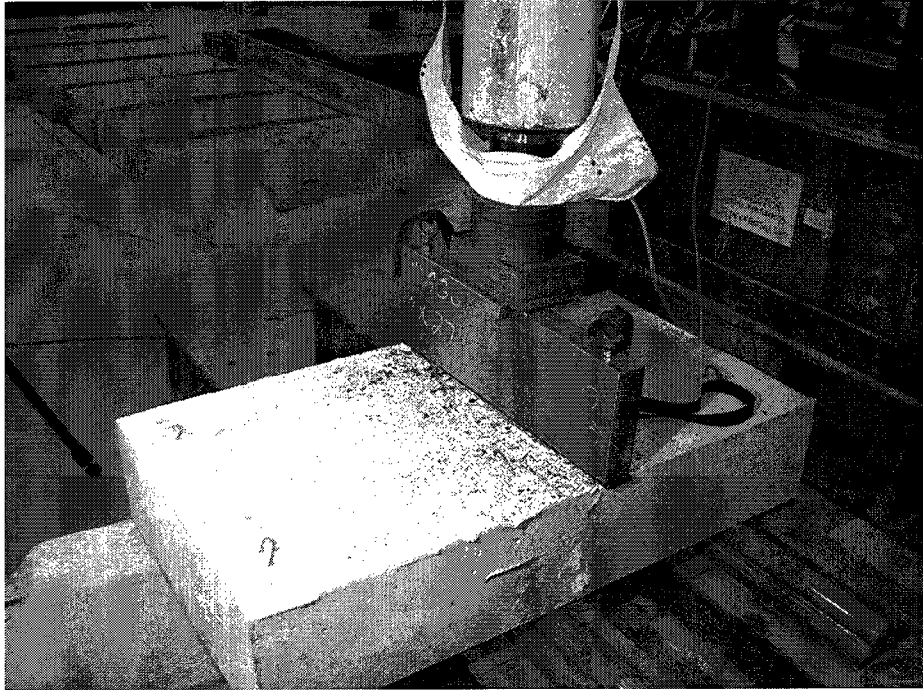


Figure 4-6: Slab test loading setup

The foremost purpose of the tests was to determine the maximum load the joint could take before failing. The load cell was connected to a DAQ NI1200 SCX to acquire loading data. However, the deflection of the panels was also of interest, since excessive deflection would hinder the serviceability of the installed panels. Several methods of deflection measurement were considered, but ultimately the DIC system was selected because it was the only non-contacting measurement type available. Given the destructive nature of the tests, other instrumentation could have been damaged.

The area of the slab next to the load point was painted white, and then speckled with black spray paint to produce a high-contrast speckle pattern. The cameras were set up adjacent to the slab and both mounted on the same tripod. Lights were clamped to the steel load frame to provide sufficient lighting (see Figure 4-7). The “Auto Plane Fit”

feature in Vic 3D was used to collect data out of plane of the slab surface. In other words, Vic 3D automatically located the vertical deflection no matter the orientation or location of the camera setup, provided the cameras were appropriately calibrated.

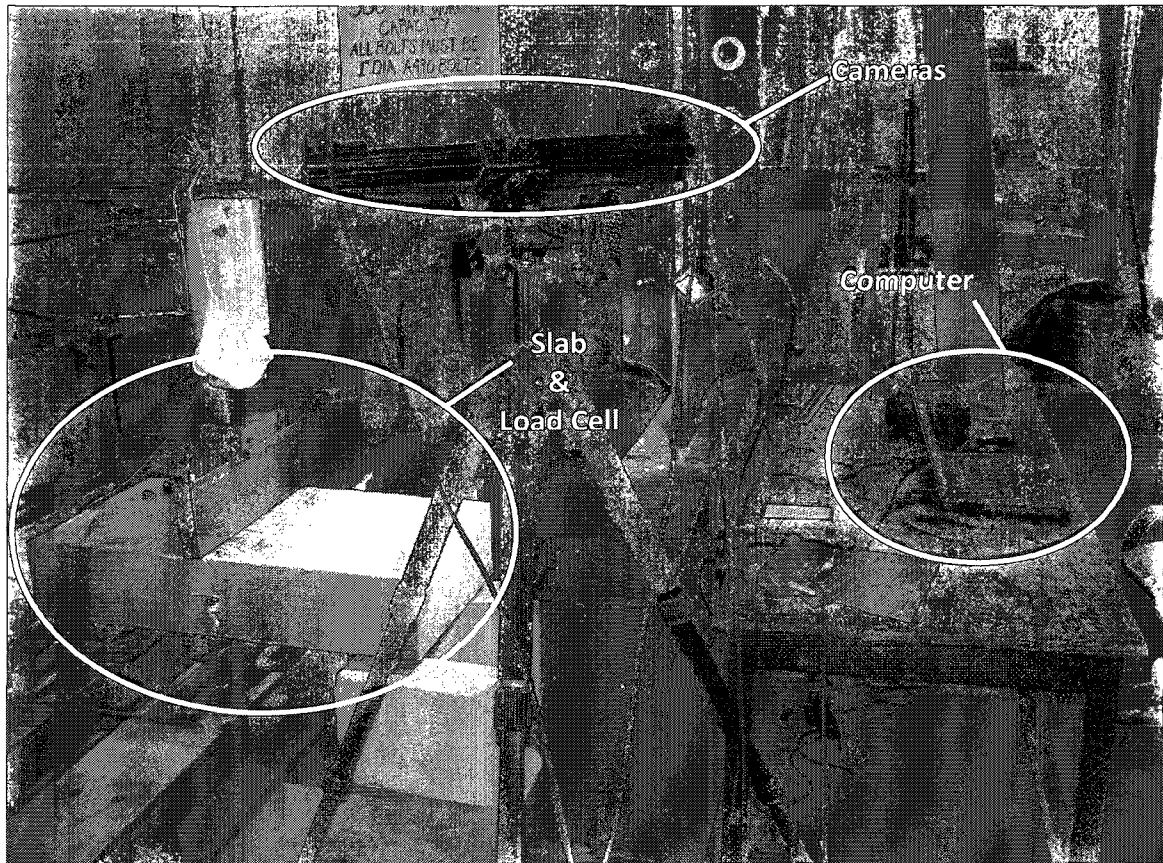


Figure 4-7: Slab test DIC setup with cameras, loaded slab, and computer

The load was applied cyclically to the panel. The service load of the slab was 16 kips (71.2 kN) per NHDOT specification. Therefore, a load of 16 kips was applied, then the load was removed. This was done three times; then, a load of 32 kips (two times the service load) was applied, and then removed, three times in succession. This process was repeated with successively higher loads until the slab failed (see Figure 4-8).



Figure 4-8: Slab after failure

Results. A series of photos were taken before any loading took place to compose a graph of the “Ambient” condition. Notice in Figure 4-9 that it appears the slab is moving dramatically; however, upon further inspection, it is realized the deflection is only on the order of plus or minus one ten-thousandth of an inch, or the thickness of a piece of paper. This amount of displacement cannot even be recorded by most dial gauges; therefore it was concluded that the cameras were behaving accurately, and further testing could proceed.

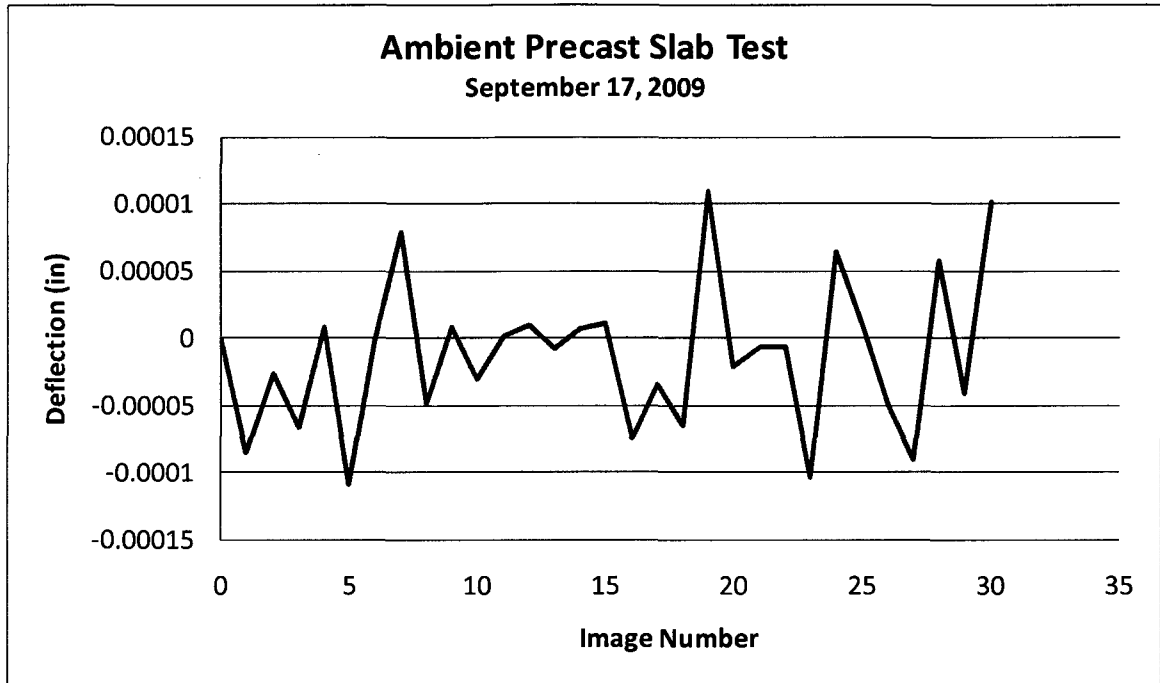


Figure 4-9: Precast Slab test ambient data

Figure 4-10 shows the graph for the first slab test. As mentioned previously, the first three load points are receiving 16 kips of pressure and the next three are 32 kips. The graph ends at the zero point because the slab failed before reaching the 48 kip load, and no data was acquired. The slope of the line drawn across the top and bottom points of the graph is included in the figure. The slope is consistently a negative number on the order of 10^{-4} . This gradual vertical deflection of the slab over time may be due to either creep or plastic deformation of the material. In addition, the load path changed from load to load as the steel blocks that transferred the load shifted with each cycle. This effect will hereafter be referred to as “plastic deformation” for simplicity.

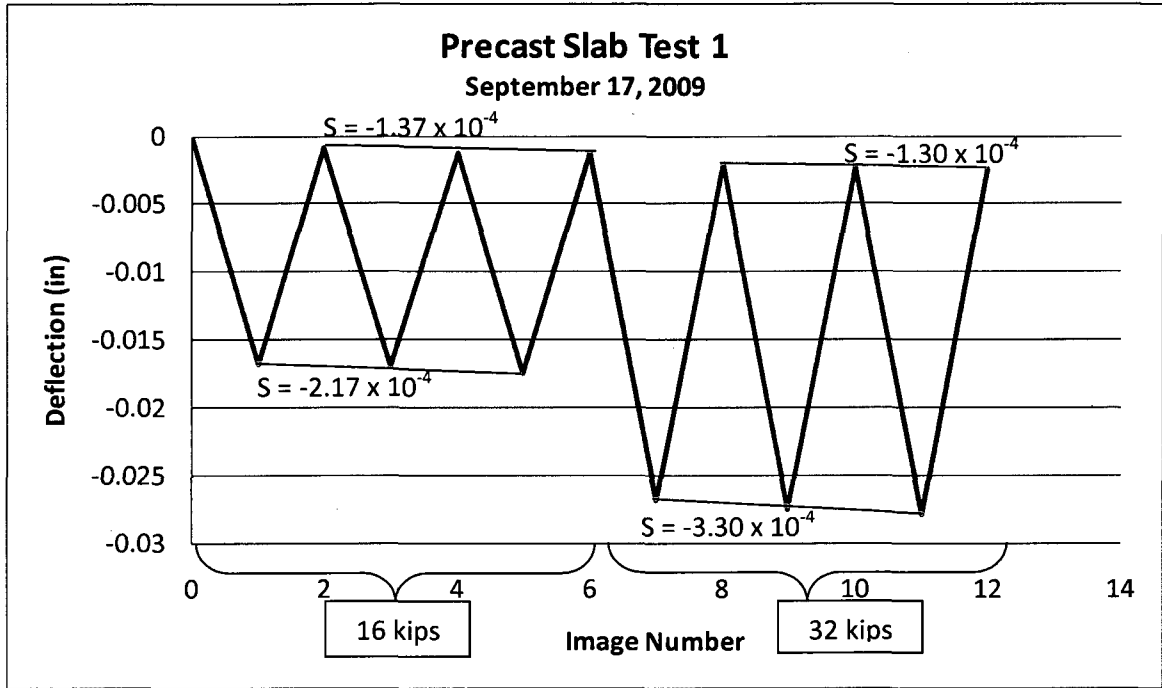


Figure 4-10: Precast slab Test 1

Test 2 (Figure 4-11) shows very similar data to that of Test 1. However, in this case, the slab reached a load of 48 kips three times before failing. When the load was first increased from 32 kips to 48 kips, an image was taken approximately every three kips in case the slab failed before reaching 48 kips, as it had the previous time. This is indicated by the nearly straight line between images thirteen and eighteen. Note once again that the rate of plastic deformation between load cycles is on the order of 10^{-4} . However, when the load reaches the 48-kip range, the rate of plastic deformation decreases. The data from Test 2 implies that the rate of plastic deformation decreases as the slab nears its ultimate capacity.

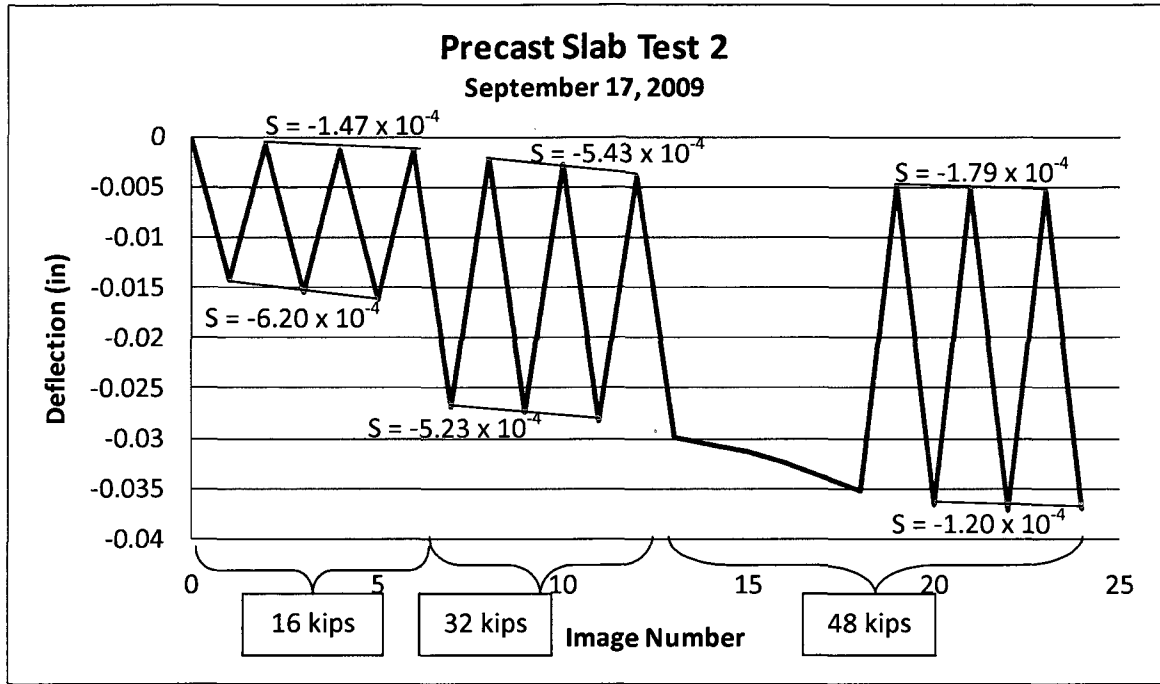


Figure 4-11: Precast slab Test 2

In Test 3, the slab makes it through both the 16 kip and the 32 kip load cycles, but fails just before reaching the 48-kip load. Again, after the third 32-kip load cycle, images were taken about every three kips until the slab failed. There is a noticeable difference in the plastic deformation in this case. The slope of the plastic deformation is lower here than in the two previous tests, and at one point is actually positive. The reason for the smaller slope values could be a factor of the joint type, different material properties, or a more consistent load path.

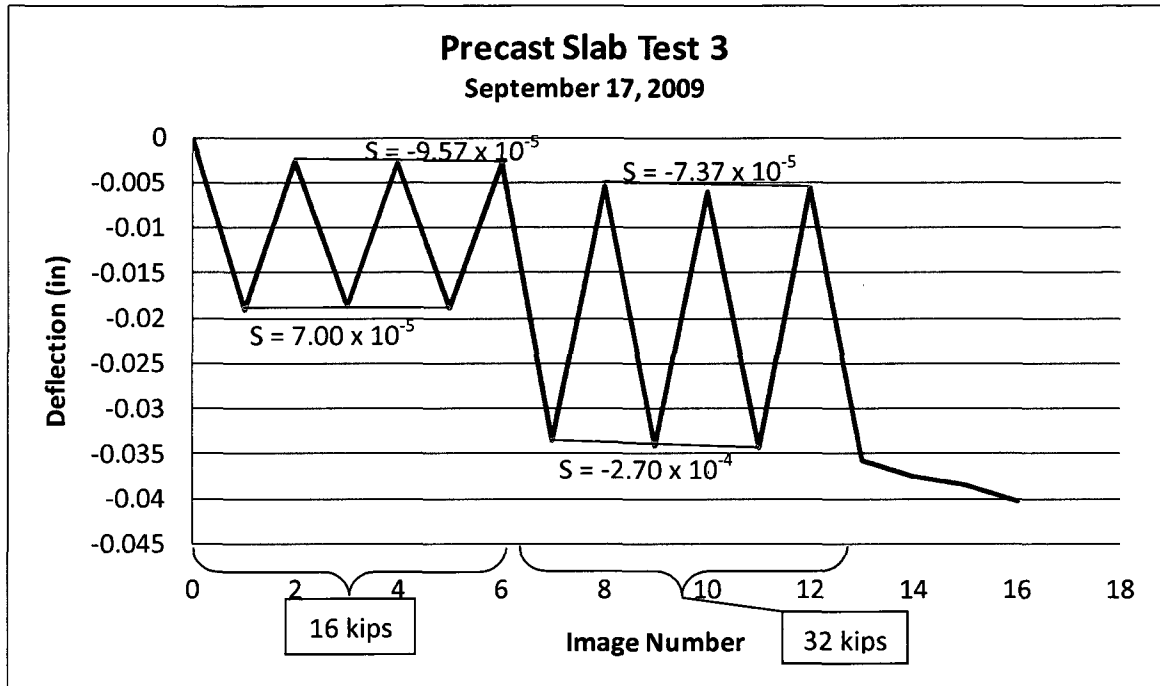


Figure 4-12: Precast slab Test 3

Remarks. The slab testing is another successful demonstration of the low-speed DIC system in the laboratory. The test also proved that the axes can be successfully manipulated in Vic-3D to collect data along the desired axes. In this case, the auto plane-fit feature allowed for out-of-plane measurements regardless of the camera location.

4.1.3 - Shake Table Tests

The Civil Engineering department at the University of New Hampshire designed and constructed a medium-sized shake table to conduct seismological tests of steel frames and other structures. Typically, accelerometers are used with a DAQ system to gather acceleration data during such a test. It had already been proven that the DIC system could provide accurate displacement information during a low-speed test.

However, the system was untested at high-speed. It was decided that it would be expedient to use the DIC setup during a shake-table test to gather high-speed deflections. See Figure 4-13 for the test setup.

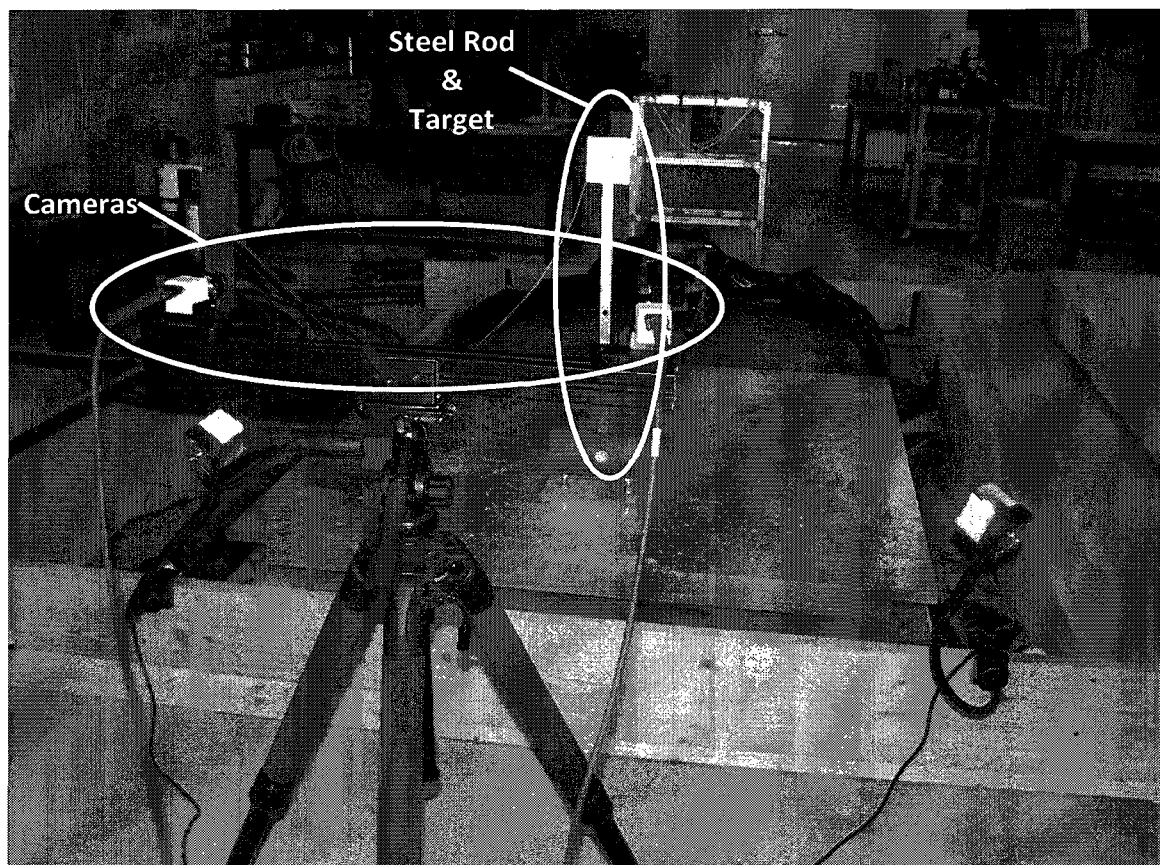


Figure 4-13: Shake table DIC setup

Images were collected at 1,000 frames per second, while an accelerometer recorded the accelerations at the top of a steel rod mounted to the shake table. The rod was A36 steel, 31.25" long, 3/8" thick, and 1" wide. Vic-3D software was used to calculate displacement data from the images. After averaging the DIC data and filtering the accelerometer data, the accelerations obtained from both were nearly identical. Two tests will be examined in detail here. A third is included in Appendix A.

Test One. In the first test, images were captured at one thousand frames per second. The high-speed DIC system is able to store 4,090 images at a time, so this amounted to a test length of about 4.09 seconds. The shake table was excited with a tapered sine function, an amplitude of 1.5 inches, and a frequency of three Hertz. The accelerometer and DIC data acquisition systems, on separate computers, were initiated as close to the same time as possible to simplify post-processing (data would later be corrected to eliminate any time-correlation error). The accelerometer was placed on the mass, which was speckled for DIC data collection (see Figure 4-14).

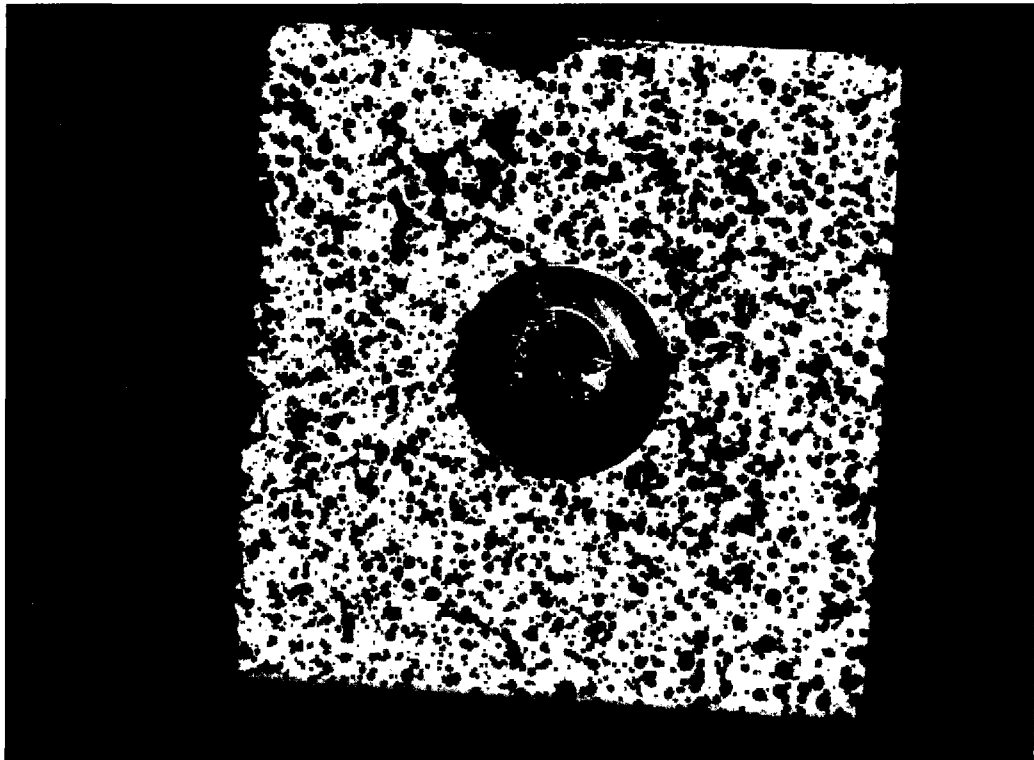


Figure 4-14: Shake table speckle target

The first graph below (Figure 4-15) is a display of velocity in feet per second and acceleration in terms of gravitational force (g) versus time in seconds as processed from

the DIC system. Of particular note is the fact that when the velocity reaches a maximum or minimum, the acceleration is zero. This confirms a well-known scientific principle.

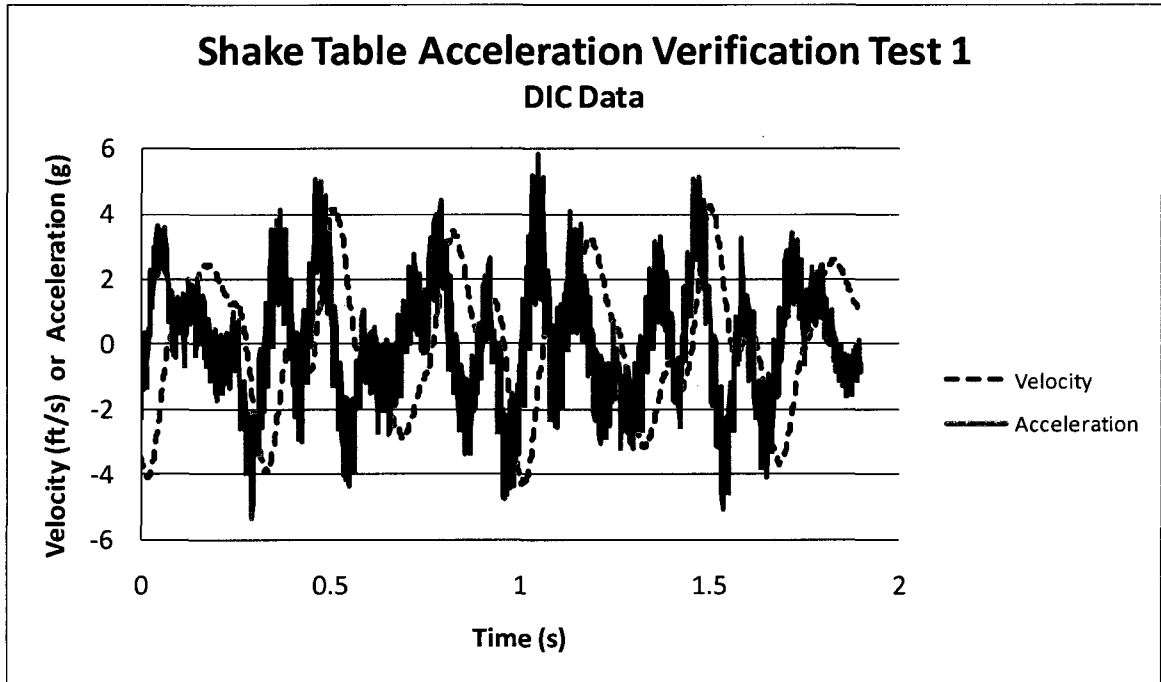


Figure 4-15: Shake table Test 1, DIC velocity and acceleration versus time

Figure 4-16 is a graph of displacement in inches and velocity in feet per second versus time in seconds from the DIC data. Note here that as the displacement reaches a maximum or minimum, the velocity is zero. This also is a commonly known fact in physics and is understandable since at maximum or minimum displacement, the target reverses direction.

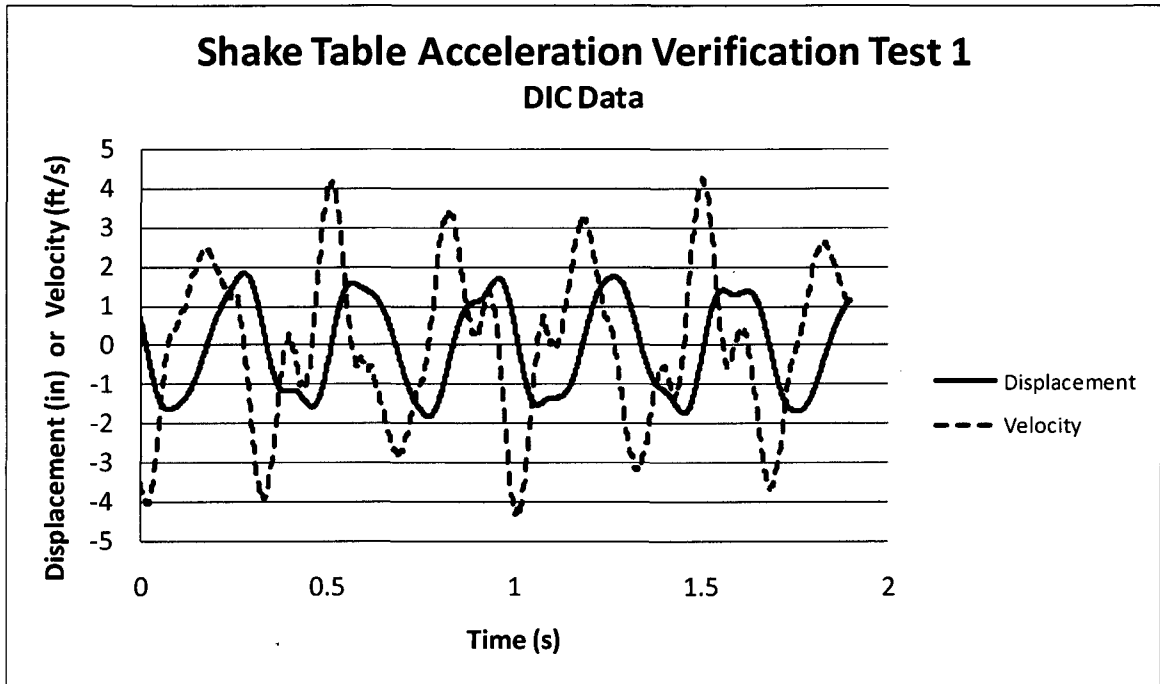


Figure 4-16: Shake table Test 2, DIC displacement and velocity versus time

For both the accelerometers and the DIC system, collected acceleration data contains significant noise. Large amounts of noise are present because of the high sampling rate; the faster data is collected, the more noise will be present. To eliminate the noise, a moving average of the collected data was used to filter the data and obtain acceptable results. In Figure 4-17, the raw data from both sources is displayed in the heavy semi-transparent lines in terms of “g” versus time. The filtered data using the moving average of every 140 data points from each source is shown in the two thinner lines. The moving average function can be adjusted to average various numbers of points until a visual match is created. The number of points that are averaged varies from test to test, and 140 was found to provide the best fit in this case.

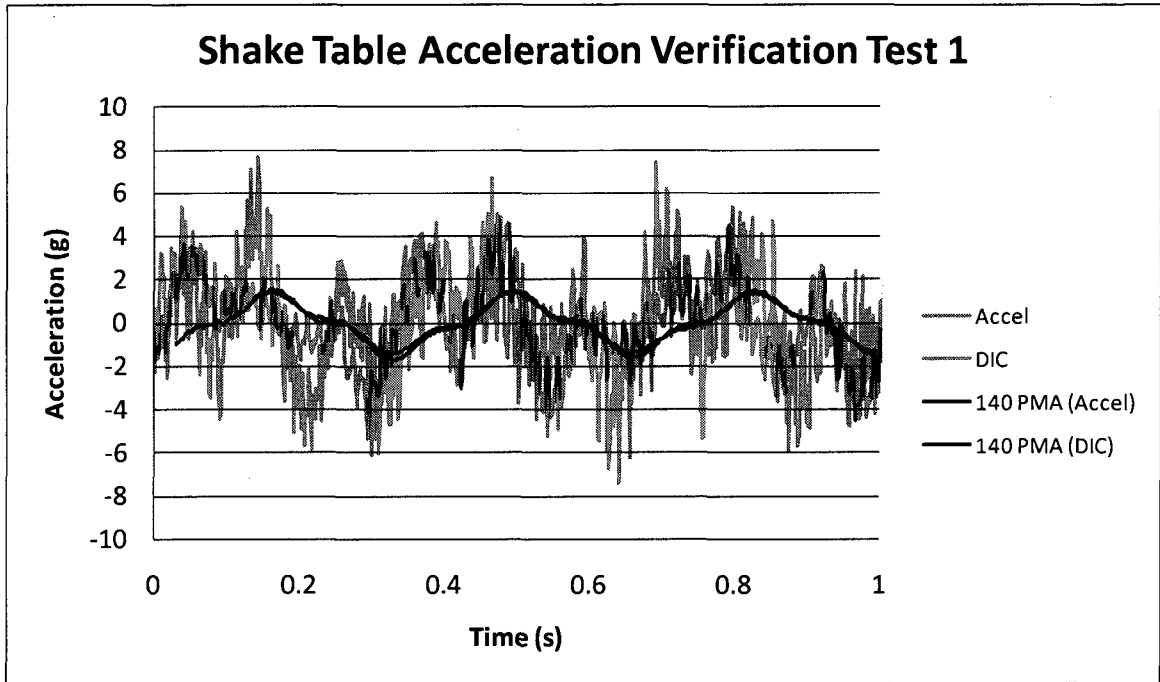


Figure 4-17: Shake table Test 1, acceleration versus time comparison

Figure 4-18 shows an enlarged view of the two Moving Average functions. Overall correlation is very clear. Note that the minima and maxima tend to be greater for the Accelerometer data. This is probably because the accelerometers have a higher sampling rate and can detect the more extreme acceleration values.

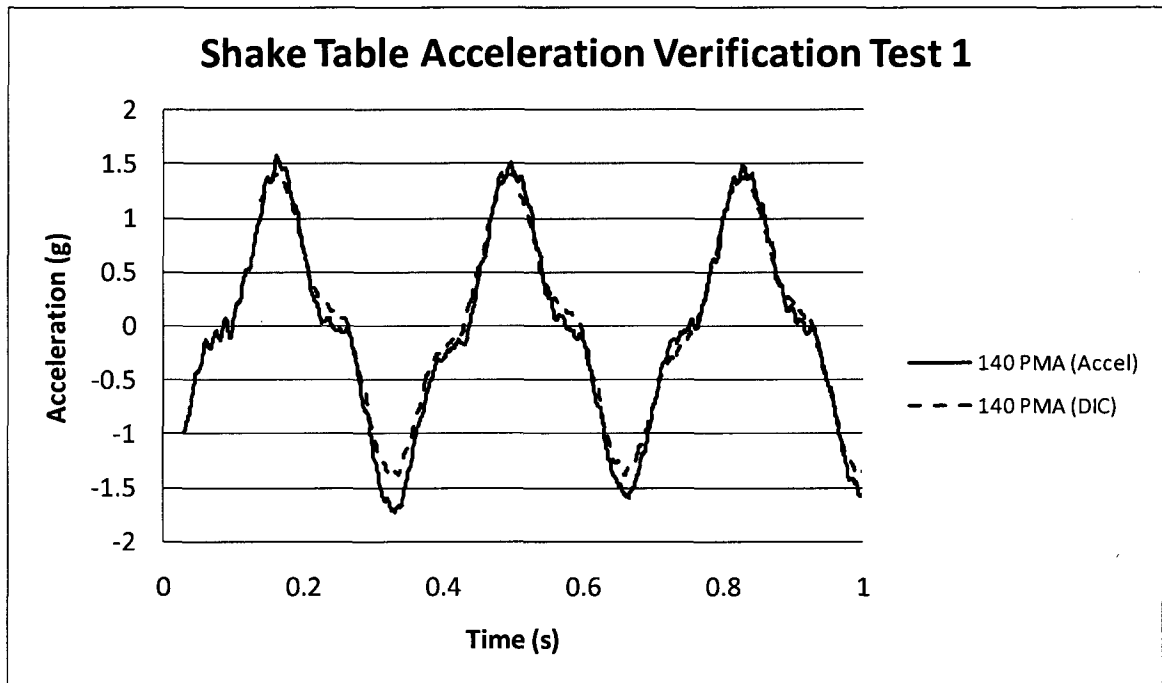


Figure 4-18: Shake table Test 1, acceleration versus time comparison detail

Test Two. A second test was conducted later with a similar DIC setup to that used in the previous case; the input motion was once again a tapered sine wave, with an amplitude of 1.5” and a frequency of 3 Hz.

To compare accelerations for this test, a much more sophisticated technique was used to filter the accelerometer data. A Fourier analysis was conducted, and the data was filtered by period using Matlab software. Colleague Heather Newton provided this information. To match the filtered accelerations, the DIC data was filtered using a moving average function, as was done previously. In this case, the average of each 93 acceleration values was selected visually to match the accelerometer data. The result is shown in Figure 4-19.

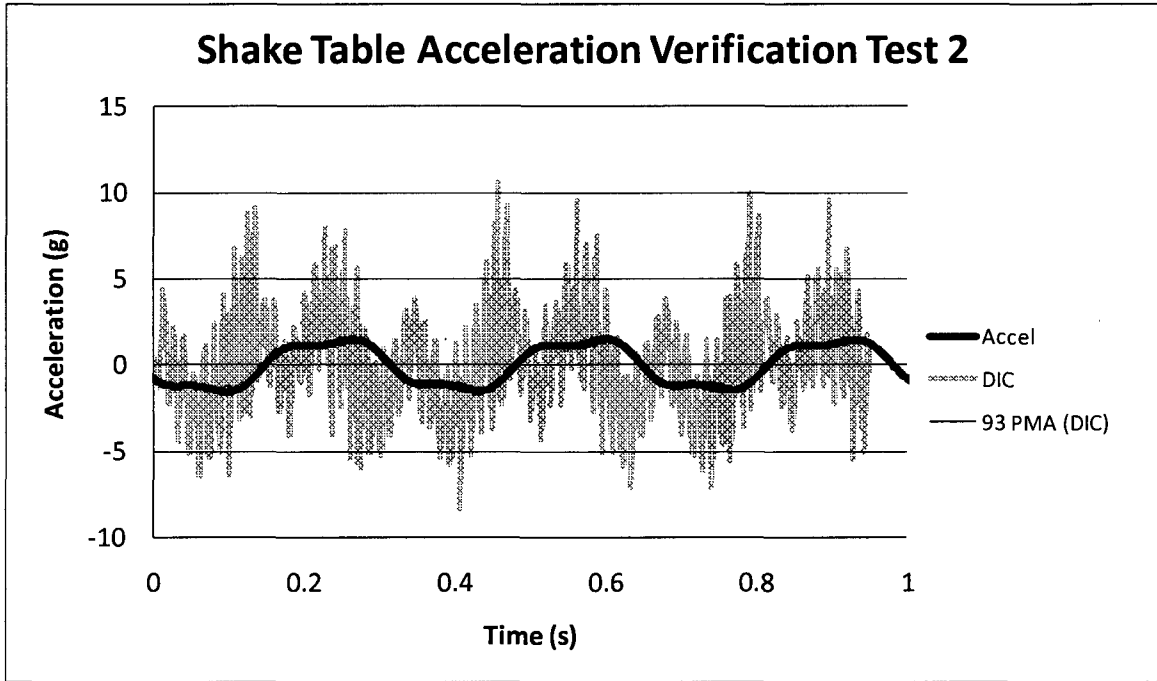


Figure 4-19: Shake table Test 2, acceleration versus time comparison

The two accelerations are too similar to differentiate, so an enlarged graph was created. Figure 4-20 enlarges the scale of the above graph and removes the raw DIC data. The accelerations match very closely, but as seen in Test 1, the accelerometers appear to detect the minima and maxima more accurately.

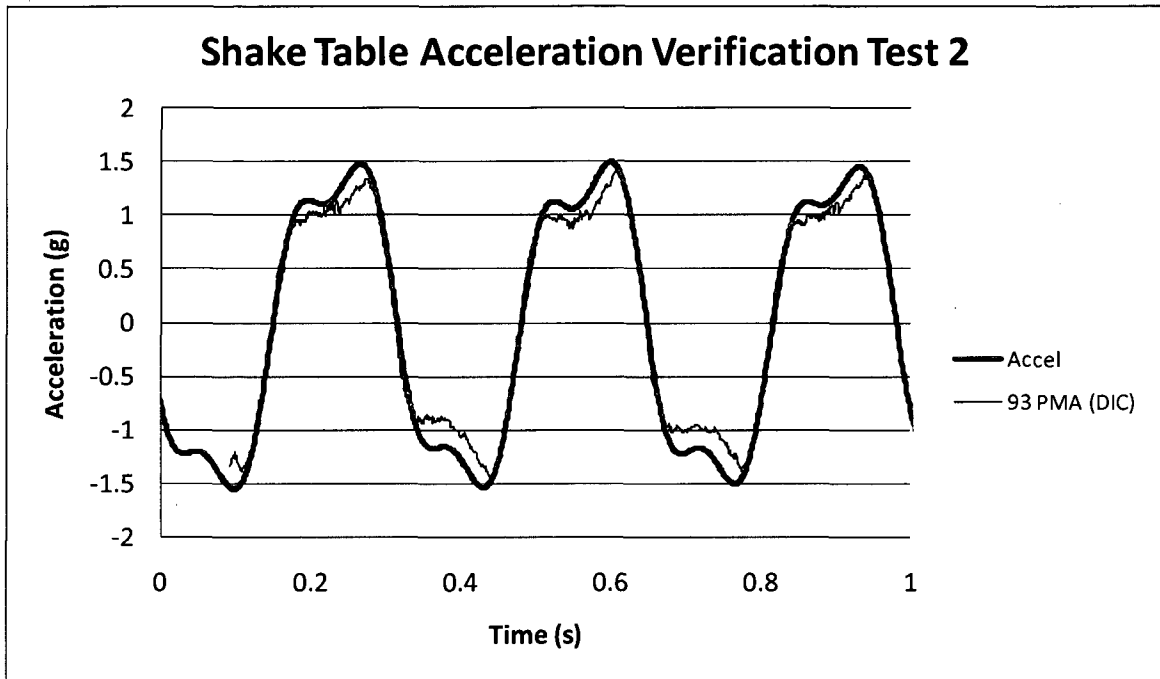


Figure 4-20: Shake table Test 2, acceleration versus time comparison detail

The data included here is only a small part of that collected at the shake table. A complete set of graphs is located in Appendix A.

Remarks. The shake table testing demonstrated the ability of DIC to accurately capture data at high speed. However, one significant problem was encountered during the shake table testing. Graduate student Heather Newton discovered that the DIC software is not able to accurately measure large out-of-plane displacements. In this case, the maximum displacement that could be accurately recorded was two inches. This number is specific to this test setup and would likely change under different circumstances. If large displacements are expected, measuring displacement in-plane will provide much more accurate results.

The limit is likely caused by the rotation of the target as it leans forward and backward. If the target did not rotate, the DIC system may be able to measure larger displacements. Further testing needs to be conducted to confirm that the rotation is the cause of the problem. If not, then the problem is likely caused by a deficient calibration calculation within the software.

4.2 - Field Experiments

4.2.1 - Pond Bridge Road Bridge Test

The bridge over Nonquit Pond on Pond Bridge Road in Tiverton, Rhode Island underwent a load test on August 17, 2009. The bridge is frequented by heavy potato trucks from a nearby farm that have no other reasonable means of egress but this bridge. The town of Tiverton was concerned that the heavy trucks were too much for the bridge to handle, so it hired Bridge Diagnostics Inc. (BDI) to perform a load test. BDI is based in Boulder, Colorado but travels the world performing bridge load testing.

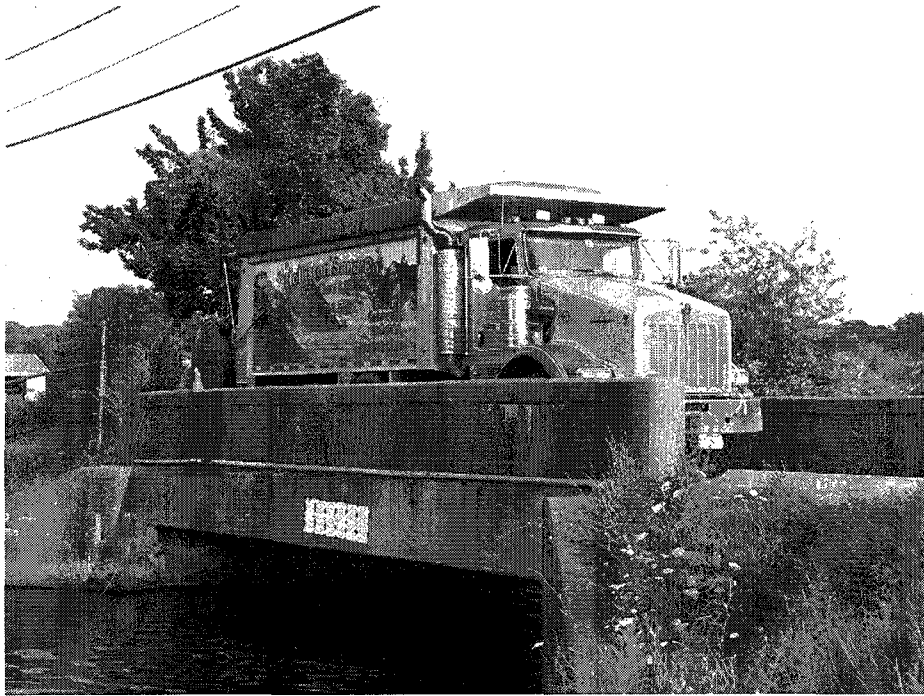


Figure 4-21: Test truck passing over the Pond Bridge Road Bridge

The Pond Bridge Road Bridge consists of steel girders encased in concrete, and a concrete deck (see Figure 4-21). BDI used strain gauges and wireless receivers to gather real-time data during the testing. A total of eleven tests were conducted as a fully loaded dump truck drove across the span at various speeds and various locations on the bridge. Table 4-1 lists each of the tests, the location on the bridge, the type of test, and how long into the test the front and rear axles crossed midspan.

Table 4-1: Pond Bridge Road Bridge testing summary

Pond Bridge Road Bridge Testing Summary				
Test Number	Location	Test Type	Front Axle over Midspan	Rear Axle over Midspan
			(Time, s)	(Time, s)
1	Near	Rolling	15.2	24.2
2	Near	Rolling	14.0	23.0
3	Near	Rolling	11.5	18.5
4	Near	Stop	11.0	23.0-58.0
5	Center	Rolling	8.5	15.5
6	Center	Rolling	10.0	16.5
7	Center	Stop	14.0	27.0-49.0
8	Far	Rolling	8.0	14.5
9	Far	Rolling	7.5	14.0
10	Far	Stop	10.0	24.5-58.0
11	Center	Fast Rolling	1.3	1.9

Setup. The bridge is directly adjacent to the dam holding back the water of Nonquit Pond. The location was quite fortunate, since the dam piers provided a convenient spot to set up the cameras. On the other hand, the pier was forty or fifty feet from the bridge structure, making accurate DIC data acquisition difficult. Also, because of the geometry provided by the dam, it was impossible to set up two separate tripods. Therefore only the deflection in two dimensions could be gathered at one location on the exterior girder. The setup is shown in Figure 4-22; the cameras are circled in white, and the bridge is to the right.



Figure 4-22: Pond Bridge Road Bridge DIC test setup

Speckle Pattern. Since the bridge material was concrete, and because the structure was over water, an innovative speckle pattern needed to be used. A random speckle pattern was developed in Microsoft Paint (see Figure 4-23). Twelve pages were printed on letter-sized paper and adhered to the side of the bridge using tape. This would not provide any accurate strain data, but it would at least allow for vertical deflection readings. Fortunately, the bridge was close enough to the water that a boat could be used to access the bridge girders. Paint could not be applied to the bridge surface because it cannot be easily removed. The opportunity to do this test came with

little warning, so there was not sufficient time to request permission to apply black chalk to the surface.

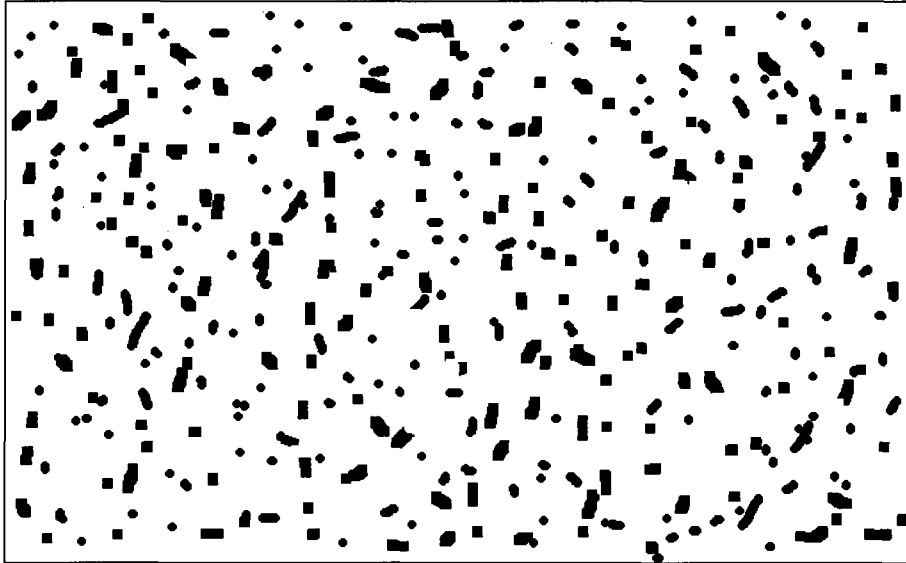


Figure 4-23: Example of the speckle pattern used at the Pond Bridge test

Calibration. Three different methods of calibration were attempted in this case. First, the typical stereo calibration was attempted. This involves rotating the calibration target in front of the camera setup. Next, a mono calibration was attempted. With this method, the calibration target is rotated in front of each of the cameras separately. Then, after the testing is completed, a special calibration process is completed using the Vic 3D software. Two points with a known separation distance must be drawn on the speckle pattern prior to testing. Using a test image and the two separate camera calibrations, the distance between the known points is entered into Vic 3D which uses that information to produce a calibration. The third method of calibration involved stereo calibration, but was done in the laboratory instead of in the field. After testing is completed, the cameras are left on the tripod in the exact orientation as they were for

the test. Back in the laboratory the stereo calibration can be completed as usual under ideal lighting and visibility conditions.

Test numbers one, four, and eleven were processed using each of the three different calibrations. The resulting error (standard deviations of residuals) for each is shown in Table 4-1. An error of 0.035 is considered a good maximum limit for data accuracy. The Mono calibration provided by far the best results, so was used as a basis for post-processing.

Table 4-2: Pond Bridge Road Bridge test error values

Pond Bridge Road Bridge Error Values			
Test Number	Field Stereo	Field Mono	Lab Stereo
1	0.9920	0.0286	0.1290
4	0.9800	0.0343	0.0598
11	0.9940	0.0435	0.0852
Average	0.9887	0.0355	0.0913

Results. Tests one through four were on the side of the bridge nearest the cameras, tests five through seven and eleven were in the center, and tests eight through ten were on the far side. Unfortunately, the only viable results were obtained during the first, fourth, and eleventh tests. It would be no surprise if only tests one through four gave reasonable results, since the truck was on the near side of the bridge and deflection would be greatest. However, the other tests on the near side of the bridge do not show any deflection. This may be explained by the large amount of error in the data that is most likely a factor of the distance from the target, windy conditions, and a poor speckle pattern application. The three tests with sensible data will now be discussed in detail; data from the remainder of the tests can be found in Appendix A.

For Test 1, the truck rolled slowly across the near side of the bridge. In Figure 4-24, it can be seen that the front axle was over the middle span of the bridge at 15.2 seconds and the rear axle was over the center at 24.2 seconds. These times correlate approximately with the two low points on the graph. What is most interesting is that the bridge appears to behave as if it were a three span structure. As the truck enters the bridge, the structure moves upward about 0.02 inches before dropping to about -0.01 inches when the front axle reaches midspan. The bridge then proceeds to return to the zero position when the truck is directly on the center of the bridge. As the rear axles reach midspan, the girder drops again to about -0.02 inches, and rises to just above the zero point as the truck exits the bridge.

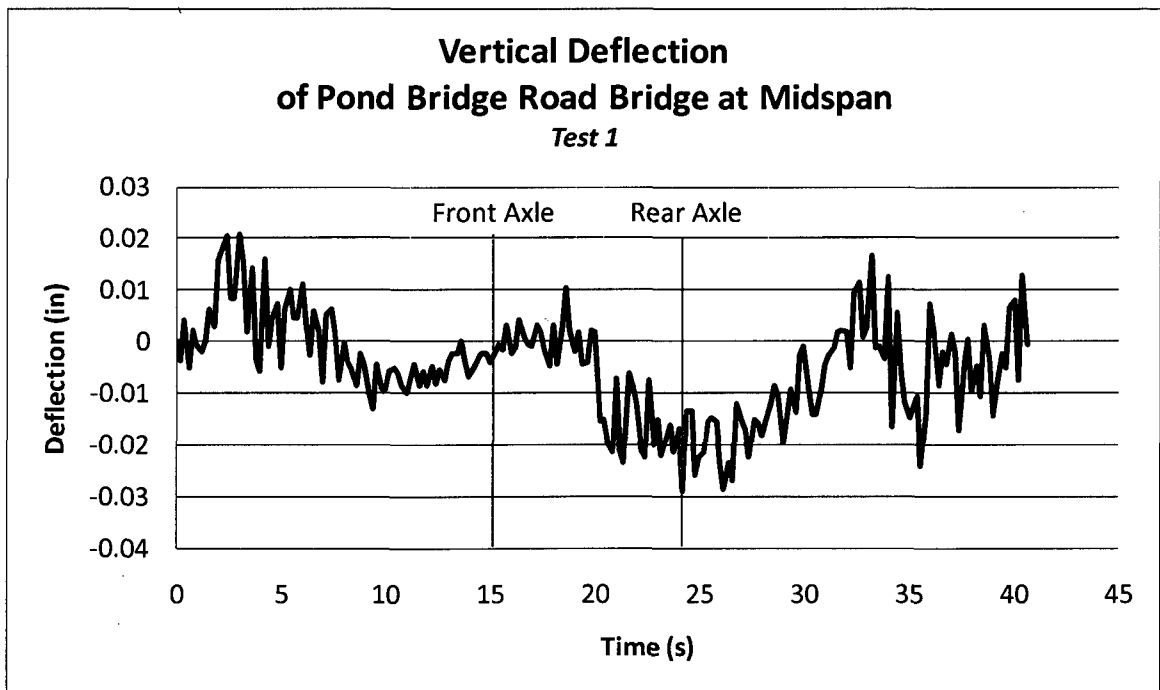


Figure 4-24: Vertical deflection of Pond Bridge Road Bridge at Midspan-Test 1

The unusual behavior of the bridge can be explained by observing the large error present in the data. During most of the test, the error appears to be ± 0.005 inches. Given the maximum deflection of about 0.02 inches, this is a very large error. Thus the positive deflections are likely due to errors introduced during testing.

Test 4 also shows some amount of deflection. Test 4 is a stop test, in which the truck stopped when it reached the middle of the bridge for about thirty seconds. Doing the test this way allows the bridge to “creep” or settle to a maximum deformation. The front axle reached the middle of the bridge at 11.0 seconds, and the rear axle remained over midspan from 23.0 to 58.0 seconds. The time of 11.0 seconds corresponds with the bridge deflecting downward about 0.02 inches, as seen in Figure 4-25. The bridge remained deflected at or near that level until about 60 seconds into the test, at which time it rose back up to about -0.01 inches, not quite to the original level. This corresponds quite well with the time the truck started to travel off the bridge at 58.0 seconds. However, all of this data is merely anecdotal because of the high error present. It can be observed that the error or noise in the data is ± 0.01 inches, or about half the maximum deflection.

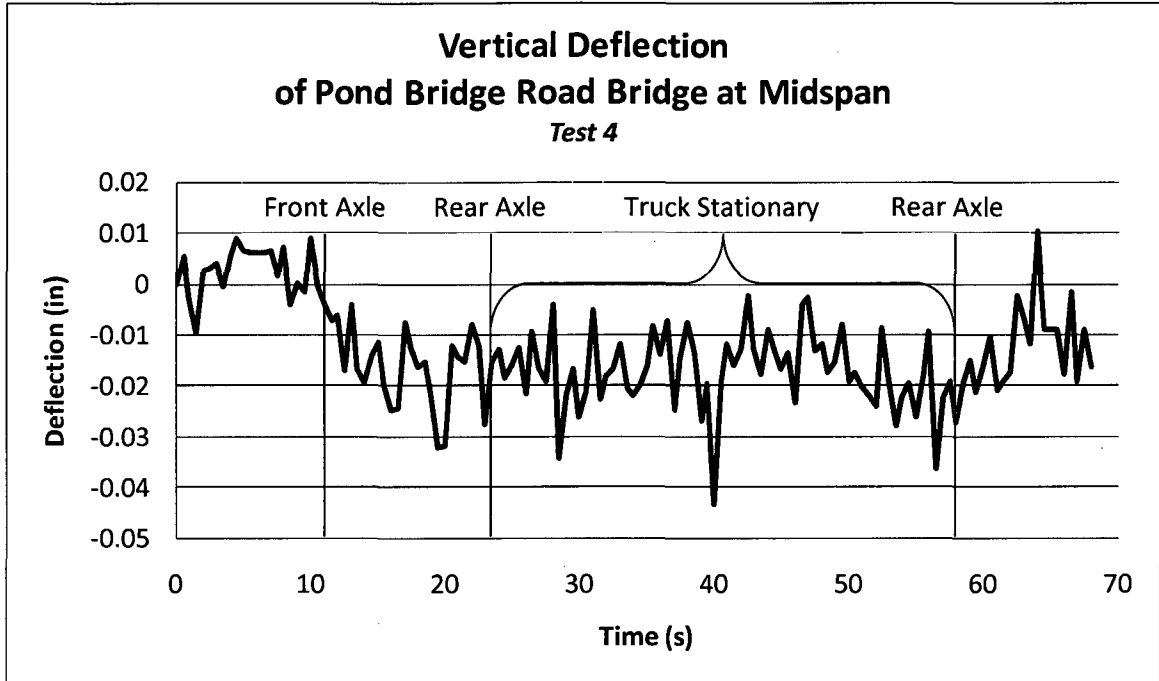


Figure 4-25: Vertical deflection of Pond Bridge Road Bridge at Midspan-Test 4

Test 11 was a high-speed rolling test in which the truck traveled at about 20 miles per hour down the center of the bridge. The front axle reached midspan at 1.3 seconds, and the rear axle at 1.9. Because of the high-speed nature of the test, very little data was collected while the truck was actually on the bridge, in spite of a fast collection rate of ten images per second. It can be seen in Figure 4-26 that the bridge starts to deflect at 1.2 seconds, reaches a maximum of -0.028 inches at 2.0 seconds, and then rises rapidly back up to near the zero position. Given the previous discussion, however, it is likely that the data point showing deflection of -0.028 inches is inaccurate. High amounts of noise are visible in this test as well, again negating the results.

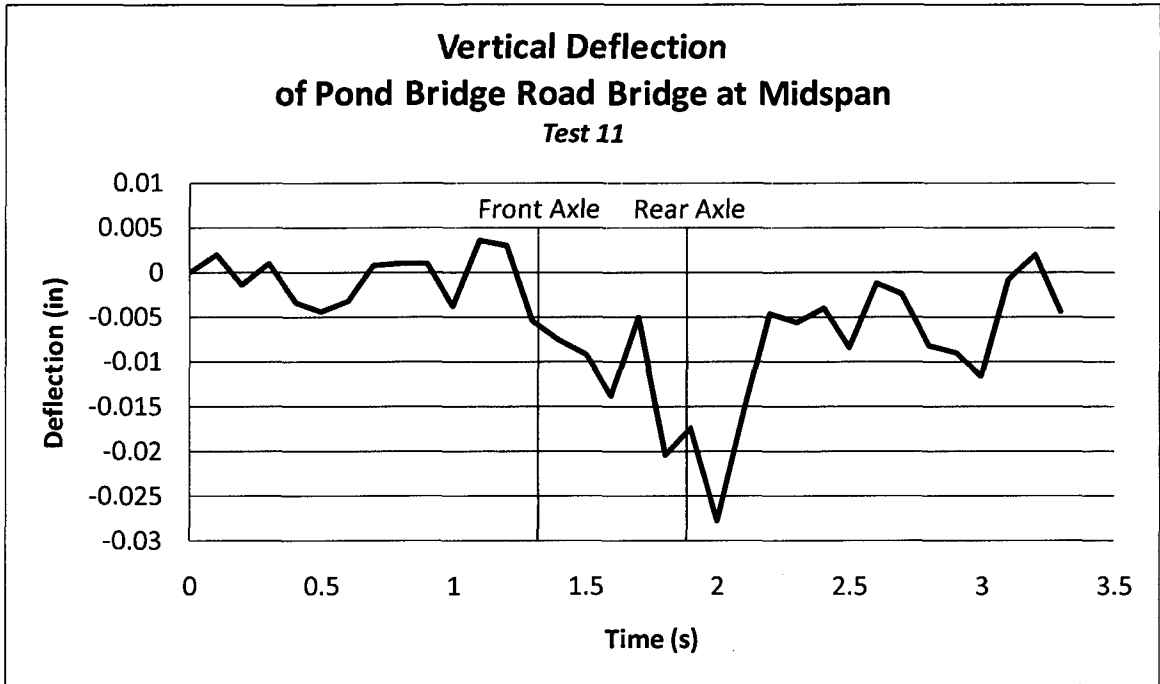


Figure 4-26: Vertical deflection of Pond Bridge Road Bridge at Midspan-Test 11

BDI Data. BDI provided deflection data from their finite-element computer model of the structure. The data was obtained by conducting a structural analysis of the bridge in BDI WinSAC (BDI, 2009). The graph shows the deflection for Girder 1, which is the girder facing the cameras. The deflection as the truck crosses the entire span at both the near and center lanes of the bridge is depicted in Figure 4-27. With the truck at the near side of the bridge, predicted maximum deflection is -0.0122 inches, and -0.0054 inches at center.

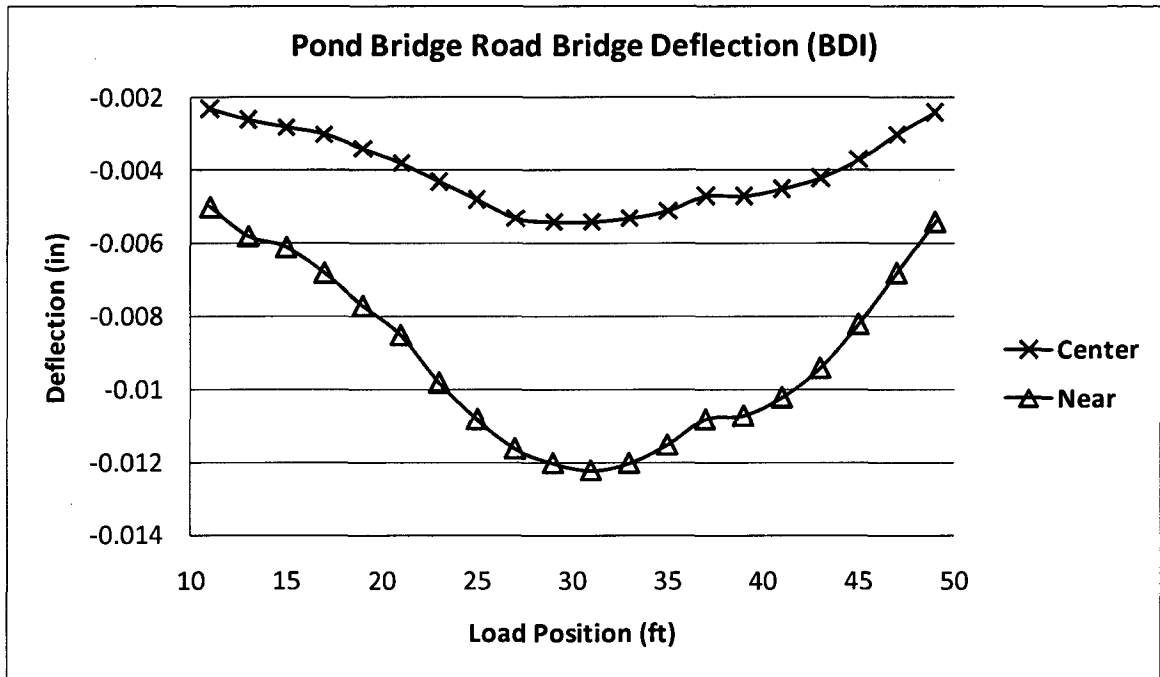


Figure 4-27: BDI data for two load truck locations at Pond Bridge Road Bridge

The maximum deflection observed in tests one and four was between -0.015 and -0.020 inches, more than that predicted by the model. However, the error in these DIC tests was anywhere from ± 0.005 inches to ± 0.01 inches, so it is no surprise that the results vary somewhat. The maximum deflection for Test 11 was -0.02 inches; the data from BDI showing a much smaller deflection seems to confirm that the DIC data is very noisy and is essentially meaningless.

Weather Conditions. The weather on the day of the test was nearly ideal. Because of the proximity of the bridge to the ocean, a thin veil of clouds had moved in across the area. Thus, the weather was cloudy but bright with temperatures near 80°F, while a few miles away it was very bright and sunny and near 90°F. The absence of direct sunlight during the test eliminated any concern with lighting of the speckle

pattern or temperature degradation caused by solar gain. However, there was a slight breeze on the test day. This could have contributed to the error by either introducing camera shake in the DIC setup or creating false displacement in the paper target on the bridge.

Remarks. The most notable aspect of the load test on Pond Bridge Road Bridge is the unpredictable quality of the data collection. It is likely that the speckle pattern printed on paper and taped to the girder is simply an unsuitable DIC target. If the target were firmly adhered to the bridge results would have likely improved. However, the distance of the cameras from the bridge was also a factor, causing an amplification of any errors present and reducing the clarity of the pixels in the test images due to insufficient resolution.

Several changes could be made to greatly improve the results from this test. First, the target on the girder could be black chalk instead of paper, eliminating the inconsistencies of the target. Secondly, multiple camera setups could be used to compare results. Lastly, cameras with higher resolution and lenses with a longer focal length would reduce the problems with resolution and pixel clarity.

4.2.2 - Vernon Avenue Test

The other field test conducted as part of this research was a load test on the Vernon Avenue Bridge in Barre, Massachusetts. This test will be discussed in full detail in the following chapter.

CHAPTER 5

Case Study—Vernon Avenue Bridge

5.1 - Introduction

The bridge across the Ware River on Vernon Avenue in Barre, Massachusetts is the focus of a case study that included the deployment of the DIC system as part of a field test. Due to the presence of a transfer station and landfill adjacent to the site, the Vernon Avenue Bridge is subjected to frequent heavy truck loading. The structure had fallen into decay in recent years. Corrosion had lead to significant section loss in the steel girders, and the deck had decayed to the point that holes had formed through the entire deck (see Figure 5-1). Heavy steel plates were used to patch the deck holes, but it was apparent that a more permanent repair was necessary (MHD, 2007).

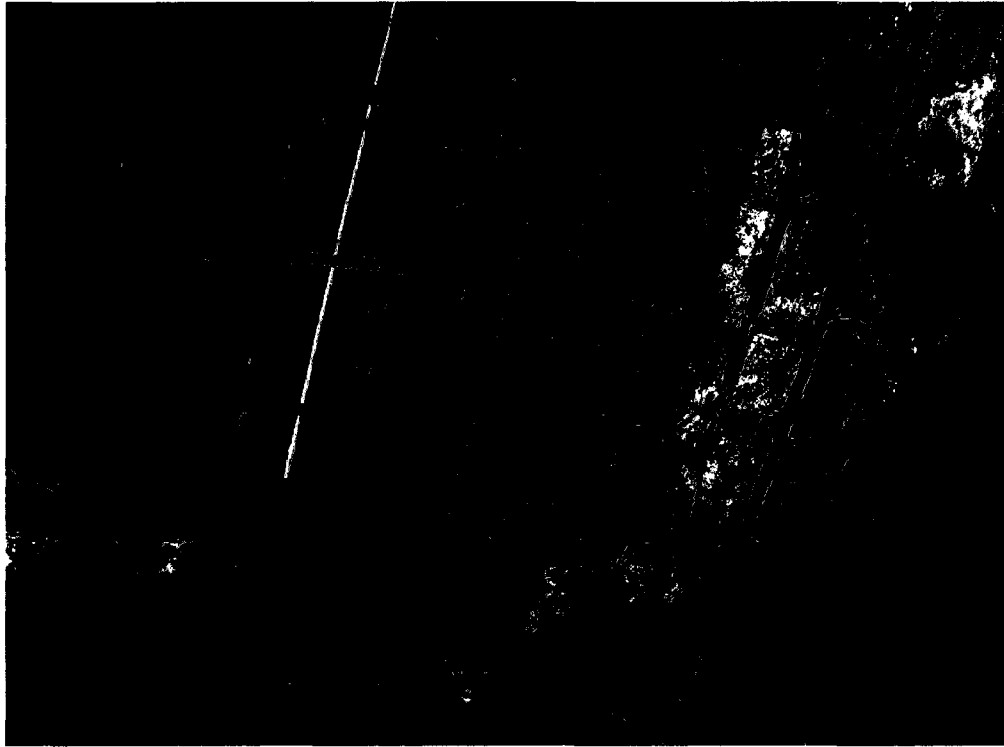


Figure 5-1: Deck spall at Vernon Avenue Bridge (MHD, 2007)

The decaying bridge was finally replaced in the summer of 2009. The bridge was designed by Fay, Spofford, and Thorndike Engineering; fabricated by High Steel; constructed by ET&L; and erected by ABE.

The structure is a three-span bridge with one lane of travel in each direction. The two outer bridge spans are about 40 feet long, and the middle span is 77 feet. Six steel girders run along the length of the bridge, and they are capped by a continuous, cast-in-place eight-inch concrete deck. Metal studs create composite action of the steel girders and concrete deck. Seven lines of steel diaphragms brace the girders (Sanayei, Brenner, Santini-Bell, Sipple, Phelps, & Lefebvre, 2010).

A research team from the University of New Hampshire and Tufts University collaborated to install instrumentation on the bridge as part of a research grant to study SHM instrumentation for long-term bridge monitoring. The team members traveled to Lancaster, Pennsylvania to install the sensors on the steel girders at the High Steel fabrication plant. The team installed 100 strain gauges, 36 girder thermistors, 30 concrete thermistors, 16 bi-axial tiltmeters, and 16 uni-axial accelerometers on the bridge (Sanayei et. al., 2010). A speckle pattern using white magnets was applied to the web of the outer girder at the bridge site for DIC testing (see Figure 5-2).



Figure 5-2: Girder 1 being installation with speckle pattern in place

5.2 - Concrete Deck Pour Test

5.2.1 - Setup

To complete a trial run of the DIC system at the bridge site, as well as gain important data, it was decided that a test should be run during the pour of the concrete deck. This would give insight into the best camera placement, proper speckle pattern configuration, weather concerns, and overall functionality of the DIC setup in advance of the more demanding load test. The cameras were set up on two separate tripods on the embankment below the bridge. The camera separation provided for sufficient depth perception, making three-dimensional readings possible.

Images were gathered at a rate of about three per minute through the duration of the placement, beginning at roughly 7:00 AM and concluding around noon. Weather conditions were clear and sunny, not necessarily the best for DIC, as will be discussed later.

5.2.2 - Speckle Pattern Issues

Unfortunately, it was discovered after processing the data that the speckle pattern that was placed on the bridge girder before installation was too coarse for the post-processing software to analyze. Not only that, but steel struts that were placed against the web of the girder to support the sidewalk forms blocked part of the speckle pattern, further inhibiting data acquisition (see Figure 5-3).



Figure 5-3: Vernon Avenue Bridge speckle pattern with obstructions

Correlated Solutions, the manufacturer of the DIC system in operation, was contacted to determine whether any data could be garnered from the images. A new beta version of the Vic-3D software had just been released, and was able acquire some data with some manipulation.

5.2.3 - Results

The VIC 3D post-processing software was able to interpret data for the first half of the concrete placement only. It appears that at some point during the middle of the placement, the cameras were disturbed, and the calibration was corrupted. Because of the poor speckle pattern, the data is very noisy.

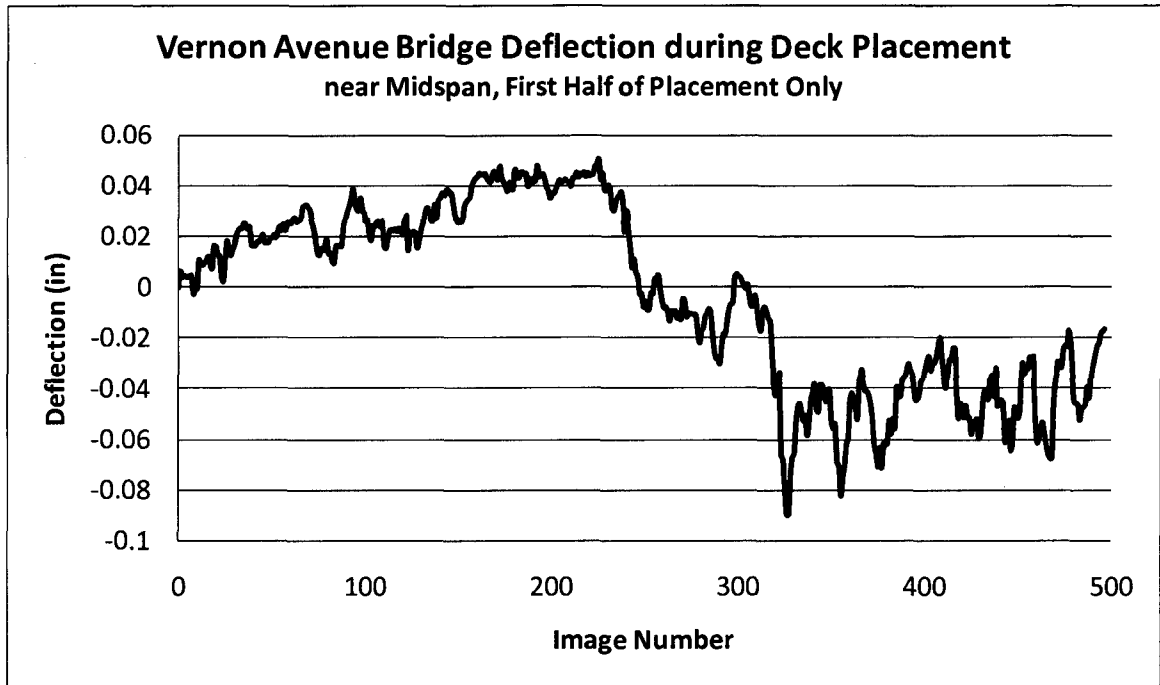


Figure 5-4: Vernon Ave Bridge deflection during concrete deck pour

The deck was poured starting at the south end, and working toward the north. The data shown in Figure 5-4 is from the beginning of the pour until the concrete reached midspan. Since deflection measurements were obtained near midspan of the bridge, it would be expected that in the early stages of the placement, the center span would actually rise slightly as the south span was depressed by the concrete. Then, once the concrete began to be placed between the two piers in the middle span, the center span would begin to sag. This behavior can clearly be seen in Figure 5-4. From the first frame to image number 220, the girder rose slightly to 0.05 inches above its original elevation. Then, over the course of the rest of the data, the girder drops to nearly 0.1 inches below its static level.

Near the end of the graph a slight rebound in the deflection may be noted. This is probably due to the fact that there was a heavy Bidwell Machine (see Figure 5-5) riding along the bridge to scarify the concrete; at the low point in the graph, the equipment was probably near midspan. The small perturbations in the deck deflection are probably due to the Bidwell Machine moving back and forth on the bridge.



Figure 5-5: Concrete deck pour and heavy equipment operation

5.3 - Load Test

5.3.1 - Background

The load test took place on September 3, 2009 using a loaded dump truck driving across the bridge several times at various locations and speeds. Three different types of tests were conducted. In the rolling tests the truck simply drove across the bridge at low speed. In the stop tests, the truck stopped for ten seconds every ten feet at fifteen stations across the span of the bridge. The impact tests involved the truck driving over a

speed bump on the bridge to induce vibration (see Figure 5-16). The truck followed three different lines down the length of the bridge: one on the west side, one in the center, and one on the east side.

Table 5-1 defines each test that was conducted.

Table 5-1: Load test schedule

Test #	Test Name	Test Type	Truck Location	Camera Data
Ambient	Ambient	Ambient	N/A	South
Ambient	Ambient 1	Ambient	N/A	North
1	1-X2-1	Rolling	Center	North/South
2	2-X2-2	Rolling	Center	North/South
102	102-X2-3	Rolling	Center	North/South
103a	103-X2-4_1	Rolling	Center	North/South
103b	103-X2-4_2	Rolling	Center	North/South
3	3-X1-1	Stop	West	North/South
4	4-X1-2	Stop	West	North/South
5	5-X1-3	Stop	West	North/South
6	6-X2-1	Stop	Center	North/South
7	7-X2-2	Stop	Center	North/South
8	8-X2-3	Stop	Center	North/South
10	10-X3-2	Stop	East	North
11	11-X3-3	Stop	East	North
12	12-X1-1	Rolling	West	North/South
13	13-X1-2	Rolling	West	North/South
14	14-X1-3	Rolling	West	North/South
15	15-X2-1	Rolling	Center	North
16	16-X2-2	Rolling	Center	North
17a	17-X2-3_1	Rolling	Center	North
17b	17-X2-3_2	Rolling	Center	North
18	18-X3-1	Rolling	East	North
19	19-X3-2	Rolling	East	North
20	20-X3-3	Rolling	East	North
22	22-X3-1	Impact	East	North
23	23-X3-2	Impact	East	North
24	24-X3-3	Impact	East	North
25	25-X1-1	Impact	West	North

The Test Name shown in Table 5-1 indicates the test number, the lane, and the trial number at that location. For example, Test 3-X1-1 is the third test, is in Lane 1, and is the first trial at that location. Lane 1 is on the west side of the bridge, Lane 2 is in the center, and Lane 3 is on the east side. Two camera setups were used for this test—one at the south span and one at the middle span. Figure 5-6 shows the three lanes and two camera setups on a plan view of the bridge.

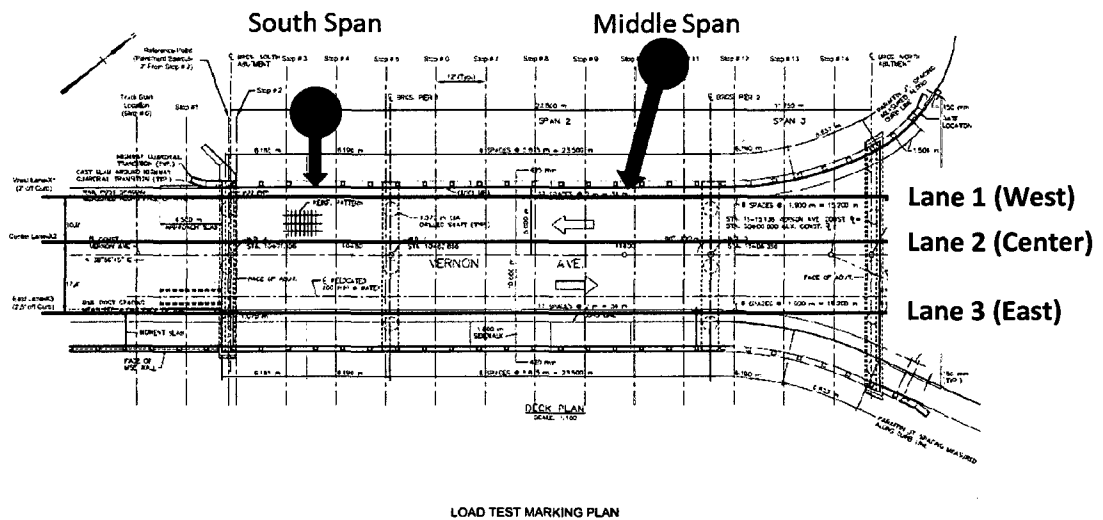


Figure 5-6: Vernon Ave plan showing truck lanes and DIC setup locations

5.3.2 - Center Span Data

Setup. The cameras were mounted on separate tripods about ten feet apart to allow enough separation distance to get data in all three directions. The angle between the cameras should be between 15 and 45 degrees for three-dimensional data acquisition (CSI, 2007). The cameras were thirty to forty feet from and ten to twelve feet below the face of the girder. Although the girder was in the shadow of the concrete

deck above, the ambient light was sufficient to acquire data without lamps being used as seen in Figure 5-7.



Figure 5-7: Middle span DIC setup

Speckle Pattern. The speckle pattern on the center span of the bridge was the same as that used to collect the placement data; however, one section of the speckle pattern was removed and replaced with a much smaller pattern of magnets. This provided a much better data acquisition platform which provided a reasonable contrast for DIC post-processing (see Figure 5-8).



Figure 5-8: Updated speckle pattern at middle span

Calibration. The calibration process proved rather difficult. Since the cameras were spaced far apart, it was necessary to hold the calibration target close to the bridge so that both cameras could see the target at the same time (stereo calibration). Also, because the ground was far below the bridge girders, the calibration target needed to be held at about ten feet above the ground. To accomplish this, a 35mm calibration target was tied to the end of a 2x6 piece of wood, and moved around to get ample calibration images (see Figure 5-9).

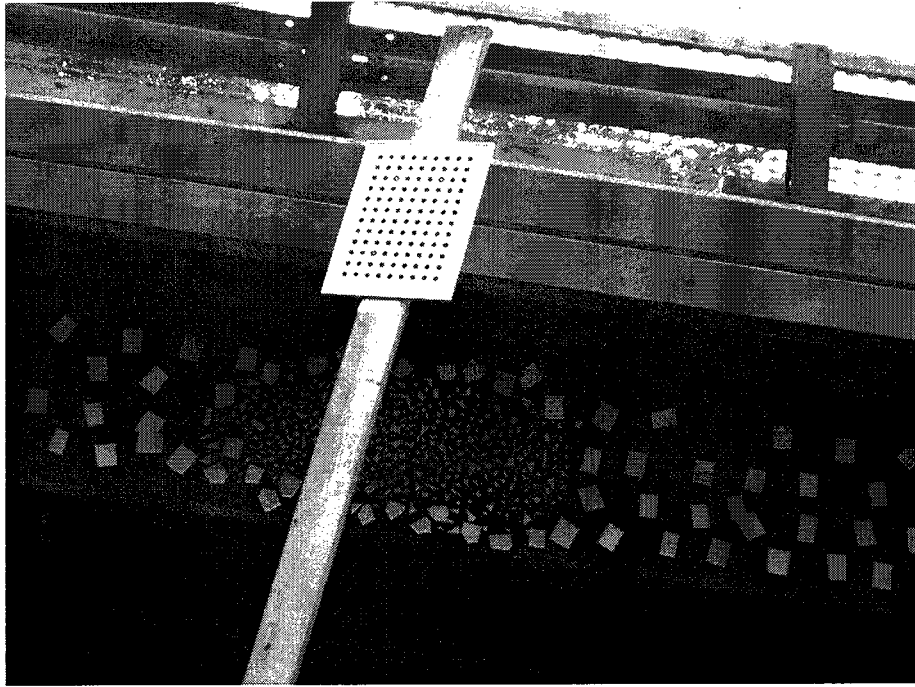


Figure 5-9: Calibration target in front of the speckle pattern at the middle span

5.3.3 - South Span Data

Setup. Since the cameras at the south span were near the end of the bridge, they were able to be set up very close to the bridge girder. Also, due to this close proximity of about eight feet, the cameras were set up on the same tripod about 18 inches apart, while still allowing for three-dimensional data acquisition. The response would also be less due to the shorter span at the south end of the bridge (see Figure 5-10).



Figure 5-10: DIC setup at south span

Speckle Pattern. The speckle pattern was very unique and innovative on the south side. A simple piece of white chalk was rubbed across the web of the girder, applying a high-contrast pattern to the weathering steel surface. In fact, the pattern created was a series of tiny, well-defined dots that were evenly distributed. The speckle pattern was applied to the lower part of the web and the edge of the bottom flange as seen in Figure 5-11.

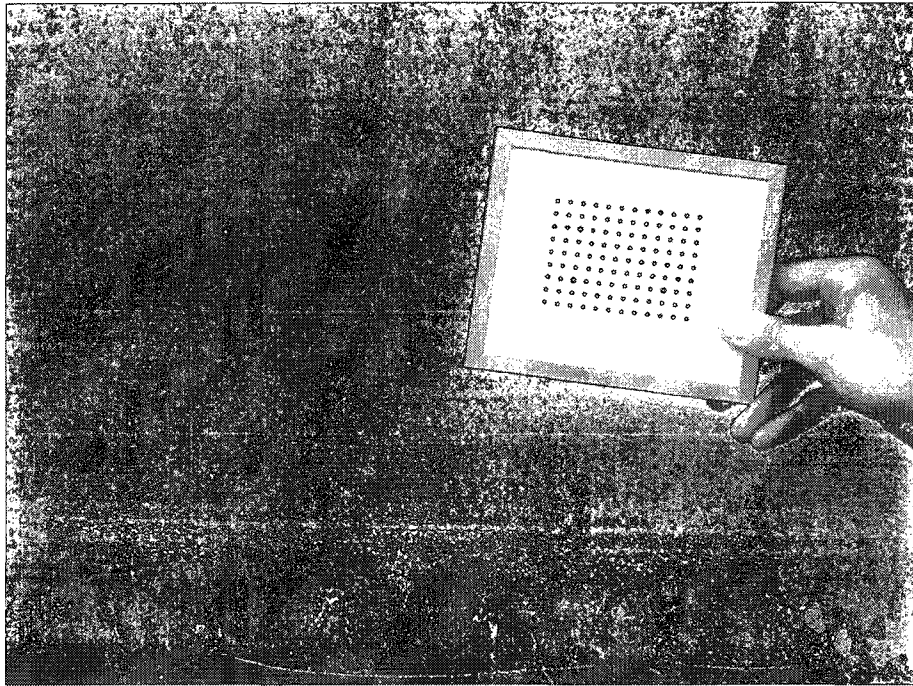


Figure 5-11: Speckle pattern and calibration target at south span

Calibration. The calibration was much simpler because the cameras were close together. A 7mm calibration target was rotated against the girder web to collect calibration images (Figure 5-11).

5.3.4 - Results

A sampling of results will be included here. Complete results for all truck runs during the load test are included in Appendix A. The truck runs that provided the cleanest data were those on the west (camera) side and in the center of the bridge. The results for the runs on the east side did not produce usable data as will be discussed later.

The first test to be considered is Test 3-X1-1. Figure 5-12 includes a schematic of the bridge showing which lane the truck is in; the rectangle on the side of the bridge indicates which span the data is from. In this case, data from both spans is included and the truck is in Lane 1. Test 3-X1-1 is a stop test, meaning the truck drove ten feet, stopped for ten seconds, drove another ten feet, stopped for ten seconds, and so on across the bridge.

The graph shows very clear deflection in the bridge girder. Initially, the middle span shifts upward as the truck begins to roll onto the south span; this upward movement is on the order of 0.02 inches. As the truck goes farther, the middle span drops quickly, finally reaching a low point of -0.16 inches. The girder then rises quickly, and continues slightly above the zero point. This is when the truck is over the north span and lifts the middle span upward, this time about 0.03 inches. The girder then proceeds to settle back down toward its original position at 0.00 inches.

Each truck stop location can be clearly seen as a horizontal portion of the curve. Some amount of noise is evident, but the results are very clear overall considering the distance at which the cameras were located from the bridge and the magnitude of deflections in consideration.

As seen in Figure 5-12, the south span drops to a maximum value of about -0.048 inches when the truck crosses the south span. When the truck enters the middle span, the girder lifts very rapidly, reaching 0.025 inches above the initial point. At the very end of the run, when the truck is over the north span, the girder drops back down very

slightly to -0.002 inches. Data from the south span has been included for the truck backing across the bridge after the test for observational purposes only. This can be seen at the end of the graph. Note that the minimum and maximum values are nearly identical for the stop test as they are for the truck backing over the bridge.

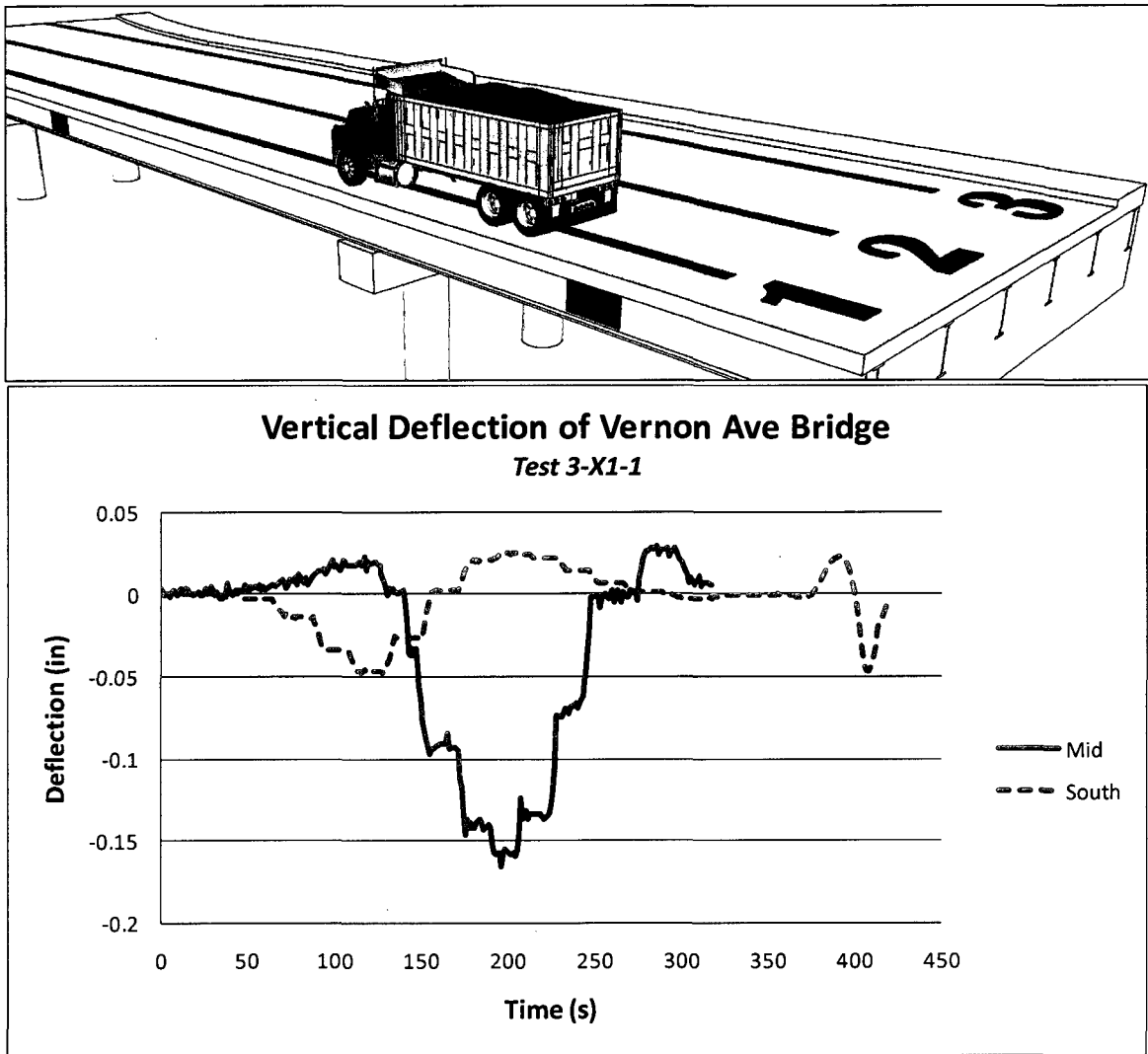


Figure 5-12: Vertical deflection of Vernon Ave Bridge at both spans-Test 3-X1-1

The next example is also a stop test, but this time the truck is traveling down the center of the bridge. Figure 5-13 shows the graph of Test 8-X2-3. Most noticeable is the

presence of significantly more noise at midspan than in the previous example, although the shapes are very similar.

Many of the stops in the middle span data are indistinguishable from adjacent stops or are so full of noise they are far from their ideal horizontal position. The presence of so much noise can be explained by realizing that because the truck passed over the center of the bridge, it was farther away from the outside girder that was being measured, resulting in smaller deflection values. The deflection decreased by a factor of nearly three when the truck moved from the west side of the bridge to the center. Accordingly, it should be no surprise that the error appears to be magnified for the tests in the center lane. The error itself has not necessarily increased; rather, its apparent magnitude has increased.

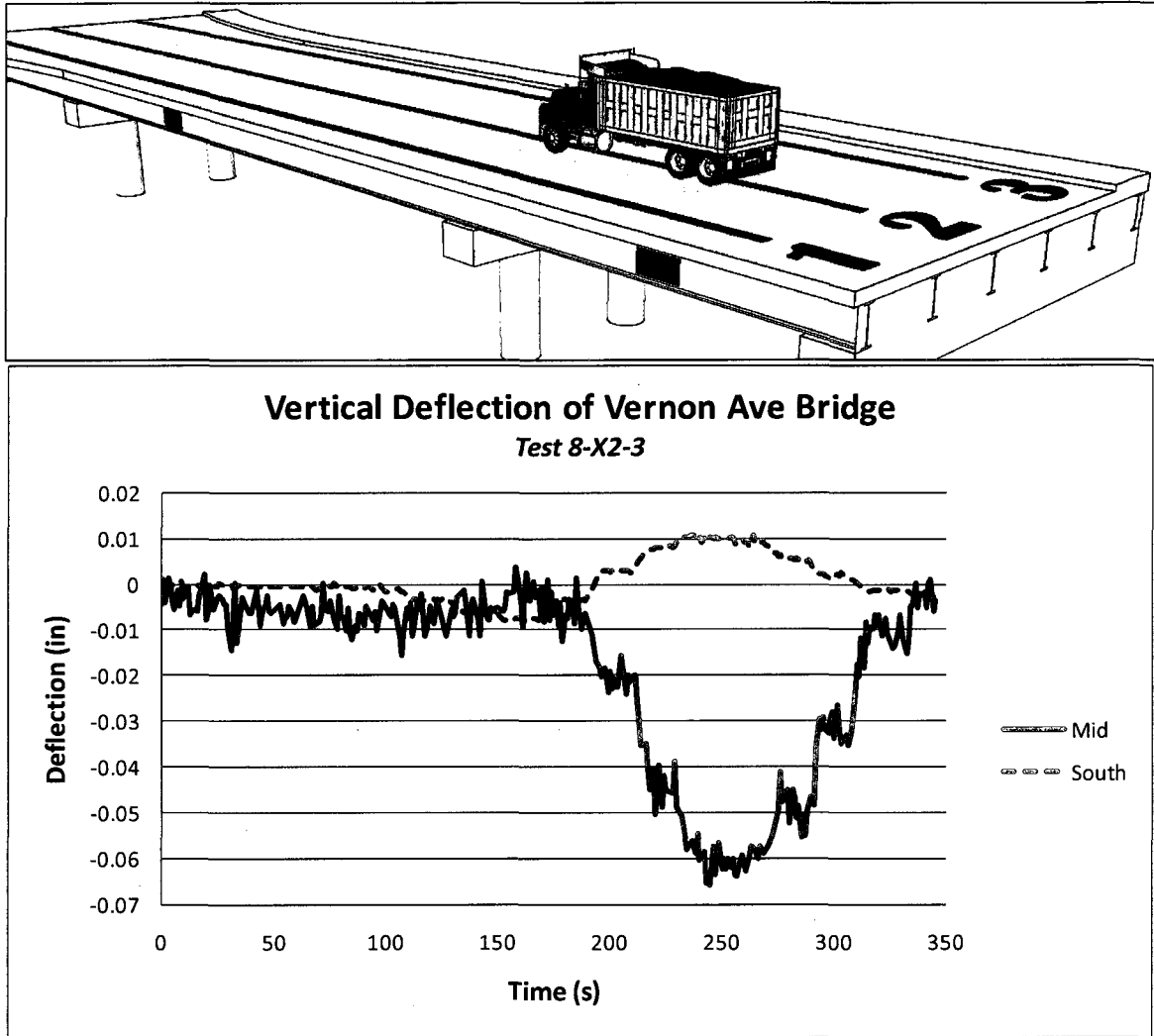


Figure 5-13: Vertical deflection of Vernon Ave Bridge at both spans-Test 8-X2-3

Another type of test was the rolling, or crawl-speed test. Test number 14-X1-3 (Figure 5-14) is shown below. Notice the smoothness of the curve compared to that of the stop tests because the truck rolled steadily across the bridge. It should be pointed out that the shapes seen here are essentially an influence line of the deflected shape of the bridge. Note also that maximum deflection values here are nearly identical to those measured in Test 3-X1-1, a stop test.

In a multiple-span bridge, deflection is typically in opposing directions in adjacent spans. This can be seen here—each time the middle span moves upward, the south span moves downward, and vice versa.

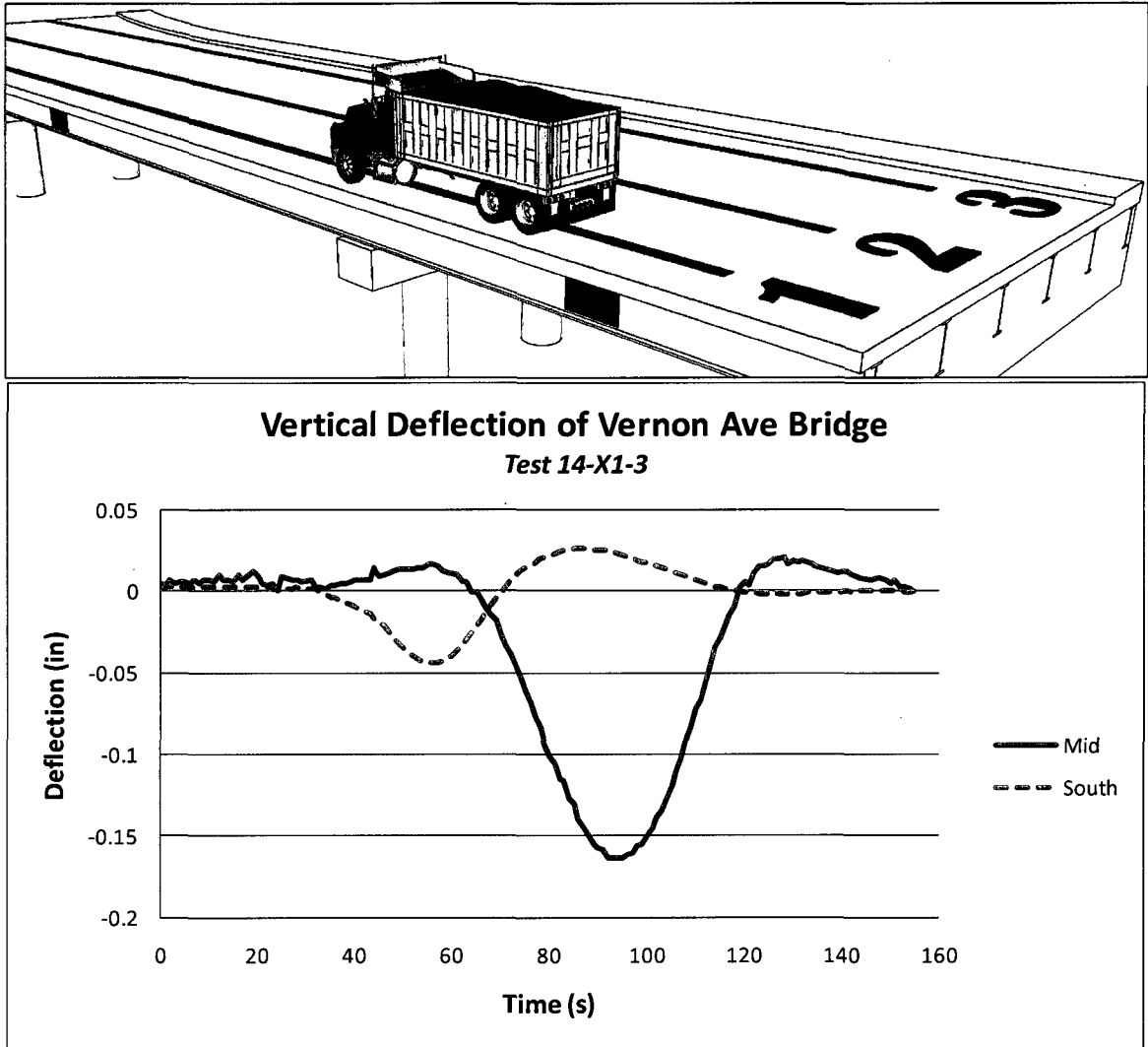


Figure 5-14: Vertical deflection of Vernon Ave Bridge near midspan-Test 14-X1-3

Test 103-X2-4_1 (Figure 5-15) is a rolling test with the truck at the center of the bridge. Again, notice that deflections here are very similar to those seen in stop test number 8-X2-3 (Figure 5-13) for both spans. Maximum deflection at the middle span is

about -0.053 inches, very similar to the -0.06 inches reached in Test 8-X2-3. In this case the bridge deflected slightly less in the rolling test versus the stop test. This is not surprising since the bridge is allowed to fully settle, or creep, with time if the truck remains on the span for an extended period.

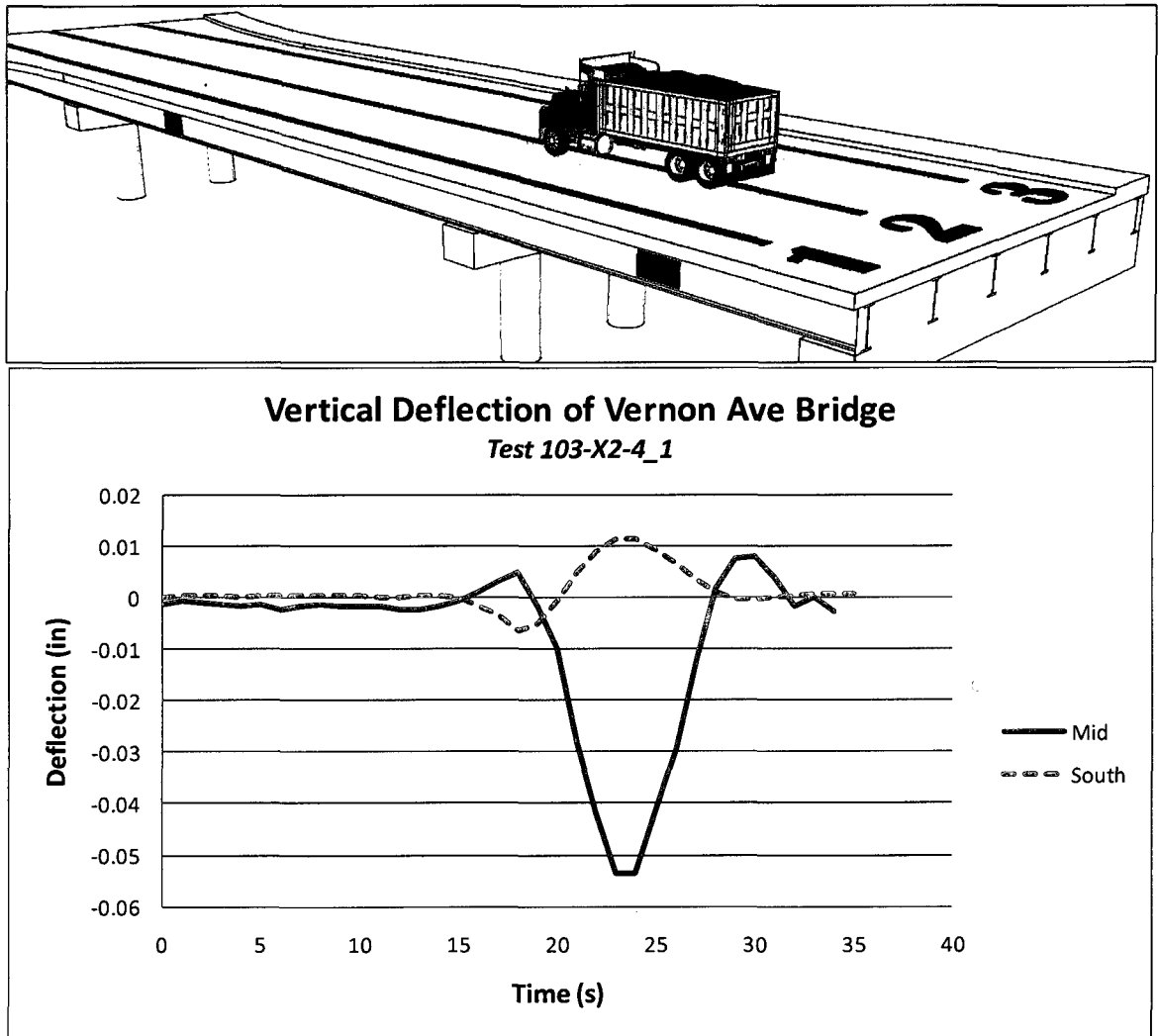


Figure 5-15: Vertical deflection of Vernon Ave Bridge near midspan-Test 103-X2-4_1

The final type of test is the impact, or dynamic test. Data was only collected at the middle span during this test. Shown here is Test 25-X1-1, in which the truck rolled

across the west side of the bridge (Lane 1), over a speed bump, and induced vibration in the structure (see Figure 5-16).



Figure 5-16: Load truck hitting speed bump during impact test

On the downward side of the curve, notice the sharp peak in the deflection, then two more sharp peaks near the bottom of the curve (Figure 5-17). The truck used in the load test had one front axle and two rear axles. Therefore, the first peak is the front axle hitting the speed bump and impacting the bridge deck. Then, the two rear (and much heavier) axles impacted the speed bump, vibrating the bridge with about double the amplitude as the front axle. The weight of the front axle of the test truck was 19.6 kips, and the two rear axles were each 26.6 kips, or a total of 53.2 kips. Also notice the excitation after each point of impact as the bridge vibrates briefly.

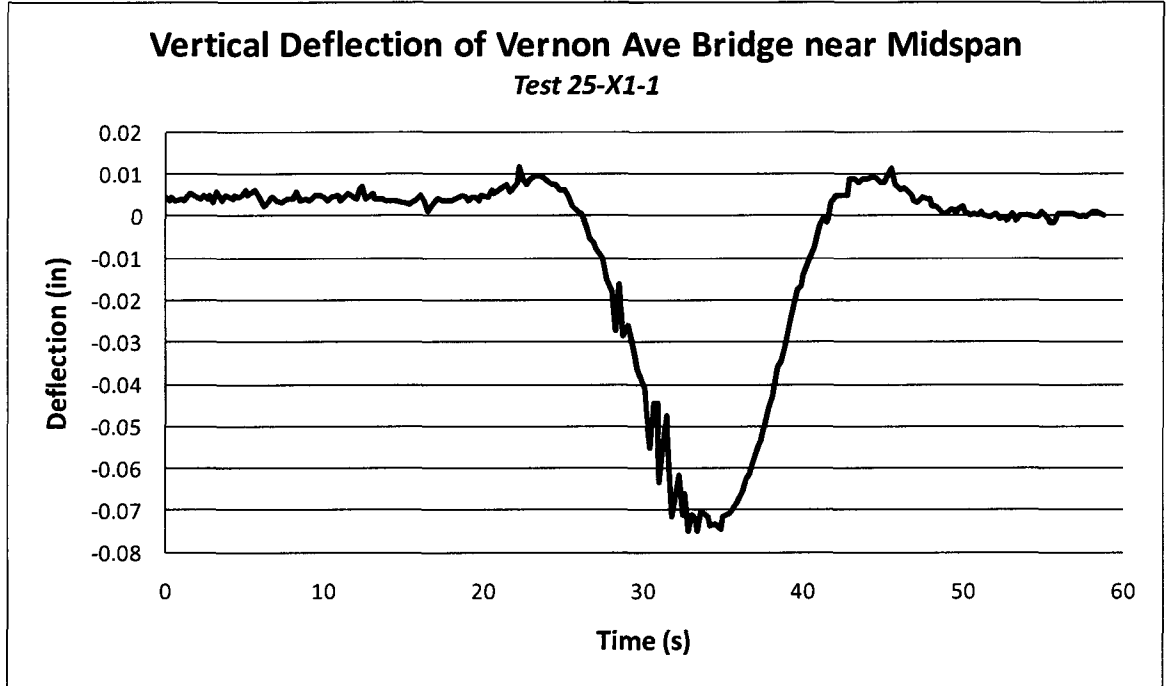
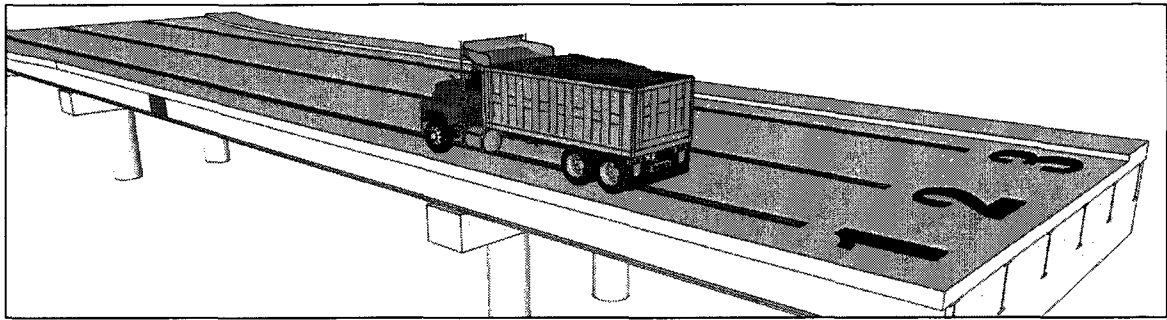


Figure 5-17: Vertical deflection of Vernon Ave Bridge near midspan-Test 25-X1-1

Note that the deflections are less than those of Test 14-X1-3 by a factor of about three. Because of the higher truck speed, the resolution of the images was reduced to increase the frame rate of the cameras. As a result, the error produced in post-processing was much greater than that in the other tests. This most likely explains the smaller deflection values.

5.3.5 - SAP2000 Model Deflection Comparison

A structural model of the Vernon Avenue Bridge was created in SAP2000 by fellow graduate student Paul Lefebvre. Figure 5-18 shows a screenshot of the model. SAP2000 is a civil engineering modeling application distributed by Computers and Structures, Inc. of Berkeley, California. Deflection data from two different models of the bridge were extracted from the program and compared to measured values from the stop tests.



Figure 5-18: SAP2000 model of the Vernon Avenue Bridge

The original model was created using the Bridge Modeling application of SAP2000. The model consisted of shell elements for the deck, and frame elements for the girders. Supports were treated as simple pin-roller-roller-roller connections from North to South. The deck was treated as homogeneous concrete, with no steel reinforcing.

The model was later updated to increase accuracy. The pin and roller connections were replaced with springs to simulate the elastomeric bearing pads that support the actual bridge. An eight-inch curb was added along both sides of the bridge. The deck was divided into layered shell elements so that a layer of steel reinforcing could be added to the deck structure. The material properties of the concrete deck were updated to reflect results from cylinder tests in the laboratory of the actual concrete used at the bridge.

In both cases, the truck load was applied as individual wheel weights. SAP2000 includes a truck modeling application that allows for manual input of truck characteristics. The axle spacing, width, wheel weights, and truck lanes were defined in the software to match the actual truck and test setup used in the load test. Data was collected from the software for truck locations at every ten feet across the span, at the same locations as in the stop tests.

Figure 5-19 is a compilation of four graphs showing a comparison between the measured data from DIC and the deflection values extracted from both SAP2000 models. Data from the old model is referred to as "SAP1" in the figure, and data from the new model is "SAP2." For nearly every data point, the data from the new model matches the actual measured values more closely than the data from the old model. Paul Lefebvre is studying the extent to which a model needs to be refined to produce realistic results. It is clear from these graphs that the refinements he made in his model made a large improvement in the accuracy. A complete array of graphs showing the

data comparison for tests three through eight can be found in Appendix A. A more thorough explanation of the modeling procedure can be found in Paul Lefebvre's thesis.

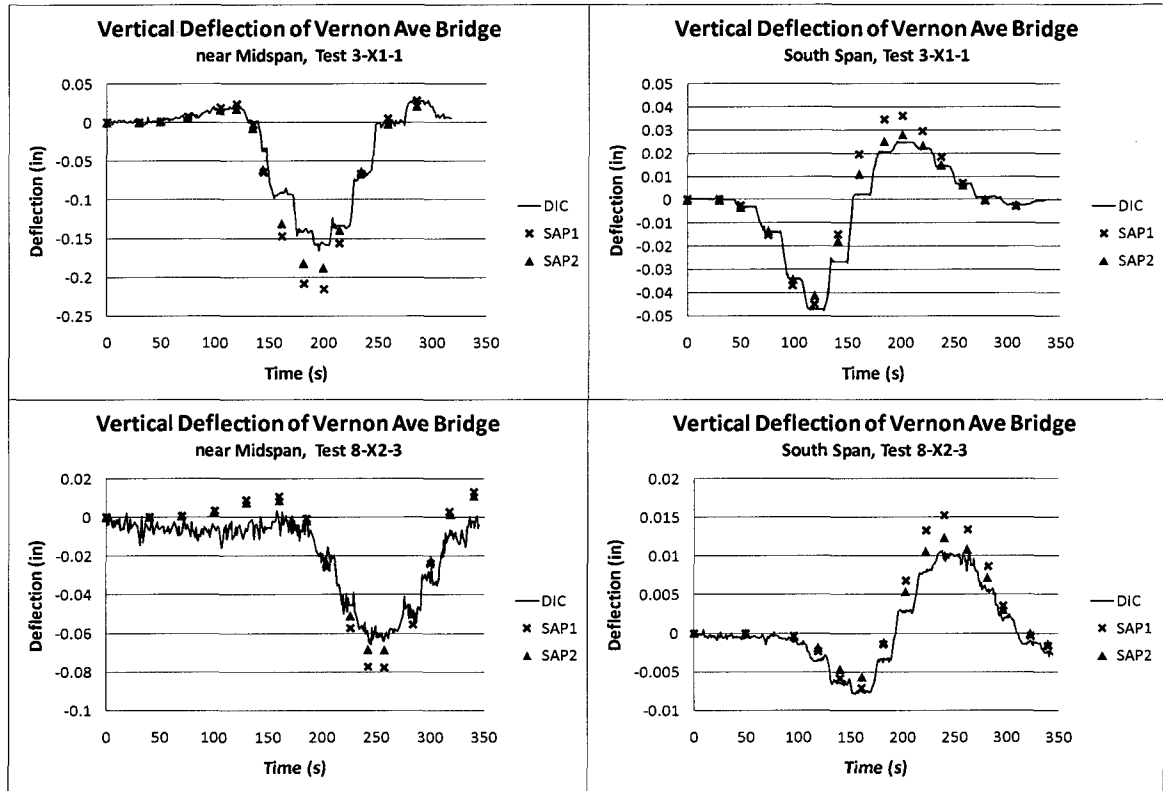


Figure 5-19: SAP2000 model deflection data versus DIC data from Vernon Ave Load Test

5.3.6 - Speckle Pattern Comparison

Clearly, there were vast differences in the speckle patterns employed in the Vernon Avenue Bridge tests. In retrospect, it appears that the finer the speckle pattern, the better quality the data will be. The speckle pattern used during the deck placement was far too coarse, and even after being refined for the load test, could still have been made much finer.

When dealing with weathering steel, it seems that white chalk is the material of choice for creating speckle patterns because it produces a high-contrast pattern on the surface. Of course, this pattern is very fine, and would only be useable up to a given distance from the target or with high resolution cameras. It is unclear whether white chalk could have been used in place of the magnets on the middle span due to the great distance of the cameras from the bridge. Further study needs to be done as to the practical limits of the chalk pattern.

5.3.7 - Weather Conditions

Weather conditions on the morning of the load test were cool and sunny, a slight breeze. The sun would not have been an issue had it not been for the fact that it was rising up from behind the bridge from the point of view of the cameras at the middle span. This not only cast the speckle pattern into a dark shadow, but it also created glare that impacted the image collection. Due to the low angle of the cameras, as the sun rose over the bridge it shone almost directly into the camera lenses. This made it nearly impossible to block the sun from reaching the lenses with any type of cover, and caused the images to be washed out by the ambient light.

In order to continue data collection, a cardboard box had to be held by fellow graduate student Antonio Garcia Palencia on the bridge to block the sun from reaching the cameras. This worked until the sun rose too high for him to reach with the box. Fortunately, by this time the sun was high enough for a cardboard visor to be taped to the top of the cameras to provide shade (see Figure 5-20).

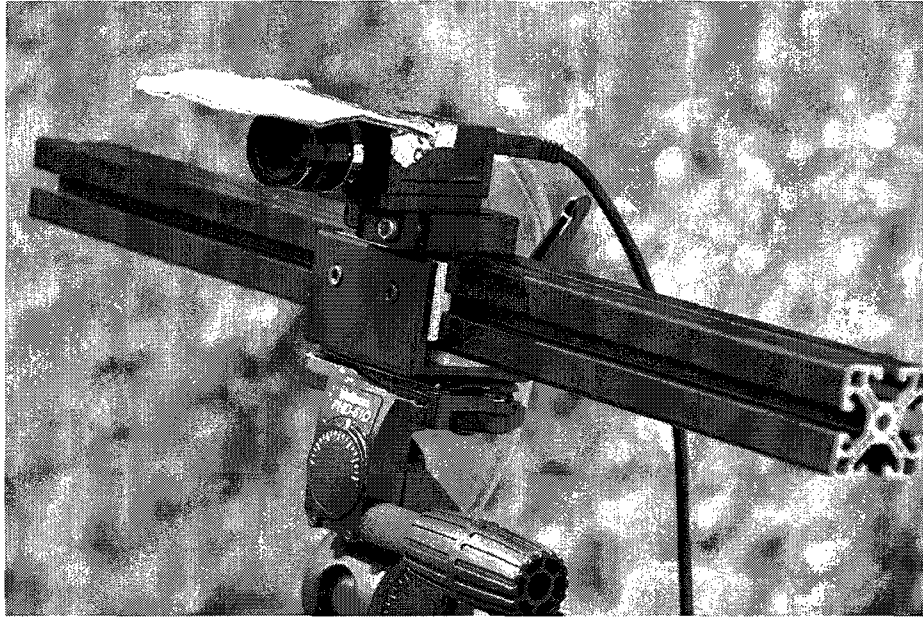


Figure 5-20: DIC camera with visor

The morning started out cool, but towards the end of the testing, the temperatures rose to around 80° F. The rapid warming during the test, combined with direct sunlight on the cameras, is definite cause for concern. Since the cameras are mounted on metal tripods which are prone to temperature shrinkage and expansion, there is significant likelihood that the cameras aberrated slightly throughout the morning. Both the tripods and the cameras themselves are black in color, absorbing a maximum of solar energy and potentially expanding significantly.

The sun also caused problems with the camera exposure settings. When the sun was behind the bridge, the exposure time had to be increased because the speckle pattern was in the shadows. However, as the sun came around to the near side, the exposure time had to be decreased as the ambient light increased. Fortunately, the Vic Snap software can perform that function without interfering with the calibration.

5.3.8 - Examples of Poor Data

Solar Glare. The sun was noticeably shining directly into one or both cameras during parts of tests 4-X1-2 and 7-X2-2. The deflection graph for test 7-X2-2 is shown in Figure 5-21 below. There is severe drifting and jumping of the deflection curve. Although this is a stop test, there is almost no horizontal portion of the graph visible anywhere. Many of the images during that test were entirely washed out, eliminating any data during those time periods.

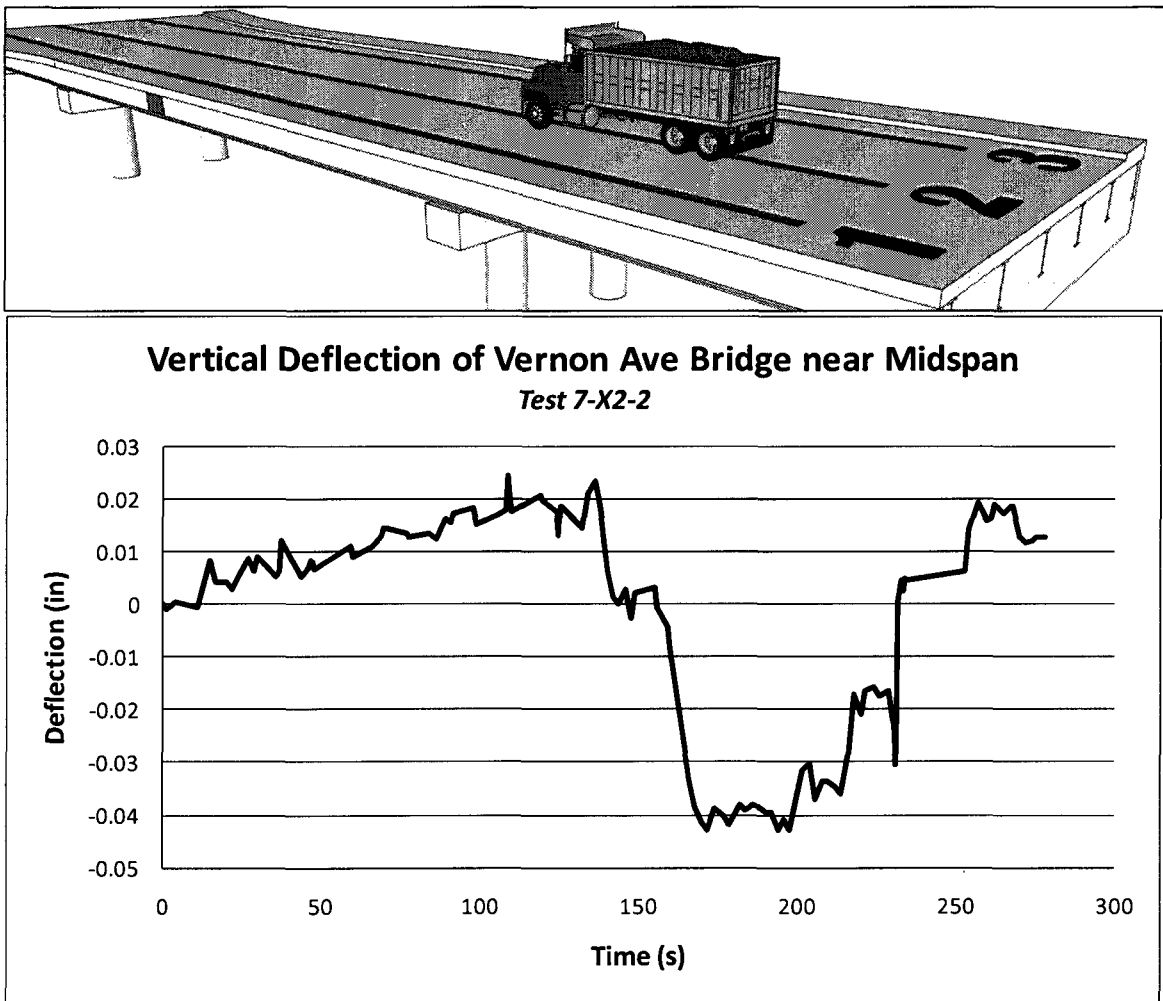


Figure 5-21: Vertical deflection of Vernon Ave Bridge near midspan-Test 7-X2-2

Computer Difficulties. Problems with the computer at the middle span also interfered with many of the tests. The day of the load test the computer was having difficulty maintaining the desired image frequency of one per second. Although Vic Snap was programmed for that frequency, the computer would take several frames per second, and then pause for ten or twenty seconds without taking any images. Two tests were noticeably plagued by this problem, including tests 4-X1-2 (Figure 5-22) and 102-X2-3 (see Appendix A). It is believed that there was a compatibility issue between Vic Snap and the Windows XP Operating System Service Pack 3. After the test Correlated Solutions provided a fix to downgrade the operating system to Service Pack 2, which corrected the problem.

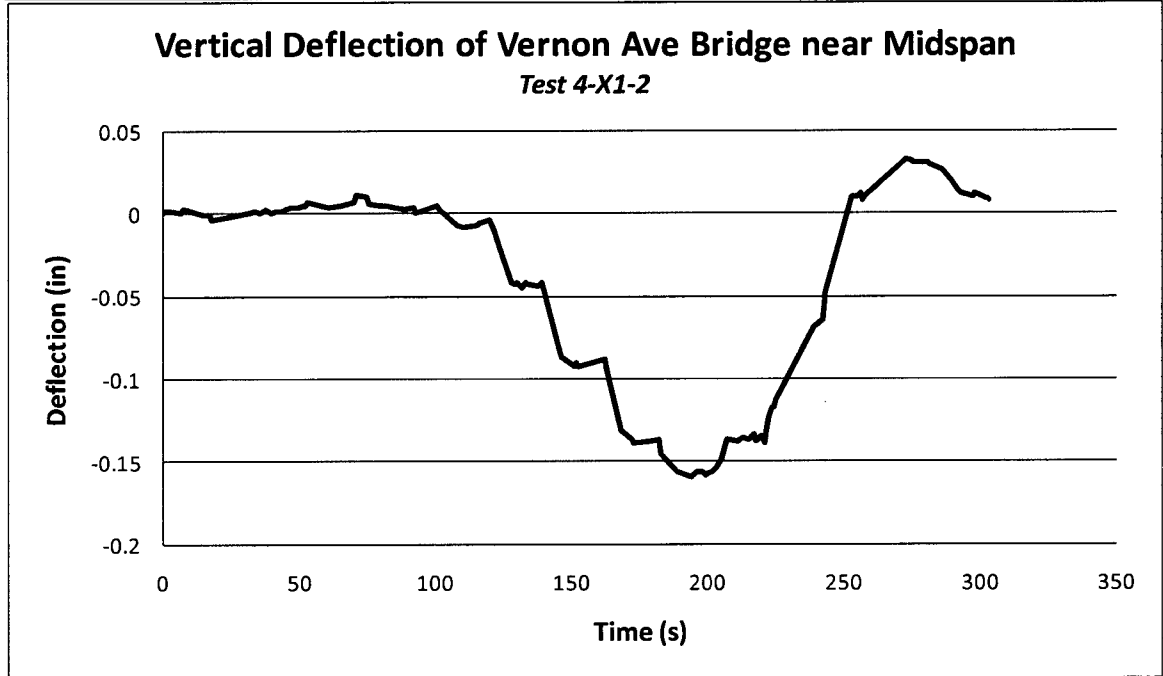
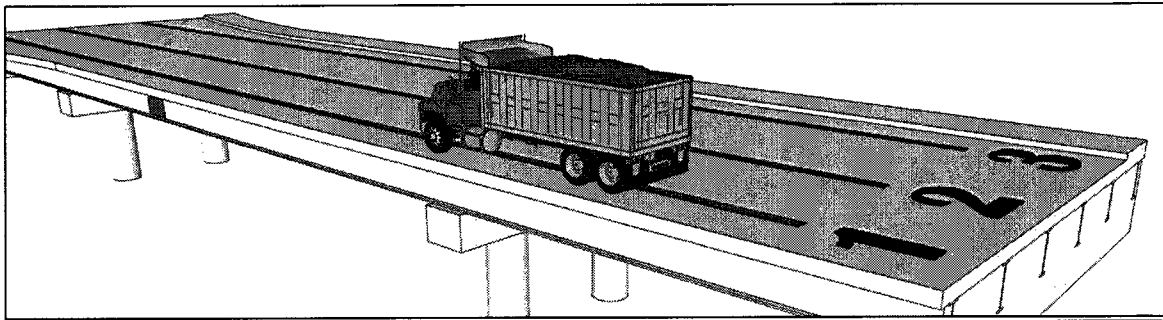


Figure 5-22: Computer error at Vernon Avenue Bridge-Test 4-X1-2

Trending. Another problem that was apparent in many of the tests was trending, or unexpected rising or dropping of the bridge girder. This was most evident in the Ambient tests as well as tests 10-X3-2 and 11-X3-3. The data from Test 10-X3-2 is shown in Figure 5-23.

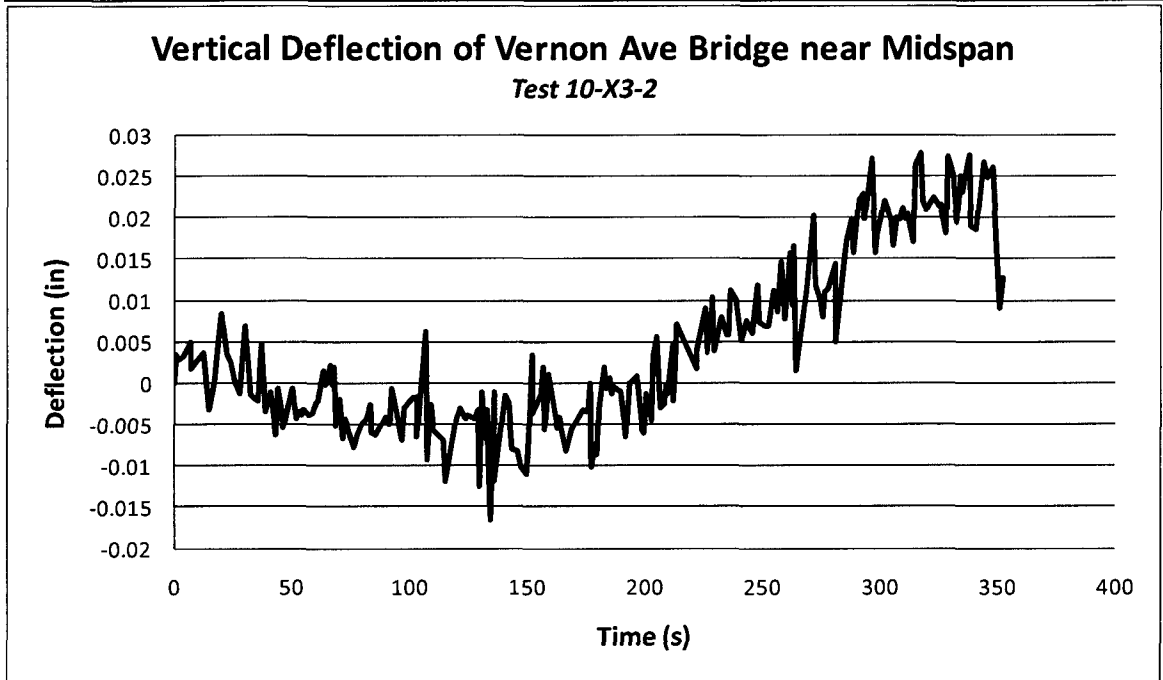
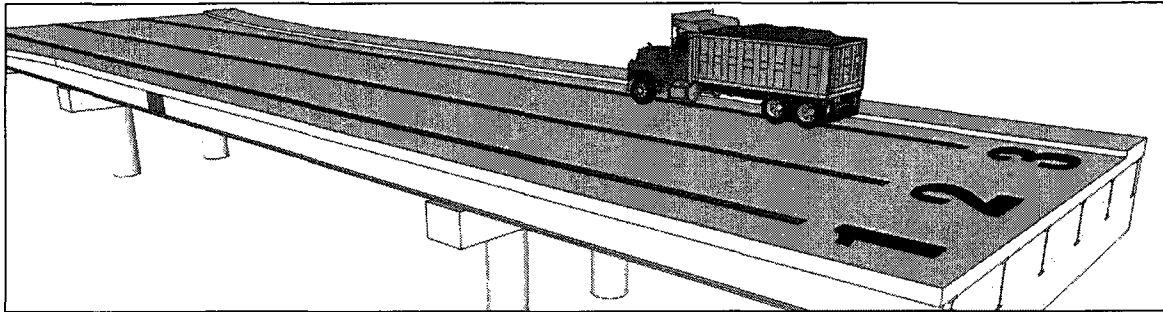


Figure 5-23: Trending of Vernon Avenue data near midspan-Test 10-X3-2

This effect was most evident during tests when the girders were not moving at all (Ambient tests) or when the deflection was so small that the cameras could not detect any deflection, such as when the truck was traveling on the east side of the bridge. The particularly intriguing aspect of this trending is that there appears to be no well-defined pattern of movement. For example, the deflection trends positive in test 10-X3-2, while it drifts negative in test 11-X3-3 (See Appendix A). It could be surmised that the effect of the heat from the sun caused the cameras to shift or the bridge to move slightly; however, a number of problems discussed in Chapter 3 probably

contributed to the error. The amount of deflection with the truck in the East lane can be expected to be very small; therefore it is quite possible that any error present would disguise the results.

5.3.9 - Remarks

Many lessons can be learned from the errors encountered during the deck pour and the load test at Vernon Avenue. It is clearly best to employ as fine a speckle pattern as possible while still maintaining a large enough pattern for the cameras to resolve. Cameras should be placed as close as possible to the testing surface to allow for a fine speckle pattern and reduce camera shake and distortion from temperature changes.

In this case, only the outside girder on one side of the bridge was tested. It would be much more useful to test both outside girders to get an accurate comparison of the deflections on both sides of the bridge. The ideal test would place the cameras under the bridge. The speckle pattern would be applied to the underside of the bottom flange of each girder. This would most likely require artificial lighting, but would provide by far the greatest amount of data. Then the deflection across the entire section could be acquired and structural symmetry observed.

The weather played a tremendous factor in the errors produced in the load test. In future tests, camera placement should be decided carefully to avoid solar glare, and if possible, avoid direct sunlight entirely. If possible, the test should be conducted on an overcast day; this minimizes glare and limits temperature changes, which in turn greatly stabilizes the camera setup. Night testing may even be considered. This could be

especially useful in high-traffic areas, and is quite possible with sufficient artificial lighting. Of course, setting up the cameras under the bridge deck will negate many of these problems.

CHAPTER 6

CONCLUSIONS AND RECOMMENDATIONS FOR FUTURE WORK

6.1 - Conclusions

All of the examples discussed in Chapters 4 and 5 demonstrate the diverse applications for DIC in civil engineering. Whether in the laboratory or in the field, DIC has demonstrated that it has great potential in the lineup of developing SHM technologies. However, there are several challenges and special considerations that must be considered.

Using the DIC system obtained by the University of New Hampshire as a baseline, the anticipated price of a DIC setup sufficient for bridge testing is between \$70,000 and \$80,000. The major cost of DIC is the processing software. A package of image capture software and post-processing software can cost \$40,000 to \$50,000. The cameras, lenses, tripod, and other components are between \$20,000 and \$30,000.

Many may argue that the high capital cost of DIC is overwhelming and cannot be regained in the lifespan of the system. However, if one considers the amount of labor that can potentially be eliminated, the cost of DIC becomes more agreeable. An instrumented bridge can have several thousand feet of cable running along its length. DIC requires very little labor or preparation time. The cost of DIC is clearly a hurdle to

widespread implementation, but considering the labor that it saves, it will pay for itself quickly.

6.2 - Future Work

This research has demonstrated that DIC is capable of accurate data measurement in laboratory testing. The testing did expose several problems, however, especially when the DIC system was used in the field. Tests revealed that large displacements or rotations of the target object can prevent accurate data collection. Also, controlled lighting conditions are nearly essential for accurate testing. Bringing DIC out into the field uncovered a plethora of problems that outdoor conditions create in DIC testing. Sun, wind, temperature, vibrations, lighting, and site conditions are some of the factors that can all have a large impact on the accuracy of the test data. The more these factors can be controlled during a test, the more likely that error will be held to a minimum.

Most of the tests in this research were conducted as a supplement to other research conducted by fellow graduate students. Ideally, DIC testing needs to be independent and completely controlled. The tests described here produced largely satisfactory results, but they did not prove that DIC is a completely effective tool for bridge testing. Several variables remain unknown; in nearly all of the field tests significant error was present. The source of this error can be surmised, but in reality it cannot be unequivocally attributed to any specific cause.

A series of controlled experiments will need to be conducted to determine the root of these errors. These tests must be highly controlled, with all but one variable remaining constant during each series of tests. These variables include:

- Camera distance from target
- Camera angle with respect to target
- Camera separation
- Camera resolution
- Focal length
- Aperture
- Speckle pattern types
- Speckle pattern “dot” sizes
- Calibration target sizes
- Target rotation
- Temperature
- Wind speed
- Lighting conditions (artificial lighting, sunny versus cloudy, etc.)

After this testing is conducted, a table of allowable values for each of these variables can be constructed. For example, the table would specify how far the cameras can be placed from the target surface with a certain size speckle pattern to produce an acceptably low error value, given the temperature and wind speed during the test. The table will also provide guidance to develop a filtering technique to reduce the noise in DIC data. Once the relationship between the aforementioned variables is realized, filters can be applied to the data to correct for the conditions during a specific test. Most importantly, the table will provide objectivity to the DIC testing process and specify the limits of the technology so that future researchers and test engineers can successfully apply DIC to bridge health monitoring.

Objectivity in DIC testing methodology will enable the technology to become a major asset to bridge managers who are trying to initiate long-term bridge monitoring. The DIC system could be employed as a supplement to visual inspection and be used to develop a baseline which is especially critical for long-term monitoring. With further testing, DIC has the potential to be a vital cog in the effort to transform bridge management.

WORKS CITED

- A&M University. (2004). *Transportation Images - Highway Transportation*. Retrieved April 30, 2010, from Texas Transportation Institute:
http://tti.tamu.edu/groups/cpd/resources/images/highway_transportation.htm
- AASHTO. (2008). *Bridging the Gap-Restoring and Rebuilding the Nation's Bridges*. Washington, D.C.: American Association of State Highway and Transportation Officials.
- Applied Geomechanics*. (2010). Retrieved April 30, 2010, from 900 Series Tiltmeters and Clinometers: <http://www.carboceramics.com/agi/900-series/>
- ASCE. (2010). *Report Card for America's Infrastructure*. Retrieved April 22, 2010, from <http://www.infrastructurereportcard.org/>
- Aydilek, A. H., Oguz, S. H., & Edil, T. B. (2002). Digital Image Analysis to Determine Pore Opening Size Distribution of Nonwoven Geotextiles. *Journal of Computing in Civil Engineering*, 16 (4), 280-290.
- BDI. (2009). *FIELD TESTING AND LOAD RATING REPORT: RIDOT#292 – TIVERTON, RI*.
- Bell, E. S., Sanayei, M., Javdekar, C. N., & Slavsky, E. (2007, August). Multiresponse Parameter Estimation for Finite-Element Model Updating Using Nondestructive Test Data. *Journal of Structural Engineering*, 1067-1079.
- CSI. (2007). *Vic-3D 2007 Testing Guide*. Columbia, South Carolina: Correlated Solutions.
- CS1a. (2009). *CSI History*. Retrieved April 24, 2010, from <http://www.correlatedsolutions.com/index.php/about-us>
- CS1b. (2009). *Easily Quantify Strain Measurements with the Vic-3D System*. Retrieved April 23, 2010, from <http://www.correlatedsolutions.com/index.php/component/content/article/78>
- Dantec Dynamics. (2010). *Digital Image Correlation for Deformation Measurement*. Retrieved April 30, 2010, from <http://www.dantecdynamics.com/Default.aspx?ID=1030>
- Digi-key. (2010). *LVDTs-Sensors, Transducers*. Retrieved April 22, 2010, from <http://parts.digikey.com/1/parts-cats/index23.html>

FHWA. (2006, November 16). *Freeway Management and Operations Handbook*. Retrieved April 23, 2010, from U.S. Department of Transportation Federal Highway Administration: http://ops.fhwa.dot.gov/freewaymgmt/publications/frwy_mgmt_handbook/chapter15_01.htm

FHWA. (2010). *History of the Interstate Highway System*. Retrieved April 22, 2010, from U.S. Department of Transportation Federal Highway Administration: <http://www.fhwa.dot.gov/interstate/history.htm>

FHWA. (2004). *Status of the Nation's Highways, Bridges, and Transit: 2004 Conditions and Performance*. Retrieved May 01, 2010, from <http://www.fhwa.dot.gov/policy/2004cpr/chap15c.htm>

Fuchs, P. A., Washer, G. A., Chase, S. B., & Moore, M. (2004, November). Laser-Based Instrumentation for Bridge Load Testing. *Journal of Performance of Constructed Facilities* , 213-219.

Gamache, R., & Santini-Bell, E. (2009). Non-intrusive Digital Optical Means to Develop Bridge Performance Information. *Non-Destructive Testing in Civil Engineering* .

ISHMII. (2010). *About ISHMII*. Retrieved April 30, 2010, from <http://www.ishmii.org/AboutIshmii/AboutIshmii.html>

Japanese Ministry of Land, I. T. (2008). *What's ITS*. Retrieved April 22, 2010, from http://www.mlit.go.jp/road/ITS/topindex/topindex_g02_1.html

Lee, J. J., & Shinozuka, M. (2006). A Vision-based System for Remote Sensing of Bridge Displacement. *NDT&E International* (39), 425-431.

Macro Sensors. (2009). Retrieved April 23, 2010, from LVDT Basics: http://www.macrosensors.com/lvdt_tutorial.html

Mayer, L., Yanev, B., Olson, L. D., & Smyth, A. W. (2010). Monitoring of the Manhattan Bridge for Vertical and Torsional Performance with GPS and Interferometric Radar Systems. *Transportation Research Board Annual Meeting 2010*. New York: TRB.

MHD. (2007). *Structures Inspection Field Report*. Barre: Massachusetts Highway Department.

NJDOT. (2010, March 8). *Roadway Information and Traffic Counts: Weigh-in-Motion System*. Retrieved April 23, 2010, from <http://www.state.nj.us/transportation/refdata/roadway/truckwt.shtm>

Phares, B. M., Rolander, D. D., Graybeal, B. A., & Washer, G. A. (2000). Studying the Reliability of Bridge Inspection. *Public Roads* , 64 (3).

Reiker. (2010). *Accelerometers: Linear Static and Dynamic*. Retrieved April 22, 2010, from <http://www.riekerinc.com/Accelerometers.htm>

Robert, C. W. (2009). *Transverse Joint Configuration Development and Testing for a Modular Bridge Deck Replacement System*.

Sanayei, M., Brenner, B. R., Santini-Bell, E., Sipple, J. D., Phelps, J. E., & Lefebvre, P. J. (2010). Baseline Model Updating During Bridge Construction Using Measured Strains. *ASCE Structures Congress* .

Sipple, J. D. (2008). *Structural Modeling and Monitoring of the Rollins Road Bridge for Condition Assesment*.

Sleiman, S. (2009, February). Smart Bridges-Bridging the Visual Gap. *Roads & Bridges* , pp. 50-53.

Strain Gauges. (2010). Retrieved April 22, 2010, from All About Circuits:
http://www.allaboutcircuits.com/vol_1/chpt_9/7.html

Washer, G. A. (1998). Developments for the Non-destructive Evaluation of Highway Bridges in the USA. *NDT&E International* , 31 (4), 245-249.

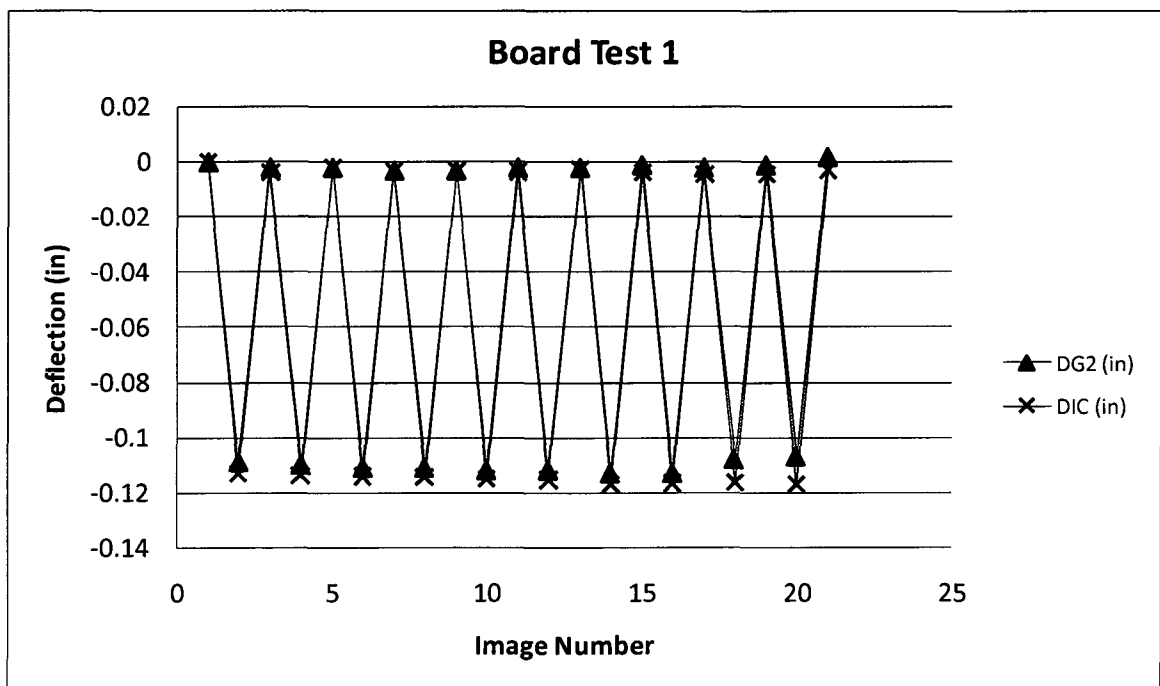
APPENDICES

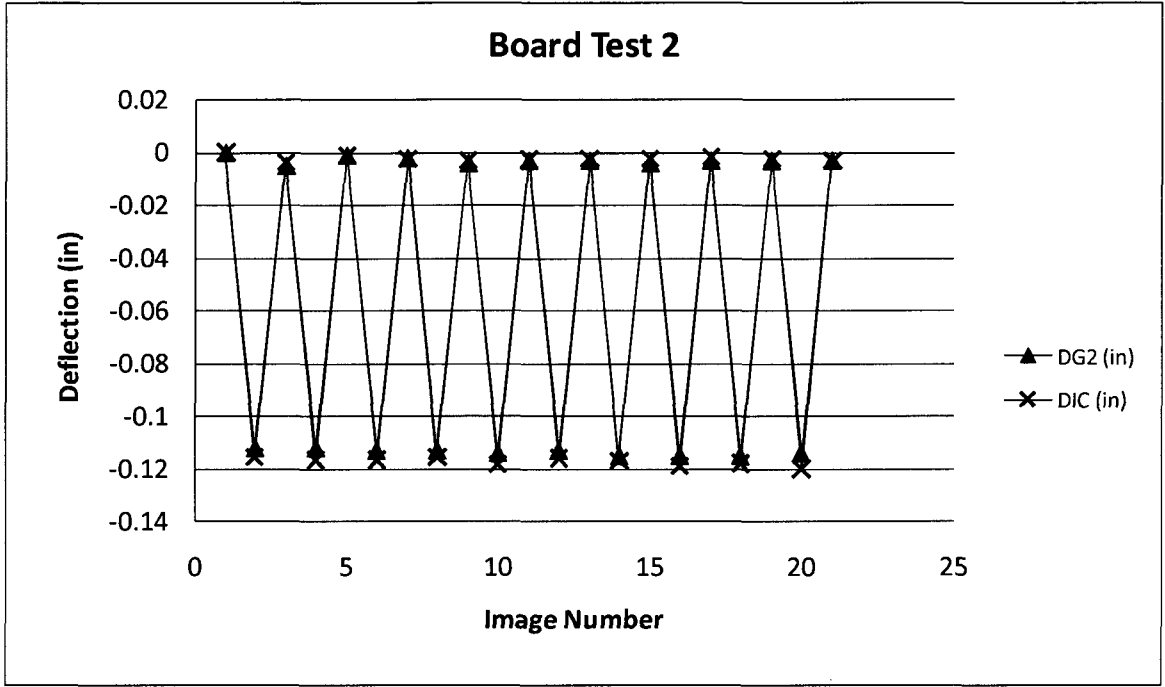
APPENDIX A

TEST RESULTS

Board Test

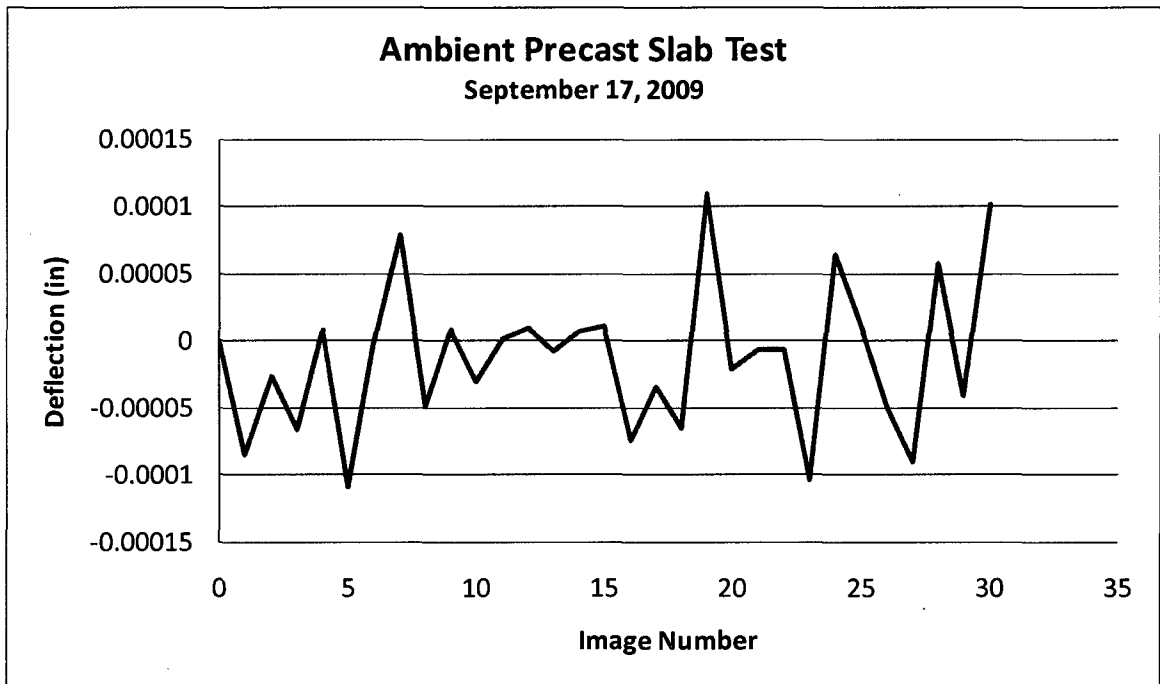
The first test conducted as part of this research at the University of New Hampshire using the DIC system was a simple verification of the accuracy of the cameras and the functionality of the post-processing software.

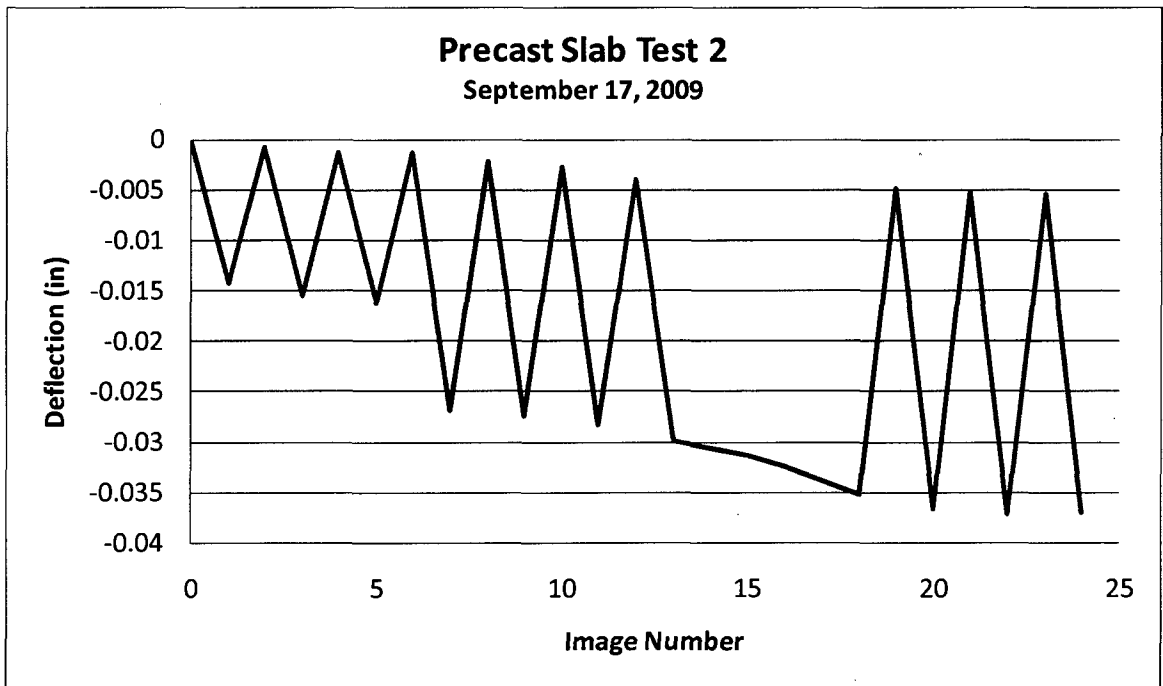
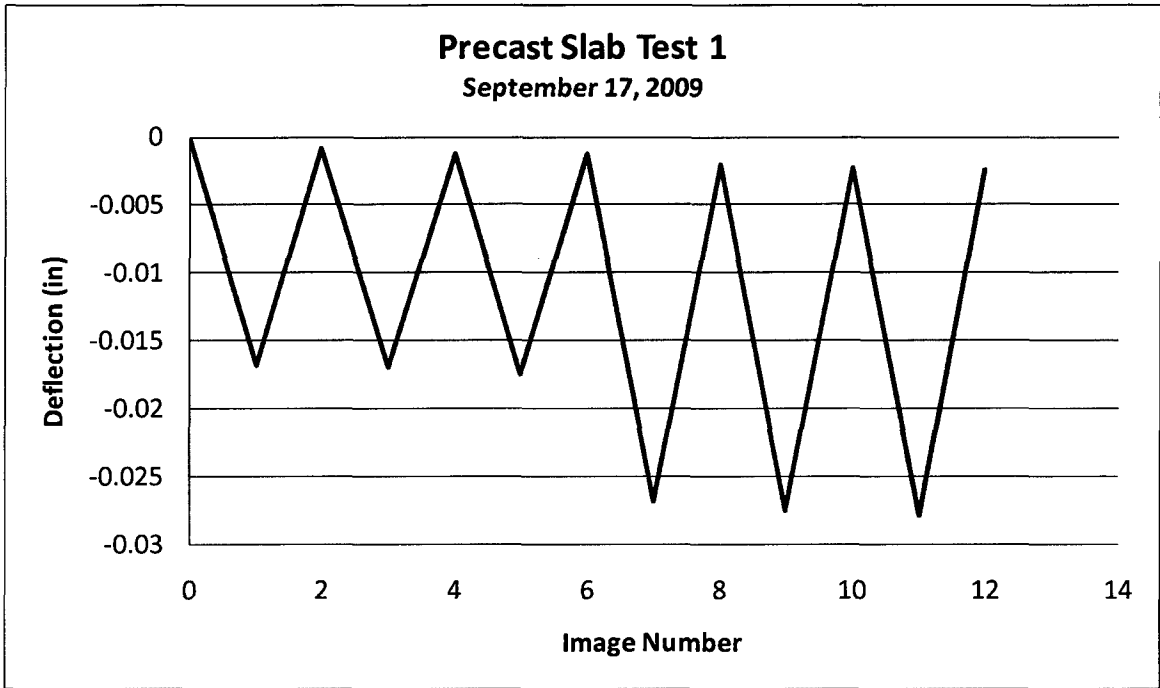




Slab Tests

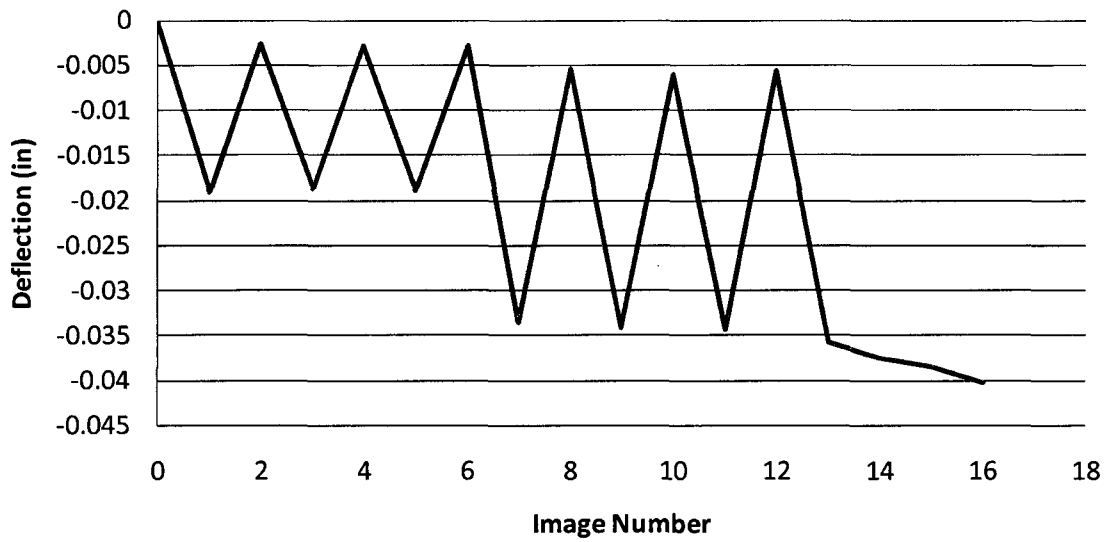
Three tests were conducted on precast concrete slabs to determine their maximum allowable service for a rapid bridge deck replacement system. The DIC system was used to collect deflection data.





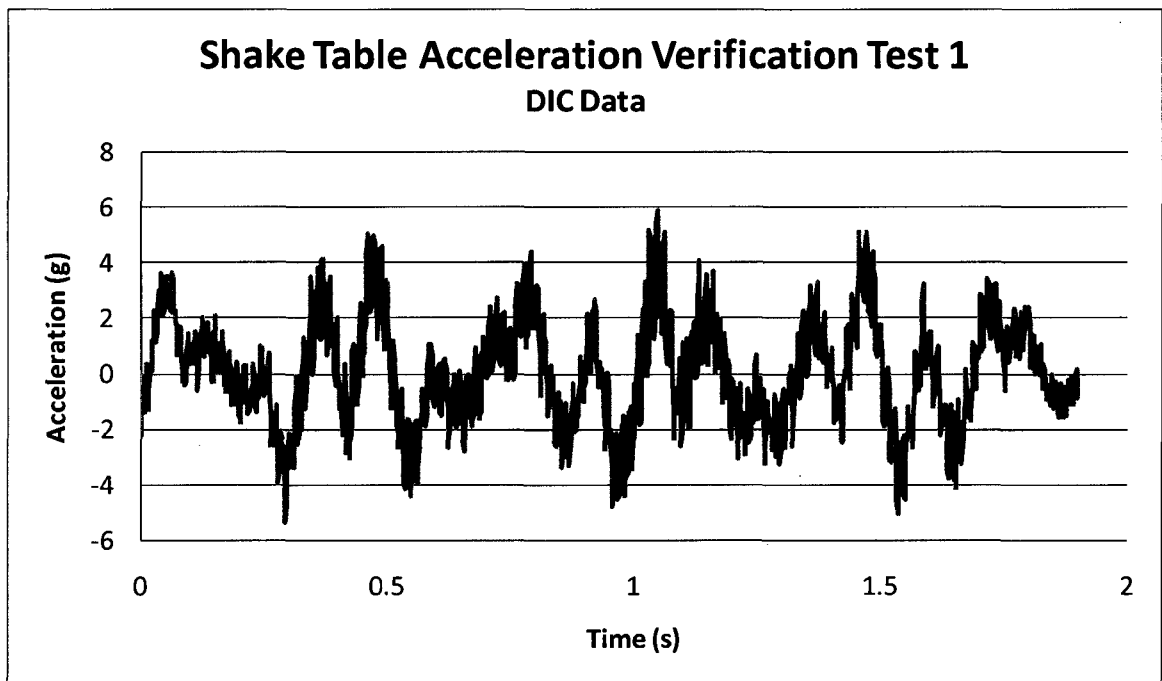
Precast Slab Test 3

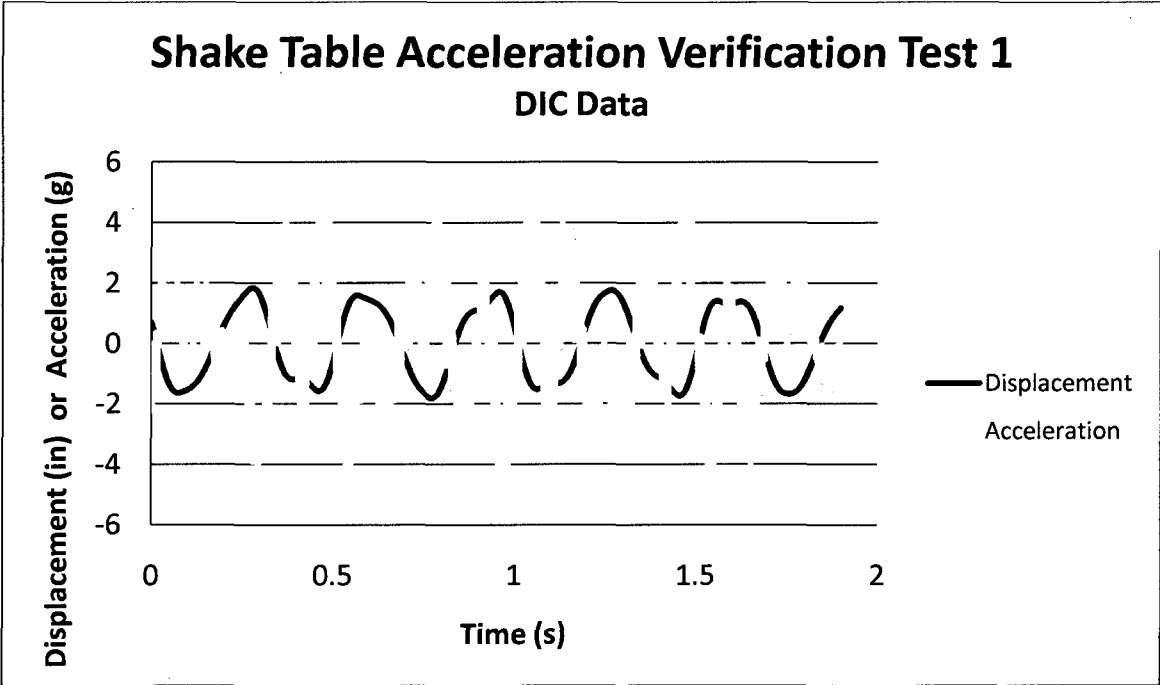
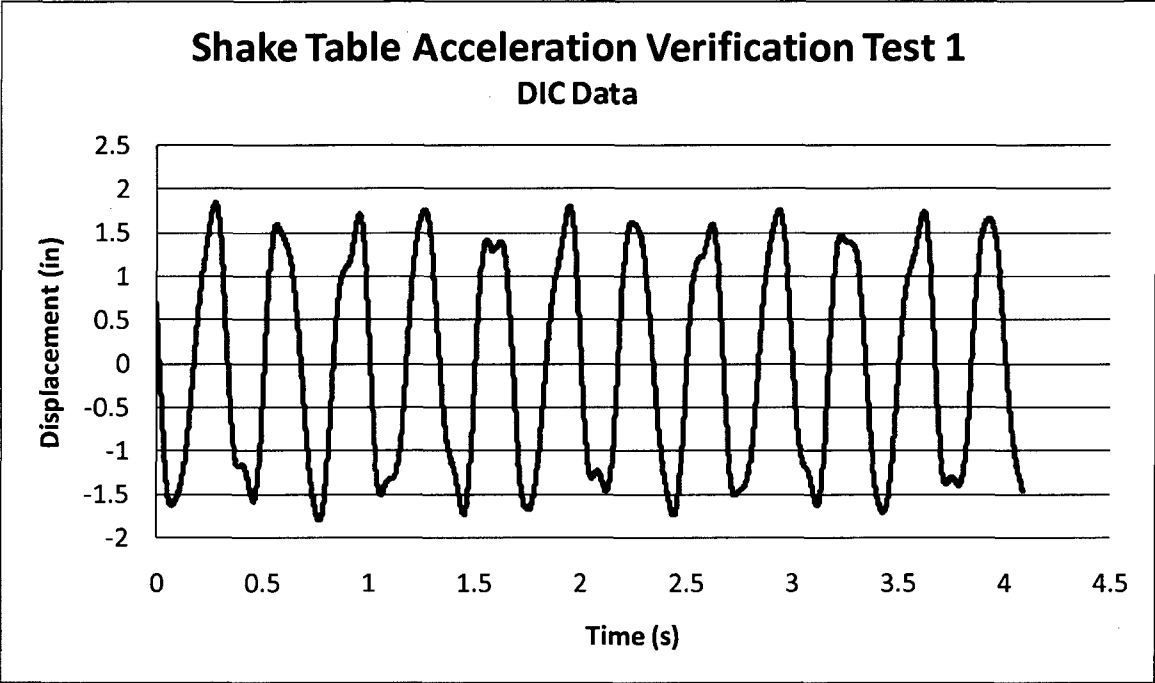
September 17, 2009



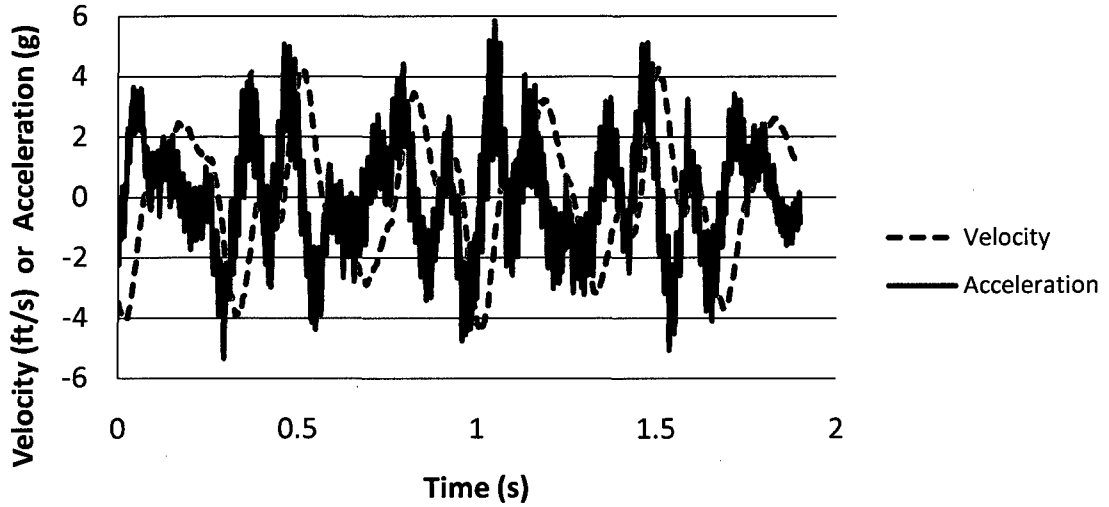
Shake Table Tests

Three tests were conducted using a stick model on the UNH shake table to verify an analytical computer model. The DIC system collected displacement data and accelerometers gathered acceleration data during testing. Acceleration was calculated from the DIC displacement data and compared to the acceleration measured by the accelerometers.

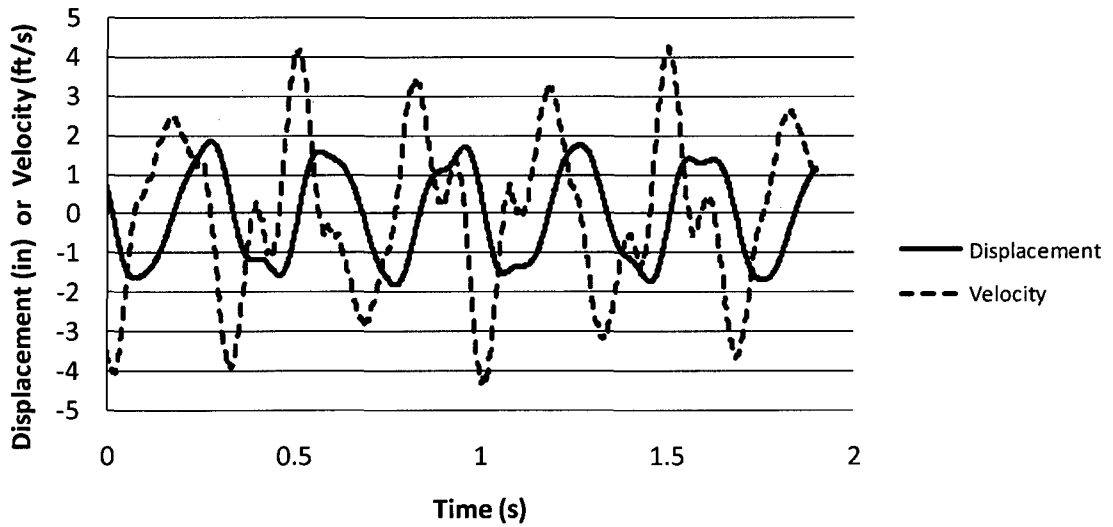


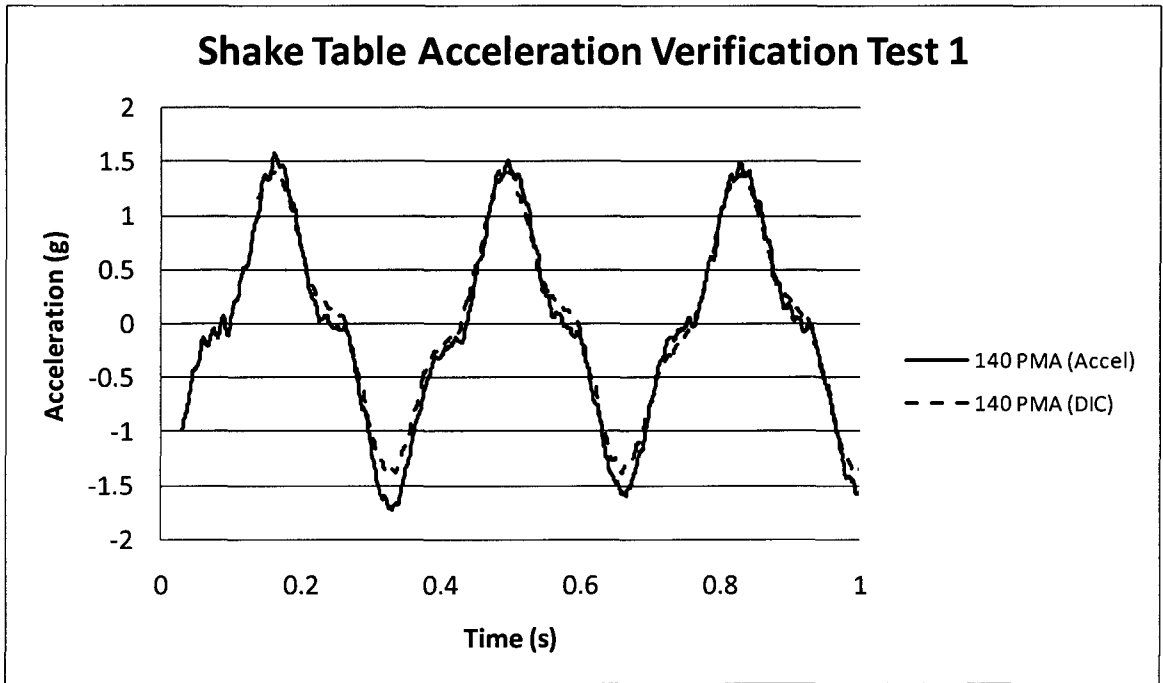
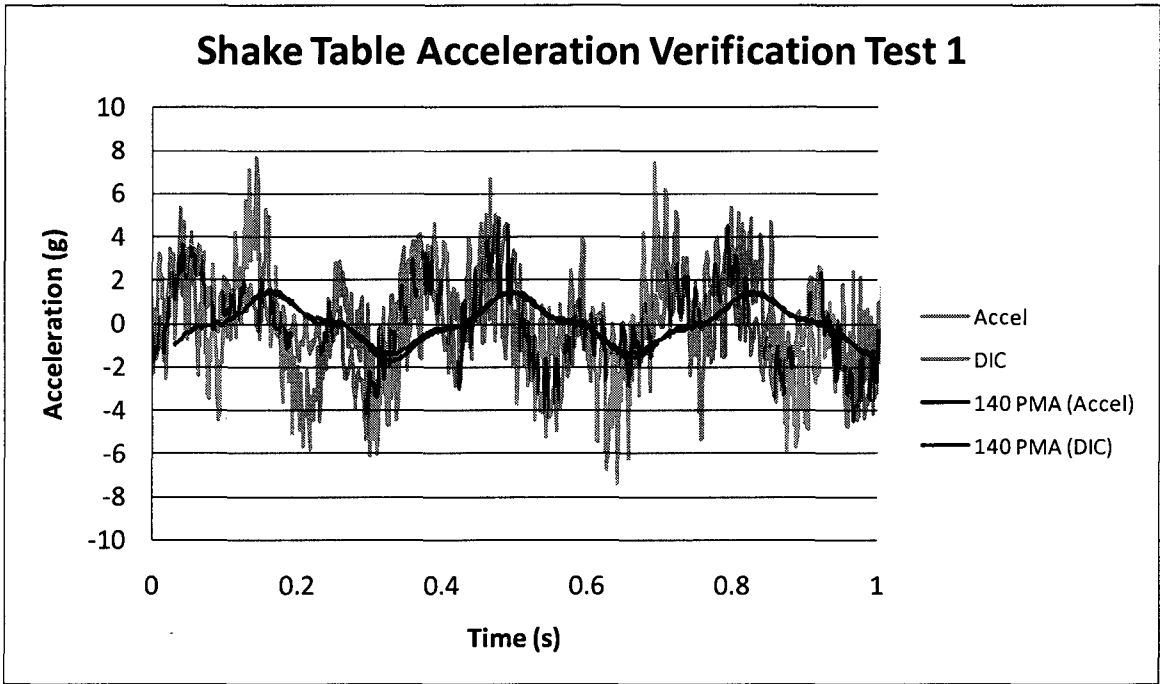


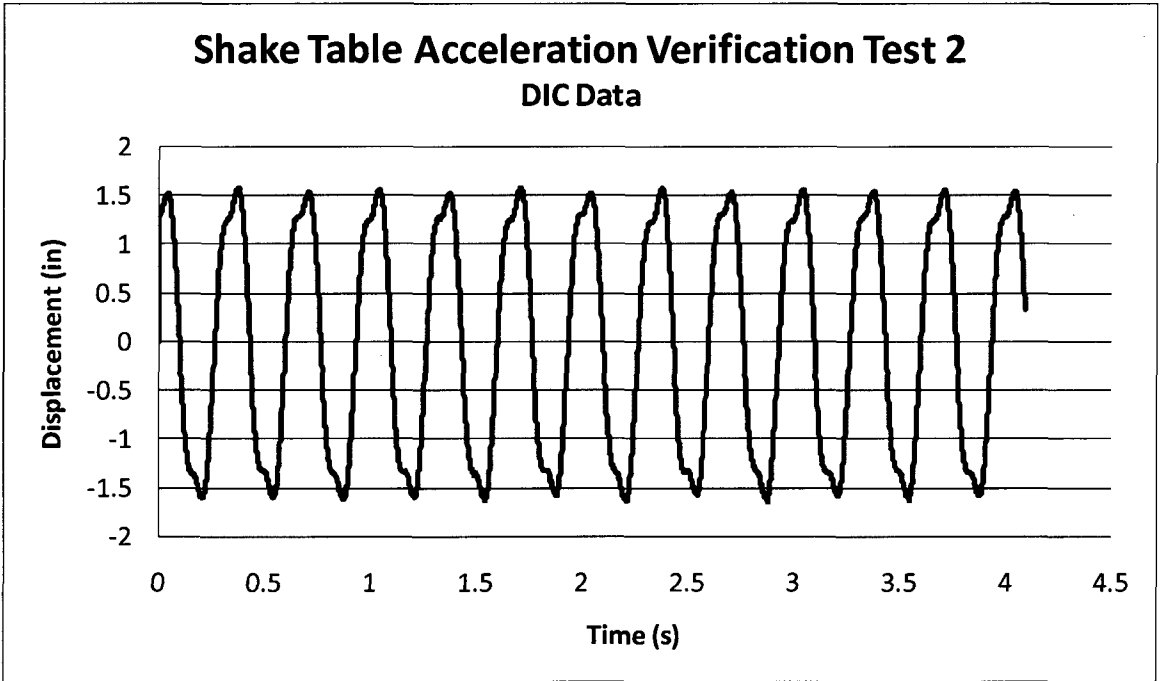
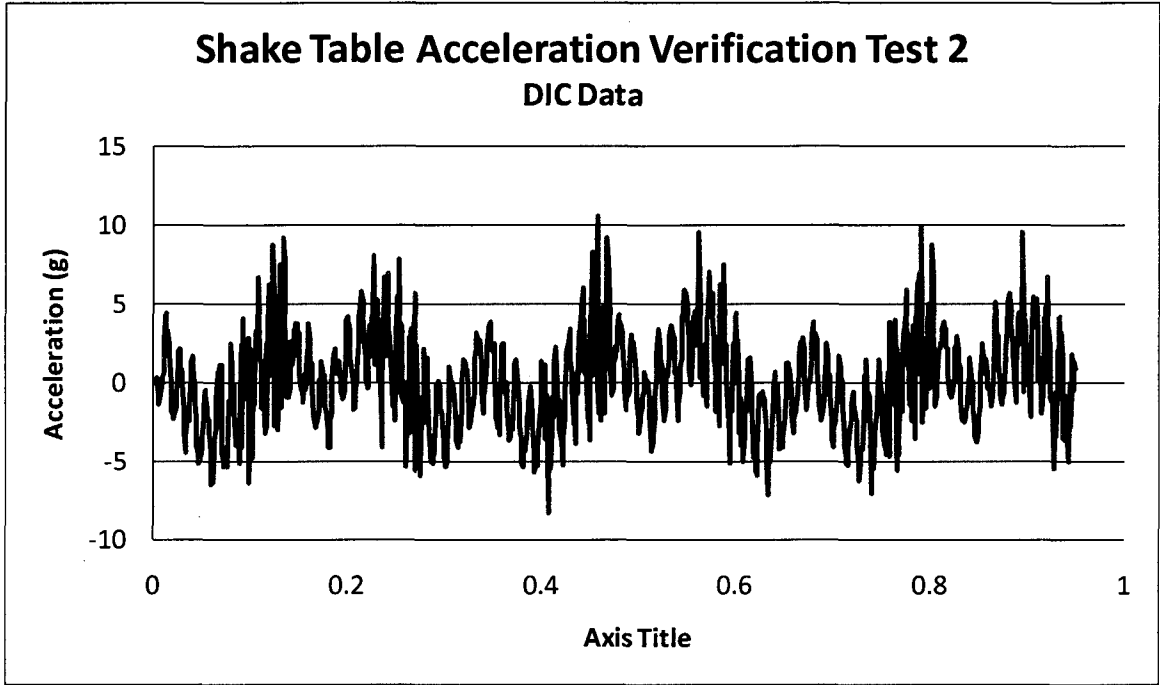
Shake Table Acceleration Verification Test 1 DIC Data

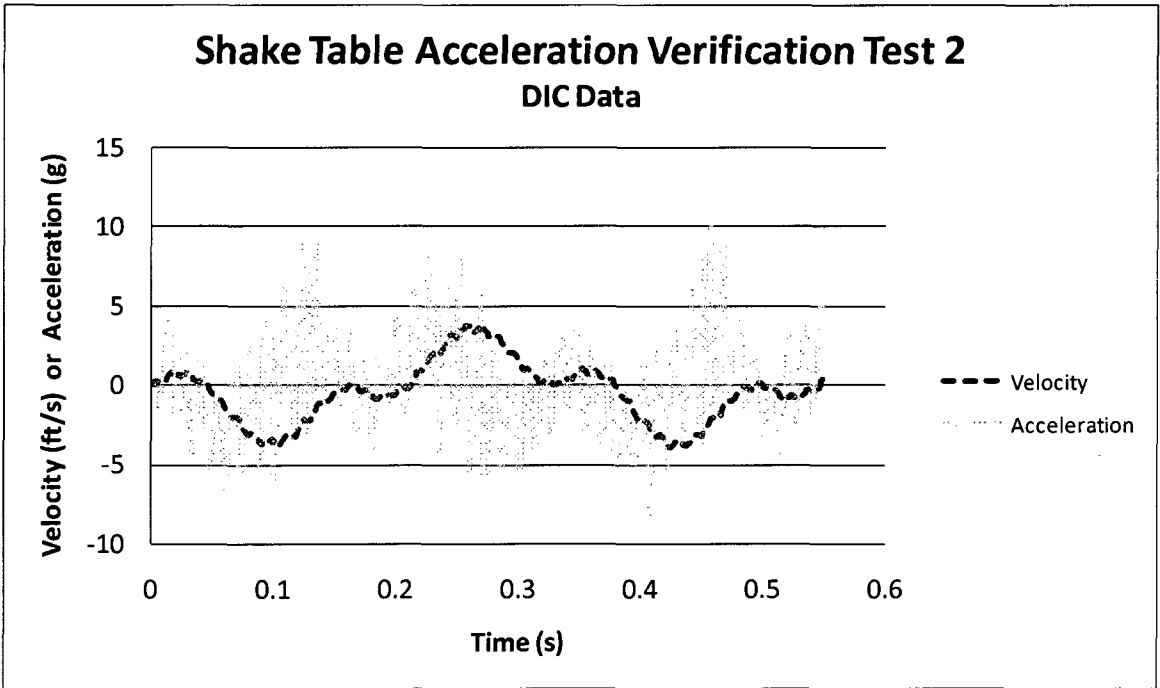
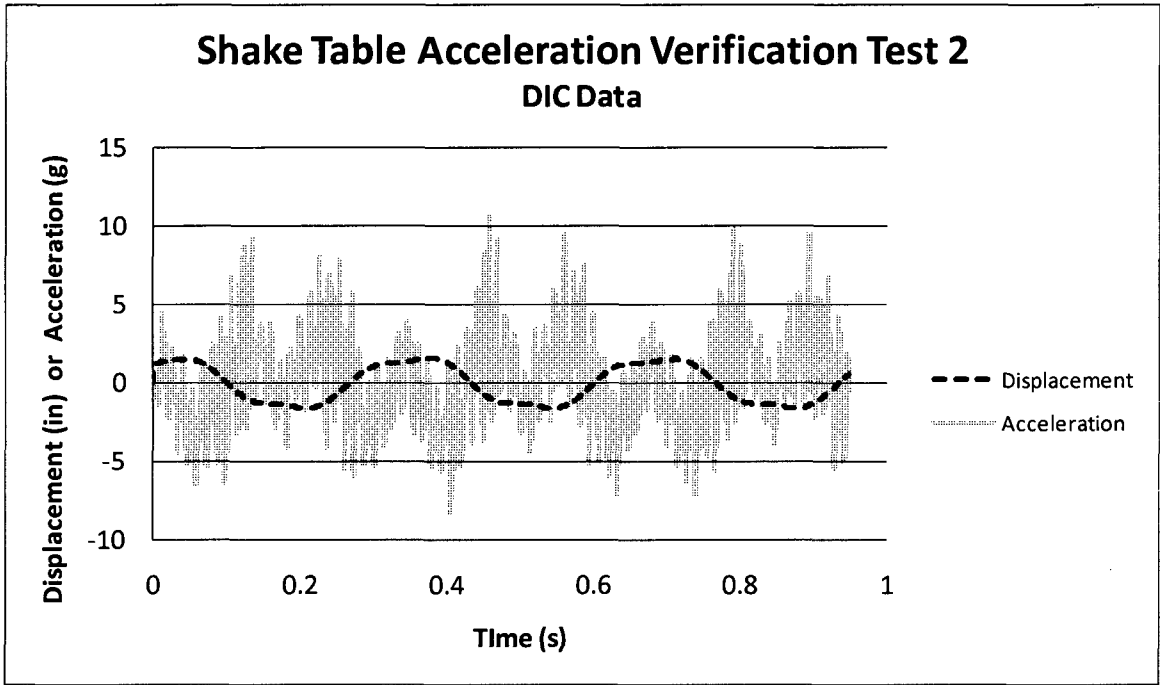


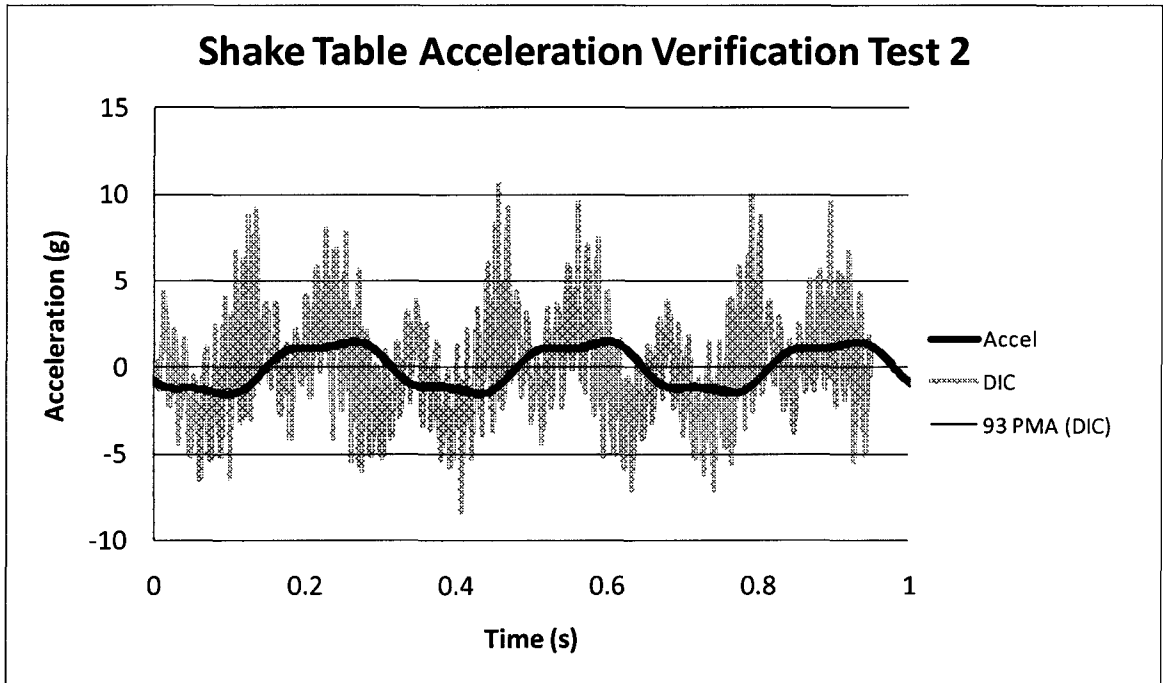
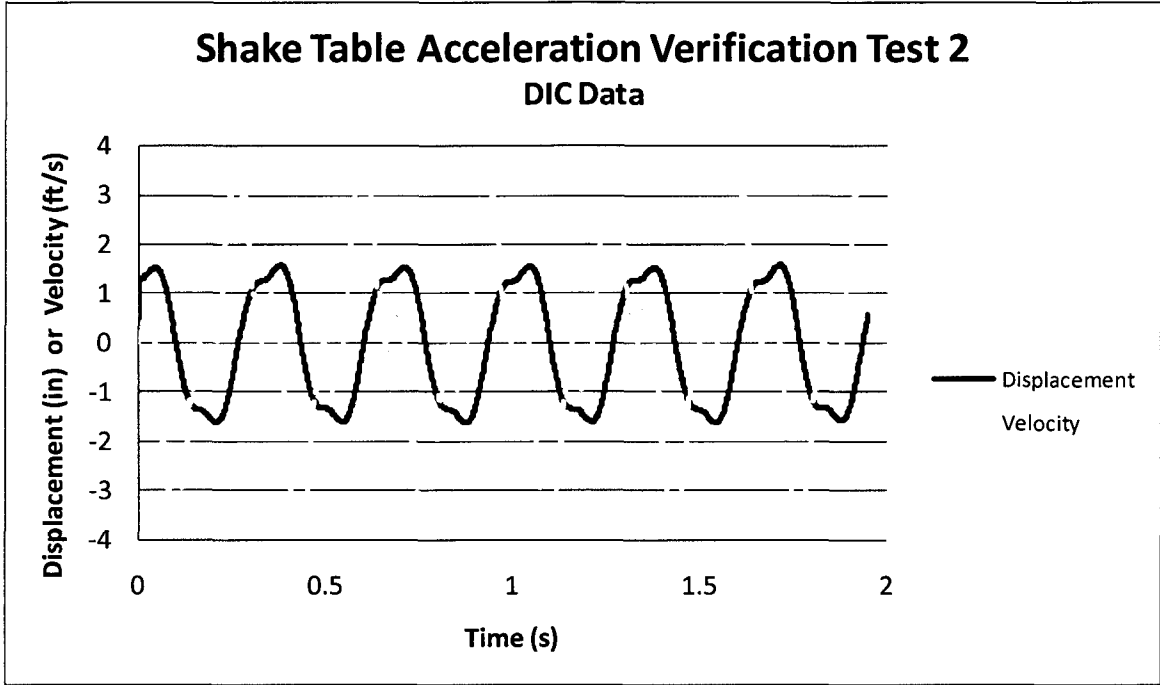
Shake Table Acceleration Verification Test 1 DIC Data

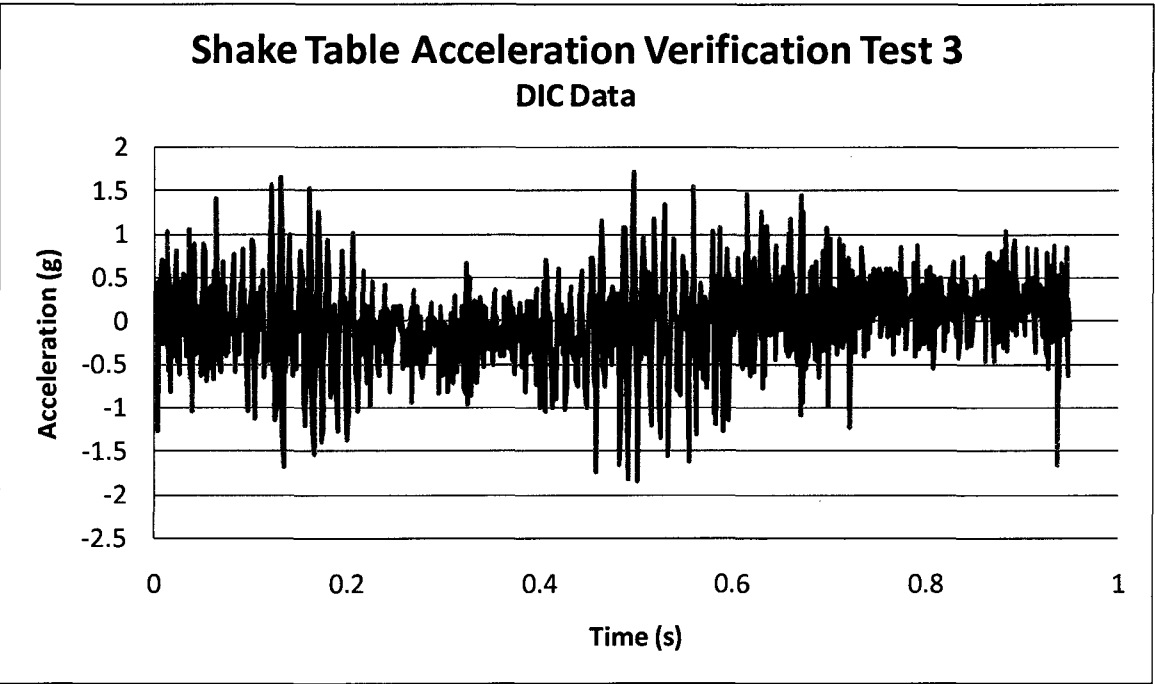
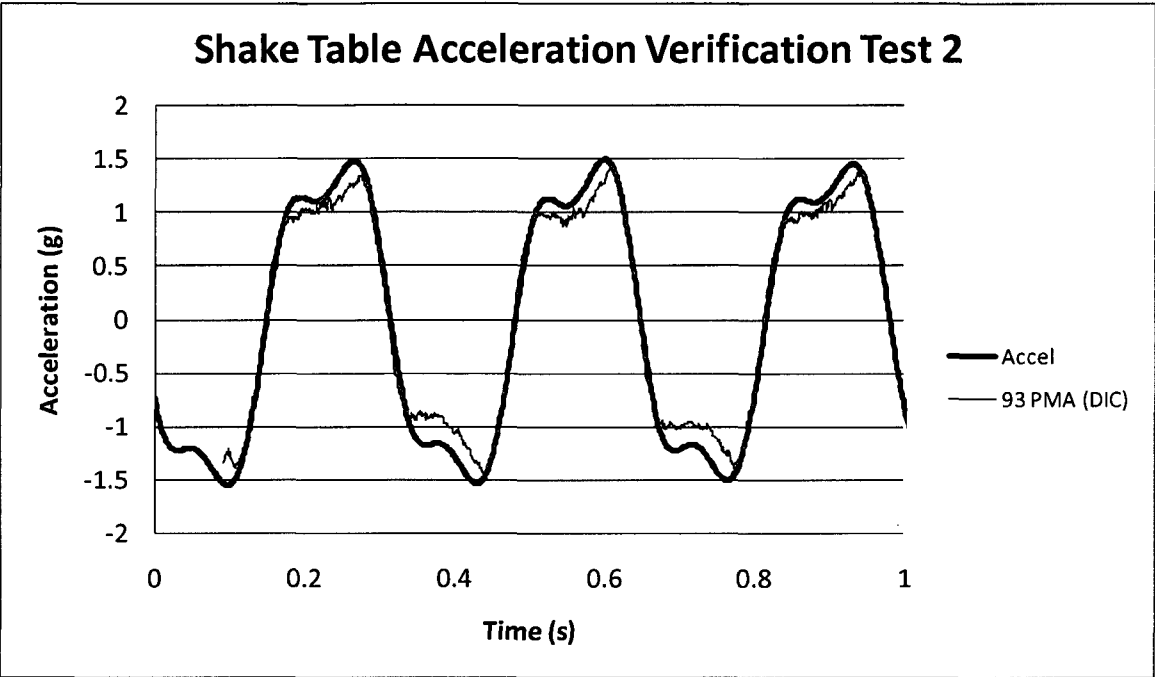


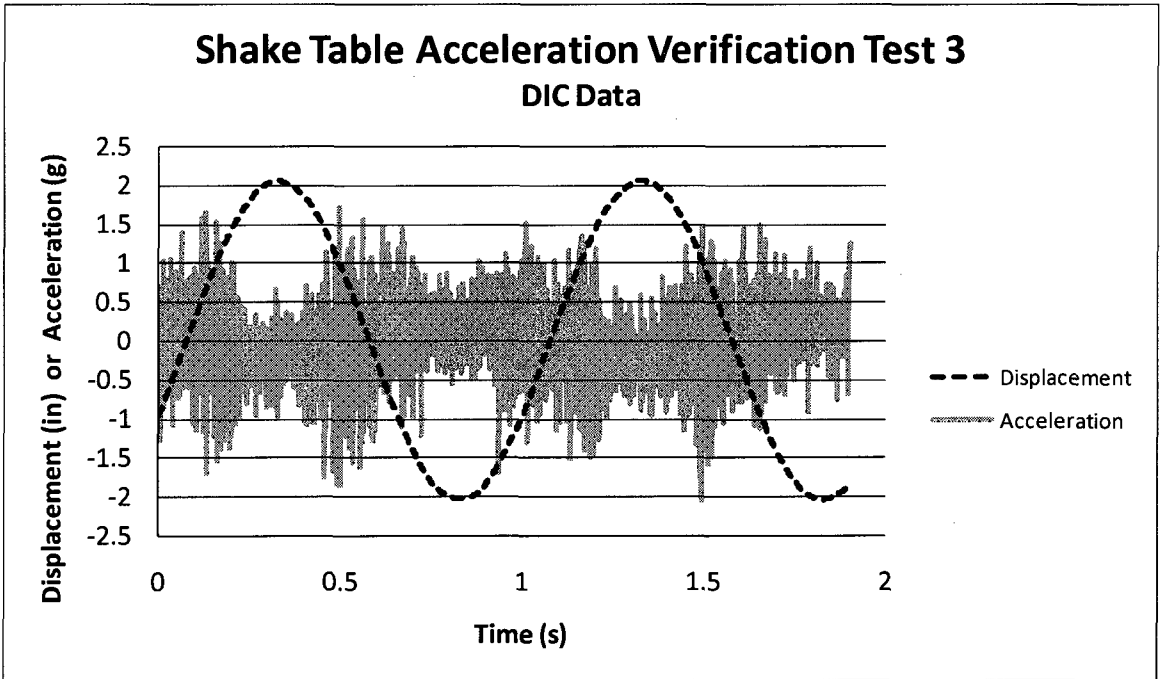
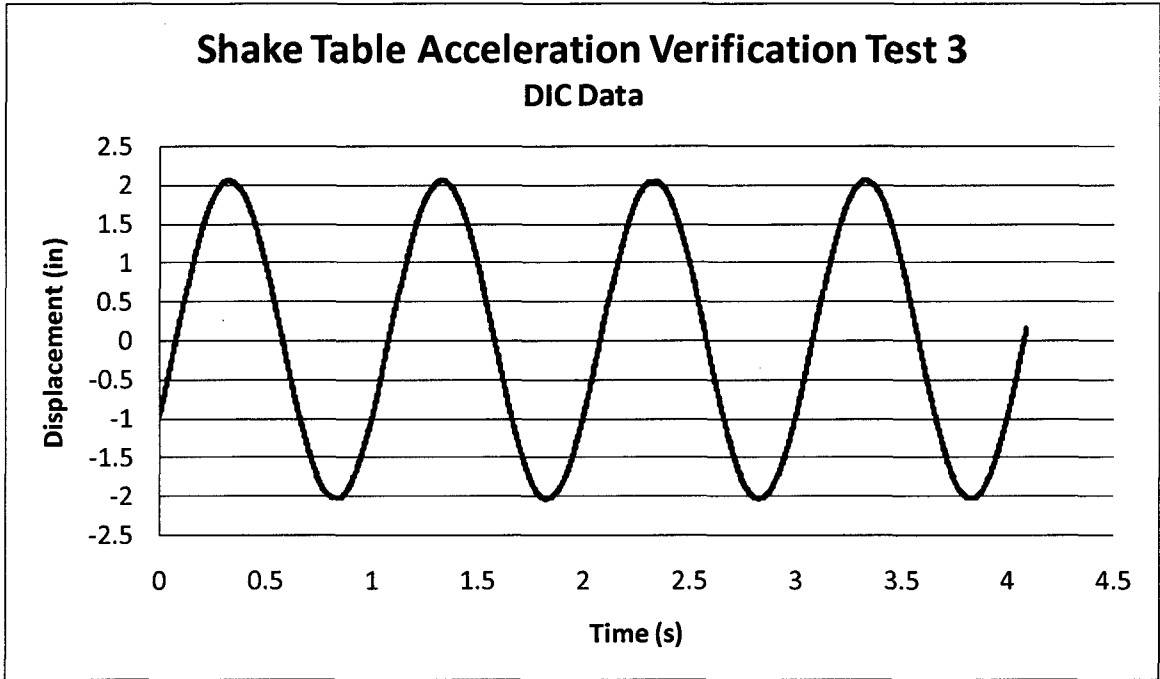




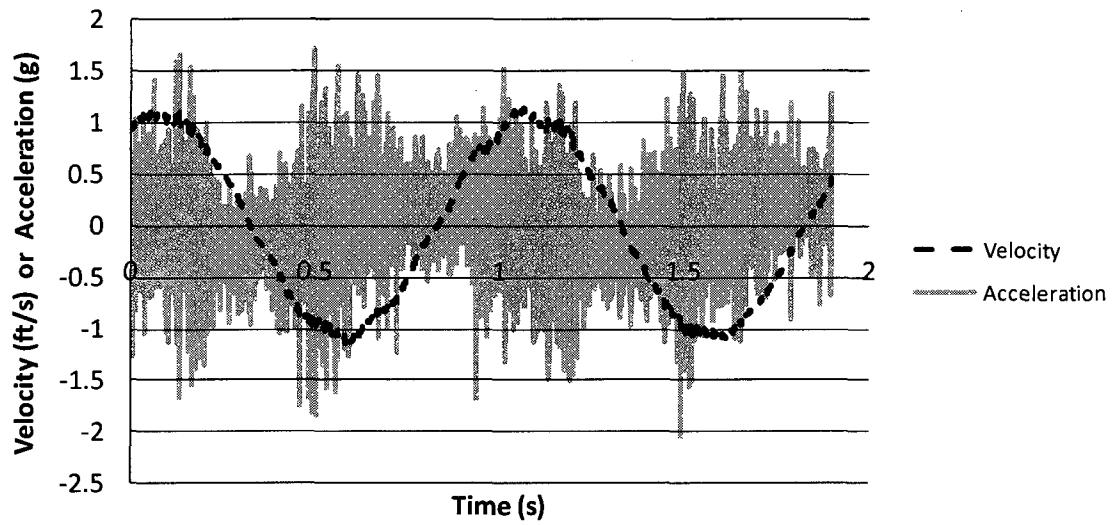




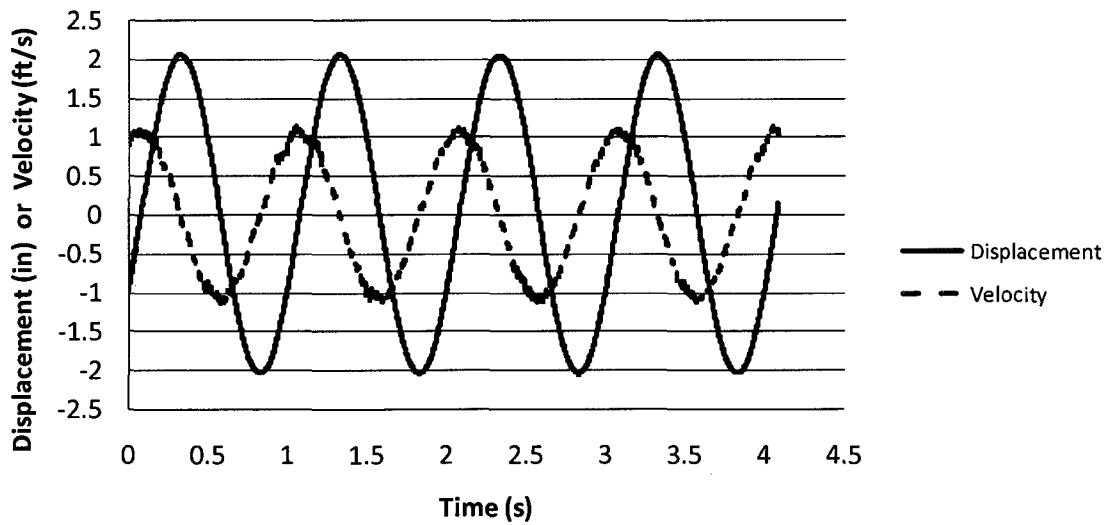


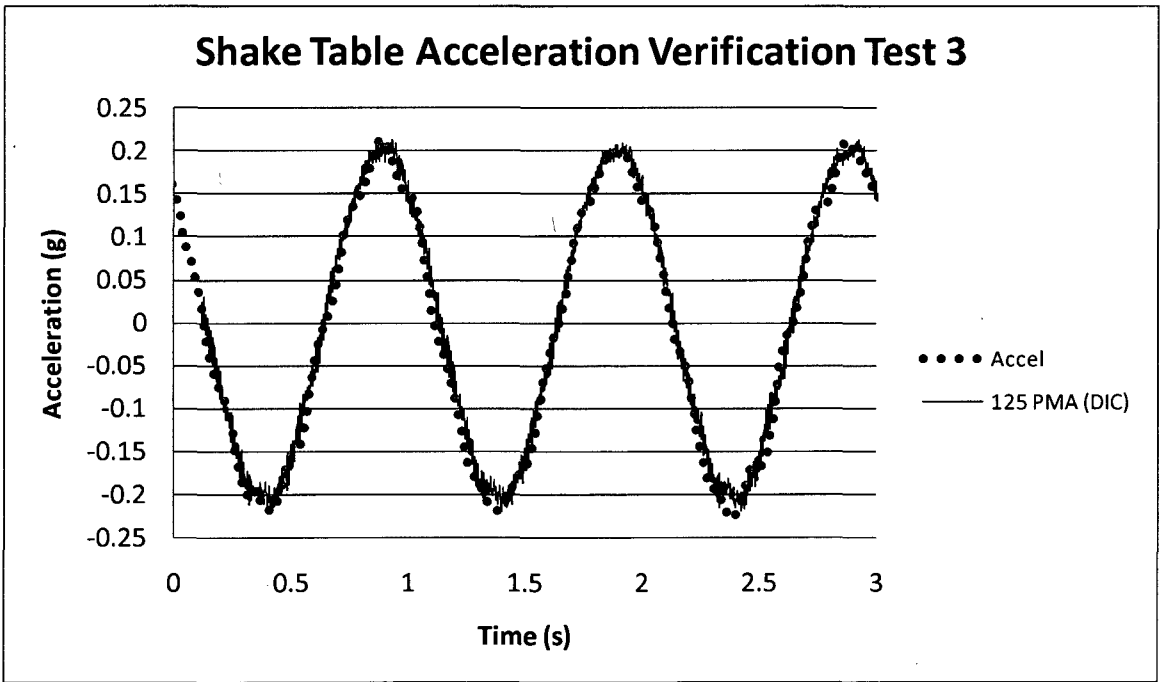
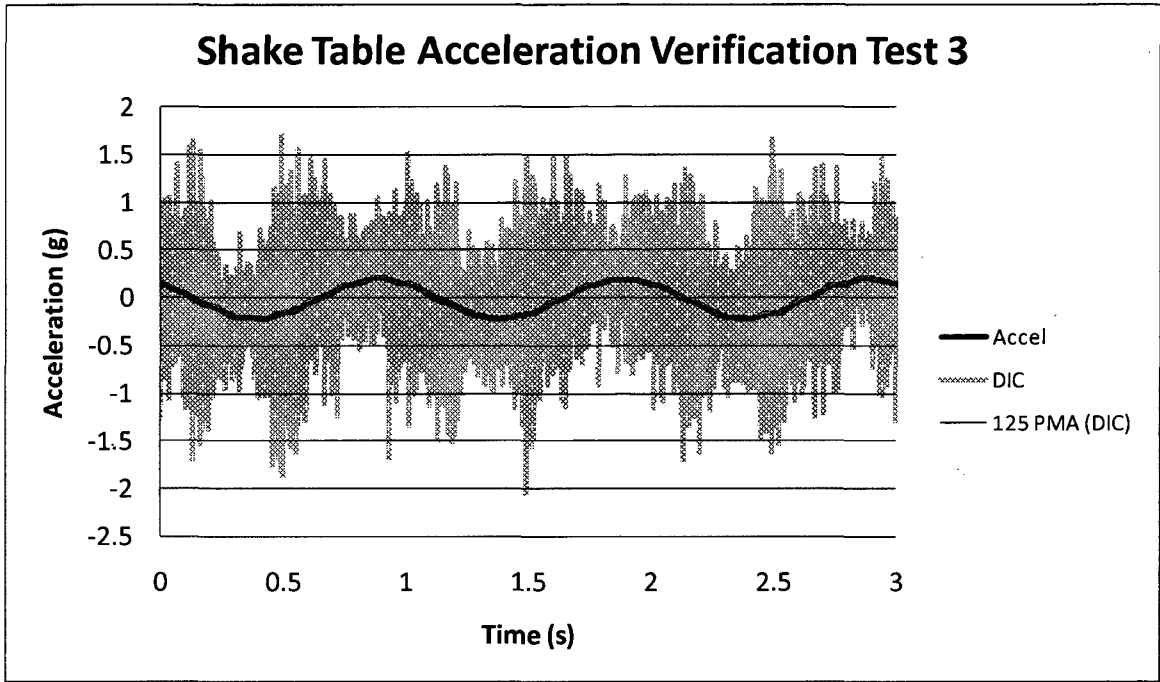


Shake Table Acceleration Verification Test 3 DIC Data



Shake Table Acceleration Verification Test 3 DIC Data

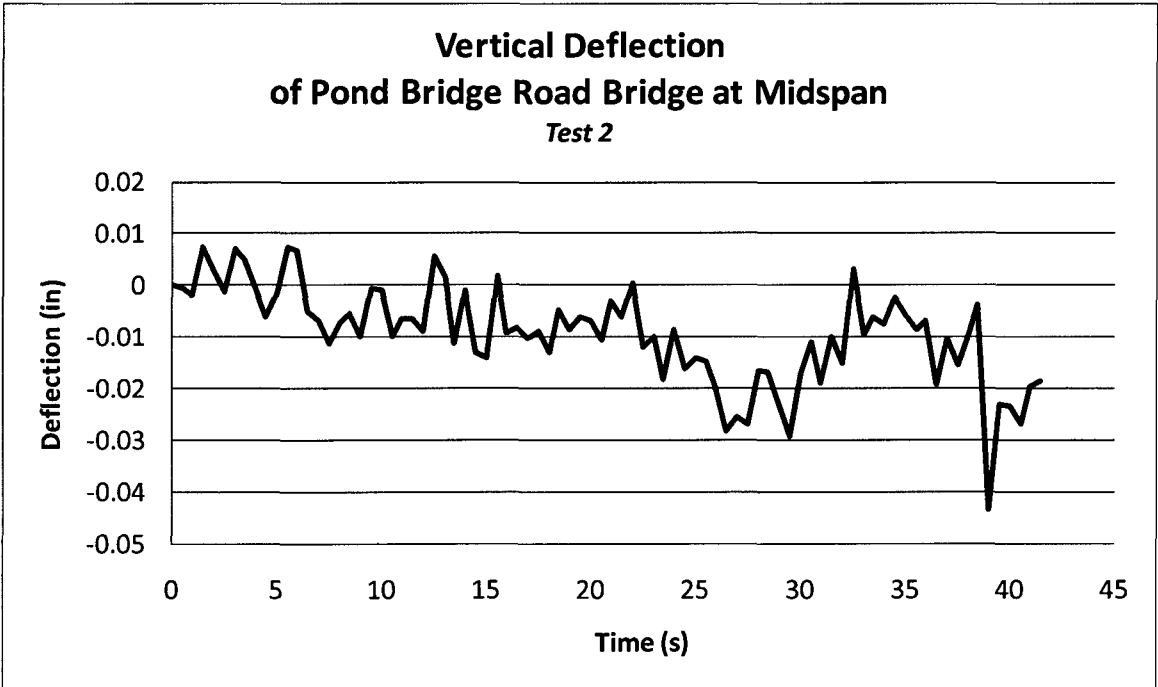
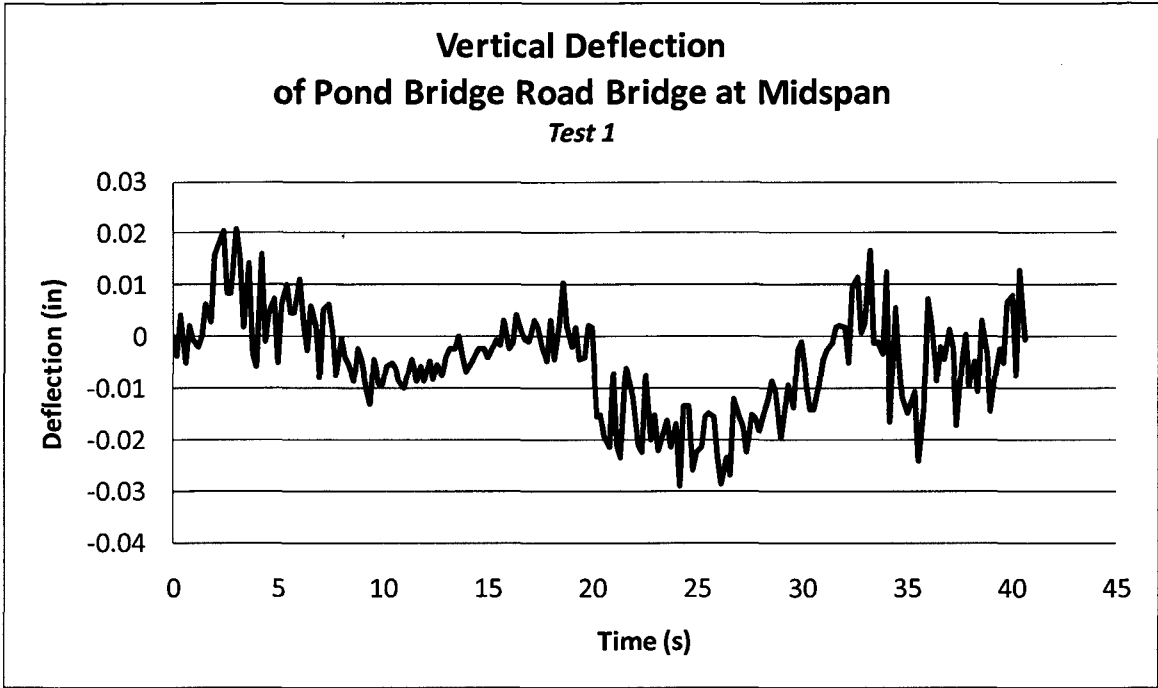


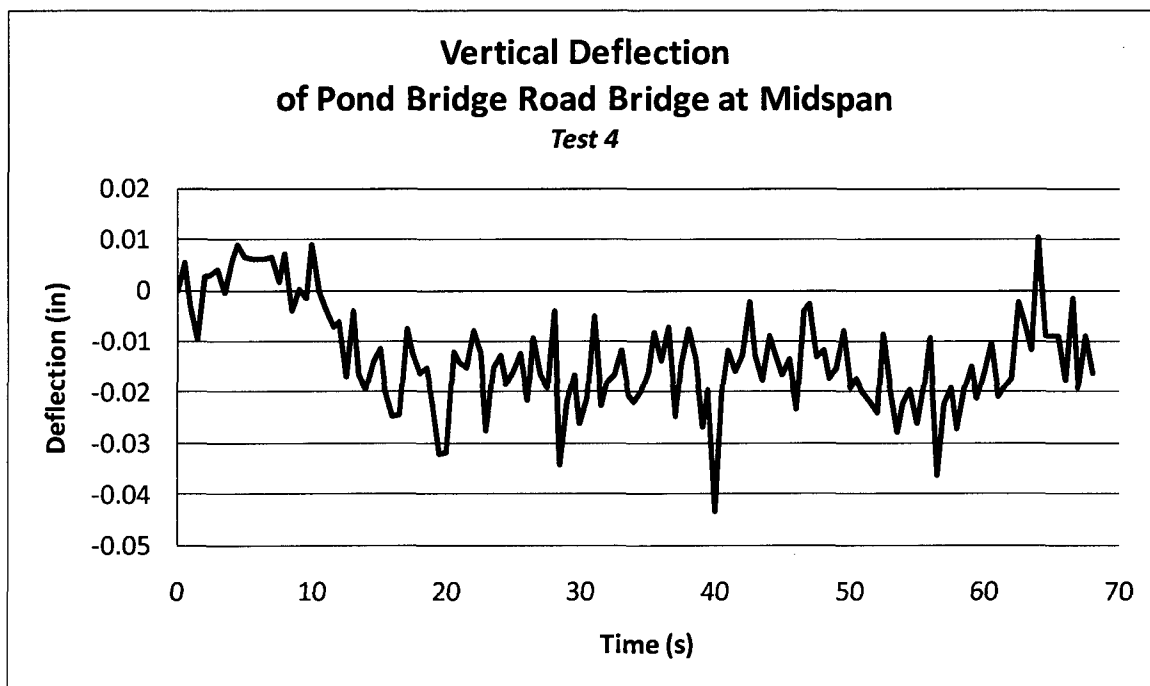
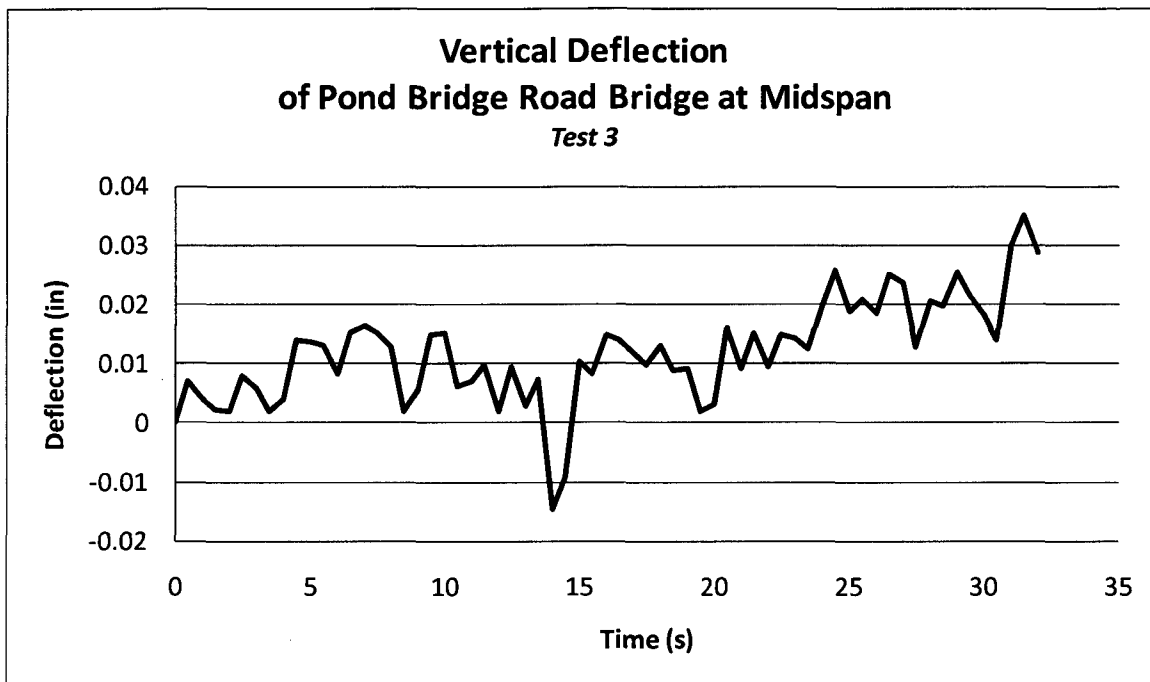


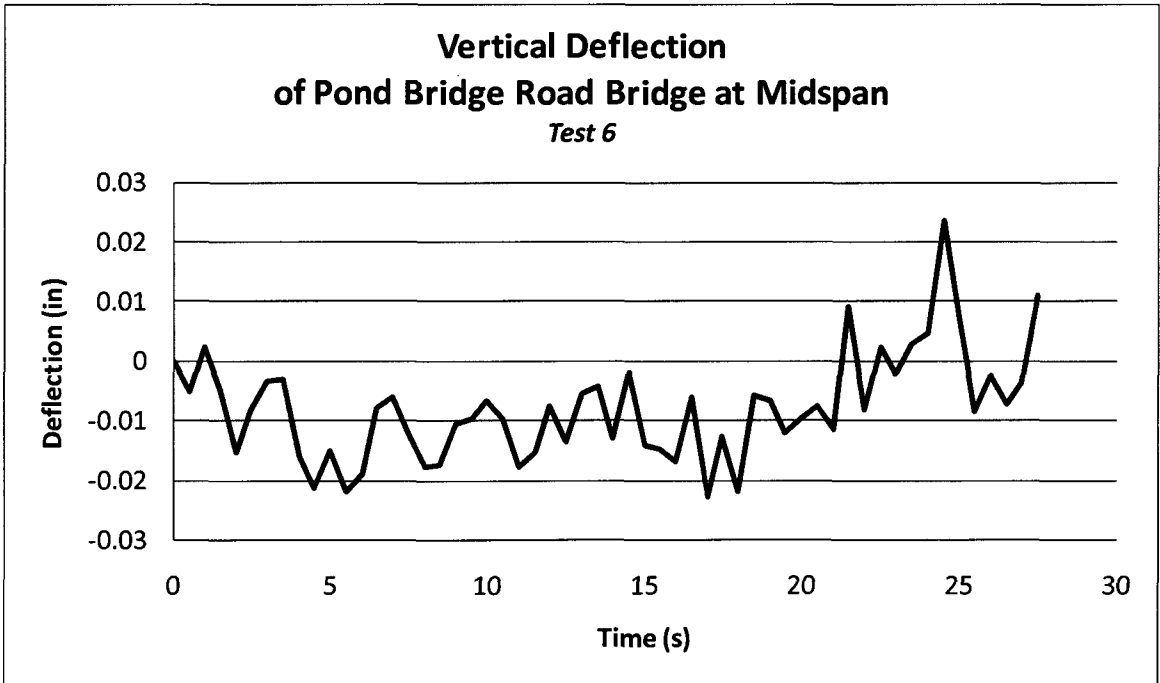
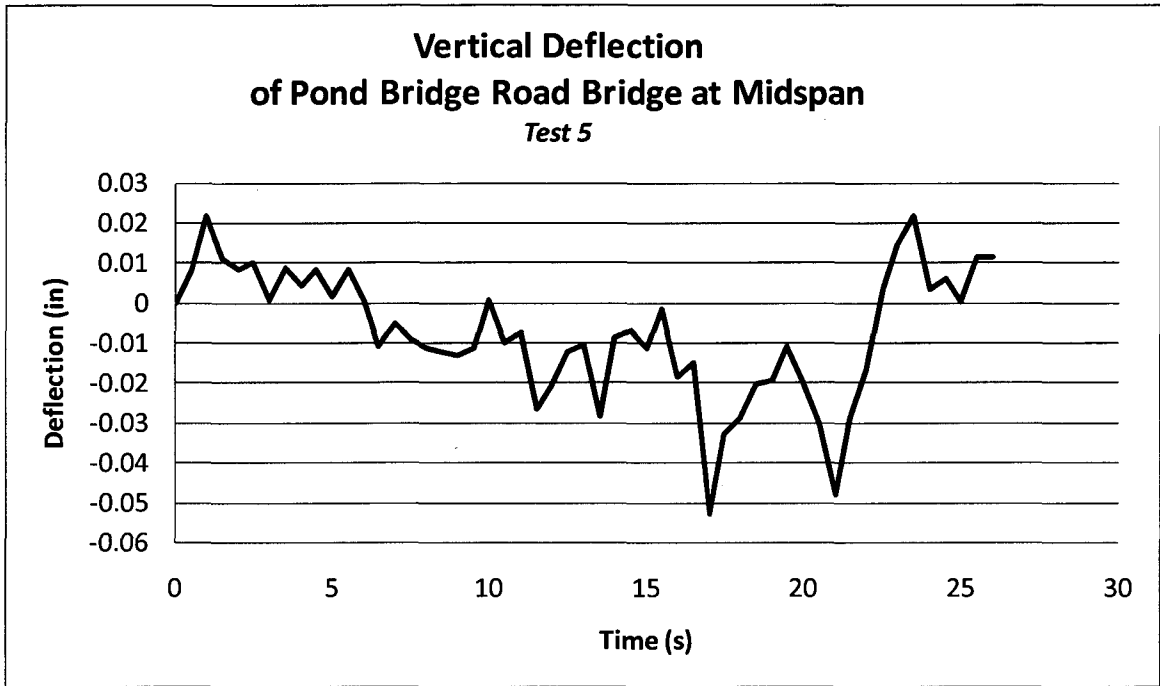
Pond Bridge Road Bridge Tests

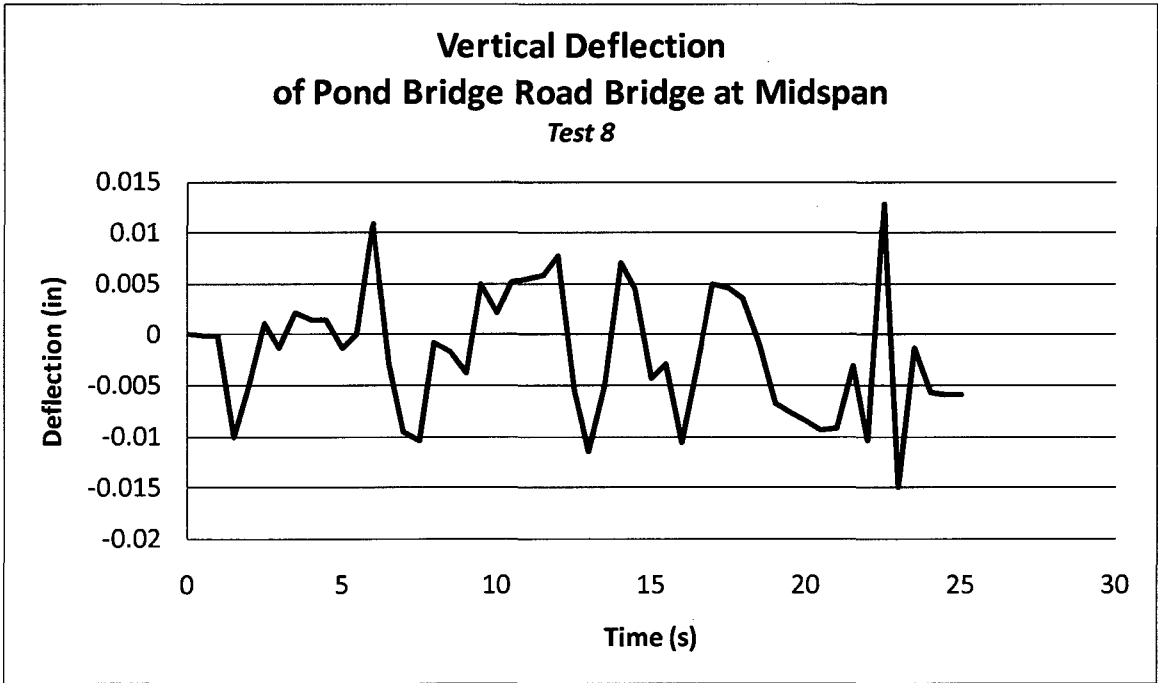
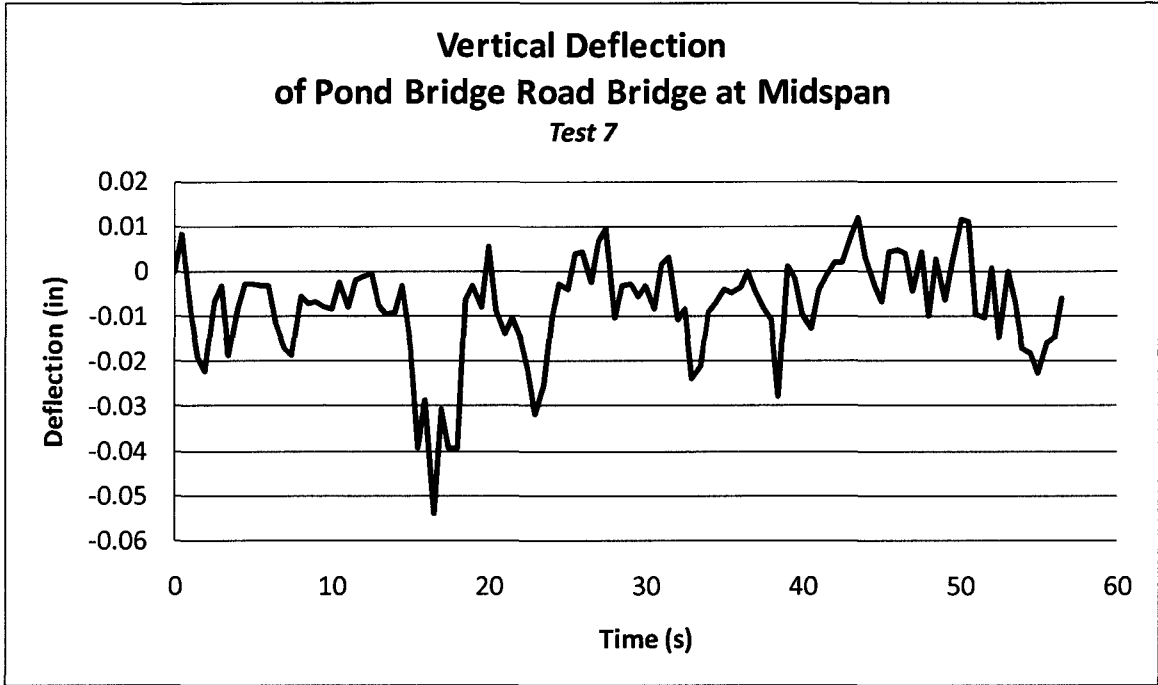
The DIC system was used to collect deflection data during a load test on the Pond Bridge Road Bridge in Tiverton, Rhode Island. The test involved a loaded truck making eleven passes across the bridge in three different lanes and three different speeds. The table below shows the information for each test.

Pond Bridge Road Bridge Testing Summary				
Test Number	Location	Test Type	Front Axle over Midspan	Rear Axle over Midspan
			(Time, s)	(Time, s)
1	Near	Rolling	15.2	24.2
2	Near	Rolling	14.0	23.0
3	Near	Rolling	11.5	18.5
4	Near	Stop	11.0	23.0-58.0
5	Center	Rolling	8.5	15.5
6	Center	Rolling	10.0	16.5
7	Center	Stop	14.0	27.0-49.0
8	Far	Rolling	8.0	14.5
9	Far	Rolling	7.5	14.0
10	Far	Stop	10.0	24.5-58.0
11	Center	Fast Rolling	1.3	1.9



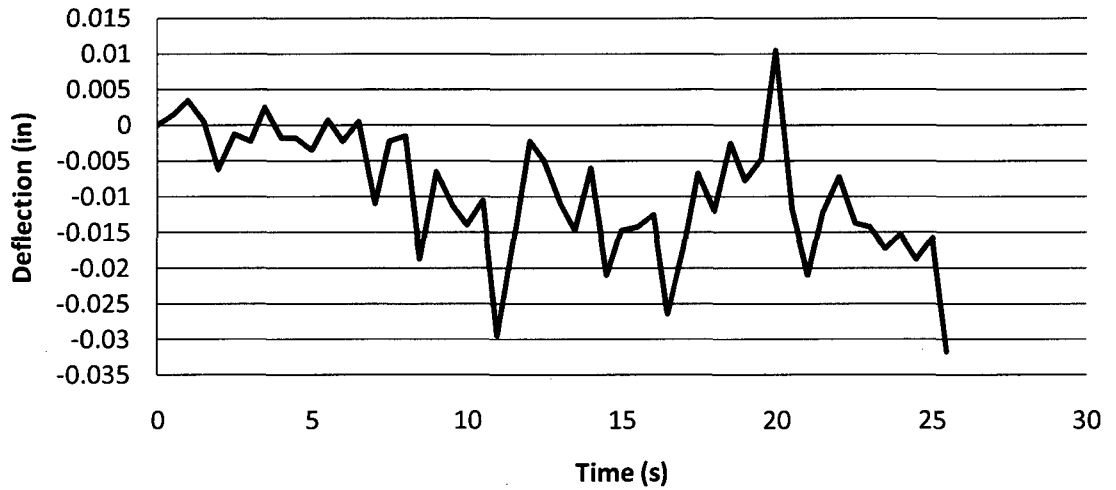






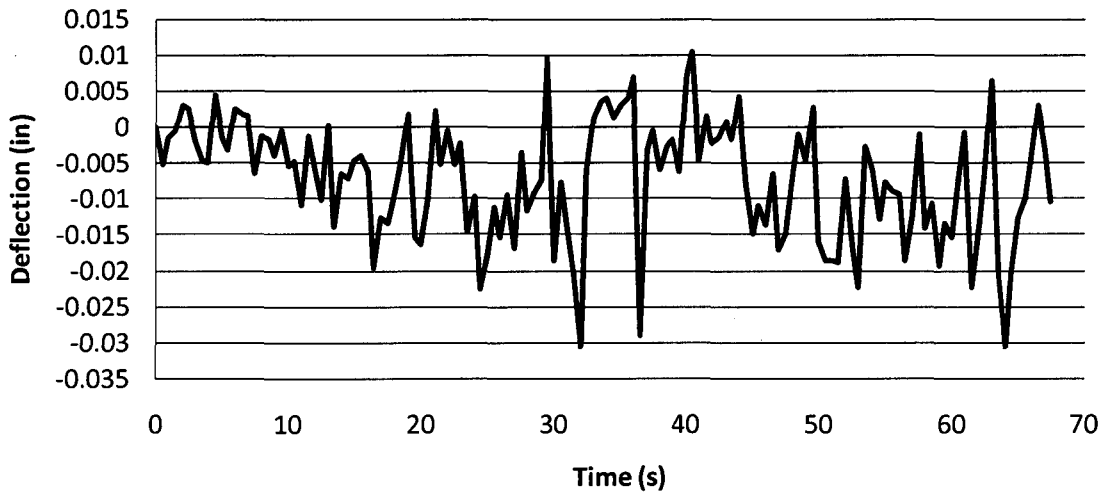
**Vertical Deflection
of Pond Bridge Road Bridge at Midspan**

Test 9

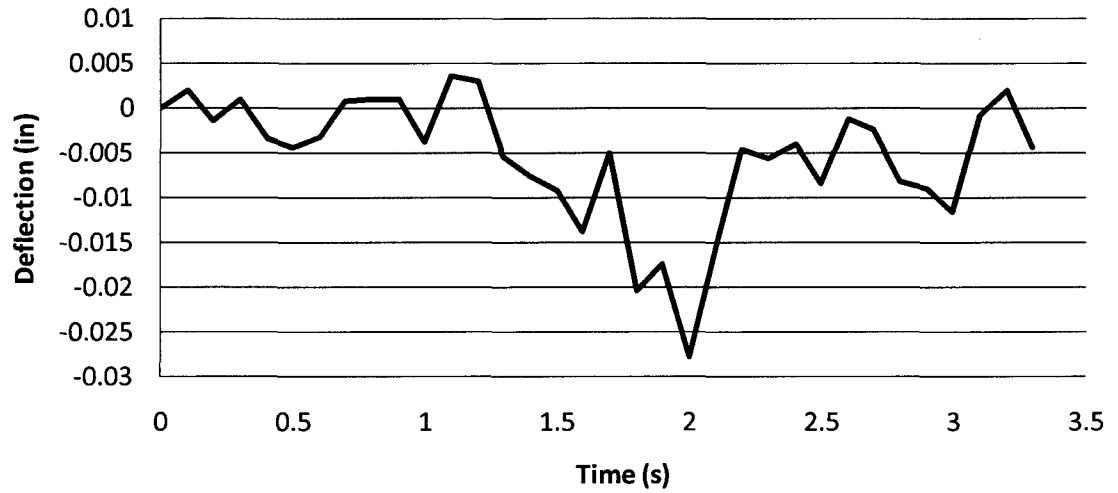


**Vertical Deflection
of Pond Bridge Road Bridge at Midspan**

Test 10

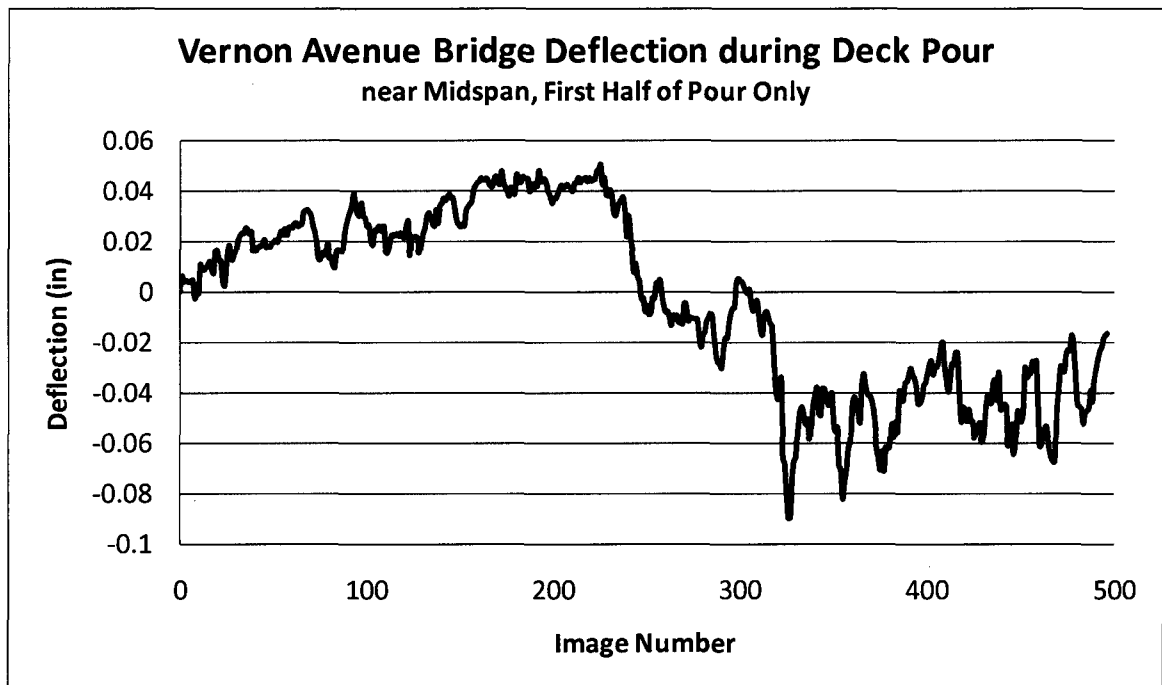


**Vertical Deflection
of Pond Bridge Road Bridge at Midspan**
Test 11



Vernon Avenue Concrete Placement Test

The three-span bridge across the Ware River on Vernon Avenue in Barre, Massachusetts is the focus of a case study that included the deployment of the DIC system as part of a second field test. The DIC system was used to collect data during the first half of the concrete deck placement.

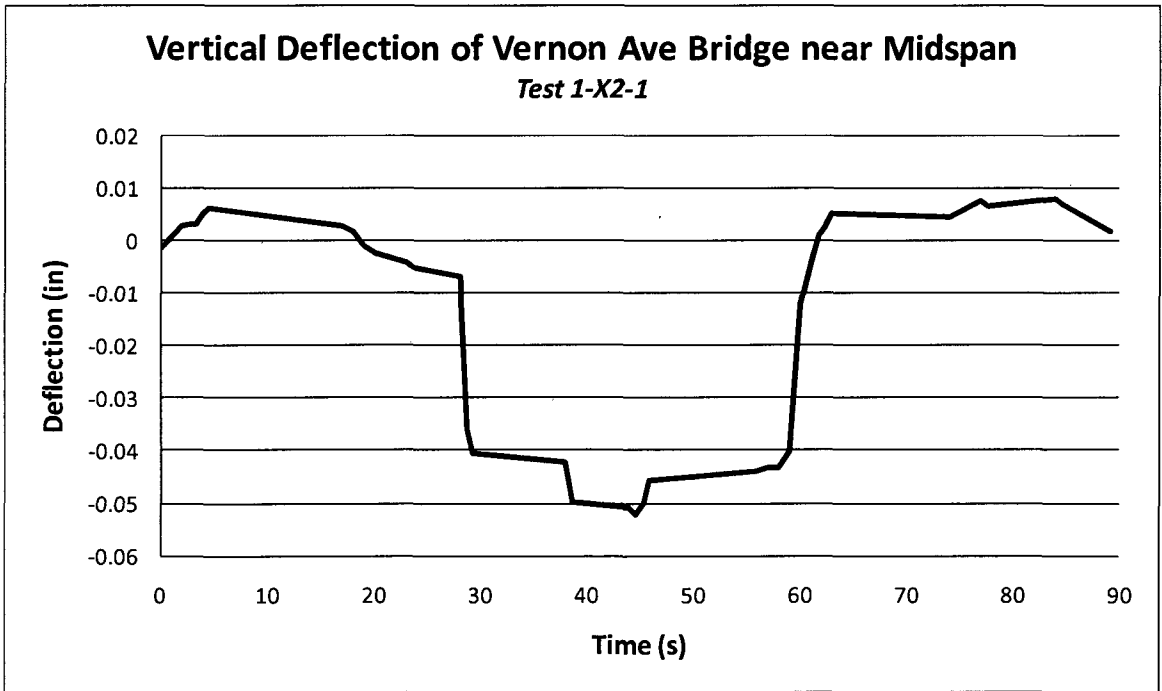
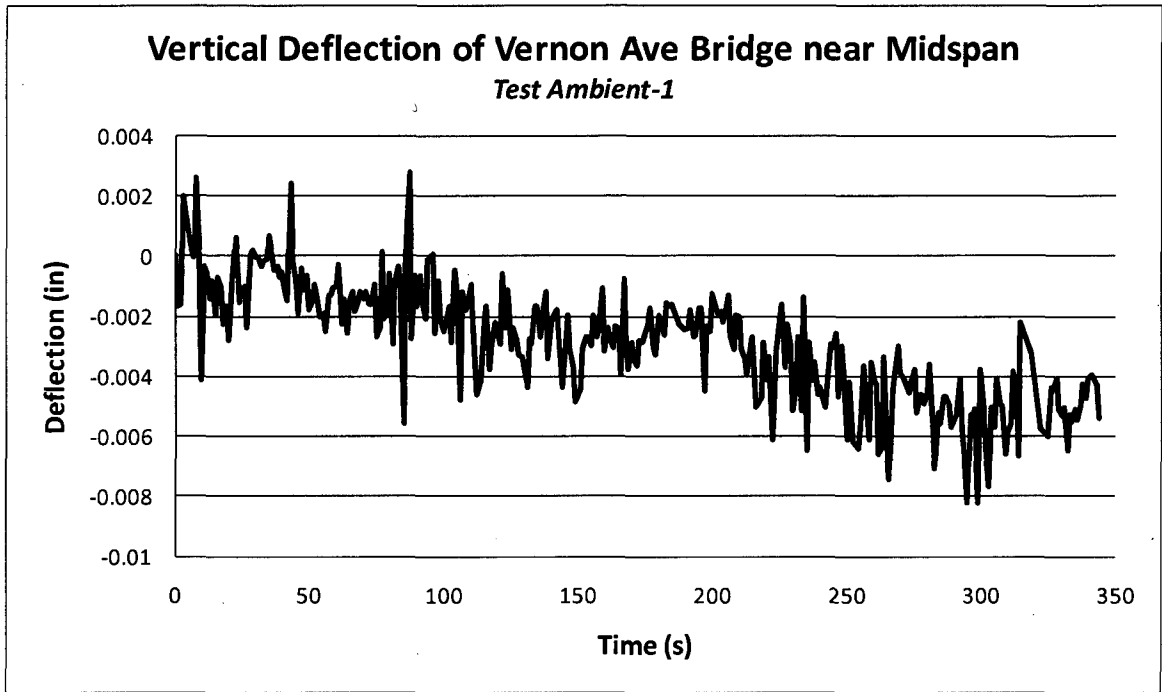


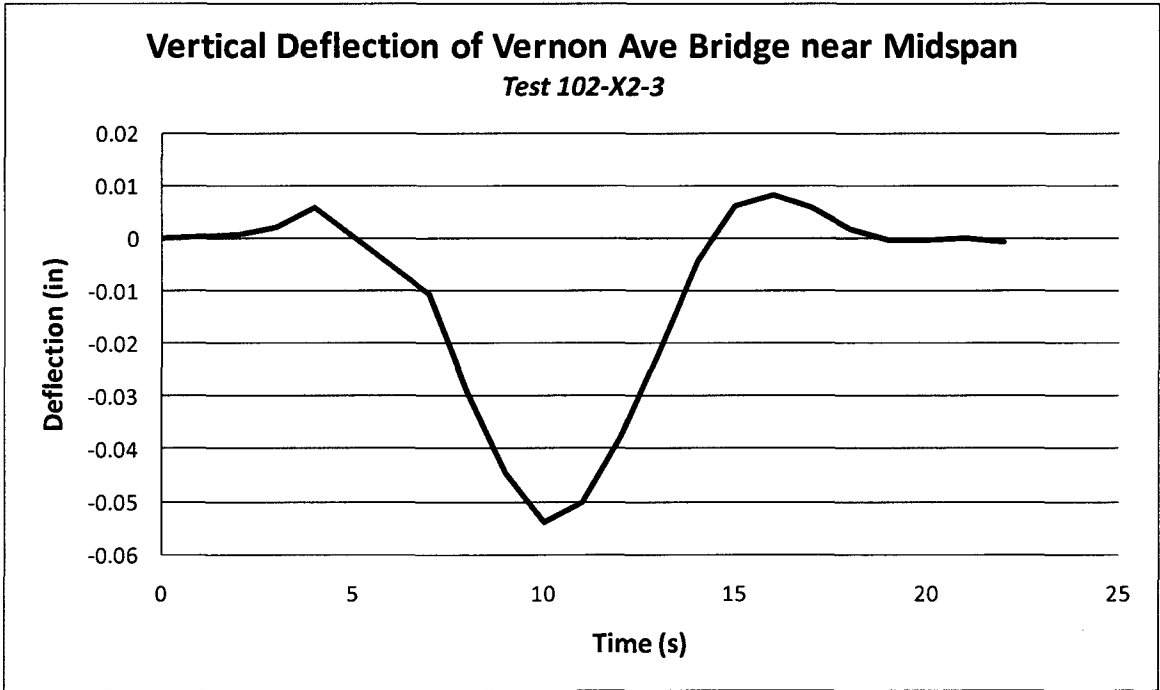
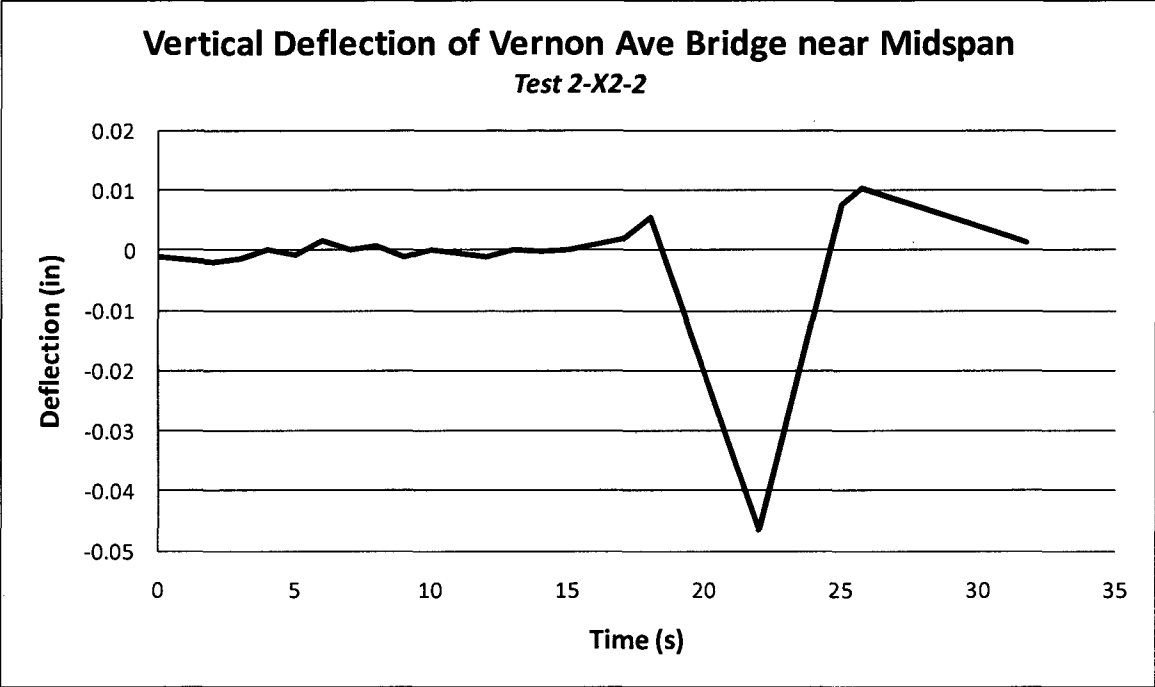
Vernon Avenue Load Test

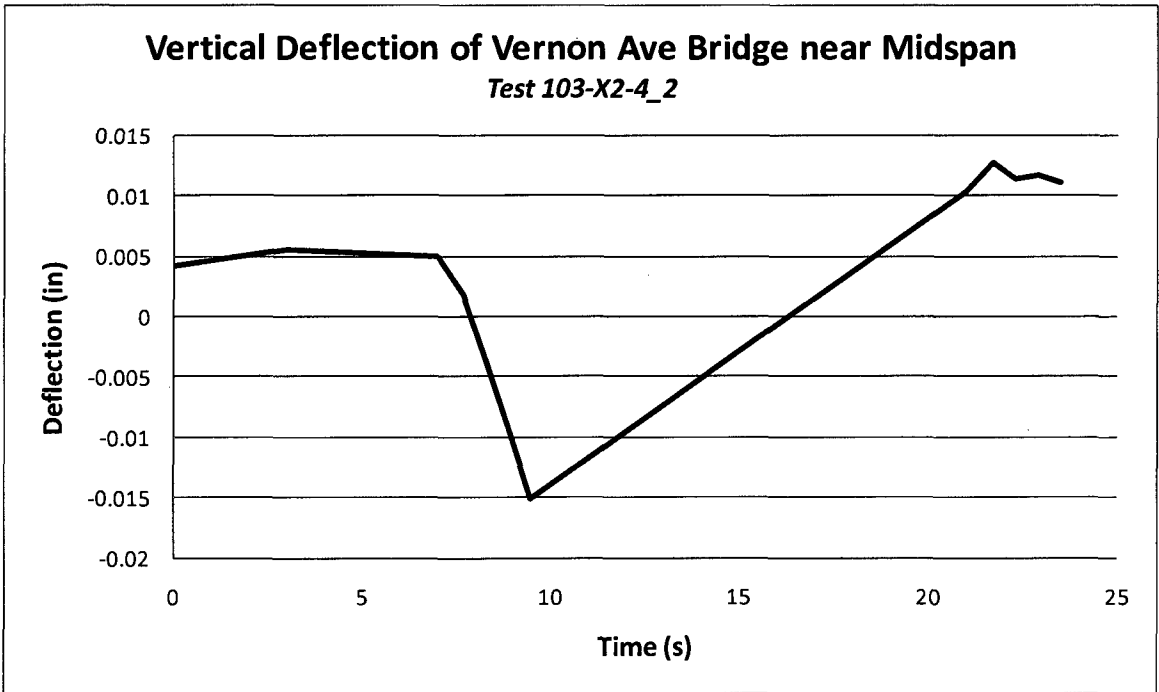
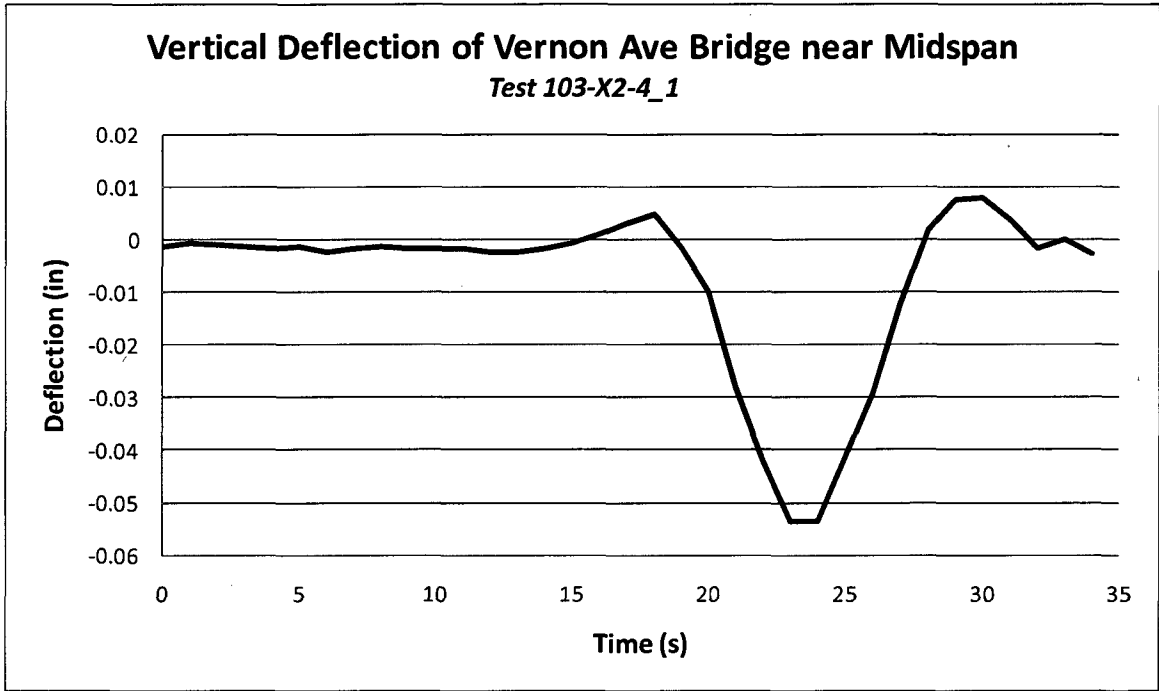
A load test was conducted on the Vernon Avenue Bridge on September 3, 2009.

The test involved a loaded truck making 25 passes across the bridge in three different lanes and three different speeds. Two DIC systems were used to collect data from two different spans of the bridge. The table below shows the information pertaining to each test.

Test #	Test Name	Test Type	Truck Location	Camera Data
Ambient	Ambient	Ambient	N/A	South
Ambient	Ambient 1	Ambient	N/A	North
1	1-X2-1	Rolling	Center	North/South
2	2-X2-2	Rolling	Center	North/South
102	102-X2-3	Rolling	Center	North/South
103a	103-X2-4_1	Rolling	Center	North/South
103b	103-X2-4_2	Rolling	Center	North/South
3	3-X1-1	Stop	West	North/South
4	4-X1-2	Stop	West	North/South
5	5-X1-3	Stop	West	North/South
6	6-X2-1	Stop	Center	North/South
7	7-X2-2	Stop	Center	North/South
8	8-X2-3	Stop	Center	North/South
10	10-X3-2	Stop	East	North
11	11-X3-3	Stop	East	North
12	12-X1-1	Rolling	West	North/South
13	13-X1-2	Rolling	West	North/South
14	14-X1-3	Rolling	West	North/South
15	15-X2-1	Rolling	Center	North
16	16-X2-2	Rolling	Center	North
17a	17-X2-3_1	Rolling	Center	North
17b	17-X2-3_2	Rolling	Center	North
18	18-X3-1	Rolling	East	North
19	19-X3-2	Rolling	East	North
20	20-X3-3	Rolling	East	North
22	22-X3-1	Impact	East	North
23	23-X3-2	Impact	East	North
24	24-X3-3	Impact	East	North
25	25-X1-1	Impact	West	North

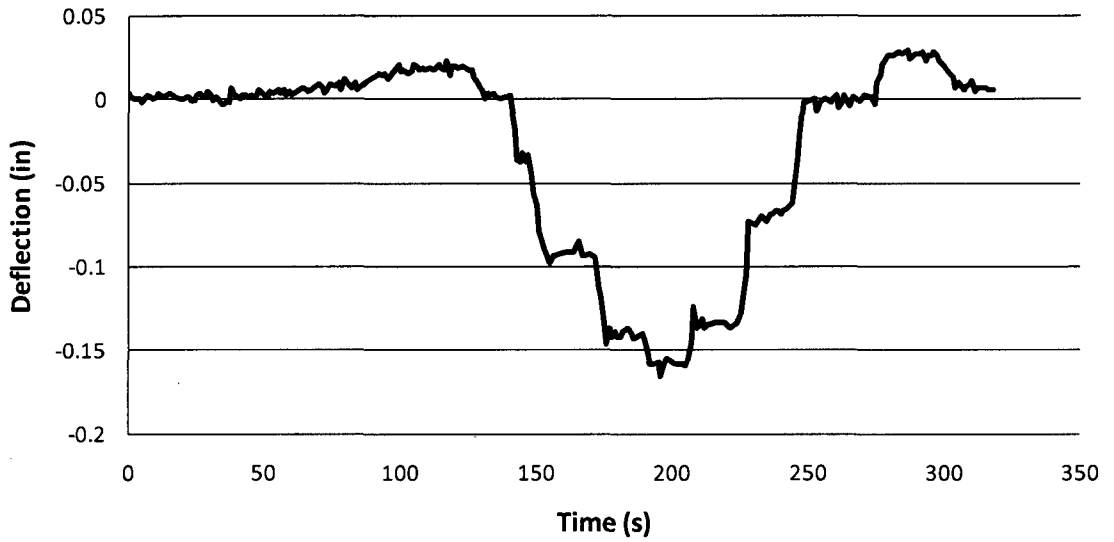






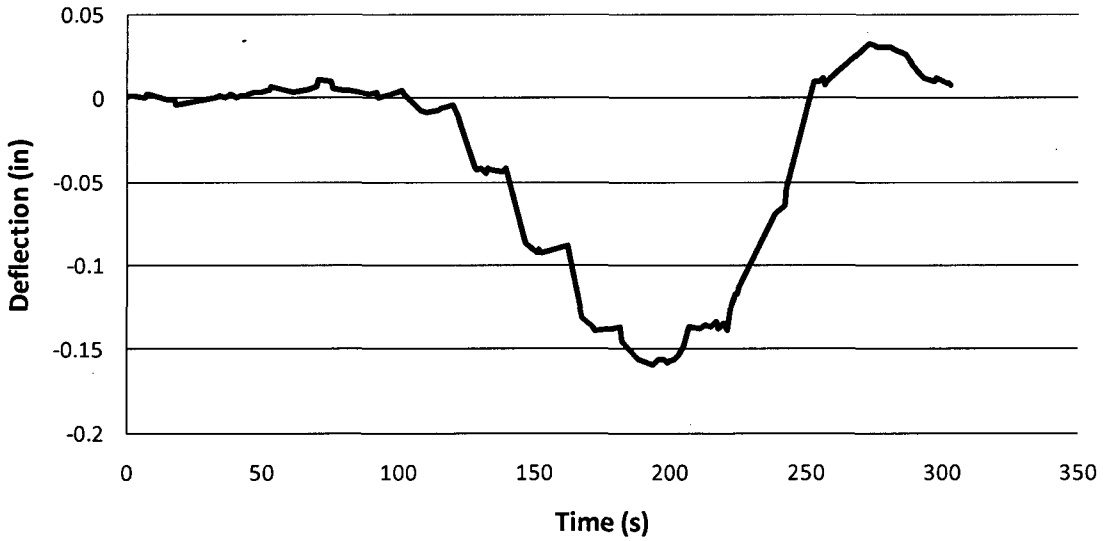
Vertical Deflection of Vernon Ave Bridge near Midspan

Test 3-X1-1



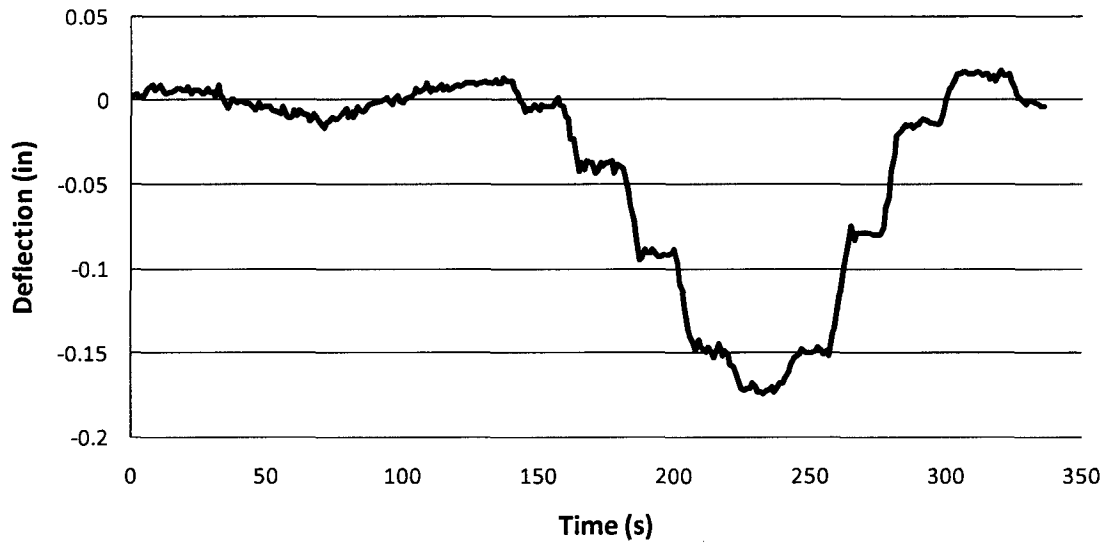
Vertical Deflection of Vernon Ave Bridge near Midspan

Test 4-X1-2



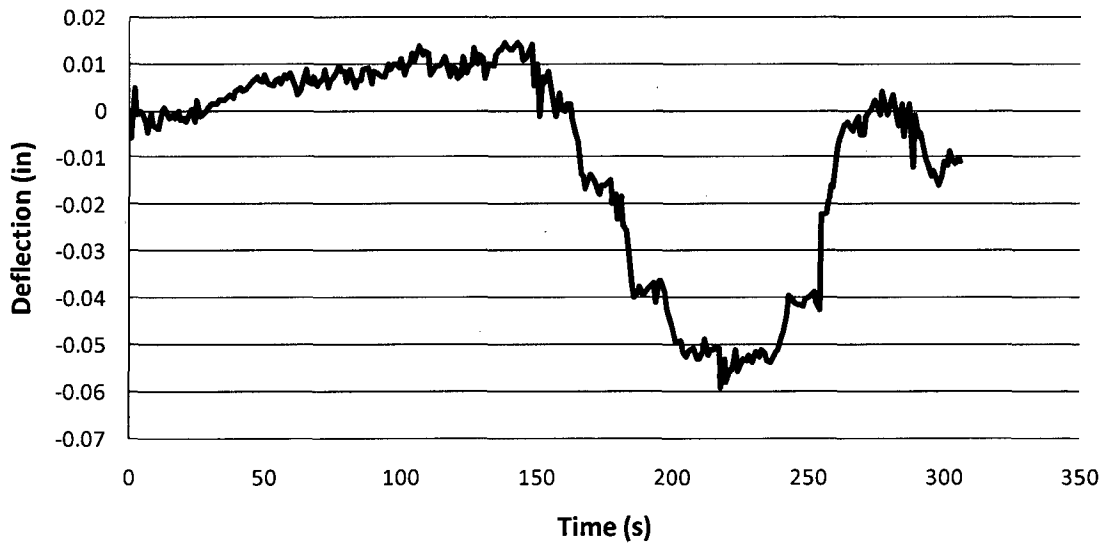
Vertical Deflection of Vernon Ave Bridge near Midspan

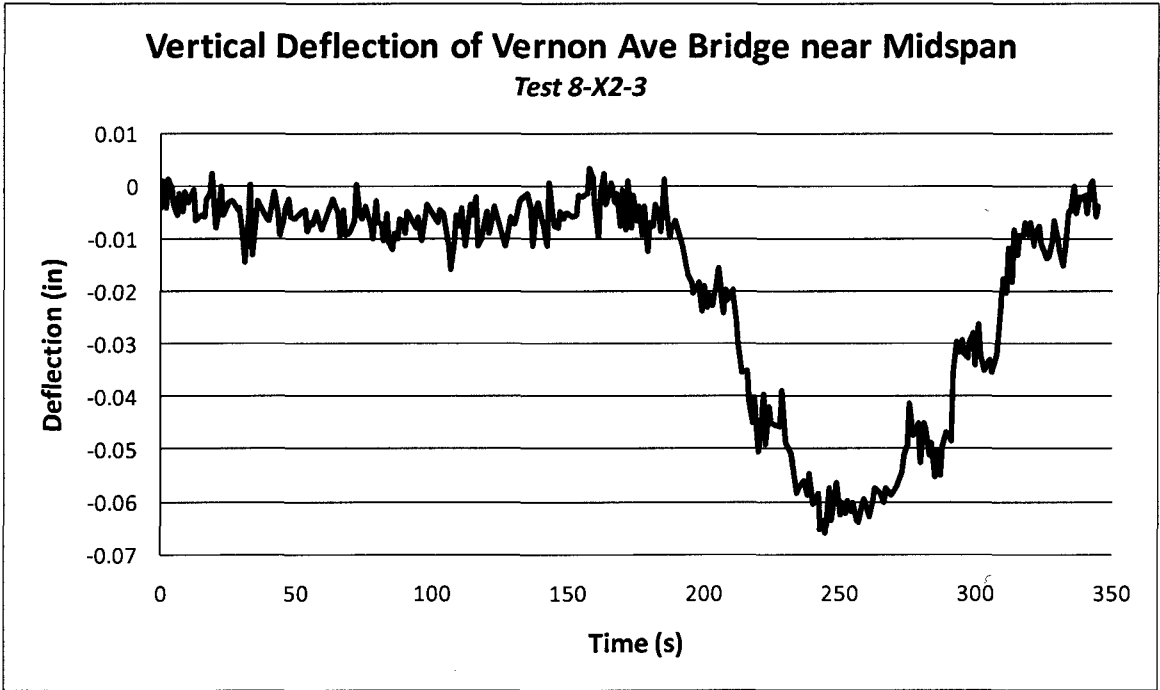
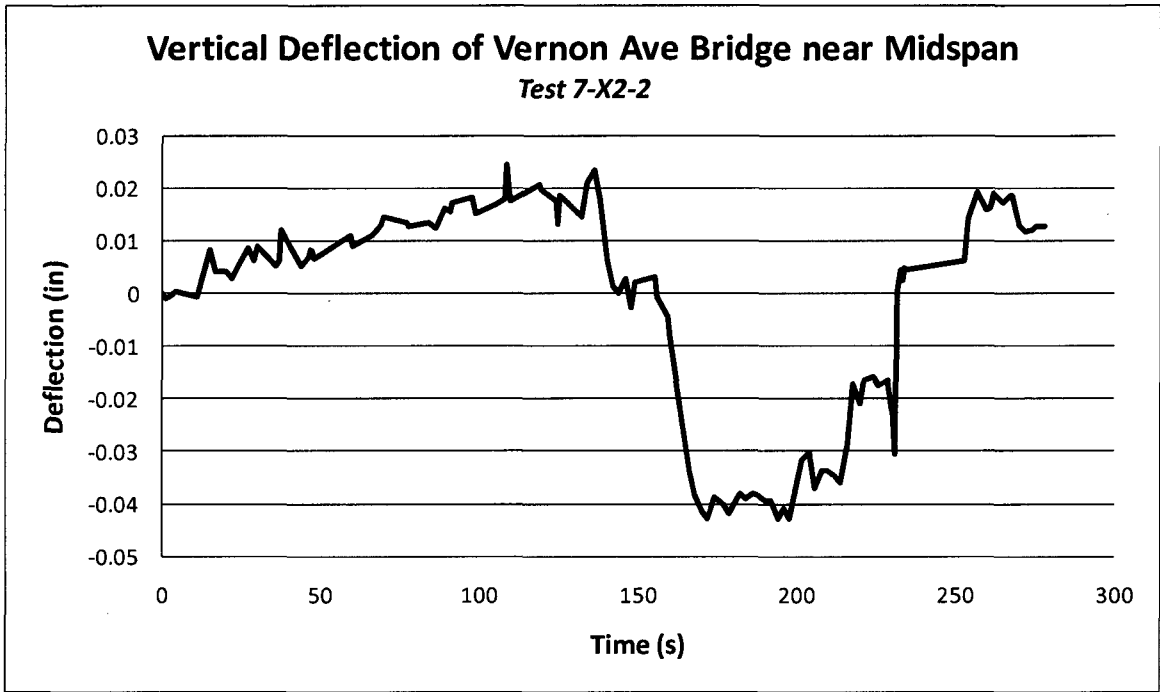
Test 5-X1-3



Vertical Deflection of Vernon Ave Bridge near Midspan

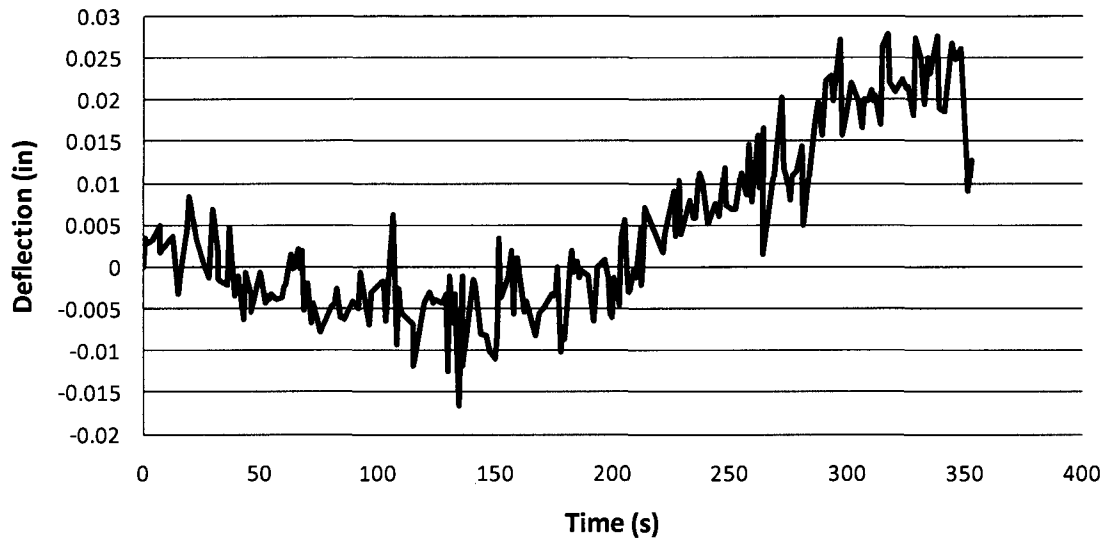
Test 6-X2-1





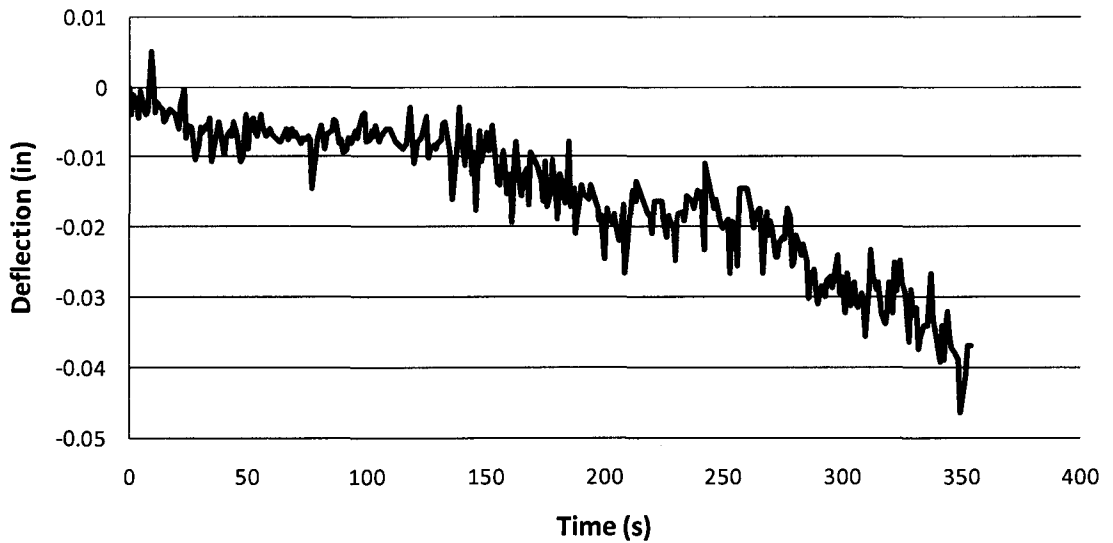
Vertical Deflection of Vernon Ave Bridge near Midspan

Test 10-X3-2



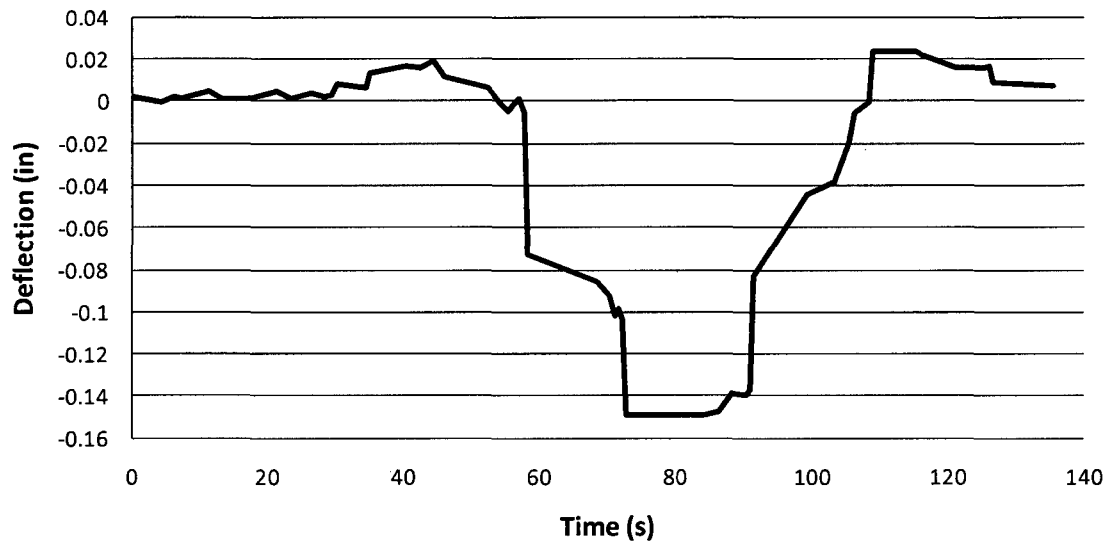
Vertical Deflection of Vernon Ave Bridge near Midspan

Test 11-X3-3



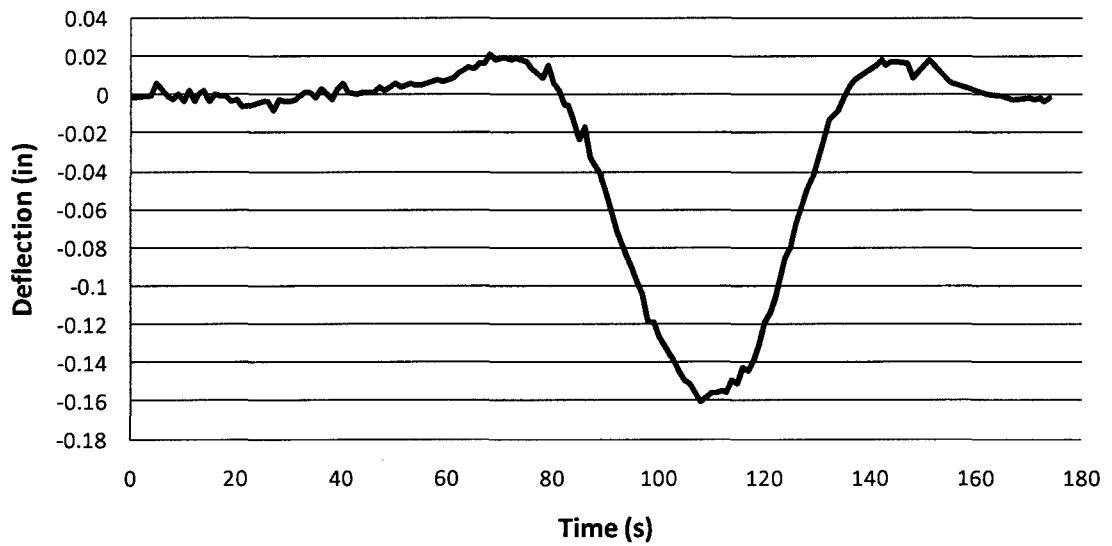
Vertical Deflection of Vernon Ave Bridge near Midspan

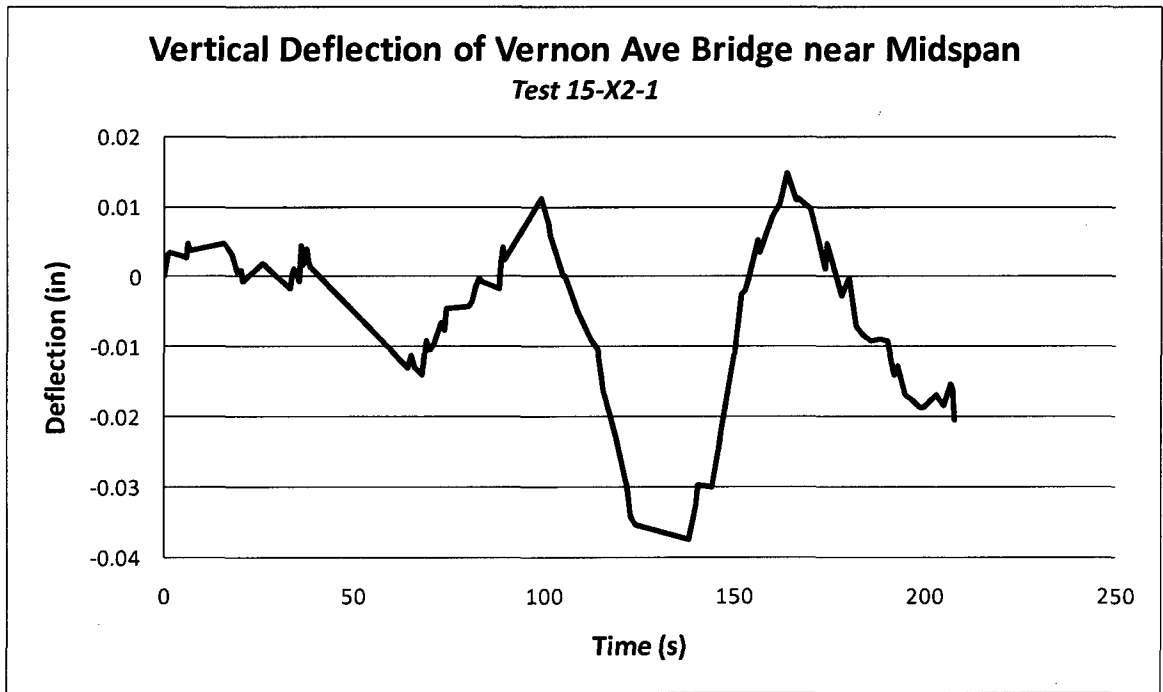
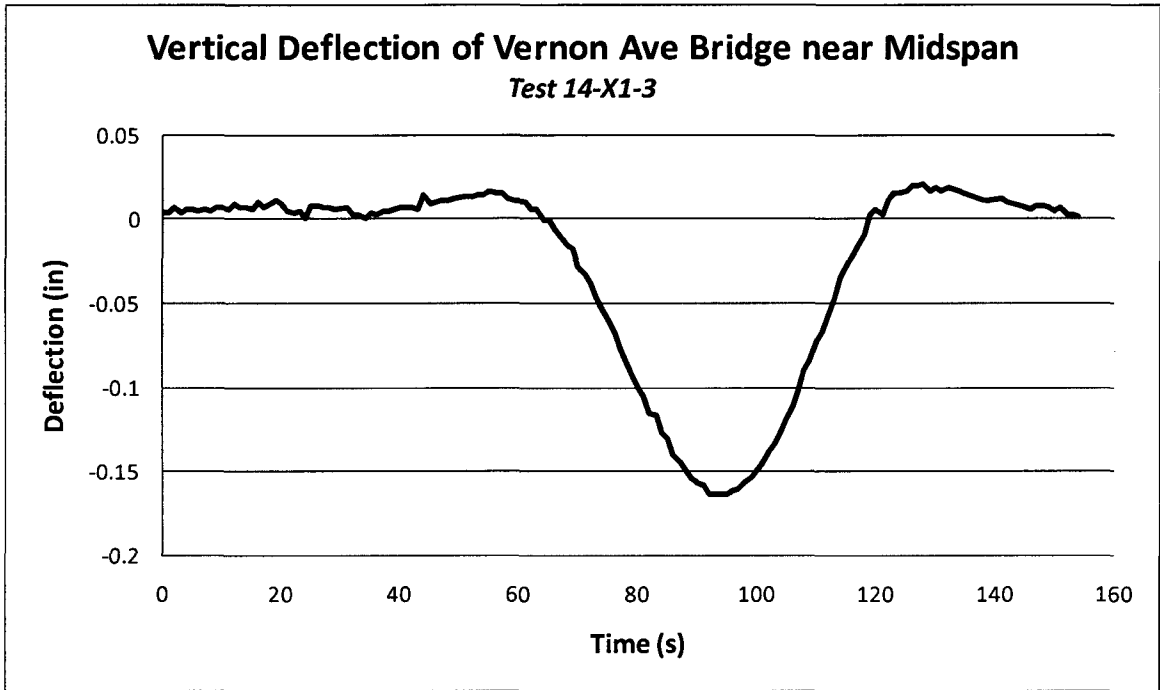
Test 12-X1-1



Vertical Deflection of Vernon Ave Bridge near Midspan

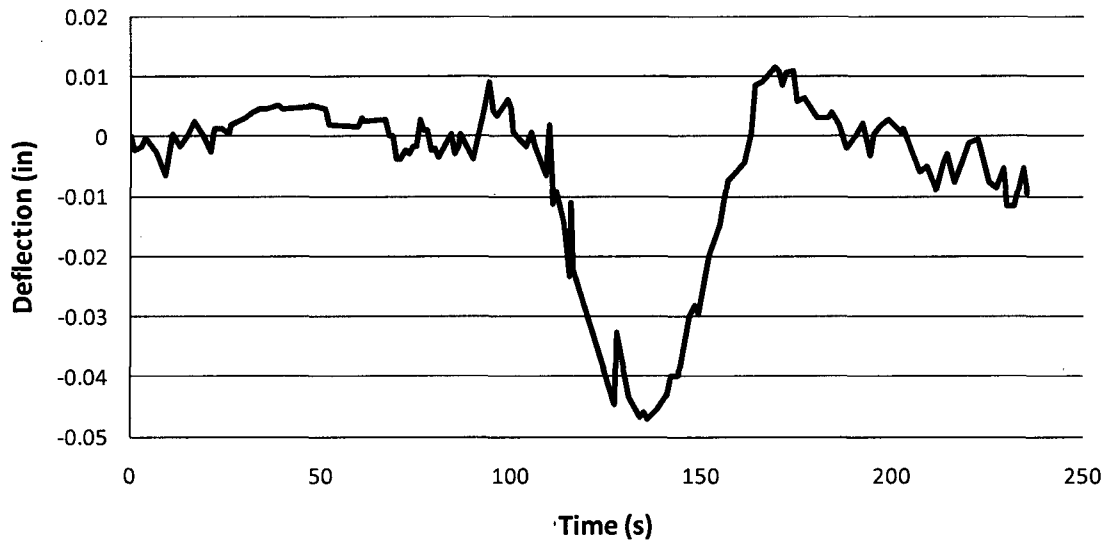
Test 13-X1-2





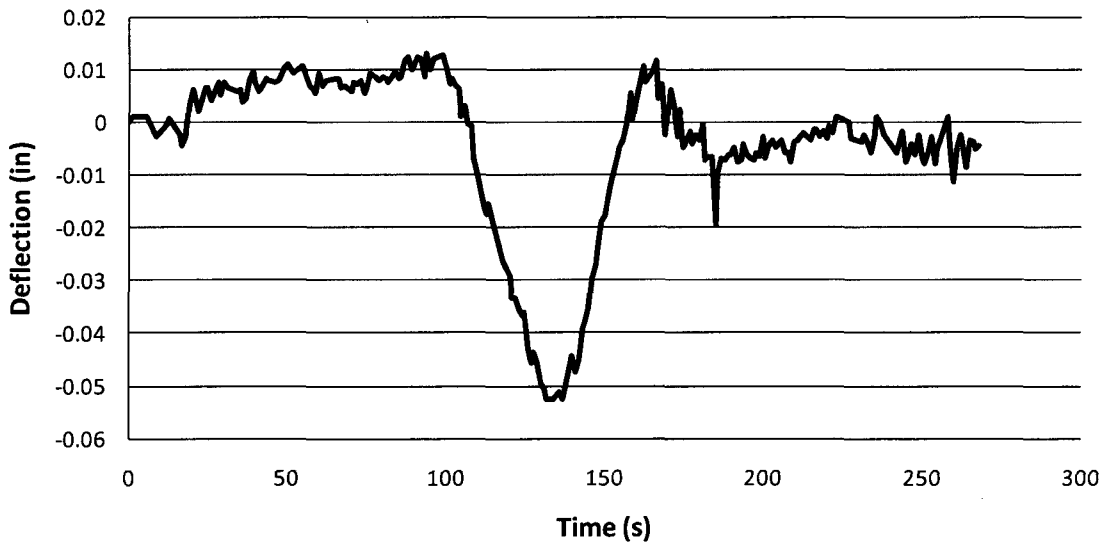
Vertical Deflection of Vernon Ave Bridge near Midspan

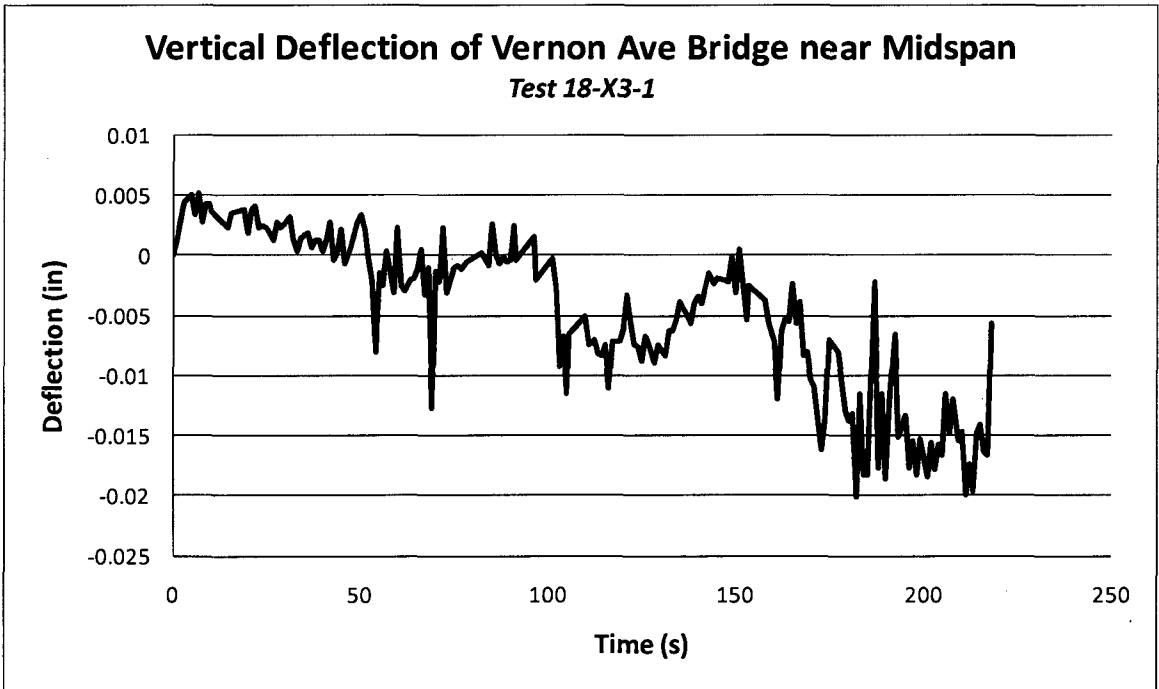
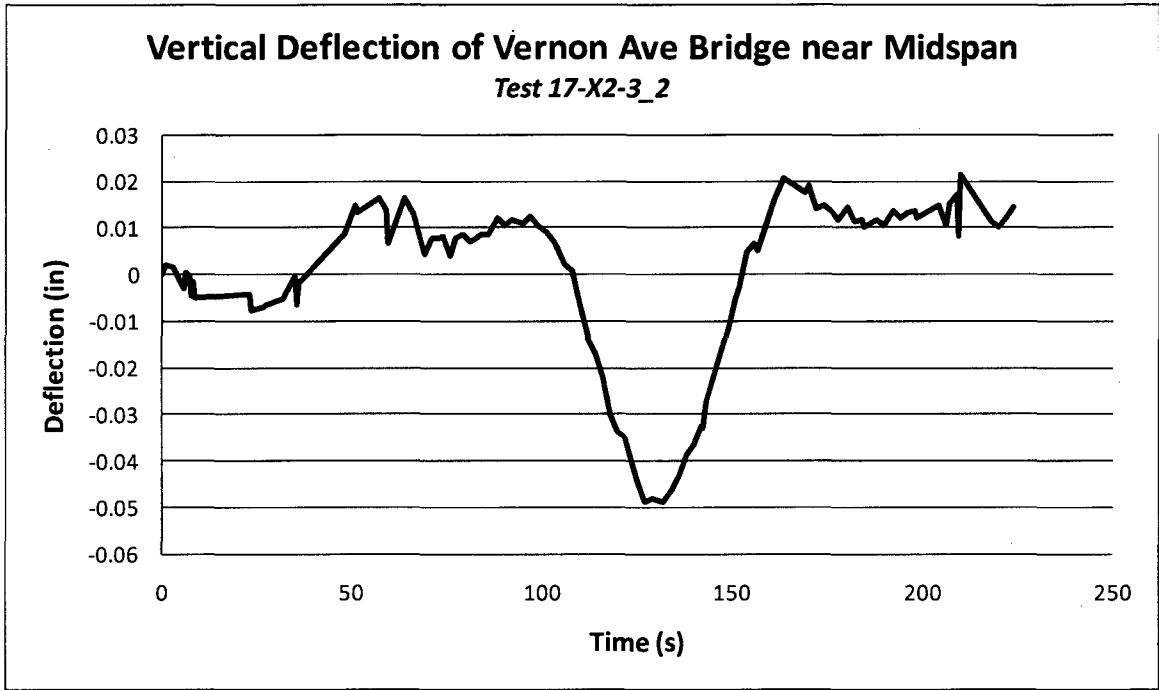
Test 16-X2-2



Vertical Deflection of Vernon Ave Bridge near Midspan

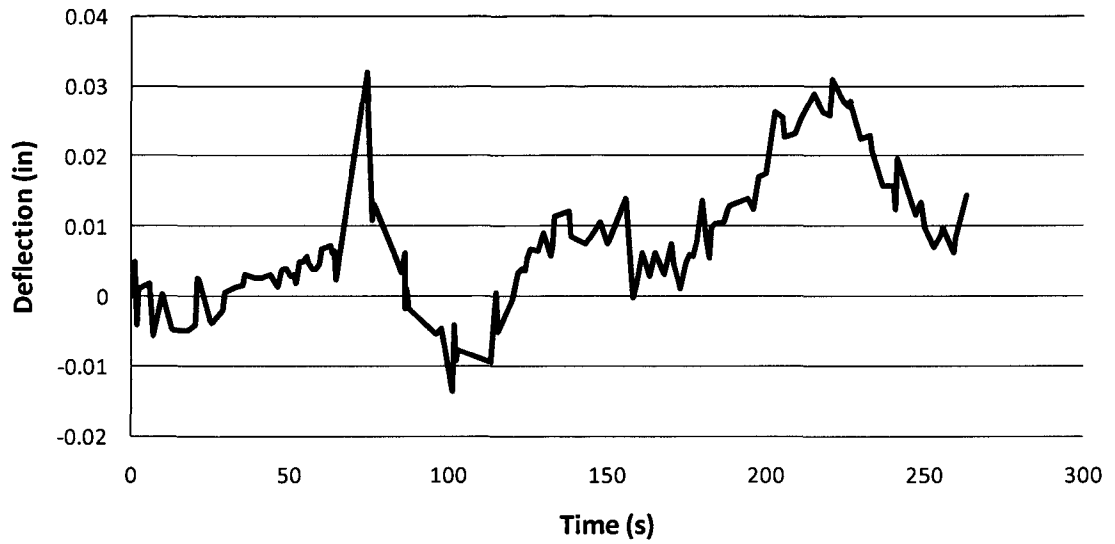
Test 17-X2-3_1





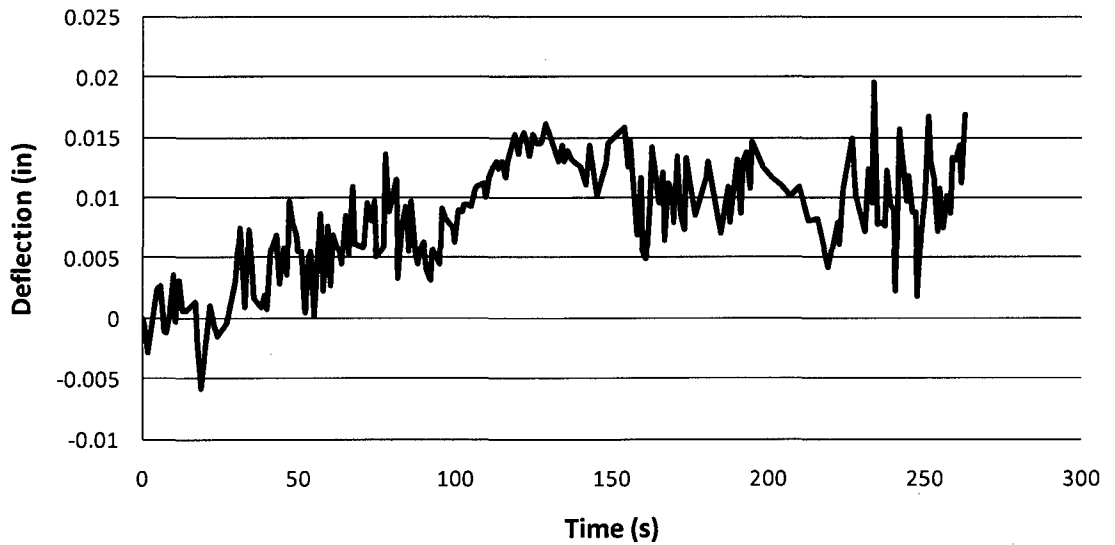
Vertical Deflection of Vernon Ave Bridge near Midspan

Test 19-X3-2

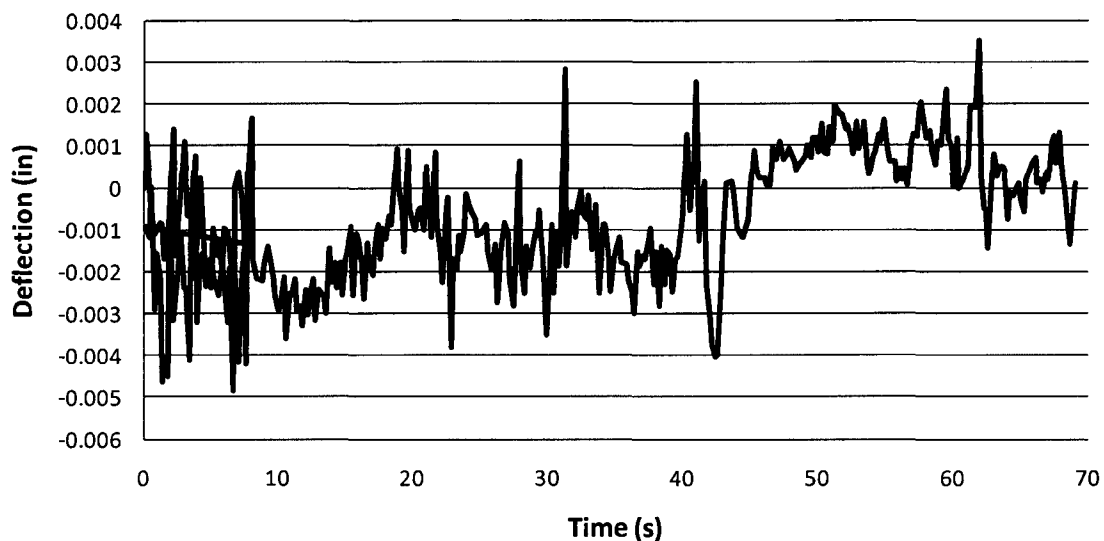


Vertical Deflection of Vernon Ave Bridge near Midspan

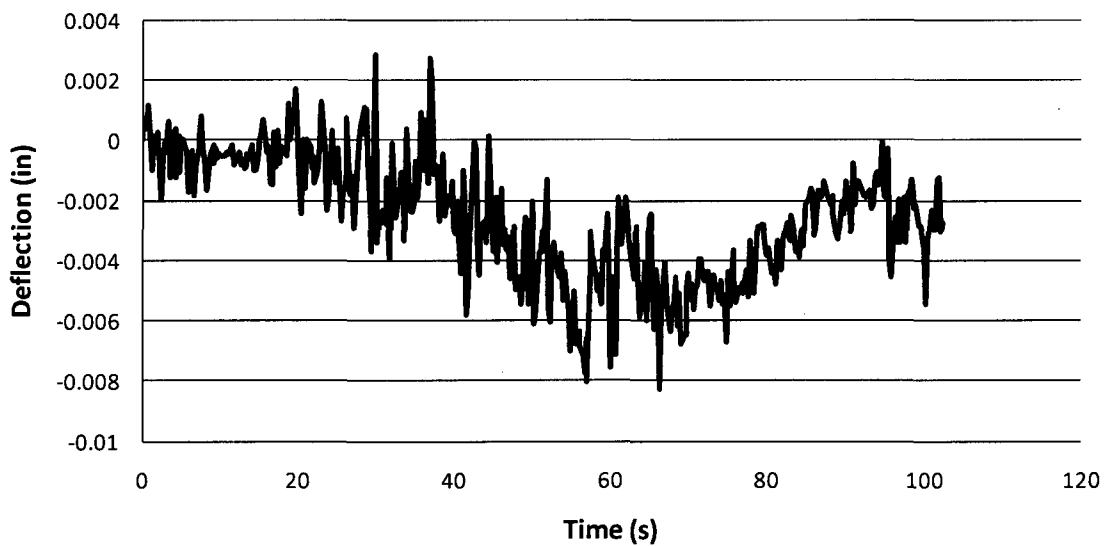
Test 20-X3-3



Vertical Deflection of Vernon Ave Bridge near Midspan
Test 22-X3-1

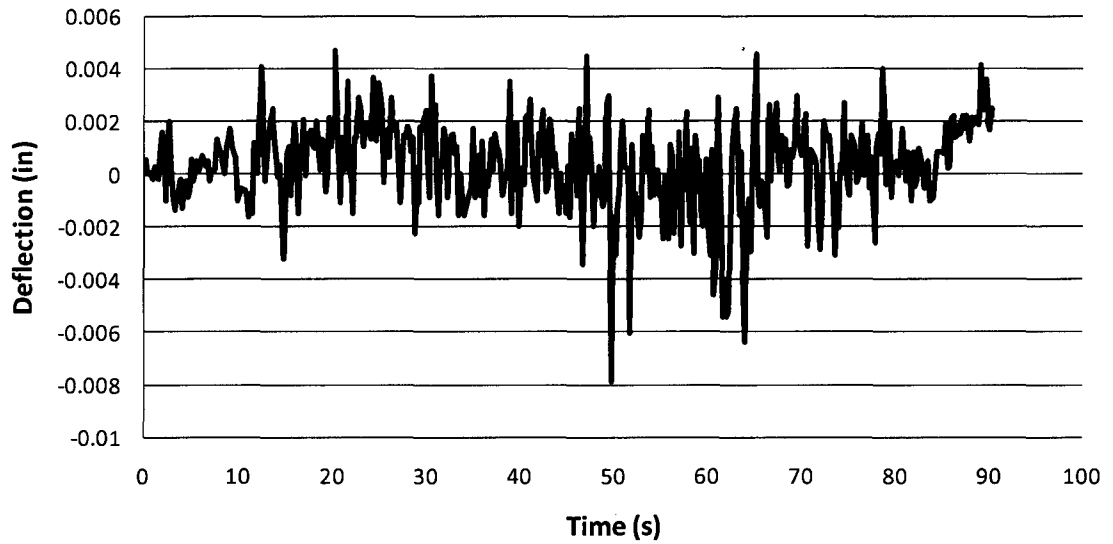


Vertical Deflection of Vernon Ave Bridge near Midspan
Test 23-X3-2



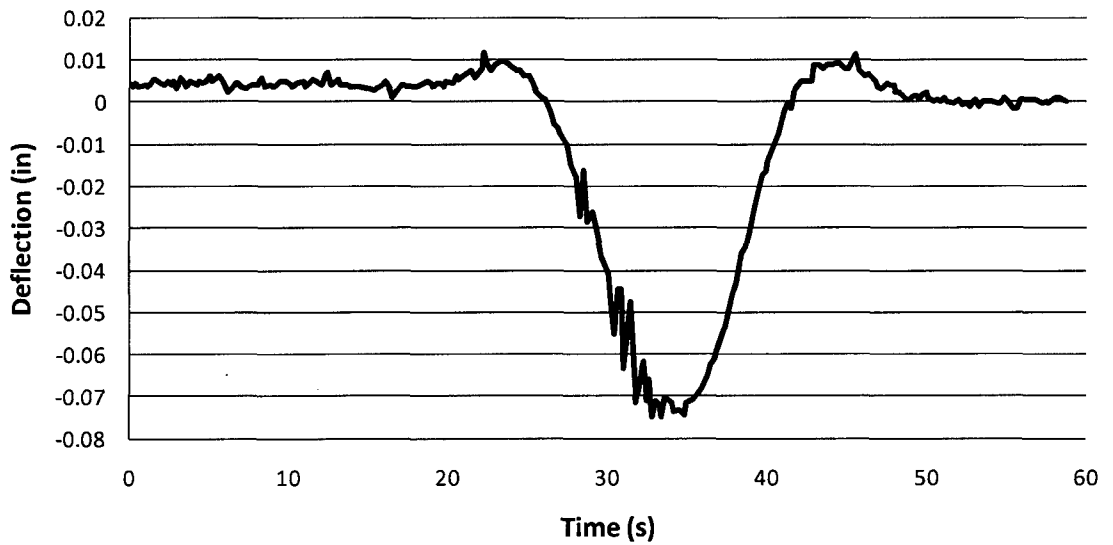
Vertical Deflection of Vernon Ave Bridge near Midspan

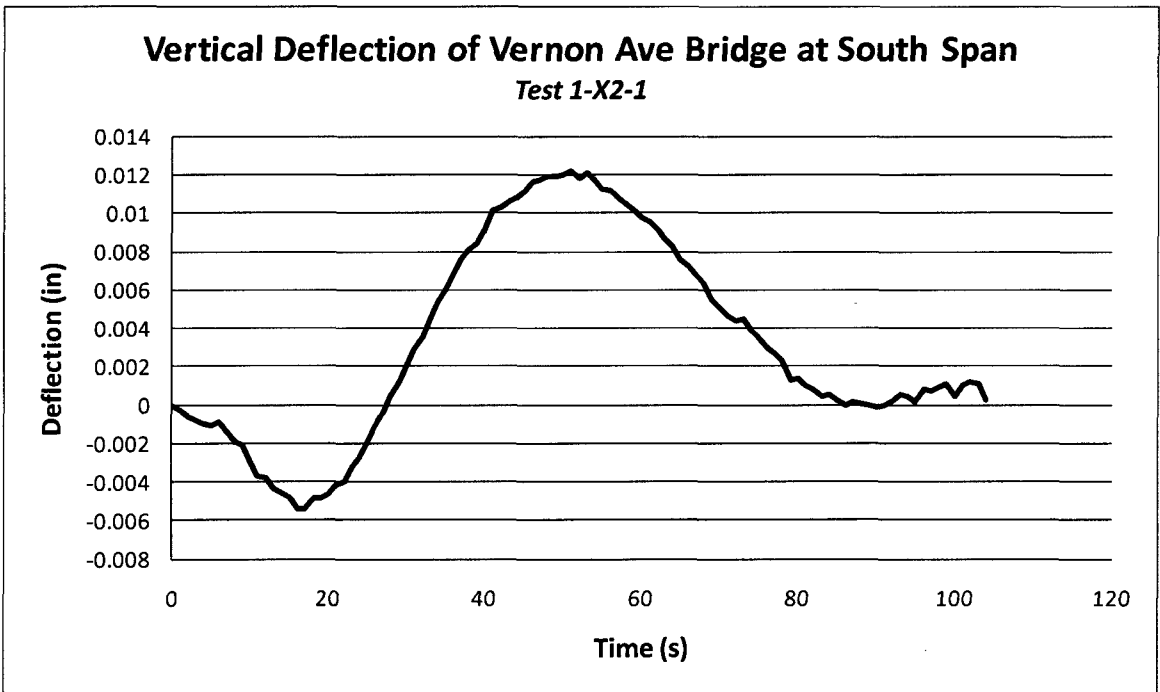
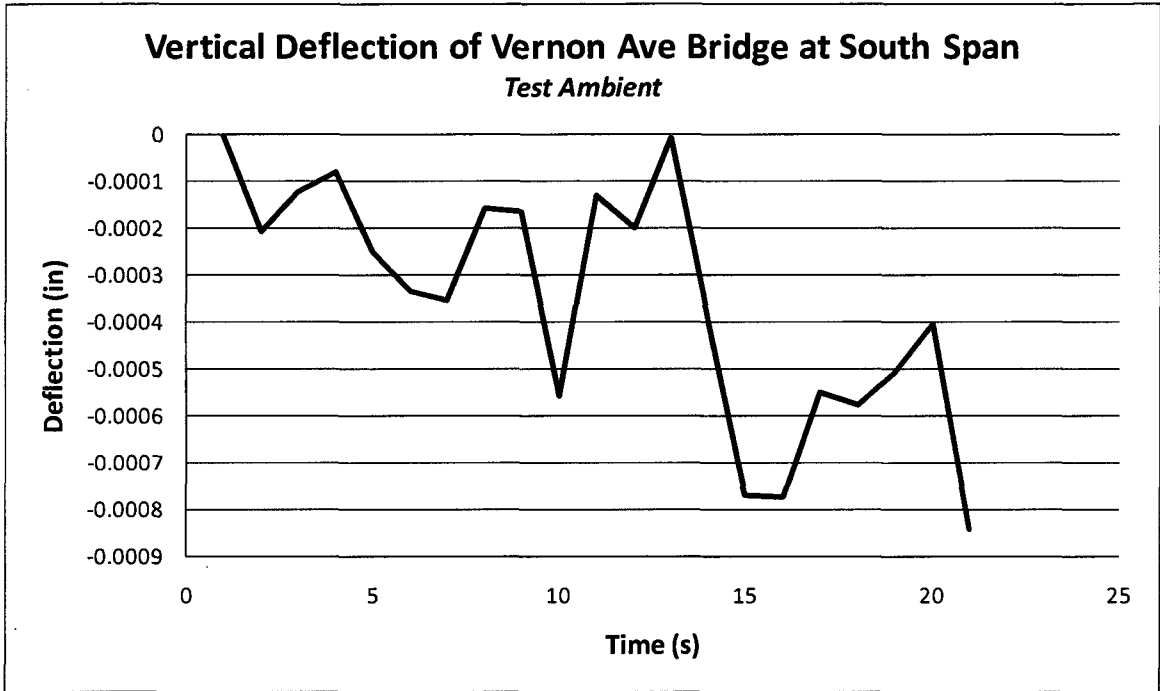
Test 24-X3-3

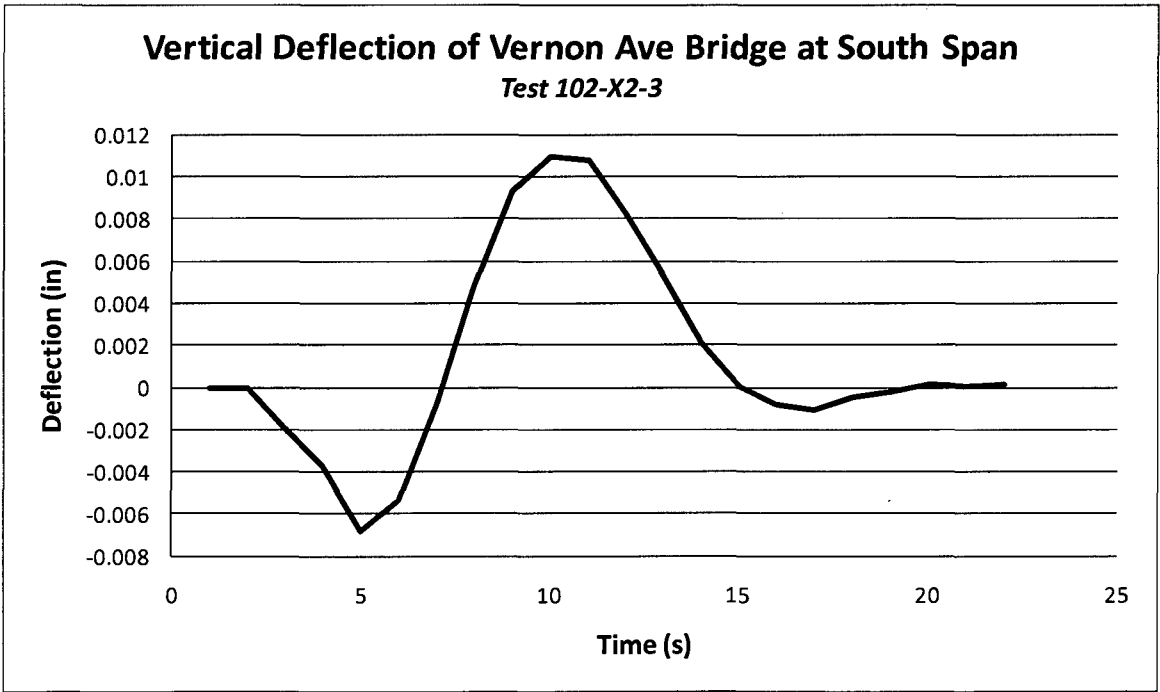
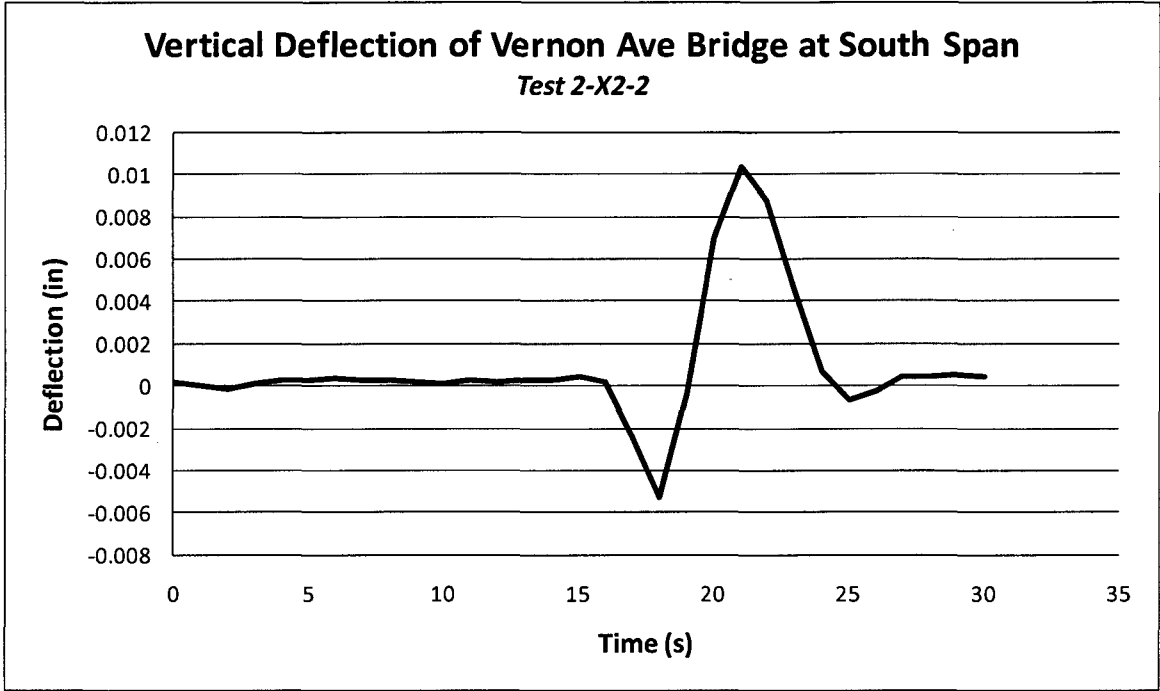


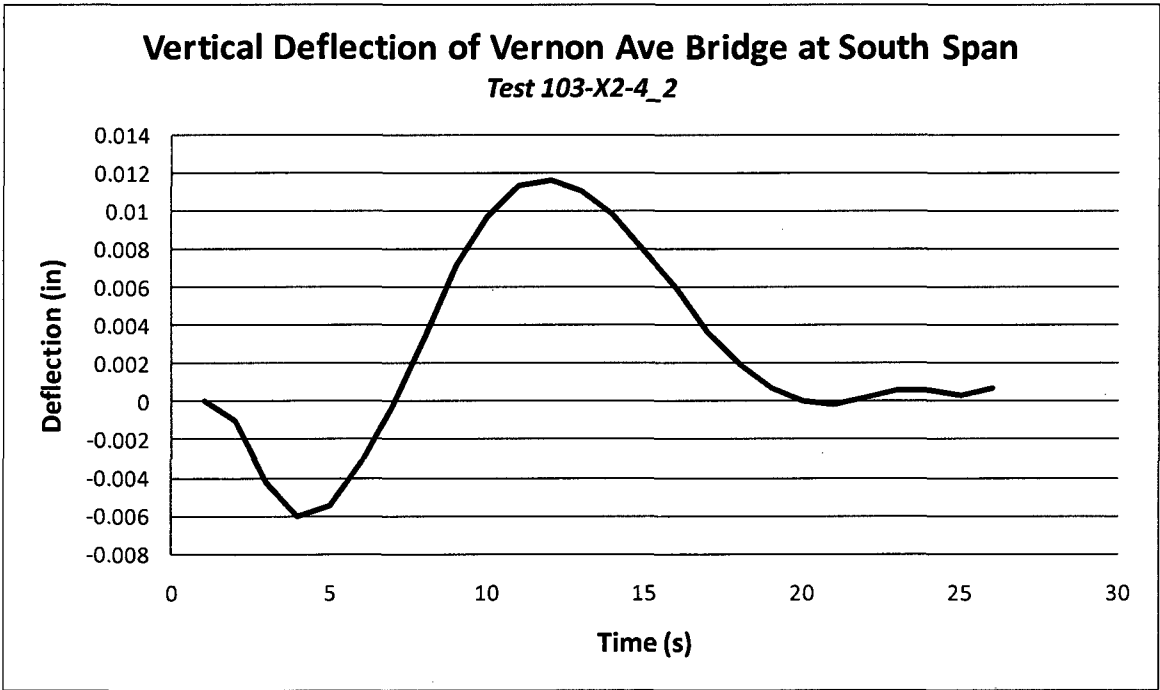
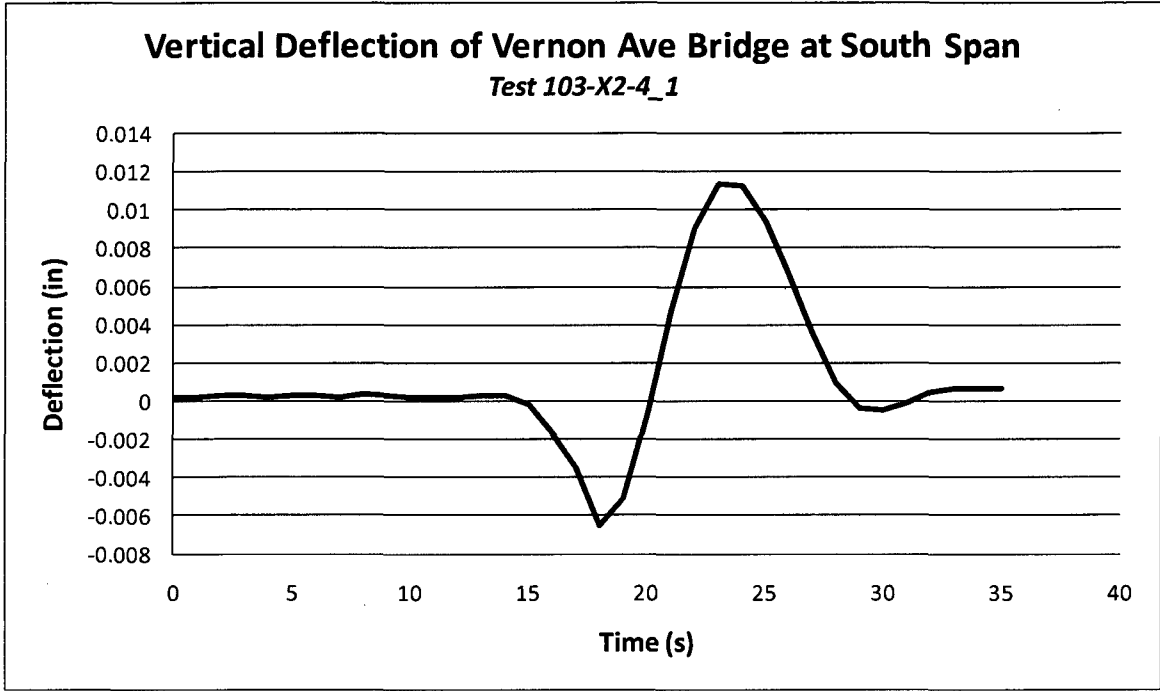
Vertical Deflection of Vernon Ave Bridge near Midspan

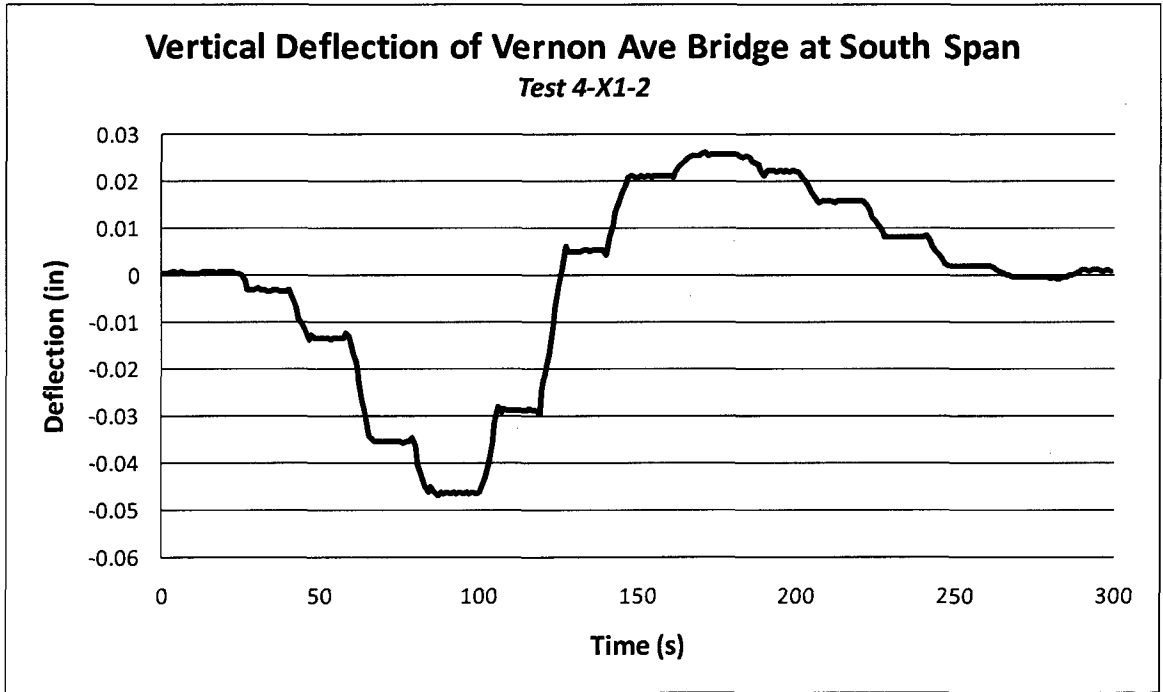
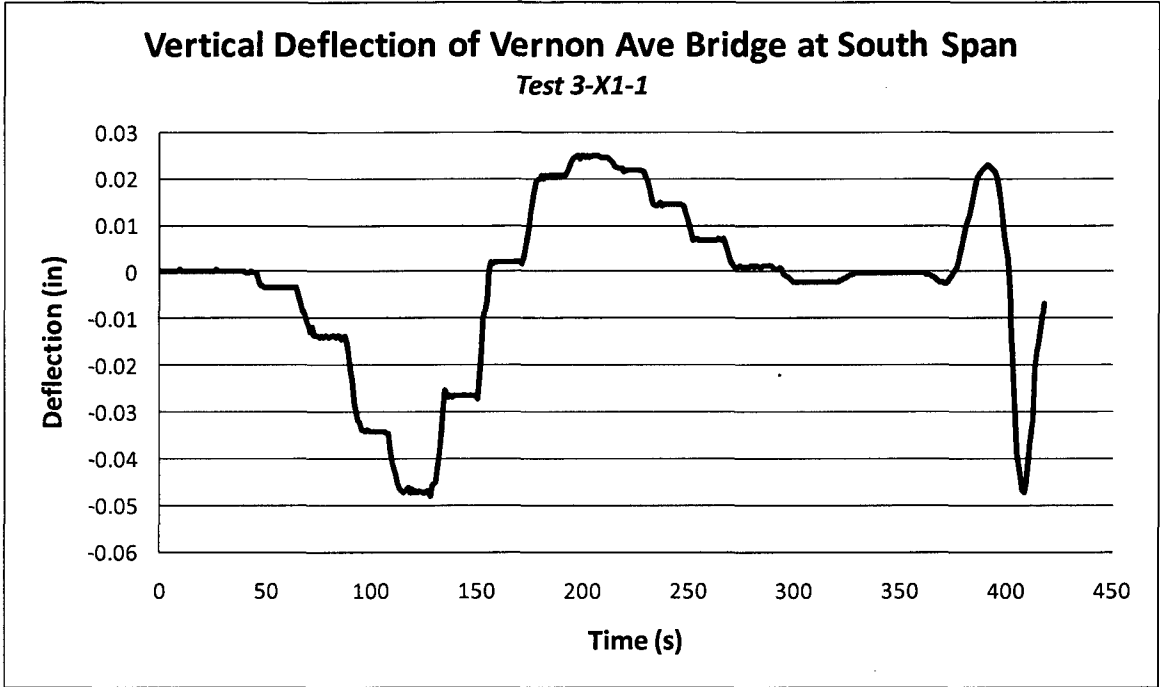
Test 25-X1-1





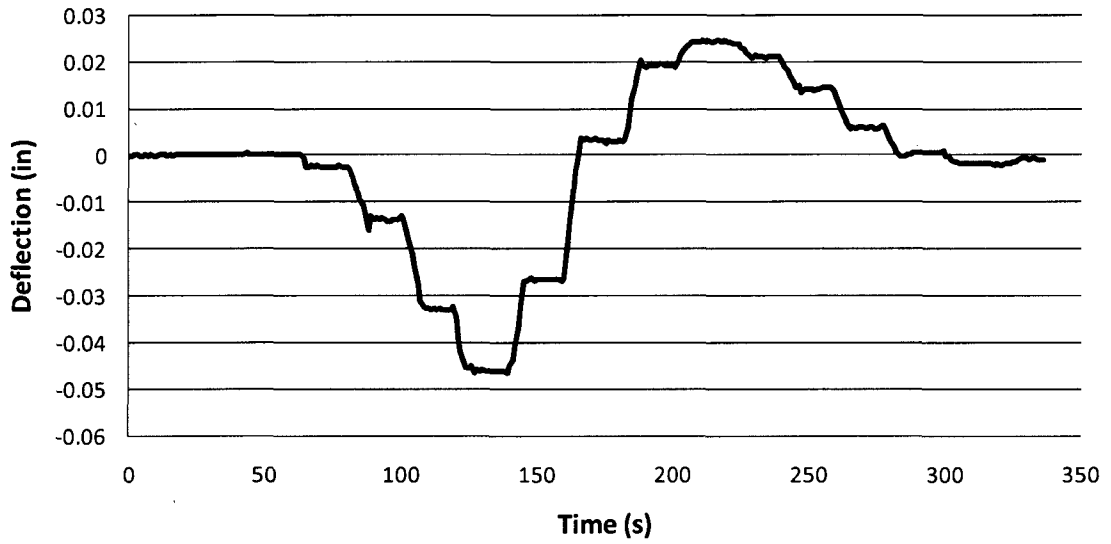






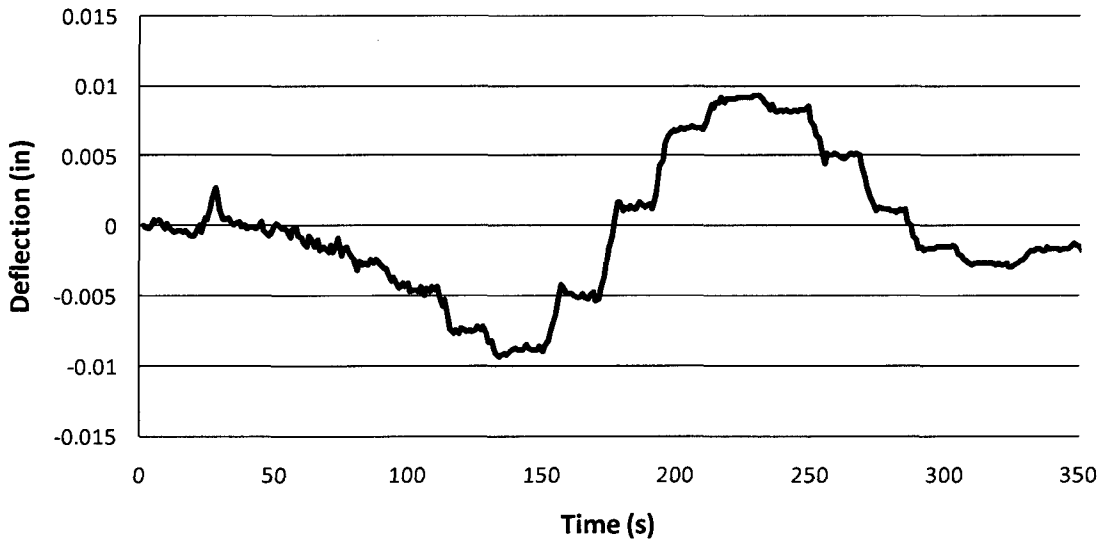
Vertical Deflection of Vernon Ave Bridge at South Span

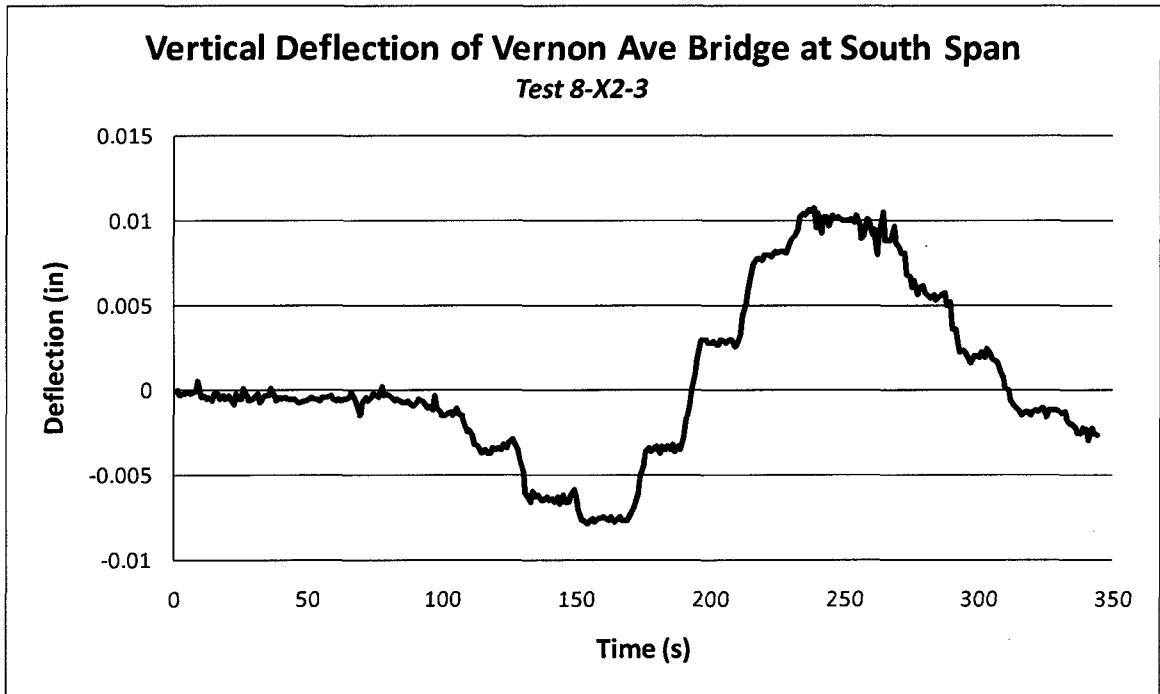
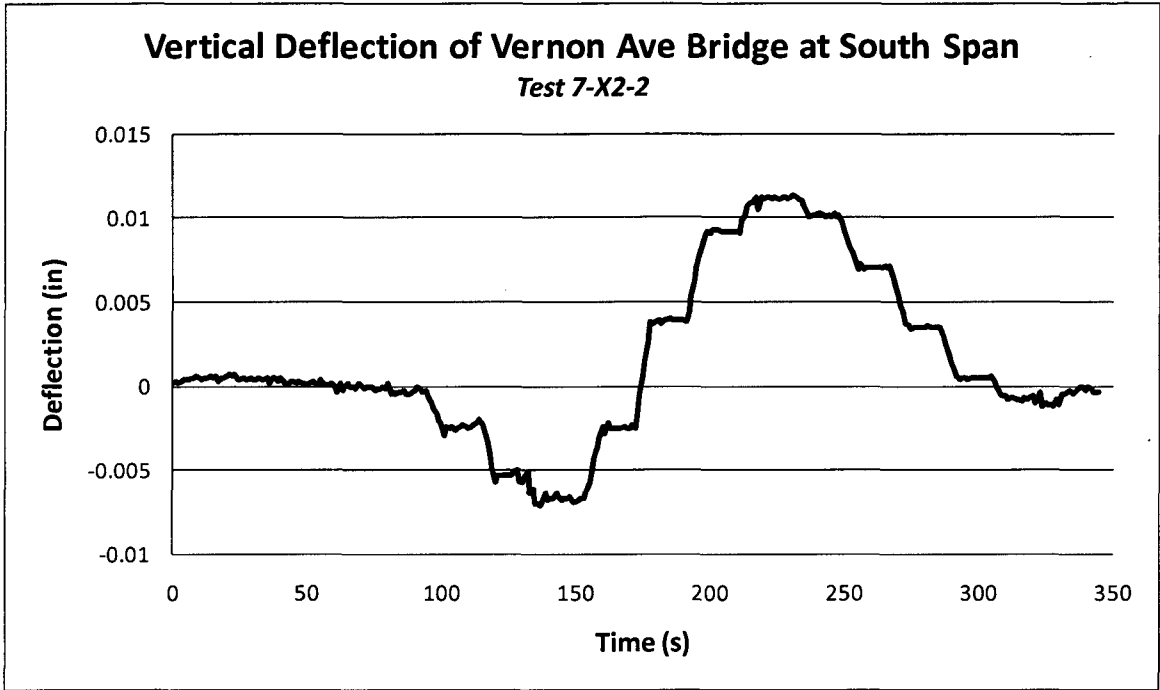
Test 5-X1-3

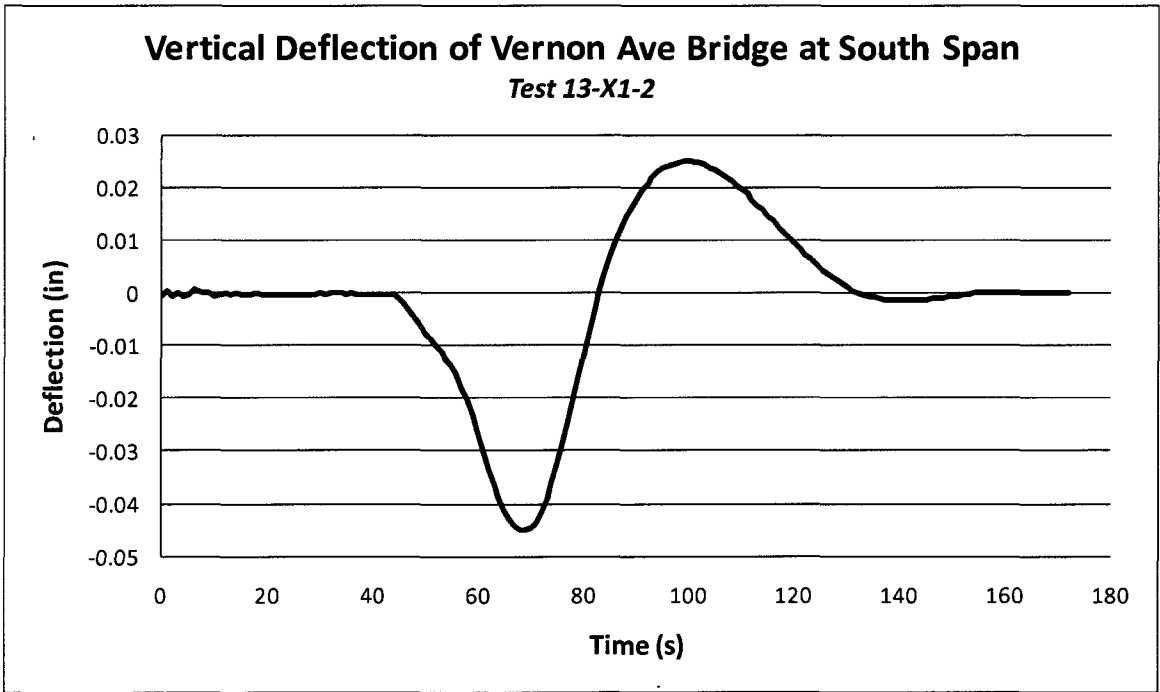
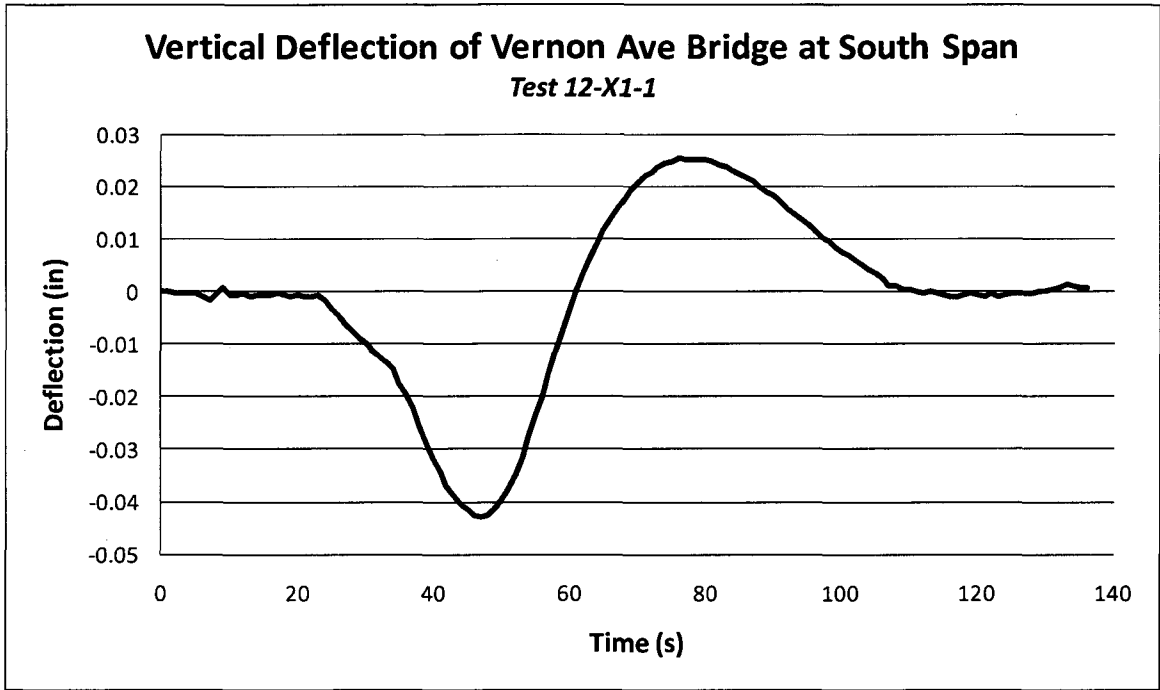


Vertical Deflection of Vernon Ave Bridge at South Span

Test 6-X2-1

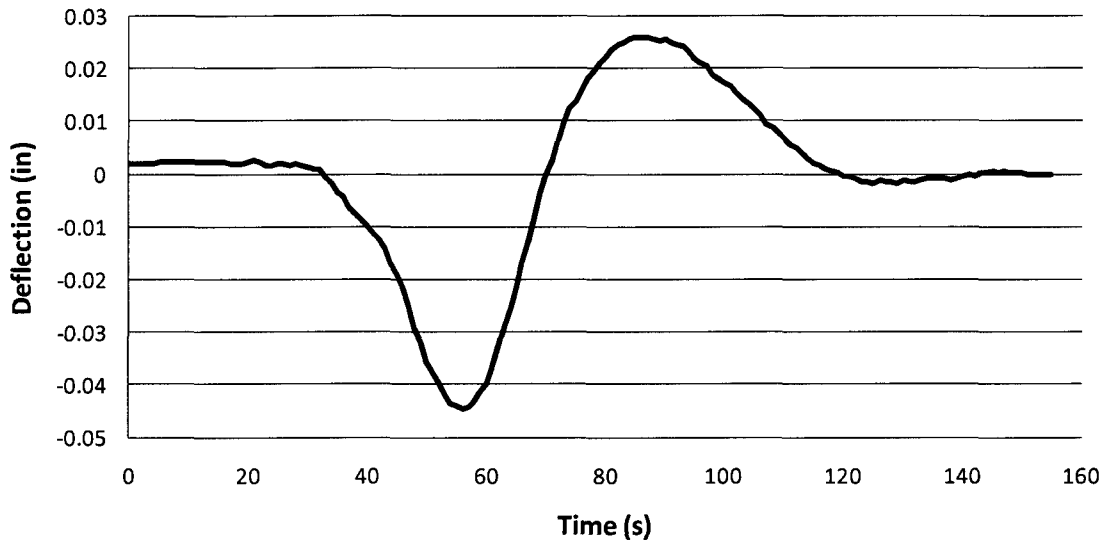






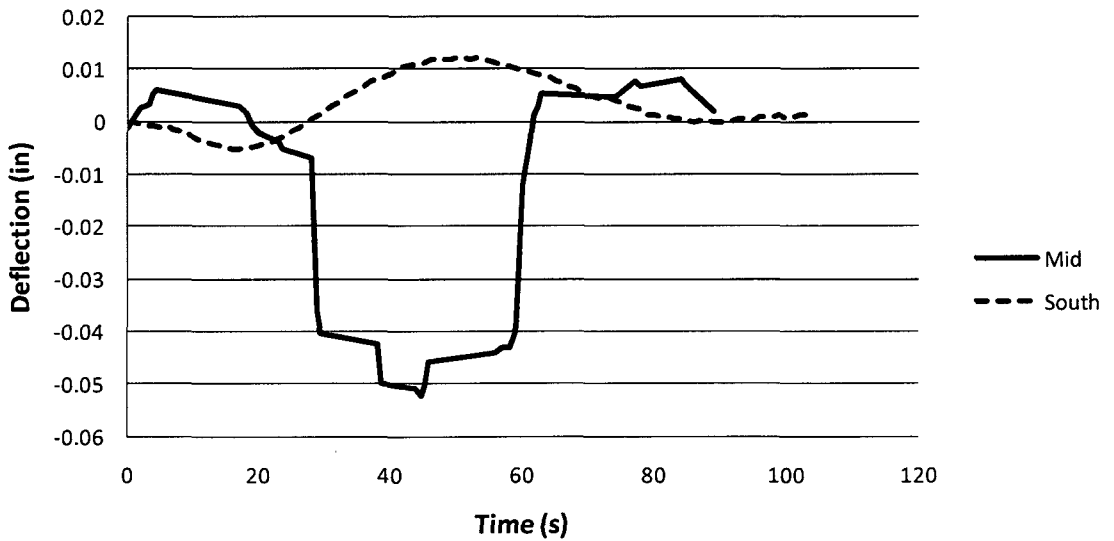
Vertical Deflection of Vernon Ave Bridge at South Span

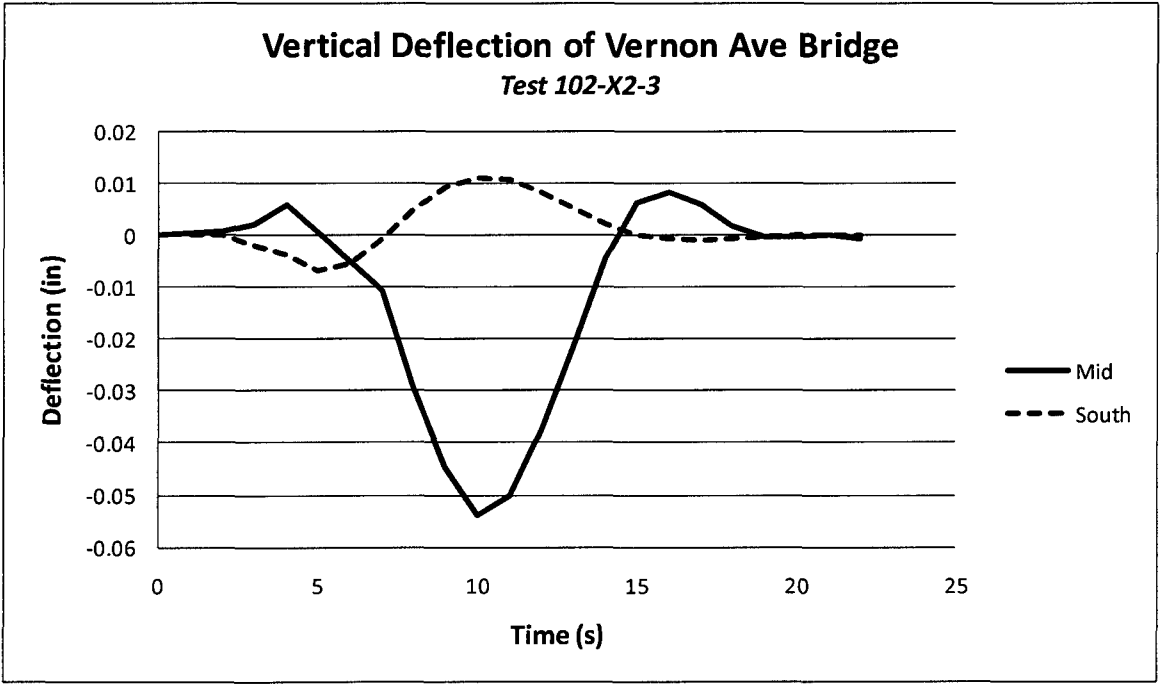
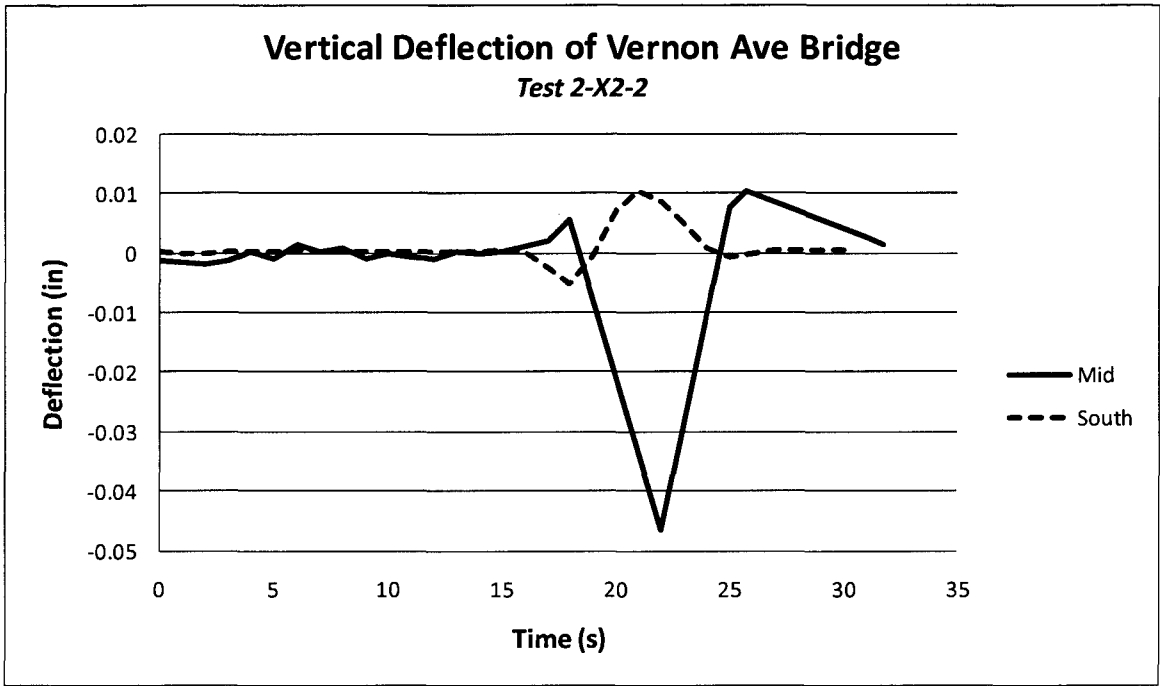
Test 14-X1-3

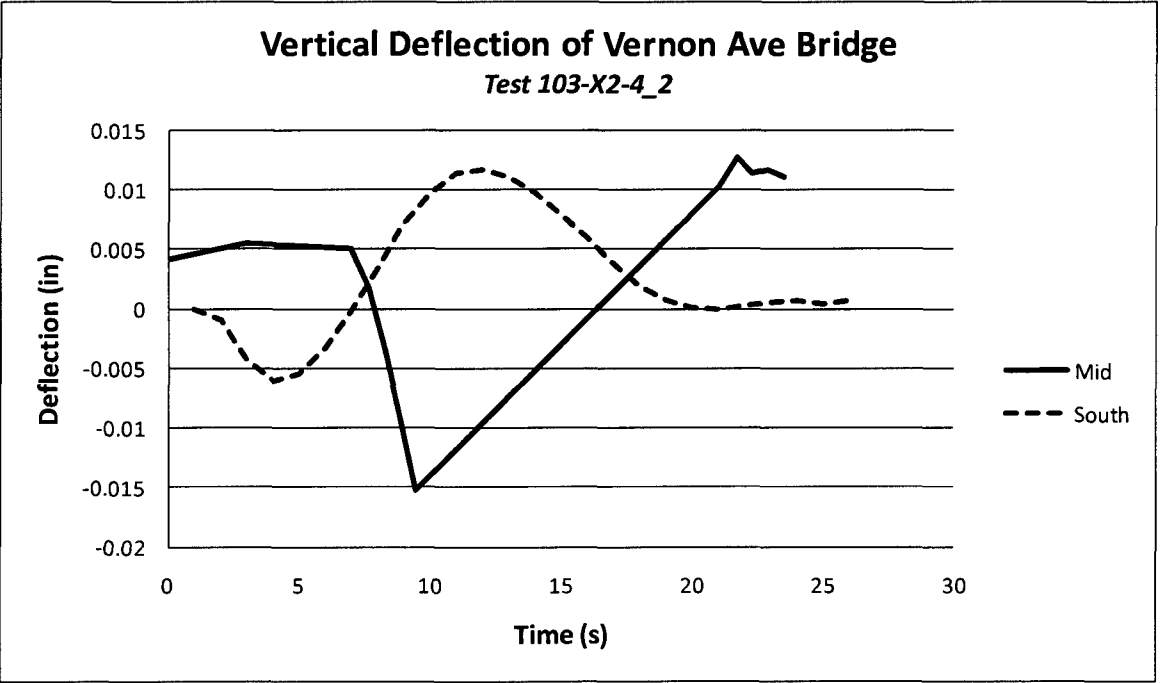
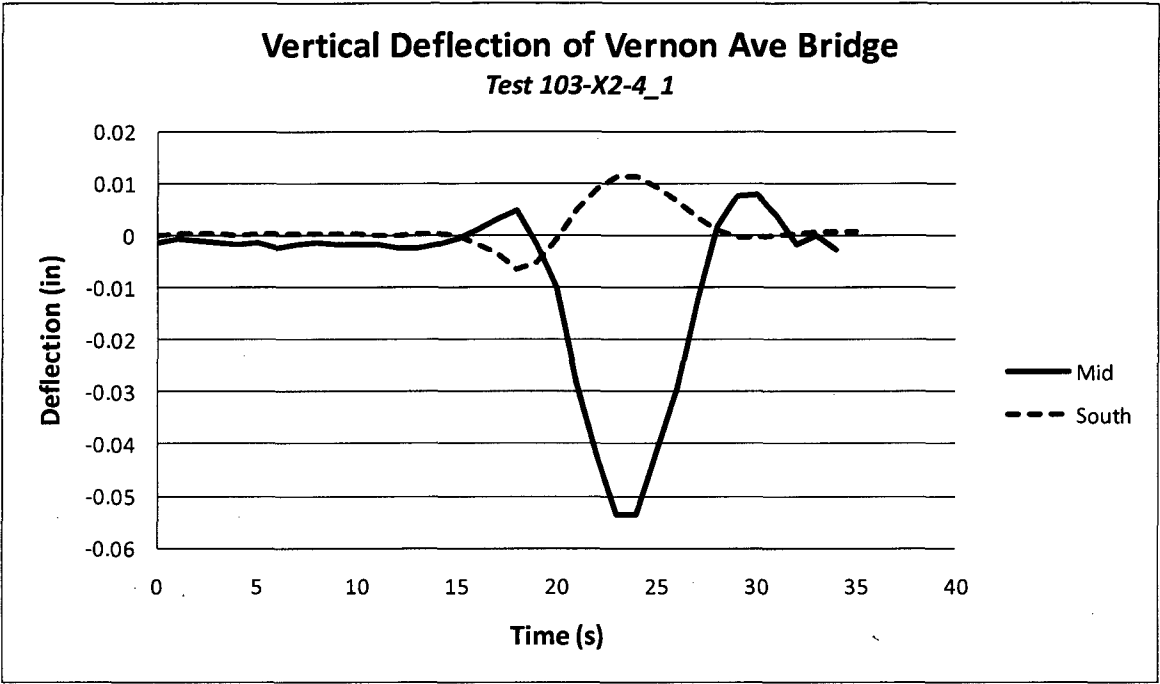


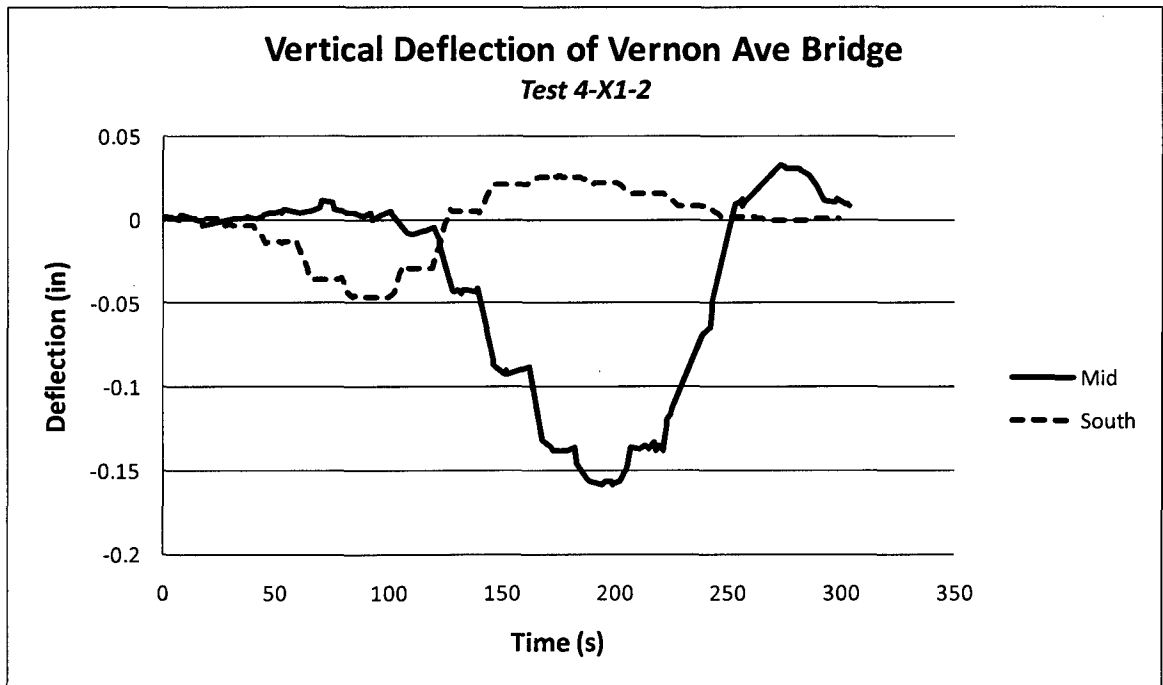
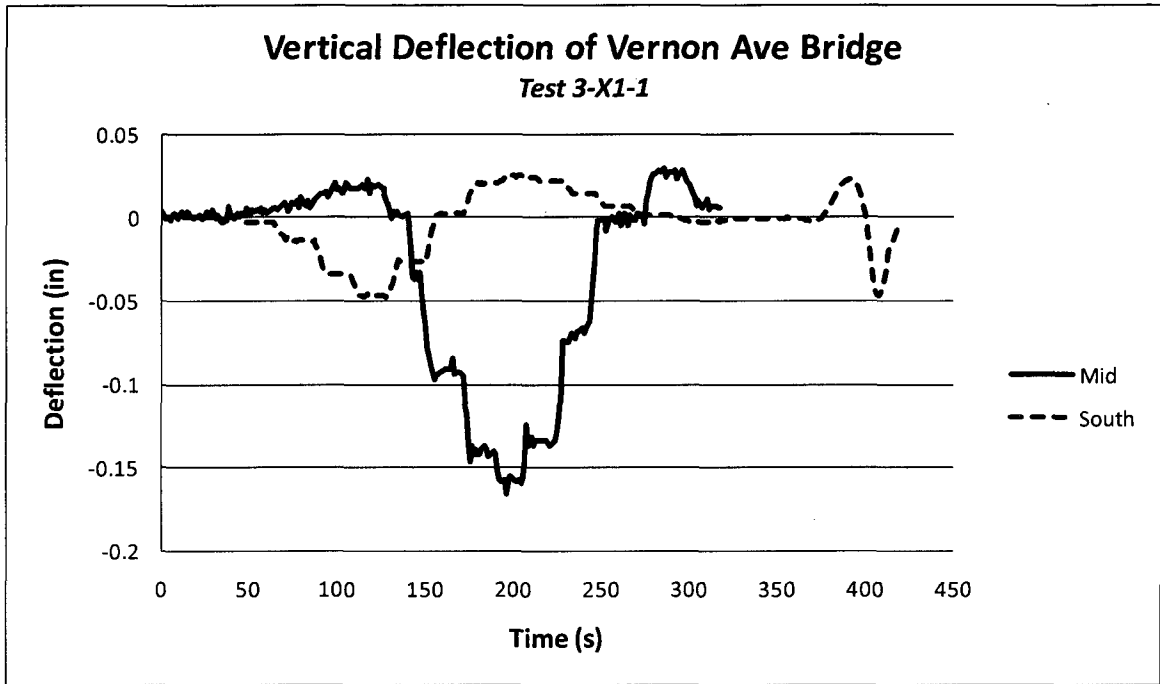
Vertical Deflection of Vernon Ave Bridge

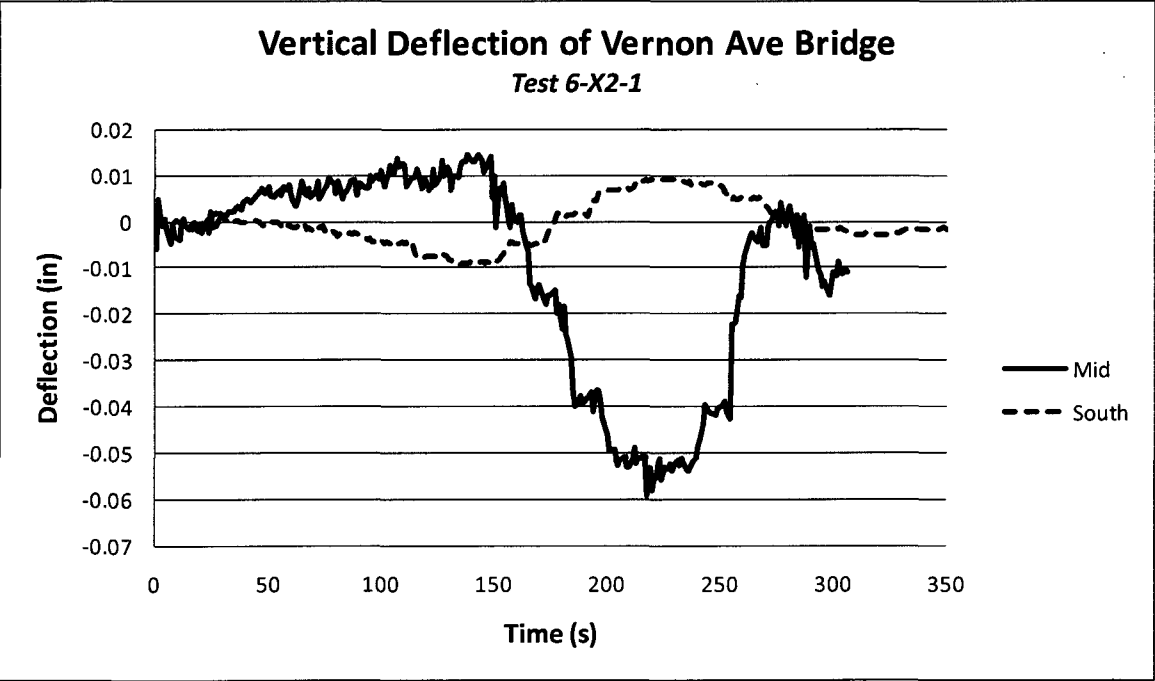
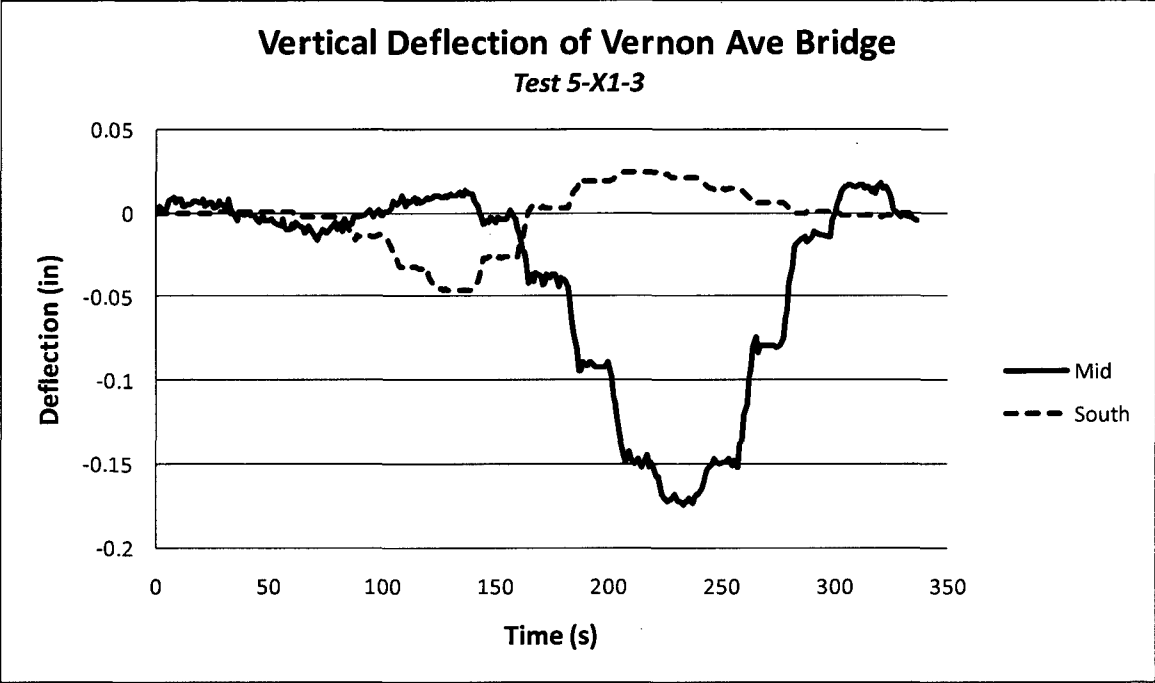
Test 1-X2-1

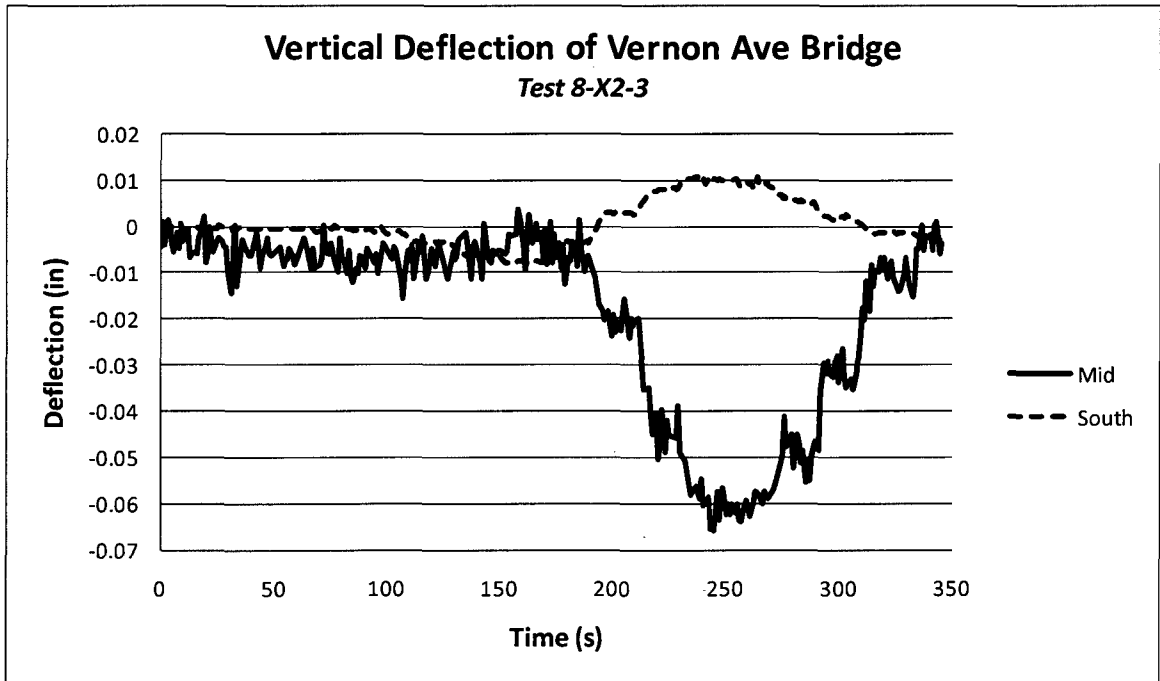
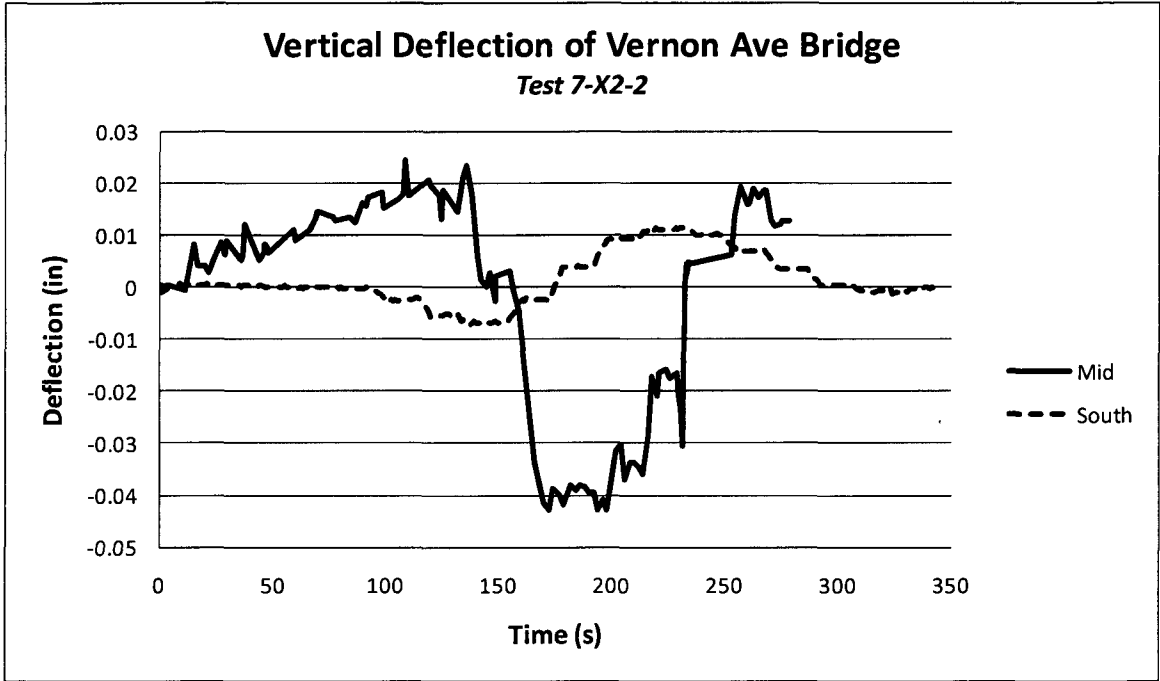


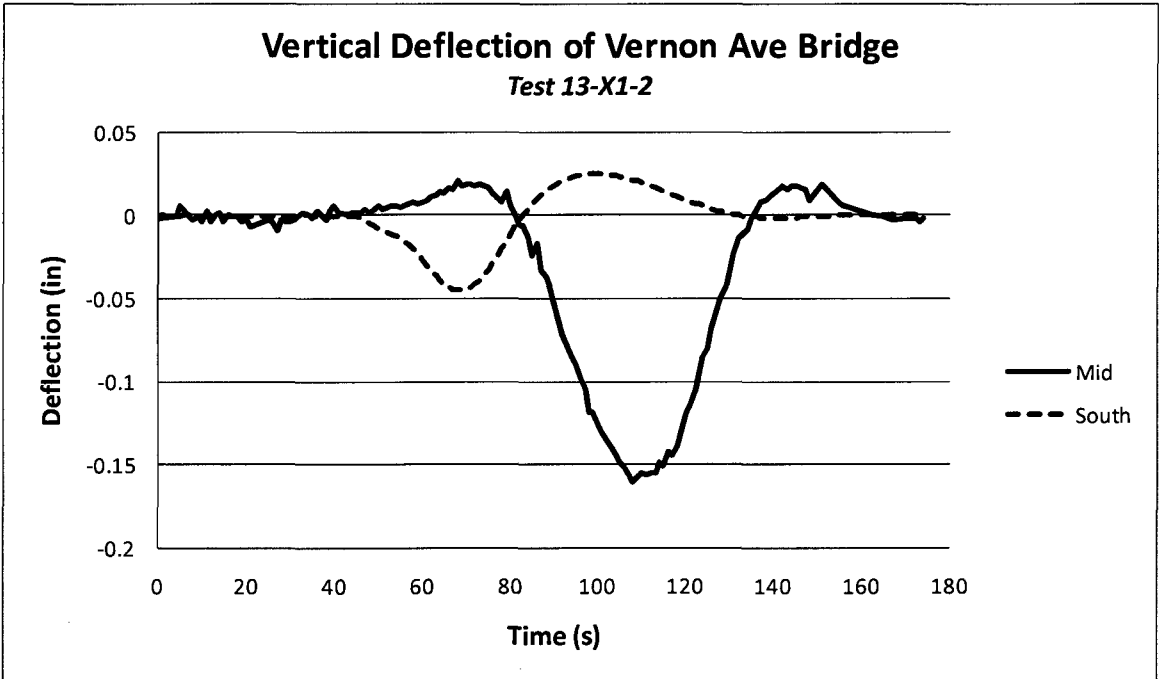
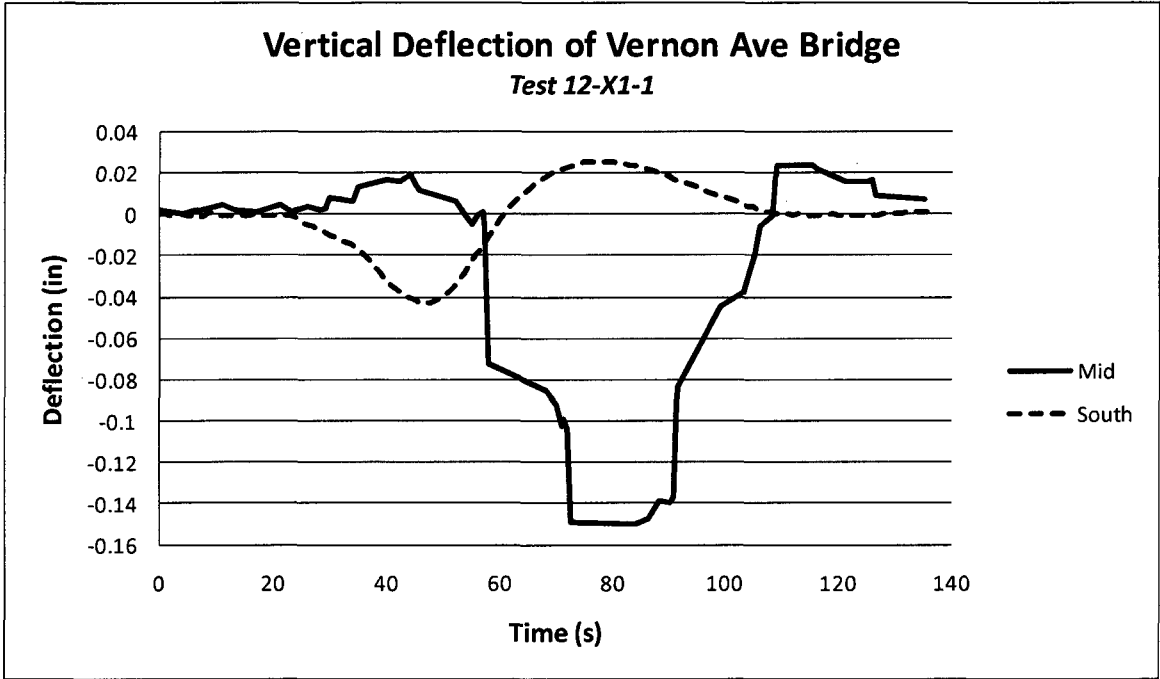






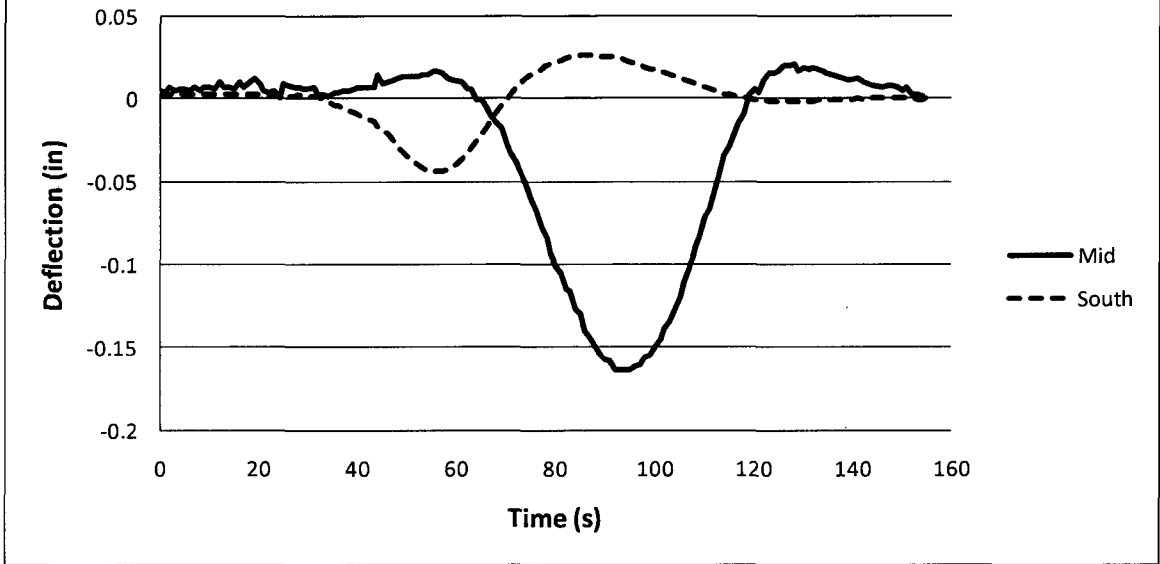






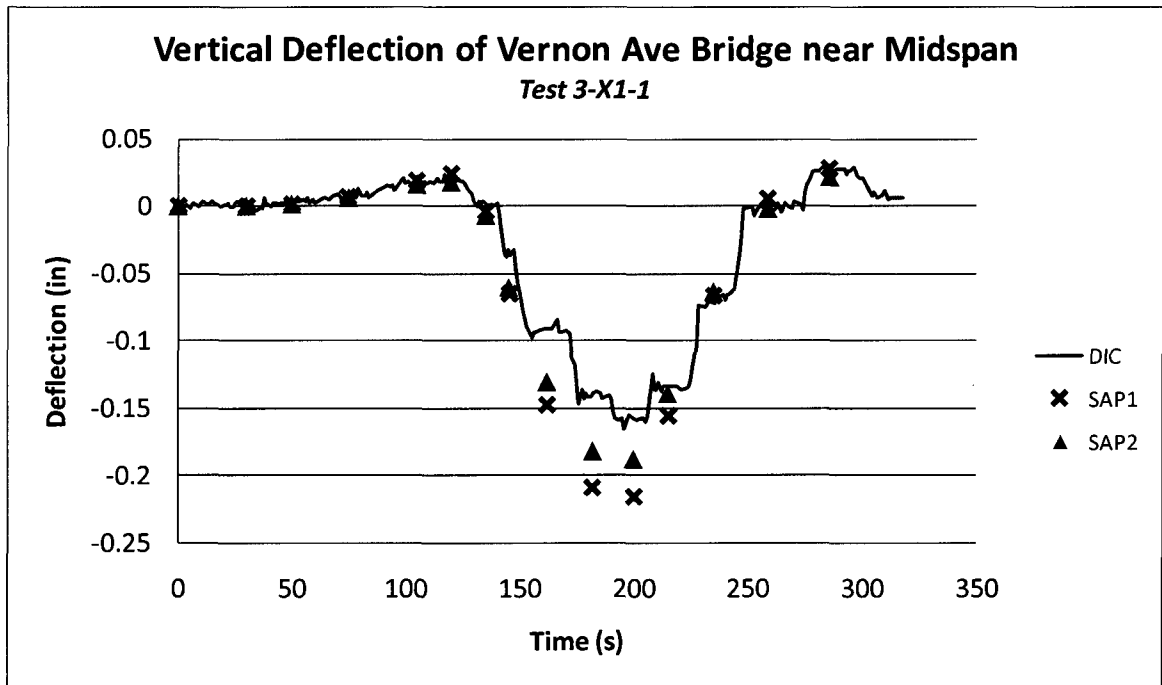
Vertical Deflection of Vernon Ave Bridge

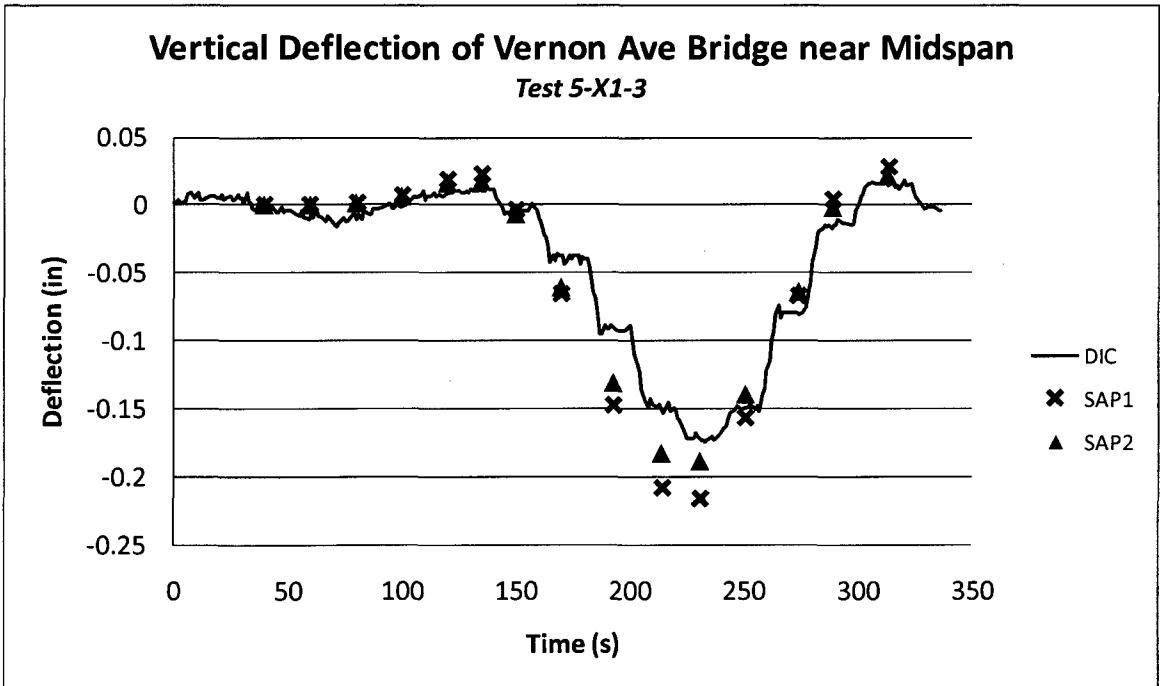
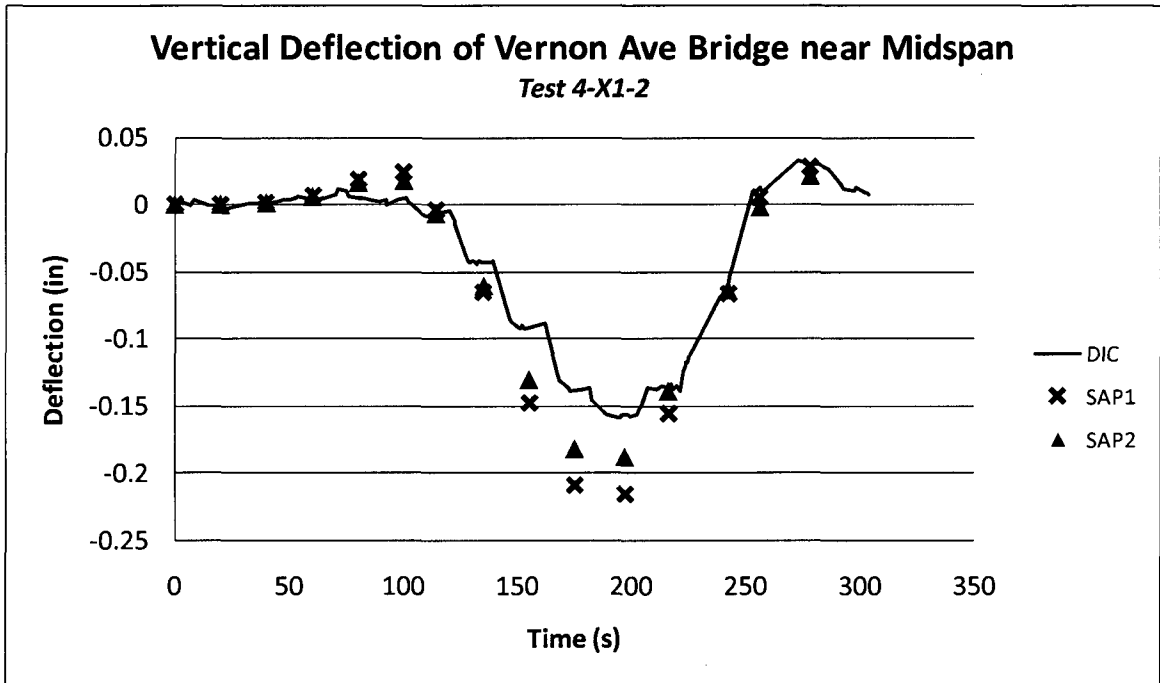
Test 14-X1-3

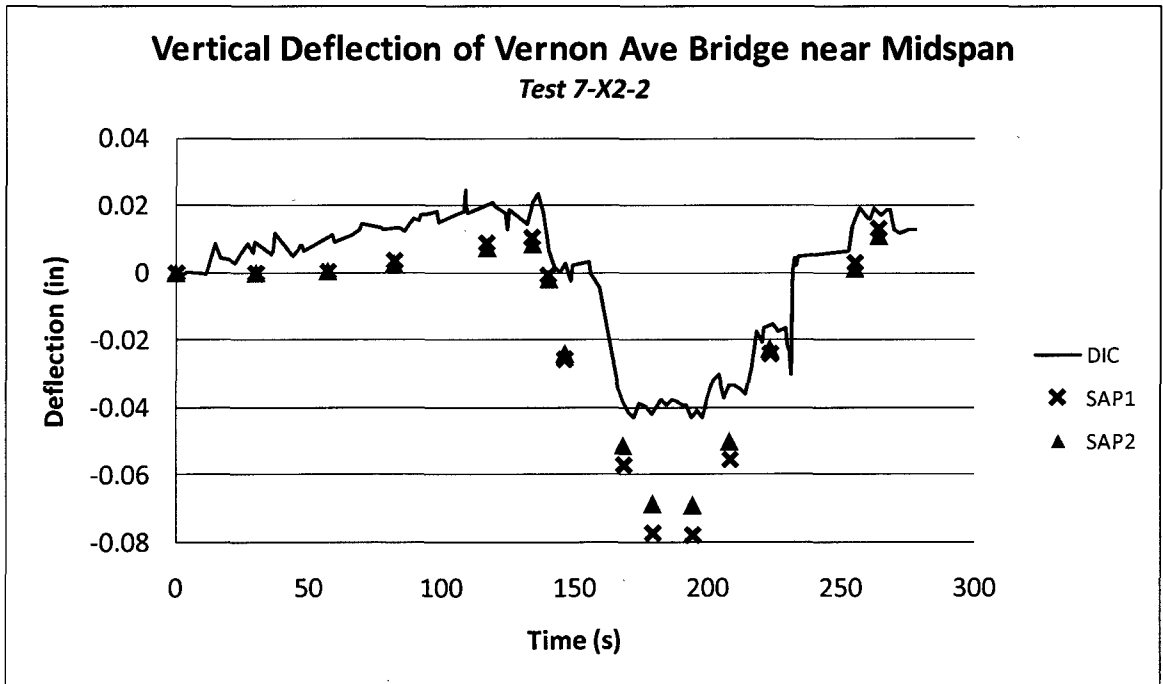
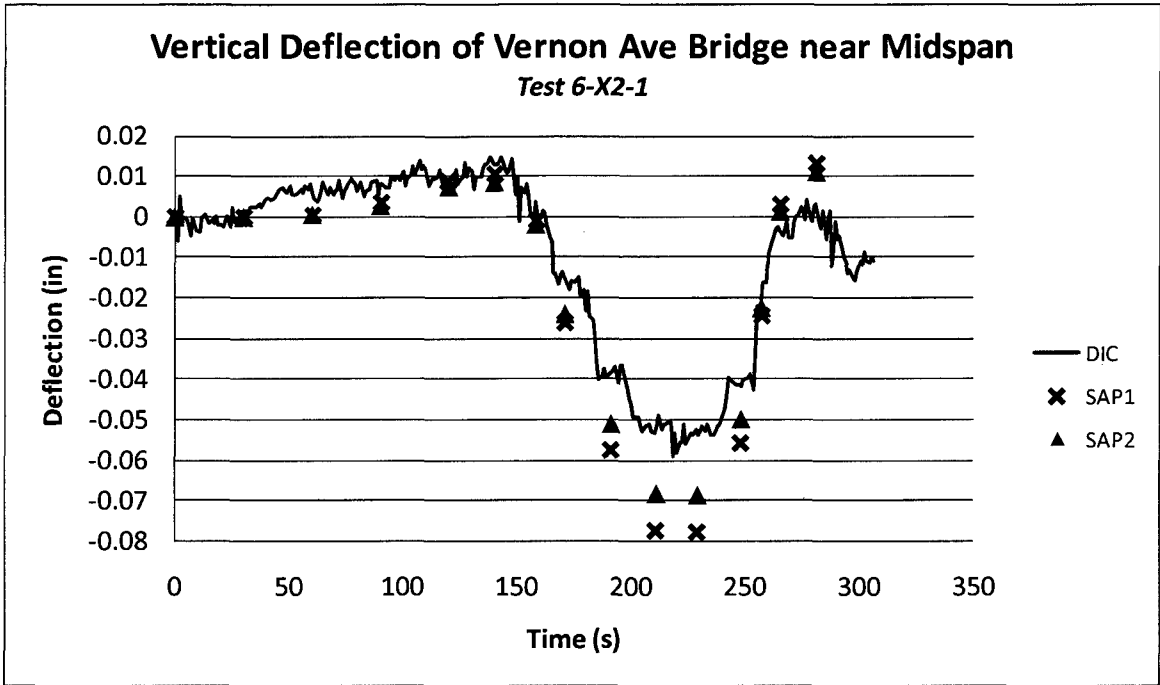


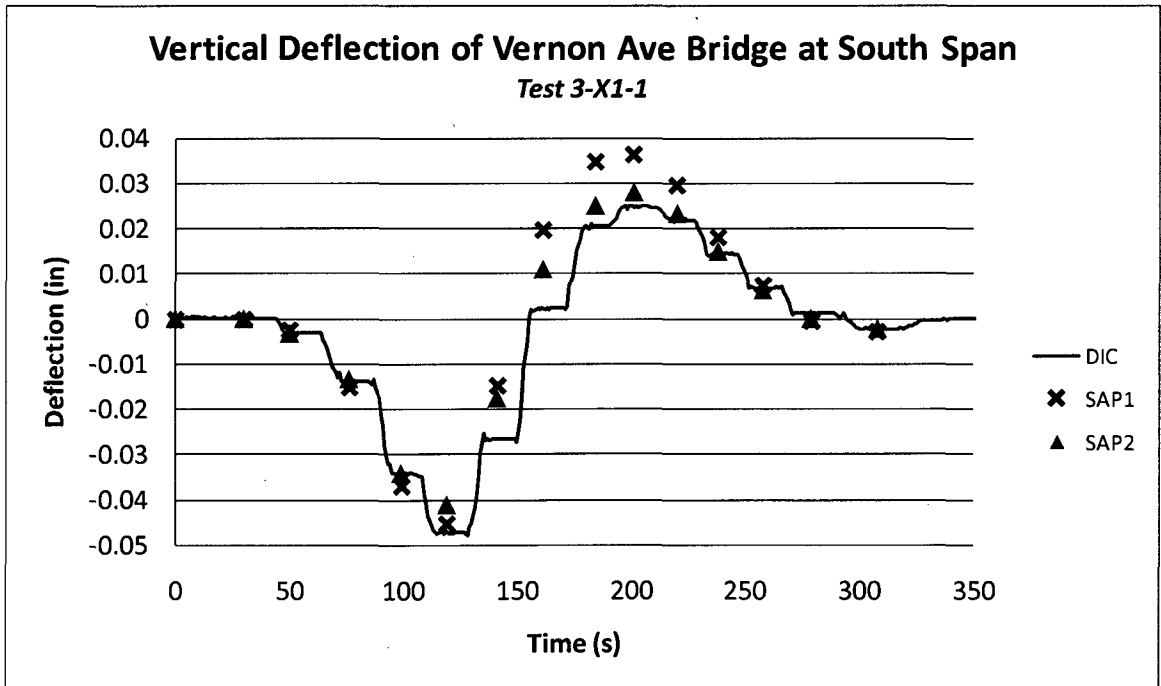
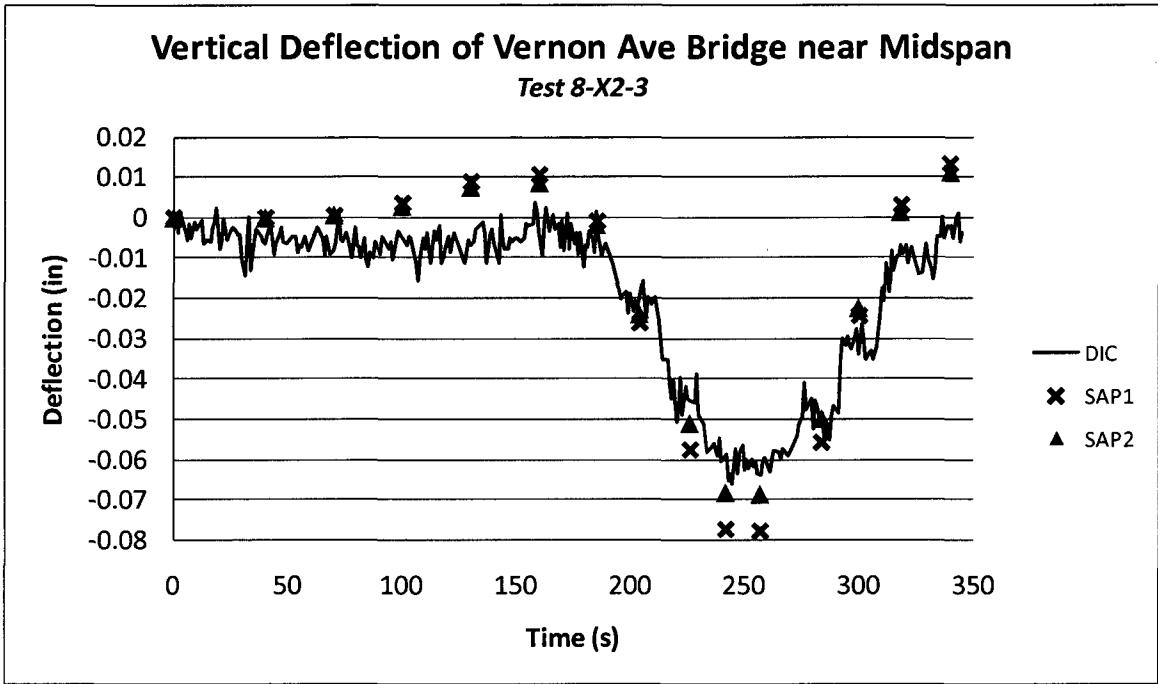
Vernon Avenue Load Test SAP2000 Comparison

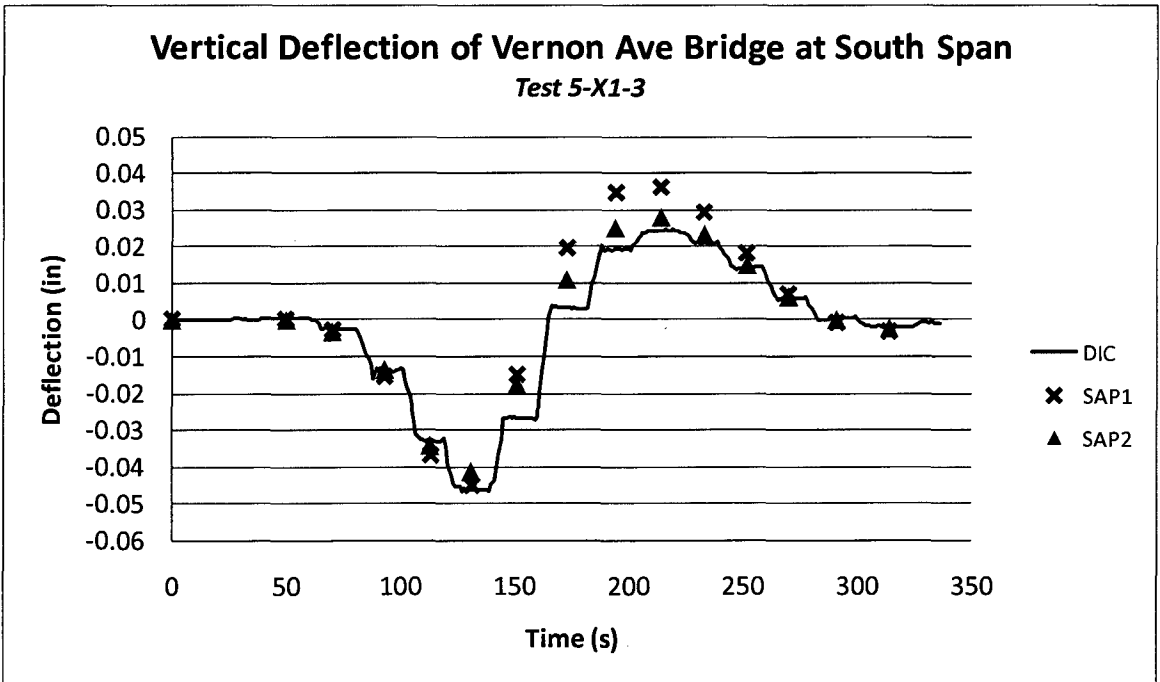
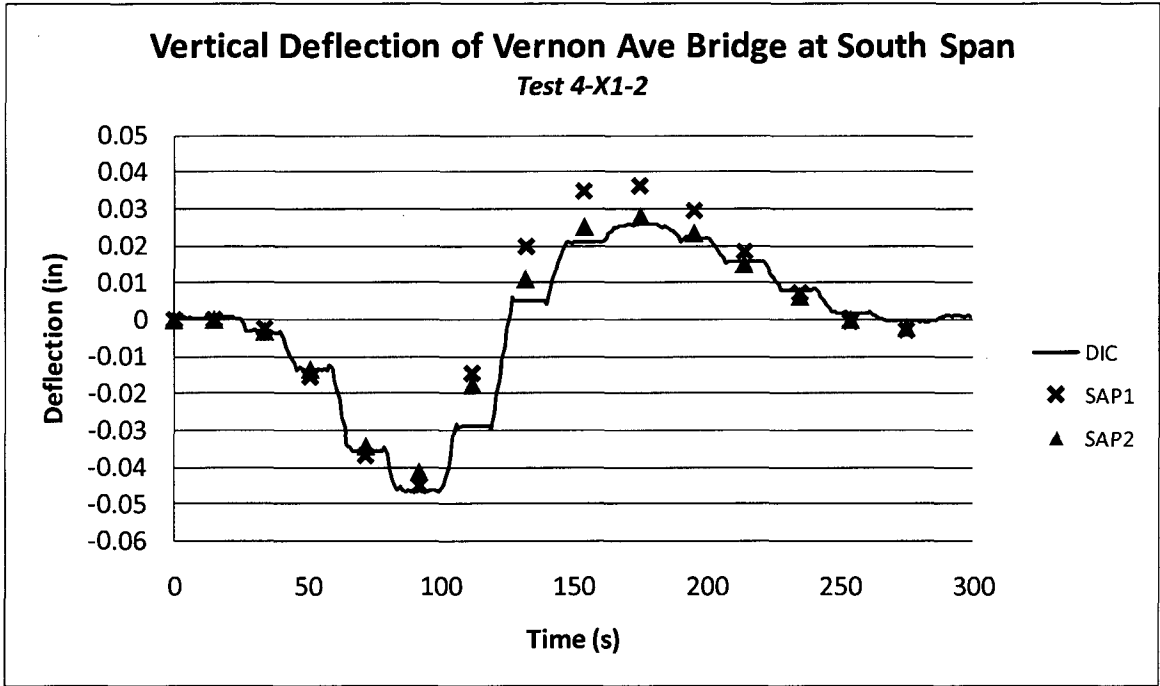
A finite element model of the Vernon Avenue Bridge was created by graduate student Paul Lefebvre. Bridge deflections during simulated stop tests were extracted from two versions of the model and compared with the deflection measured with the DIC setups.

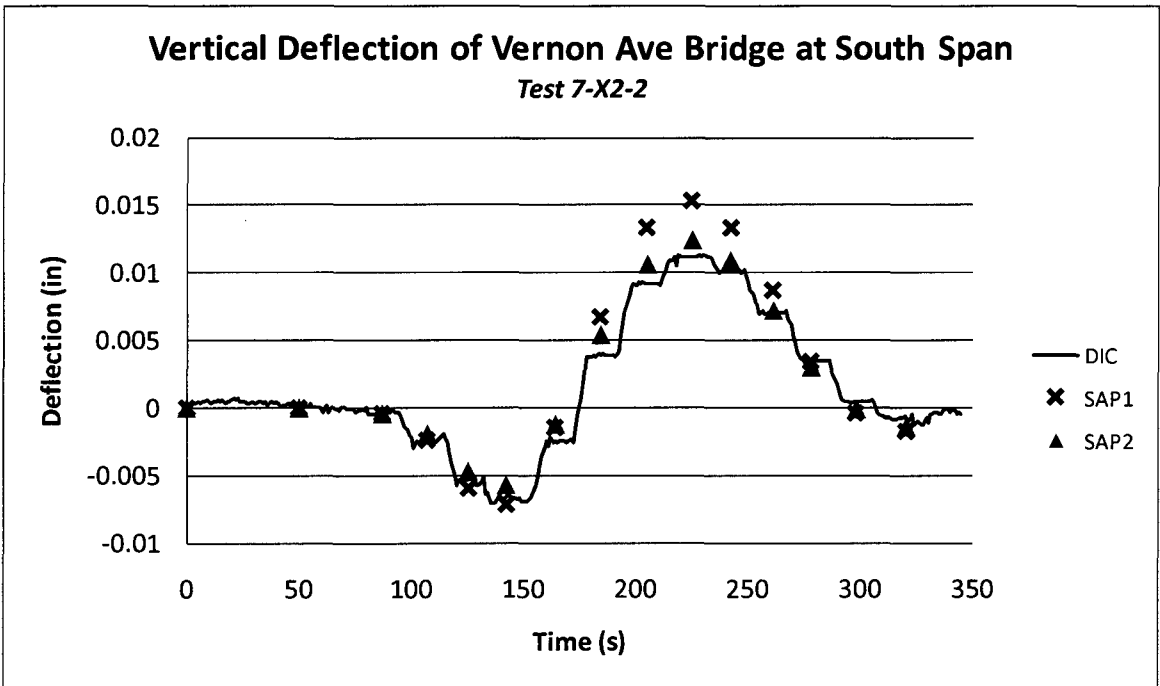
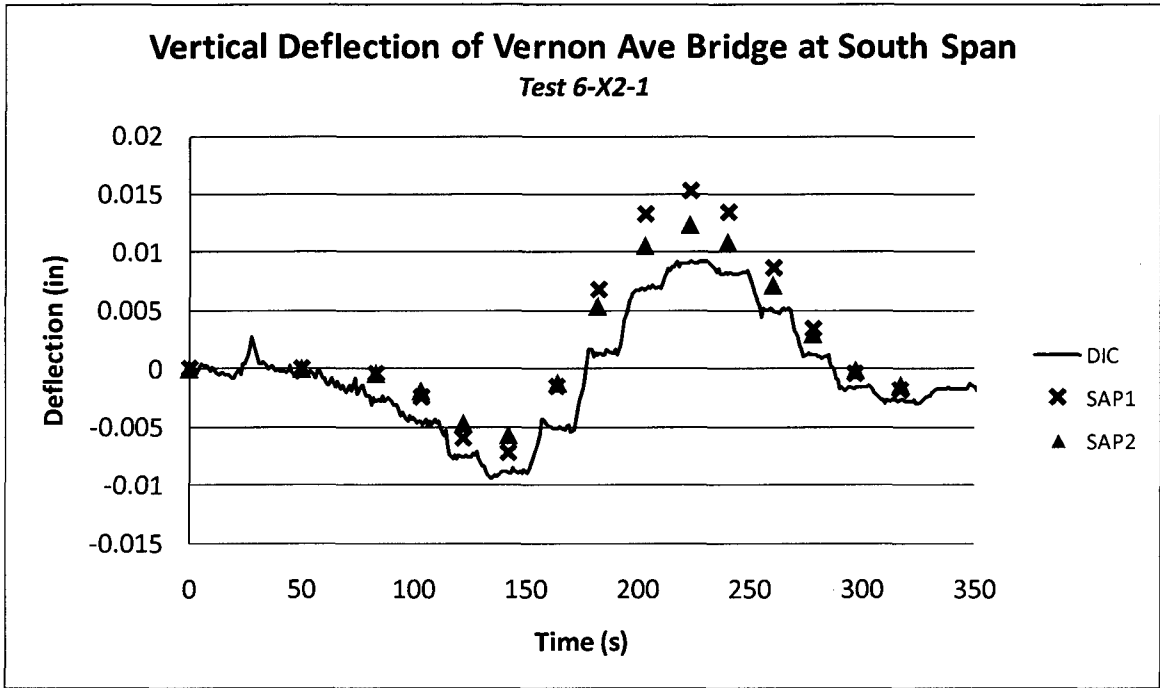






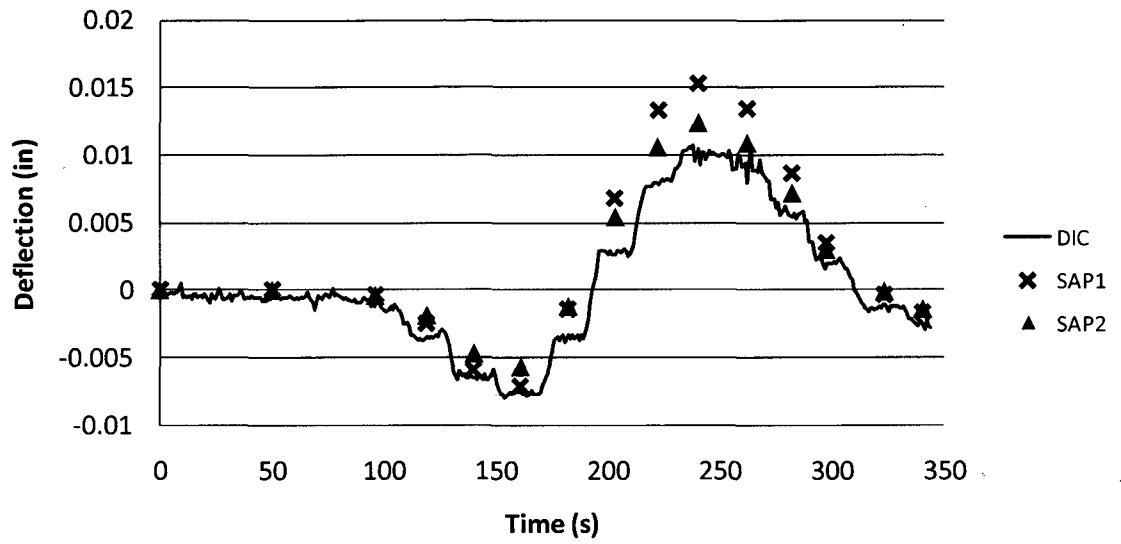






Vertical Deflection of Vernon Ave Bridge at South Span

Test 8-X2-3



APPENDIX B

SAMPLE BRIDGE INSPECTION REPORT

2-DIST 02	B.I.N. 15H	STRUCTURES INSPECTION FIELD REPORT ROUTINE & SPECIAL MEMBER INSPECTION	BR. DEPT NO. B-02-012
---------------------	----------------------	---	---------------------------------

CITY/TOWN BARRE	3-STRUCTURE NO. B02012-15H-MUN-NBI	11-Kilo. POINT 005.182	41-STATUS A:OPEN	99-ROUTINE INSP. DATE JAN 24, 2007
07-FACILITY CARRIED HWY VERNON AVE	MEMORIAL NAME/LOCAL NAME POWDER-MILL BRIDGE	27-YR BUILT 1937	106-YR REBUILT 0000	YR REHAB'D (NON 106) 0000
06-FEATURES INTERSECTED WATER WARE RIVER	26-FUNCTIONAL CLASS Major Collector	DIST. BRIDGE INSPECTION ENGINEER F. R. Heming		
43-STRUCTURE TYPE Steel continuous Stringer/Girder	22-OWNER Town Agency	21-MAINTAINER Town Agency	TEAM LEADER J. A. Mankowsky	
107-DECK TYPE Concrete Cast-in-Place	WEATHER Cloudy	TEMP. (air) -6°C	TEAM MEMBERS L. R. LYNCH	

ITEM 58	3	
DECK		<i>DEF</i>
1. Wearing surface	4	S-P
2. Deck Condition	3	S-A
3. Stay in place forms	N	-
4. Curbs	6	M-P
5. Median	N	-
6. Sidewalks	4	S-P
7. Parapets	5	M-P
8. Railing	4	S-P
9. Anti Missile Fence	N	-
10. Drainage System	4	M-P
11. Lighting Standards	N	-
12. Utilities	5	M-P
13. Deck Joints	N	-
14.	N	-
15.	N	-
16.	N	-

CURB REVEAL (In millimeters)	N 215	S 230
---------------------------------	----------	----------

APPROACHES			<i>DEF</i>
a. Appr. Pavement Condition	6	M-P	
b. Appr. Roadway Settlement	5	M-P	
c. Appr. Sidewalk Settlement	N	-	
d.	N	-	

OVERHEAD SIGNS (Attached to bridge)			<i>DEF</i>
	(Y/N)	N	
a. Condition of Welds	N	-	
b. Condition of Bolts	N	-	
c. Condition of Signs	N	-	

ITEM 59	4	
SUPERSTRUCTURE		<i>DEF</i>
1. Stringers	N	-
2. Floorbeams	N	-
3. Floor System Bracing	N	-
4. Girders or Beams	4	S-P
5. Trusses - General	N	-
a. Upper Chords	N	-
b. Lower Chords	N	-
c. Web Members	N	-
d. Lateral Bracing	N	-
e. Sway Bracings	N	-
f. Portals	N	-
g. End Posts	N	-
6. Pin & Hangers	N	-
7. Conn. Plt's, Guseets & Angles	5	M-P
8. Cover Plates	N	-
9. Bearing Devices	4	S-P
10. Diaphragms/Cross Frames	4	S-P
11. Rivets & Bolts	5	S-P
12. Welds	N	-
13. Member Alignment	5	-
14. Paint/Coating	3	S-P
15.	N	-

Year Painted	X
--------------	---

COLLISION DAMAGE: *Please explain*
None () Minor () Moderate () Severe ()

LOAD DEFLECTION: *Please explain*
None () Minor () Moderate () Severe ()

LOAD VIBRATION: *Please explain*
None () Minor () Moderate () Severe ()

Any Fracture Critical Member: (Y/N) Y N

Any Cracks: (Y/N) Y N

ITEM 60	6	
SUBSTRUCTURE		<i>DEF</i>
1. Abutments		
a. Pedestals	N	N
b. Bridge Seats	N	7
c. Backwalls	N	6
d. Breastwalls	N	6
e. Wingwalls	N	7
f. Slope Paving/Rip-Rap	N	N
g. Pointing	N	N
h. Footings	N	H
i. Piles	N	H
j. Scour	N	N
k. Settlement	N	7
l. Erosion	N	5
m.	N	N
2. Piers or Bents		
a. Pedestals	N	N
b. Caps	N	6
c. Columns	7	7
d. Stems/Walls/Pierwalls	N	N
e. Pointing	N	N
f. Footing	H	H
g. Piles	X	X
h. Scour	6	H
i. Settlement	8	7
j.	N	N
k.	N	N
3. Pile Bents		
a. Pile Caps	N	N
b. Piles	N	N
c. Diagonal Bracing	N	N
d. Horizontal Bracing	N	N
e. Fasteners	N	N

UNDERMINING (Y/N) If YES please explain Y N

COLLISION DAMAGE:
None () Minor () Moderate () Severe ()

SCOUR: *Please explain*
None () Minor () Moderate () Severe ()

I-69 (Dive Report): 6 I-69 (This Report): 6

93B-U/W (DIVE) Insp **08/10/2005**

X=UNKNOWN N=NOT APPLICABLE H=HIDDEN/INACCESSIBLE R=REMOVED

KT 11/17-06

CITY/TOWN BARRE	B.I.N. 15H	BR. DEPT. NO. B-02-012	S. STRUCTURE NO. B02012-15H-MUN-NBI	INSPECTION DATE JAN 24, 2007																																																																																															
ITEM 61 CHANNEL & CHANNEL PROTECTION <table border="1" style="width:100%; border-collapse: collapse;"> <thead> <tr> <th></th> <th>Dive</th> <th>Cur</th> <th>DEF</th> </tr> </thead> <tbody> <tr><td>1.Channel Scour</td><td>6</td><td>H</td><td>-</td></tr> <tr><td>2.Embankment Erosion</td><td>7</td><td>7</td><td>-</td></tr> <tr><td>3.Debris</td><td>5</td><td>H</td><td>M-P</td></tr> <tr><td>4.Vegetation</td><td>7</td><td>7</td><td>-</td></tr> <tr><td>5.Utilities</td><td>N</td><td>N</td><td>-</td></tr> <tr><td>6.Rip-Rap/Slope Protection</td><td>7</td><td>7</td><td>-</td></tr> <tr><td>7.Aggradation</td><td>7</td><td>7</td><td>-</td></tr> <tr><td>8.Fender System</td><td>N</td><td>N</td><td>-</td></tr> </tbody> </table>			Dive	Cur	DEF	1.Channel Scour	6	H	-	2.Embankment Erosion	7	7	-	3.Debris	5	H	M-P	4.Vegetation	7	7	-	5.Utilities	N	N	-	6.Rip-Rap/Slope Protection	7	7	-	7.Aggradation	7	7	-	8.Fender System	N	N	-	ITEM 36 TRAFFIC SAFETY <table border="1" style="width:100%; border-collapse: collapse;"> <thead> <tr> <th></th> <th>36</th> <th>COND</th> <th>DEF</th> </tr> </thead> <tbody> <tr><td>A. Bridge Railing</td><td>0</td><td>4</td><td>S-P</td></tr> <tr><td>B. Transitions</td><td>0</td><td>6</td><td>M-P</td></tr> <tr><td>C. Approach Guardrail</td><td>0</td><td>6</td><td>M-P</td></tr> <tr><td>D. Approach Guardrail Ends</td><td>0</td><td>6</td><td>M-P</td></tr> </tbody> </table>			36	COND	DEF	A. Bridge Railing	0	4	S-P	B. Transitions	0	6	M-P	C. Approach Guardrail	0	6	M-P	D. Approach Guardrail Ends	0	6	M-P	ACCESSIBILITY (Y/N/P) <table border="1" style="width:100%; border-collapse: collapse;"> <thead> <tr> <th></th> <th>Needed</th> <th>Used</th> </tr> </thead> <tbody> <tr><td>Lift Bucket</td><td>N</td><td>N</td></tr> <tr><td>Ladder</td><td>P</td><td>N</td></tr> <tr><td>Boat</td><td>N</td><td>N</td></tr> <tr><td>Waders</td><td>P</td><td>N</td></tr> <tr><td>Inspector 50</td><td>Y</td><td>Y</td></tr> <tr><td>Rigging</td><td>N</td><td>N</td></tr> <tr><td>Staging</td><td>N</td><td>N</td></tr> <tr><td>Traffic Control</td><td>Y</td><td>Y</td></tr> <tr><td>RR Flagger</td><td>N</td><td>N</td></tr> <tr><td>Police</td><td>Y</td><td>Y</td></tr> <tr><td>Other:</td><td></td><td></td></tr> <tr><td>N</td><td>N</td><td>N</td></tr> </tbody> </table>		Needed	Used	Lift Bucket	N	N	Ladder	P	N	Boat	N	N	Waders	P	N	Inspector 50	Y	Y	Rigging	N	N	Staging	N	N	Traffic Control	Y	Y	RR Flagger	N	N	Police	Y	Y	Other:			N	N	N
	Dive	Cur	DEF																																																																																																
1.Channel Scour	6	H	-																																																																																																
2.Embankment Erosion	7	7	-																																																																																																
3.Debris	5	H	M-P																																																																																																
4.Vegetation	7	7	-																																																																																																
5.Utilities	N	N	-																																																																																																
6.Rip-Rap/Slope Protection	7	7	-																																																																																																
7.Aggradation	7	7	-																																																																																																
8.Fender System	N	N	-																																																																																																
	36	COND	DEF																																																																																																
A. Bridge Railing	0	4	S-P																																																																																																
B. Transitions	0	6	M-P																																																																																																
C. Approach Guardrail	0	6	M-P																																																																																																
D. Approach Guardrail Ends	0	6	M-P																																																																																																
	Needed	Used																																																																																																	
Lift Bucket	N	N																																																																																																	
Ladder	P	N																																																																																																	
Boat	N	N																																																																																																	
Waders	P	N																																																																																																	
Inspector 50	Y	Y																																																																																																	
Rigging	N	N																																																																																																	
Staging	N	N																																																																																																	
Traffic Control	Y	Y																																																																																																	
RR Flagger	N	N																																																																																																	
Police	Y	Y																																																																																																	
Other:																																																																																																			
N	N	N																																																																																																	
STREAM FLOW VELOCITY: Tidal () High () Moderate (<input checked="" type="checkbox"/>) Low () None ()		WEIGHT POSTING Not Applicable <input checked="" type="checkbox"/>		TOTAL HOURS 24																																																																																															
ITEM 61 (Dive Report): 6 ITEM 61 (This Report): 6 93b-U/W INSP. DATE: 08/10/2005		CLEARANCE POSTING Not Applicable <input type="checkbox"/>		PLANS (Y/N): N (V.C.R.) (Y/N): N TAPE#: _____ List of field tests performed: Visual & Spot sounding. Beam section loss measurements.																																																																																															
RATING Rating Report (Y/N): <input checked="" type="checkbox"/> Y Date: 08/01/1980		(To be filled out by DBIE) Request for Rating or Rerating (Y/N): <input type="checkbox"/> N If YES please give priority: HIGH () MEDIUM () LOW () REASON: Bridge is scheduled for replacement. FHK																																																																																																	
CONDITION RATING GUIDE																																																																																																			
(For Items 58, 59, 60 and 61)																																																																																																			
	CODE	CONDITION	DEFECTS																																																																																																
	N	NOT APPLICABLE																																																																																																	
G	9	EXCELLENT	Excellent condition.																																																																																																
G	8	VERY GOOD	No problem noted.																																																																																																
G	7	GOOD	Some minor problems.																																																																																																
F	6	SATISFACTORY	Structural elements show some minor deterioration.																																																																																																
F	5	FAIR	All primary structural elements are sound but may have minor section loss, cracking, spalling or scour.																																																																																																
P	4	POOR	Advance section loss, deterioration, spalling or scour.																																																																																																
P	3	SERIOUS	Loss of section, deterioration, spalling or scour have seriously affected primary structural components. Local failures are possible. Fatigue cracks in steel or shear cracks in concrete may be present.																																																																																																
C	2	CRITICAL	Advance deterioration of primary structural elements. Fatigue cracks in steel or shear cracks in concrete may be present or scour may have removed substructure support. Unless closely monitored it may be necessary to close the bridge until corrective action is taken.																																																																																																
C	1	"IMMINENT" FAILURE	Major deterioration or section loss present in critical structural components or obvious vertical or horizontal movement affecting structure stability. Bridge is closed to traffic but corrective action may put it back in light service.																																																																																																
	0	FAILED	Out of service - beyond corrective action.																																																																																																
DEFICIENCY REPORTING GUIDE																																																																																																			
DEFICIENCY: A defect in a structure that requires corrective action.																																																																																																			
CATEGORIES OF DEFICIENCIES:																																																																																																			
M= Minor Deficiency - Deficiencies which are minor in nature, generally do not impact the structural integrity of the bridge and could easily be repaired. Examples include but are not limited to: Spalled concrete, Minor potholes, Minor corrosion of steel, Minor scouring, Clogged drainage, etc.																																																																																																			
S= Severe/Major Deficiency - Deficiencies which are more extensive in nature and need more planning and effort to repair. Examples include but are not limited to: Moderate to major deterioration in concrete. Exposed and rounded rebar, Considerable settlement, Considerable scouring or undermining, Moderate to extensive corrosion to structural steel with measurable loss of section, etc.																																																																																																			
C-S= Critical Structural Deficiency - A deficiency in a structural element of a bridge that poses an extreme unsafe condition due to the failure or imminent failure of the element which will effect the structural integrity of the bridge.																																																																																																			
C-H= Critical Hazard Deficiency - A deficiency in a component or element of a bridge that poses an extreme hazard or unsafe condition to the public, but does not impact the structural integrity of the bridge. Examples include but are not limited to: Loose concrete hanging down over traffic or pedestrians, A hole in a sidewalk that may cause injuries to pedestrians, Missing section of bridge railing, etc.																																																																																																			
URGENCY OF REPAIR:																																																																																																			
I = Immediate - Inspectors immediately contact District Bridge Inspection Engineer (DBIE) to report the Deficiency and to receive further instruction from him/her.																																																																																																			
A = ASAP - Action/Repairs should be initiated by District Maintenance Engineer or the Responsible Party (if not a State owned bridge) upon receipt of the Inspection Report.																																																																																																			
P = Prioritize - Shall be prioritized by District Maintenance Engineer or the Responsible Party (if not a State owned bridge) and repairs made when funds and/or manpower is available.																																																																																																			

2-DIST 02	B.I.N. 15H	STRUCTURES INSPECTION FIELD REPORT ROUTINE & SPECIAL MEMBER INSPECTION	BR. DEPT. NO. B-02-012
---------------------	----------------------	---	----------------------------------

CITY/TOWN BARRE	8-STRUCTURE NO. B02012-15H-MUN-NBI	11-KILO POINT 005.182	90-ROUTINE INSP. DATE Jan 24, 2007	93*-SPEC. MEMB. INSP. DATE Jan 24, 2007
07-FACILITY CARRIED HWY VERNON AVE		MEMORIAL NAME/LOCAL NAME POWDER-MILL BRIDGE		27-YR BUILT 1937
106-YR REBUILT 0000		94-YR REHAB'D (NON 106) 0000		
06-FEATURES INTERSECTED WATER WARE RIVER		26-FUNCTIONAL CLASS Major Collector		DIST. BRIDGE INSPECTION ENGINEER F. R. Heming
43-STRUCTURE TYPE Steel continuous Stringer/Girder		22-OWNER Town Agency	21-MAINTAINER Town Agency	TEAM LEADER J. A. Mankowsky
107-DECK TYPE Concrete Cast-in-Place		WEATHER Cloudy	TEMP. (air) -6°C	TEAM MEMBERS L. R. LYNCH

WEIGHT POSTING		<table style="font-size: small;"> <tr> <td>H</td><td>3</td><td>352</td><td>Single</td> </tr> <tr> <td><input type="checkbox"/></td><td><input type="checkbox"/></td><td><input type="checkbox"/></td><td><input type="checkbox"/></td> </tr> </table>				H	3	352	Single	<input type="checkbox"/>	<input type="checkbox"/>	<input type="checkbox"/>	<input type="checkbox"/>	<table style="font-size: small;"> <tr> <td>At bridge</td><td>Advance</td> </tr> <tr> <td>E W</td><td>E W</td> </tr> <tr> <td><input type="checkbox"/></td><td><input type="checkbox"/></td> </tr> <tr> <td><input type="checkbox"/></td><td><input type="checkbox"/></td> </tr> </table>		At bridge	Advance	E W	E W	<input type="checkbox"/>	<input type="checkbox"/>	<input type="checkbox"/>	<input type="checkbox"/>
H	3	352	Single																				
<input type="checkbox"/>	<input type="checkbox"/>	<input type="checkbox"/>	<input type="checkbox"/>																				
At bridge	Advance																						
E W	E W																						
<input type="checkbox"/>	<input type="checkbox"/>																						
<input type="checkbox"/>	<input type="checkbox"/>																						
Actual Posting: <input checked="" type="checkbox"/> Not Applicable Recommended Posting: <input type="checkbox"/> <input type="checkbox"/> <input type="checkbox"/> <input type="checkbox"/>		Signs In Place (Y=Yes, N=No, NR=Not Required): <input type="checkbox"/> <input type="checkbox"/> <input type="checkbox"/> <input type="checkbox"/> <input type="checkbox"/> <input type="checkbox"/>																					
Waived Date: 08/30/1980		EJDMT Date: ---		Legibility/Visibility: <input type="checkbox"/> <input type="checkbox"/> <input type="checkbox"/> <input type="checkbox"/>																			

RATING		Request for Rating or Rerating (Y/N): <input type="checkbox"/> N		If YES please give priority: HIGH () MEDIUM () LOW ()		PLANS (Y/N): <input type="checkbox"/> N	
Rating Report (Y/N): <input type="checkbox"/> Y		REASON: Bridge is scheduled for replacement. FHK				(V.C.R.) (Y/N): <input type="checkbox"/> N	
Date: 08/01/1980		TAPE#:					

SPECIAL MEMBER(S):

	MEMBER	CRACK (Y/N)	WELD'S CONDITION (0-9)	LOCATION OF CORROSION, SECTION LOSS (%), CRACKS, COLLISION DAMAGE, STRESS CONCENTRATION, ETC.	CONDITION		INV. RATING OF MEMBER			Deficiencies
					PREVIOUS (0-9)	PRESENT (0-9)	H-20	3	352	
A	Item 58.1 - Wearing surface	N		See remarks in comments section.	5	4	Not Rated			S-P
B	Item 58.2 - Deck Condition	N		See remarks in comments section.	3	3	19	37	57	S-A
C	Item 58.6 - Sidewalks	N		See remarks in comments section.	4	4	Not Rated			S-P
D	Item 58.8 - Railing	N		See remarks in comments section.	4	4	Not Rated			S-P
E	Item 59.4 - Girders or Beams	N		See remarks in comments section.	5	4	29	34	45	S-P

List of field tests performed: Visual & Spot sounding, Beam section loss measurements.	<table style="font-size: x-small;"> <tr> <td></td><td>I-58</td><td>I-59</td><td>I-60</td><td>I-62</td> </tr> <tr> <td>(Overall Previous Condition)</td> <td style="border: 1px solid black; text-align: center;">3</td> <td style="border: 1px solid black; text-align: center;">4</td> <td style="border: 1px solid black; text-align: center;">6</td> <td style="border: 1px solid black; text-align: center;">-</td> </tr> <tr> <td>(Overall Current Condition)</td> <td style="border: 1px solid black; text-align: center;">3</td> <td style="border: 1px solid black; text-align: center;">4</td> <td style="border: 1px solid black; text-align: center;">6</td> <td style="border: 1px solid black; text-align: center;">-</td> </tr> </table>		I-58	I-59	I-60	I-62	(Overall Previous Condition)	3	4	6	-	(Overall Current Condition)	3	4	6	-
	I-58	I-59	I-60	I-62												
(Overall Previous Condition)	3	4	6	-												
(Overall Current Condition)	3	4	6	-												

DEFICIENCY: A defect in a structure that requires corrective action.

CATEGORIES OF DEFICIENCIES:

M= Minor Deficiency - Deficiencies which are minor in nature, generally do not impact the structural integrity of the bridge and could easily be repaired. Examples include but are not limited to: Spalled concrete, Minor pot holes, Minor corrosion of steel, Minor scouring, Clogged drainage, etc.

S= Severe/Major Deficiency - Deficiencies which are more extensive in nature and need more planning and effort to repair. Examples include but are not limited to: Moderate to major deterioration in concrete, Exposed and corroded rebar, Considerable settlement, Considerable scouring or undermining, Moderate to extensive corrosion to structural steel with measurable loss of section, etc.

C-S= Critical Structural Deficiency - A deficiency in a structural element of a bridge that poses an extreme unsafe condition due to the failure or imminent failure of the element which will affect the structural integrity of the bridge.

C-H= Critical Hazard Deficiency - A deficiency in a component or element of a bridge that poses an extreme hazard or unsafe condition to the public, but does not impair the structural integrity of the bridge. Examples include but are not limited to: Loose concrete hanging down over traffic or pedestrians, A hole in a sidewalk that may cause injuries to pedestrians, Missing section of bridge railing, etc.

URGENCY OF REPAIR:

I = Immediate - (Inspector) immediately contact District Bridge Inspection Engineer (DBIE) to report the Deficiency and to receive further instruction from him/her).

A = ASAP - (Action/Repairs should be initiated by District Maintenance Engineer or the Responsible Party (if not a State owned bridge) upon receipt of the Inspection Report).

P = Prioritize - (Should be prioritized by District Maintenance Engineer or the Responsible Party (if not a State owned bridge) and repairs made when funds and/or manpower is available).

X=UNKNOWN N=NOT APPLICABLE H=HIDDEN/INACCESSIBLE R=REMOVED

FC (1/7/99)

CITY/TOWN	B.I.N.	BR. DEPT. NO.	S. STRUCTURE NO.	INSPECTION DATE
BARRE	15H	B-02-012	B02012-15H-MUN-NBI	JAN 24, 2007
REMARKS				
<p><u>BRIDGE ORIENTATION</u></p> <p>According to the rating report, the bridge carries Vernon Avenue traffic north & south over the Ware River which flows from east to west. The abutments are labeled as "North Abutment" & "South Abutment". The 3 spans and 2 piers are numbered from south to north. The 7 continuous beams are numbered from west to east.</p>				
<p><u>GENERAL REMARKS</u></p> <p>There are several areas of heavy accumulation of debris (concrete from patched areas) under the repaired areas in Spans #1 and #3.</p>				
<p><u>ITEM 58 - DECK</u></p>				
<p><u>Item 58.1 - Wearing surface</u></p> <p>Seven <u>steel deck plates</u>, measuring 8'-0" long x 20'-0" wide x 1" thick, are in place due to severe deterioration of the wearing surface & deck over portions of Spans 1 & 2. The plates are placed transverse to the flow of traffic and cover the northern one-third of Span #1 and the southern two-thirds of Span #2. Run-off & road salt leak freely around these plates, allowing severe deterioration to the deck & superstructure below. Additionally, the plates do not provide traction. Hence, they are slippery when wet.</p> <p>Previously tack welded together, the plates now act independently due to broken welds. The plates lie uneven & have shifted in places, opening up slender gaps. Plate #2 (numbered from south to north) is sagging, causing a 1" lip between Plates #1 & #2. Please see Photo #1. A 1.5" gap exists between Plates #2 & #3. Please see Photo #2.</p> <p><u>Span #1</u> - The bituminous concrete pavement at the south end of the plates is heaved by 1". The pavement is broken up & pot-holed up to 2" deep at this location. Please see Photo #3.</p> <p><u>Span #3</u> - The surface exhibits concrete repair patches scattered about & some map-cracked area above the centerline that appears slightly settled. Please see Photo #4.</p>				
<p><u>Item 58.2 - Deck Condition</u></p> <p>The underside of the deck has extensive deterioration with large spalled areas (up to full depth x full width of bay) with exposed corroded rebars, hollow areas, numerous areas of cracking with efflorescence and/or damp areas. Steel plates rest upon the deck in portions of Spans 1 & 2 to protect against local failure. Please see Item 58.1 "Wearing Surface" for details on the plates.</p> <p><u>Span #1</u> - The soffit in Bay #5, is heavily cracked with efflorescence and is hollow sounding & slightly sagging for approximately 9' length x 3' width, next to Pier #1. At the end of the sag, the deck is spalled 2' width x 1.2' length x 5" depth with a broken rebar that is bent downward. Please see Photo #7. The spall is located just outside of the steel plates which rest on the deck topside.</p> <p><u>Span #2</u> - Extensive cracking, both longitudinal & transverse with efflorescence, hollow areas & scattered spalls are scattered about the deck soffit. The most severe condition is just north of Pier #1, between Beams #2 & #4, where the concrete deck slab has failed with several full depth spalled areas and corroded rebars. Please see Photos #5 & #6. However, this failed area has steel plates above which extend from curbline to curbline. The plates guard against localized failure.</p> <p><u>Span #3</u> - Timber form work is still in place from several previous deck repairs. Please see Photos #5 & #8. Some of the timber form work has fallen onto the the embankment below Span 3. Please see Photo #9.</p> <p><u>In Bay #5 near Pier #2</u>, a spalled area with exposed corroded rebars measures 4' length x full width of bay. Please see Photo #10.</p> <p>A spalled section 10' long x 2.5' wide x 2.5" deep exists below the East Curbline with several exposed rebars.</p>				

REM:217-40

CITY/TOWN BARRE	B.I.N. 15H	BR. DEPT. NO. B-02-012	S.-STRUCTURE NO. B02012-15H-MUN-NBI	INSPECTION DATE JAN 24, 2007
---------------------------	----------------------	----------------------------------	---	--

REMARKS

Item 58.4 - Curbs

The north end of the West Curb and a section towards the middle of the East Curb are cracked & heavily scaled.

Item 58.6 - Sidewalks

Concrete sidewalk was snow covered at the time of inspection. Previous reports indicate numerous spalls, moderate scaling, random cracks, and patched areas. The sidewalk underside has some shallow cover spalls.

Item 58.7 - Parapets

Both parapet fascias have minor to moderate scaling with light efflorescence staining. A large spalled area and cracked area measuring approximately 10' length x 7" height x 5" depth exists below the construction cold joint at the north end of the West Parapet. Please see Photo #11.

Item 58.8 - Railing

The bridge rail consists of reinforced concrete rails and posts. The bridge rails are moderately to heavily scaled with numerous areas of spalled concrete with exposed rebars and areas of horizontal cracking throughout. Please see Photo #12.

Item 58.10 - Drainage System

There are a few scattered deck drains that exhibit rusted pipes and visible deck leakage. The top side of the drains are paved over and do not allow for deck run-off.

Item 58.12 - Utilities

The water main running along the east fascia is leaking at the North end with a few areas of loose insulation wrapping.

APPROACHES

Approaches a - Appr. Pavement Condition

North Approach - Roadway has 1" width transverse cracks, and some depressions with map cracking.

South Approach - Roadway has transverse cracking at the deck end.

Approaches b - Appr. Roadway Settlement

North Approach - Roadway has some heaving & settled areas scattered randomly.

ITEM 59 - SUPERSTRUCTURE

Item 59.4 - Girders or Beams

The beams have areas of minor to moderate rusting throughout. Areas with more significant layered rusting and section loss are outlined below. The original thickness of beam flanges is 3/4" thickness.

Span 1 - Beam ends have dark layered rust with section loss around bearing areas, particularly at the pier. Please see Photo #13.

Beam #3 - The lower flange & lower web area has layered rust and average 1/16" loss for approximately 70% of the length. Lower flange section thickness remaining at the pier bearing is 1/2". (65% remaining)

Remainder of beam interiors have moderate to heavy rust along webs & flanges with some layered rusting.

Span 2 - Beams #3, #4, & #5 have layered rusting of upper & lower flanges. Section remaining at mid-span averages 9/16" (75% remaining). Please see Photo #14.

Beam ends over the Pier #1 bearing area also have 1/16" loss of section in webs & flanges.

CITY/TOWN	B.I.N.	BR. DEPT. NO.	S-STRUCTURE NO.	INSPECTION DATE
BARRE	15H	B-02-012	B02012-15H-MUN-NBI	JAN 24, 2007
REMARKS				
<p><u>Item 59.4 - Girders or Beams (Cont'd)</u></p> <p>Upper flange around Beam #3 & #4 connection plates is also severely rusted due to 100% section loss holes in the deck above. Please see Photo #6.</p> <p><u>Span #3</u> - Beams #3, #4, & #5 have layered rusting of upper & lower flanges for an average length of 20' near mid-span. Average section loss is 1/16". Please see Photo #15. Webs have flaking rust.</p> <p><u>Item 59.7 - Conn Plt's, Gussets & Angles</u></p> <p>Span 2 - Connection plates for Beams #3, #4, #5 below the spalled deck next to Pier #1 have some layered rust along the lower connection plates & bolt heads.</p> <p><u>Item 59.9 - Bearing Devices</u></p> <p>All the steel fixed & movable plate bearings exhibit moderate to heavy rusting.</p> <p><u>Pier #1</u> - Bearings have layered rust. Many of the anchor bolts were sheared off or bent.</p> <p>The remaining anchor bolts have moderate to heavy rust with deep section loss. Please see Photo # 13.</p> <p><u>Abutments</u> - Most anchor bolts at the South Abutment are missing. At the North Abutment, bolts are missing below Beams #1 & #6.</p> <p><u>Item 59.10 - Diaphragms/Cross Frames</u></p> <p>The diaphragms exhibit areas of moderate to heavy rusting throughout, especially along the bottom flanges with areas of moderate delamination.</p> <p>The end diaphragms at Pier #1 have heavy rust and delamination with areas of heavy section loss, particularly in Bay #6, where areas of 100% loss exist in the web and lower flange. Please see Photo #16.</p> <p><u>Item 59.11 - Rivets & Bolts</u></p> <p>The rivets for the connection plates and beam splice connections exhibit moderate rusting for most plates. Bolts for Beams #3, #4, & #5 along the northern side of Pier #1 have heavier rust with delamination along the lower connection plates.</p> <p><u>Item 59.13 - Member Alignment</u></p> <p>Most beams appear flat or have a slight negative camber.</p> <p><u>Item 59.14 - Paint/Coating</u></p> <p>The paint system is providing minimal protection where still attached. The existing paint is chalking, peeling and appears blistered. Please see Photos #5, #8, #14, & #15.</p> <p><u>SuperStructure Load Vibration Notes</u></p> <p>There was moderate load vibration noted during live load conditions.</p> <p><u>ITEM 60 - SUBSTRUCTURE</u></p> <p><u>Item 60.1 - Abutments</u></p> <p><u>Item 60.1.c - Backwalls</u></p> <p>Both backwalls are stained from leakage with scattered areas of hairline cracking and concrete pop-outs.</p> <p><u>South Abutment</u> - There is an area of moderate scaling with exposed rusted rebar, located in Bay #6.</p> <p><u>Item 60.1.d - Breastwalls</u></p> <p>The abutment breastwalls are lightly scaled with scattered hairline cracks and efflorescence staining.</p>				

REM 12/06

CITY/TOWN	B.I.N.	BR. DEPT. NO.	STRUCTURE NO.	INSPECTION DATE
BARRE	15H	B-02-012	B02012-15H-MUN-NBI	JAN 24, 2007
REMARKS				
<p><u>Item 60.1.i - Erosion</u> There is an area of moderate erosion at the northeast corner of the bridge.</p> <p><u>Item 60.2 - Piers or Bents</u> <u>Item 60.2.b - Caps</u> Both pier caps have minor cracking with areas of light efflorescence and rust staining from deck leakage.</p> <p><u>Pier #1, south face</u> - A small spall with exposed rebar located at the bottom edge measured approximately 6" wide x 5" high is located . A hollow area measuring 5'-0" long x 1.6' high is located under Bay #2. A horizontal crack, hairline to 1/16" width, with rust stains extends from Beam #3 to Beam #6. Area is hollow beneath the crack. Please see Photo #17. <u>Pier #1, north face</u> - An area below Bay #3 is cracked with scattered hollow sounds.</p> <p><u>Item 60.2.h - Scour</u> Underwater Inspection Report dated 08/10/05 states moderate scour along the faces of the upstream column of Pier #1.</p> <p><u>ITEM 61 - CHANNEL AND CHANNEL PROTECTION</u></p> <p><u>Item 61.6 - Rip-Rap/Slope Protection</u></p> <ul style="list-style-type: none"> The slope under the bridge showed minor gullying of the gravel slope. <p><u>TRAFFIC SAFETY</u></p> <p><u>Item 36a - Bridge Railing</u> Non-standard. The bridge rail consists of reinforced concrete rails and posts. The bridge rails are moderately to heavily scaled with numerous areas of spalled concrete with exposed rebars and areas of horizontal cracking throughout. Please see Photo #12.</p> <p><u>Item 36b - Transitions</u> Non-standard. The approach guardrail is not attached to the bridge at the south end. At the north end, the guardrail is attached to a non-standard endpost.</p> <p><u>Item 36c - Approach Guardrail</u> Non-standard. Older style single face metal guardrail exists at all 4 approaches and has minor collision damage at all corners. Please see Photo #18.</p> <p><u>Item 36d - Approach Guardrail Ends</u> Non-standard. The guardrail at the northwest corner extends beyond the limits of the bridge. The guardrail ends at the southeast and southwest corners have terminal ends. End at northeast corner is buried.</p> <p><u>Photo Log</u></p> <p>Photo 1 : Connection welds are broken between steel plates. Plate #2 sags, creating a 1" lip between Plates #1 & #2.</p> <p>Photo 2 : Looking east, welds between steel plates have failed; a 1.5" gap is present between Plates #2 & #3.</p> <p>Photo 3 : Looking east; Wearing surface has broken up & is pot-holed at the end of the steel plate above Span 1.</p> <p>Photo 4 : Wearing surface above Span 3 has areas of full depth repairs; Other areas are heavily cracked.</p>				

REM:21740

CITY/TOWN	B.T.N.	BR. DEPT. NO.	S. STRUCTURE NO.	INSPECTION DATE
BARRE	15H	B-02-012	B02012-15H-MUN-NBI	JAN 24, 2007
REMARKS				
<u>Photo Log (Cont'd)</u>				
Photo 5 : Span 2, looking south; Note the heavy cracking with efflorescence & severe spalls, some with timber repair forms.				
Photo 6 : Span 2, Close-up of typical full depth spall adjacent to Pier #1.				
Photo 7 : Span 1, Bay #5; Cracking in deck soffit is heavy. This section is directly below the southernmost steel plate on the deck surface.				
Photo 8 : Span 3; Timber repair forms remain in place at north end of Bays #3, #4, & #5.				
Photo 9 : Several of the timber repair forms have fallen to the embankment below Span 3.				
Photo 10 : Span 3, Bay #5; Spalled area with corroded rebar extends full width of the bay.				
Photo 11 : West Parapet @ northerly end; Note the spalled condition below the horizontal construction cold joint.				
Photo 12 : Heavy deterioration of concrete horizontals is typical for approximately 25% of the bridge rail system.				
Photo 13 : Span 1, Typical heavy corrosion of beam & bearing above Pier #1.				
Photo 14 : Span 2; Typical corrosion of beams.				
Photo 15 : Span 3, Beam #4 near mid-span. Upper & lower flanges have layered rust with measurable section loss. Web has flaking rust.				
Photo 16 : Bay #6 above Pier #1; Note the severe rust & section loss holes along lower web of diaphragm.				
Photo 17 : Pier Cap #1, south face; Rust stains exist below horizontal cracks.				
Photo 18 : Guardrail at southeast corner has some minor collision damage.				

REM:27/40

CITY/TOWN BARRE	B.I.N. 15H	BR. DEPT. NO. B-02-012	S. STRUCTURE NO. B02012-15H-MUN-NBI	INSPECTION DATE JAN 24, 2007
---------------------------	----------------------	----------------------------------	---	--

PHOTOS

Photo 1: Connection welds are broken between steel plates. Plate #2 sags, creating a 1" lip between Plates #1 & #2.

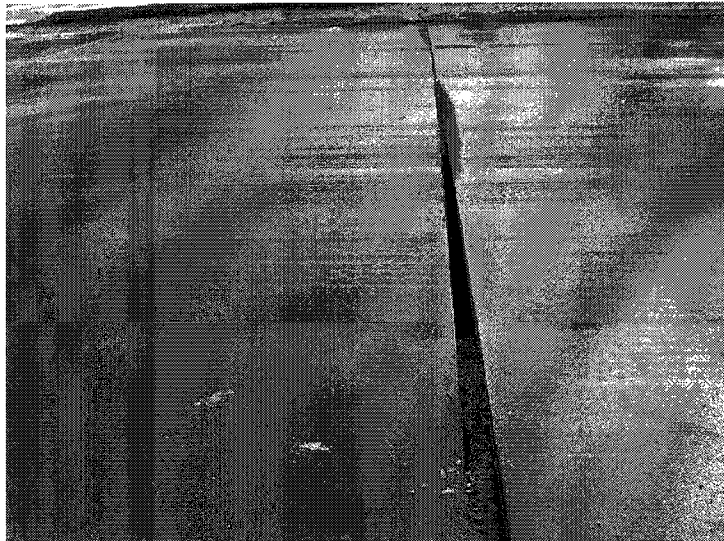


Photo 2: Looking east, welds between steel plates have failed; a 1.5" gap is present between Plates #2 & #3.

CITY/TOWN BARRE	B.I.N. 15H	BR. DEPT. NO. B-02-012	S. STRUCTURE NO. B02012-15H-MUN-NBI	INSPECTION DATE JAN 24, 2007
---------------------------	----------------------	----------------------------------	---	--

PHOTOS

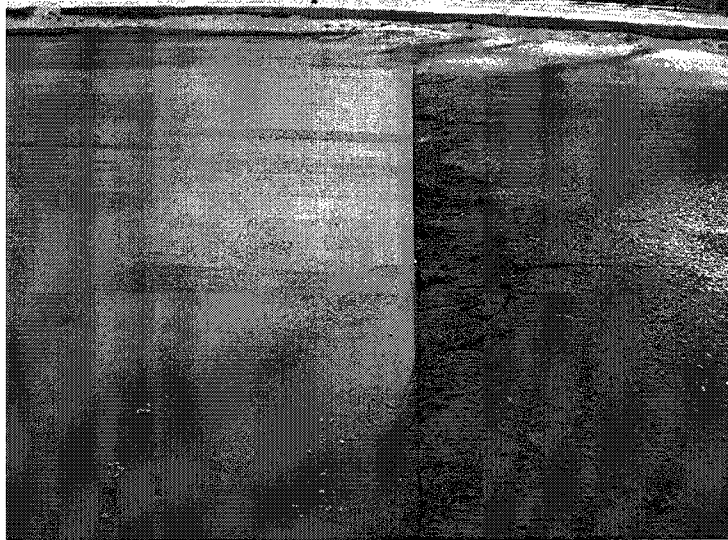


Photo 3: Looking east; Wearing surface has broken up & is pot-holed at the end of the steel plate above Span 1.



Photo 4: Wearing surface above Span 3 has areas of full depth repairs; Other areas are heavily cracked.

CITY/TOWN BARRE	B.L.N. 15H	BR. DEPT. NO. B-02-012	S. STRUCTURE NO. B02012-15H-MUN-NBI	INSPECTION DATE JAN 24, 2007
---------------------------	----------------------	----------------------------------	---	--

PHOTOS



Photo 5: Span 2, looking south; Note the heavy cracking with efflorescence & severe spalls, some with timber repair forms.



Photo 6: Span 2, Close-up of typical full depth spall adjacent to Pier #1.

CITY/TOWN BARRE	B.I.N. 15H	BR. DEPT. NO. B-02-012	8-STRUCTURE NO. B02012-15H-MUN-NBI	INSPECTION DATE JAN 24, 2007
---------------------------	----------------------	----------------------------------	--	--

PHOTOS

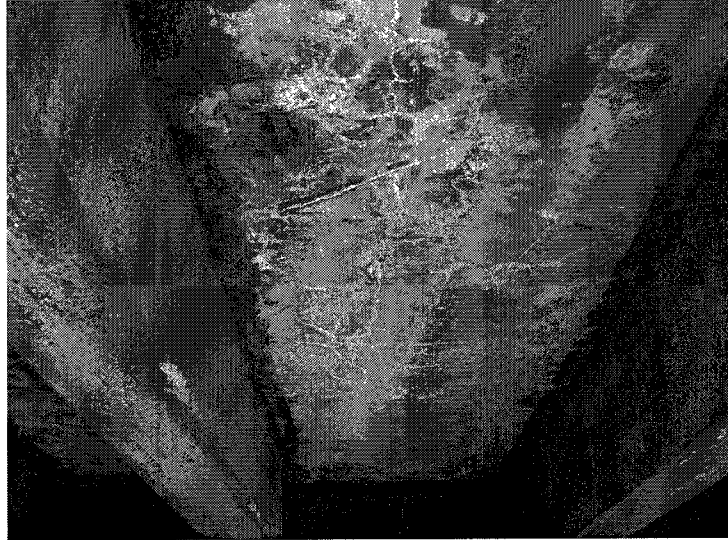


Photo 7: Span 1, Bay #5; Cracking in deck soffit is heavy. This section is directly below the southernmost steel plate on the deck surface.



Photo 8: Span 3; Timber repair forms remain in place at north end of Bays #3, #4, & #5.

CITY/TOWN BARRE	B.I.N. 15H	BR. DEPT. NO. B-02-012	S. STRUCTURE NO. B02012-15H-MUN-NBI	INSPECTION DATE JAN 24, 2007
---------------------------	----------------------	----------------------------------	---	--

PHOTOS

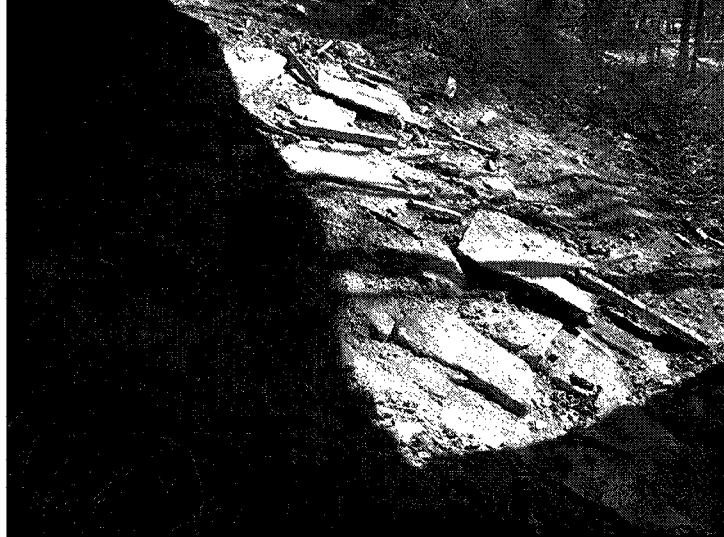


Photo 9: Several of the timber repair forms have fallen to the embankment below Span 3.

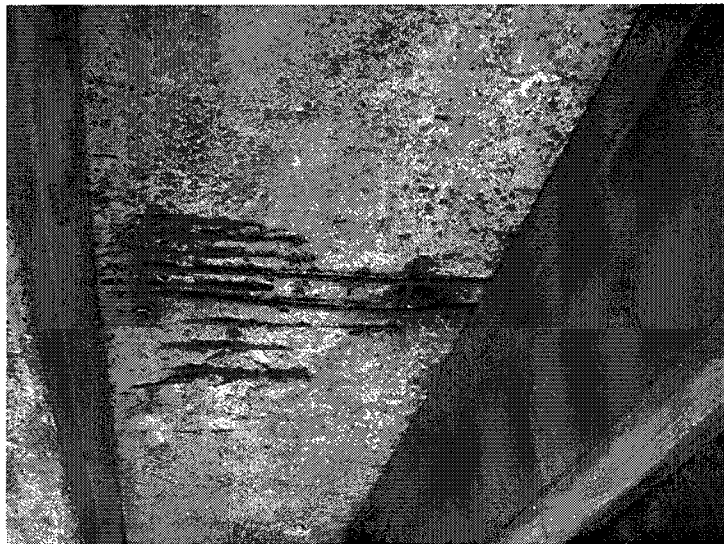


Photo 10: Span 3, Bay #5; Spalled area with corroded rebar extends full width of the bay.

REM (2/7-95)

CITY/TOWN BARRE	B.I.N. 15H	BR. DEPT. NO. B-02-012	S. STRUCTURE NO. B02012-15H-MUN-NBI	INSPECTION DATE JAN 24, 2007
---------------------------	----------------------	----------------------------------	---	--

PHOTOS

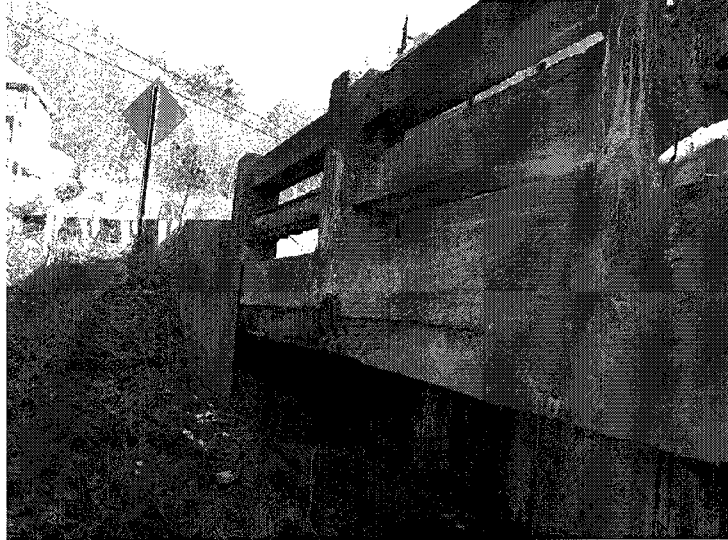


Photo 11: West Parapet @ northerly end; Note the spalled condition below the horizontal construction cold joint.



Photo 12: Heavy deterioration of concrete horizontals is typical for approximately 25% of the bridge rail system.

REN 2/7-98

CITY/TOWN BARRE	B.I.N. 15H	BR. DEPT. NO. B-02-012	S-STRUCTURE NO. B02012-15H-MUN-NBI	INSPECTION DATE JAN 24, 2007
---------------------------	----------------------	----------------------------------	--	--

PHOTOS



Photo 13: Span 1, Typical heavy corrosion of beam & bearing above Pier #1.



Photo 14: Span 2; Typical corrosion of beams.

REM 127-06

CITY/TOWN BARRE	B.I.N. 15H	BR. DEPT. NO. B-02-012	S-STRUCTURE NO. B02012-15H-MUN-NBI	INSPECTION DATE JAN 24, 2007
---------------------------	----------------------	----------------------------------	--	--

PHOTOS

Photo 15: Span 3, Beam #4 near mid-span. Upper & lower flanges have layered rust with measurable section loss. Web has flaking rust.

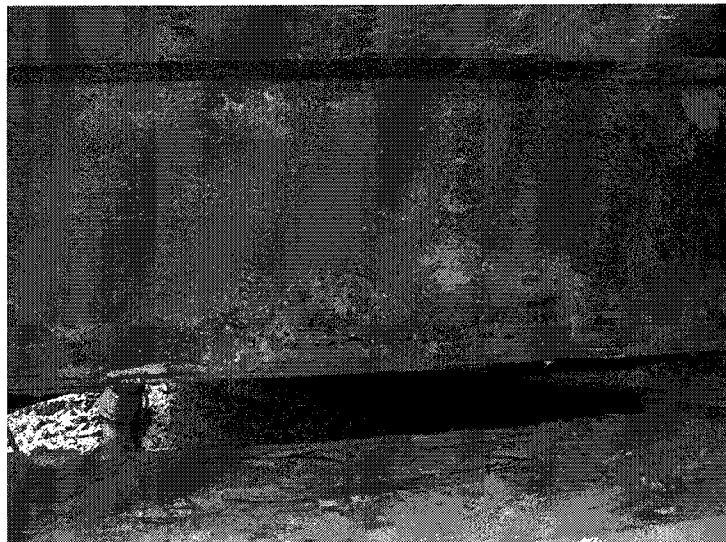


Photo 16: Bay #6 above Pier #1; Note the severe rust & section loss holes along lower web of diaphragm.

CITY/TOWN BARRE	B.I.N. 15H	BR. DEPT. NO. B-02-012	S. STRUCTURE NO. B02012-15H-MUN-NBI	INSPECTION DATE JAN 24, 2007
---------------------------	----------------------	----------------------------------	---	--

PHOTOS



Photo 17: Pier Cap #1, south face; Rust stains exist below horizontal cracks.

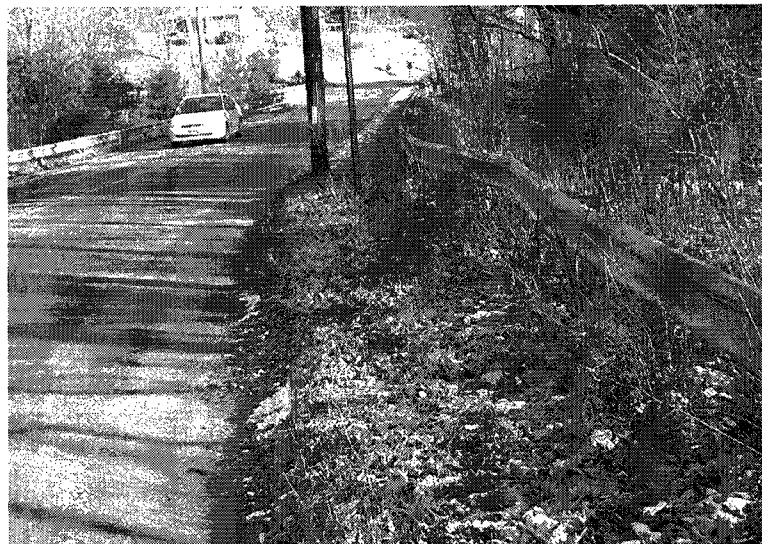


Photo 18: Guardrail at southeast corner has some minor collision damage.